

*Strategies
and Tactics
in Organic
Synthesis* *Volume 10*

Edited by
MICHAEL HARMATA



Academic Press is an imprint of Elsevier
The Boulevard, Langford Lane, Kidlington, Oxford OX5 1GB, UK
Radarweg 29, PO Box 211, 1000 AE Amsterdam, The Netherlands

© 2014 Elsevier Ltd. All rights reserved.

No part of this publication may be reproduced, stored in a retrieval system or transmitted in any form or by any means electronic, mechanical, photocopying, recording or otherwise without the prior written permission of the publisher.

Permissions may be sought directly from Elsevier's Science & Technology Rights Department in Oxford, UK: phone (+44) (0) 1865 843830; fax (+44) (0) 1865 853333; email: permissions@elsevier.com. Alternatively you can submit your request online by visiting the Elsevier web site at <http://elsevier.com/locate/permissions>, and selecting Obtaining permission to use Elsevier material.

Notice

No responsibility is assumed by the publisher or the editor for any injury and/or damage to persons or property as a matter of products liability, negligence or otherwise, or from any use or operation of any methods, products, instructions or ideas contained in the material herein. Because of rapid advances in the medical sciences, in particular, independent verification of diagnoses and drug dosages should be made.

British Library Cataloguing in Publication Data

A catalogue record for this book is available from the British Library

Library of Congress Cataloging-in-Publication Data

A catalog record for this book is available from the Library of Congress

For information on all **Academic Press** publications
visit our web site at store.elsevier.com

This book has been manufactured using Print On Demand technology. Each copy is produced to order and is limited to black ink. The online version of this book will show color figures where appropriate.

ISBN: 978-0-12-417185-5

ISSN: 1874-6004



Working together
to grow libraries in
developing countries

www.elsevier.com • www.bookaid.org

Dedication

This volume is dedicated to the memory of Andrew Harmata, November 9, 1924–October 1, 2013.



June 6, 1953

Contributors

Numbers in Parentheses indicate the pages on which the author's contributions begin.

- Tamara Arto** (33), Instituto Universitario de Química Organometálica “Enrique Moles,” Universidad de Oviedo, Julián Clavería, Oviedo, Spain
- Carlos Roque Duarte Correia** (1), Chemistry Institute, State University of Campinas—Unicamp, Campinas, São Paulo, Brazil
- Michael J. Di Maso** (225), Department of Chemistry, University of California, Davis, California, USA
- Tim G. Elford** (79), Gilead Alberta ULC, Edmonton, Alberta, Canada
- Francisco J. Fañanás** (33), Instituto Universitario de Química Organometálica “Enrique Moles,” Universidad de Oviedo, Julián Clavería, Oviedo, Spain
- Paul E. Floreancig** (183), Department of Chemistry, University of Pittsburgh, Pittsburgh, Pennsylvania, USA
- Laura Furst** (207), Department of Chemistry, University of Michigan, Ann Arbor, Michigan, USA
- Charles I. Grove** (225), Department of Chemistry, University of California, Davis, California, USA
- Dennis G. Hall** (79), Department of Chemistry, University of Alberta, Edmonton, Alberta, Canada
- Carrie Johnson** (131), Department of Biochemistry, The University of Texas Southwestern Medical Center at Dallas, Dallas, Texas, USA
- Taek Kang** (271), Department of Chemistry, KAIST (Korea Advanced Institute of Science and Technology), Yuseong, Daejeon, South Korea
- Hee-Yoon Lee** (271), Department of Chemistry, KAIST (Korea Advanced Institute of Science and Technology), Yuseong, Daejeon, South Korea
- Hee Nam Lim** (51), Department of Chemistry, Stony Brook University, Stony Brook, New York, USA
- Jeremy A. May** (113), Department of Chemistry, University of Houston, Houston, Texas, USA
- Abraham Mendoza** (33), Instituto Universitario de Química Organometálica “Enrique Moles,” Universidad de Oviedo, Julián Clavería, Oviedo, Spain
- E. Zachary Oblak** (155), Department of Pharmaceutical Sciences, and Department of Chemistry, University of Connecticut, Storrs, Connecticut, USA
- Caio Costa Oliveira** (1), Chemistry Institute, State University of Campinas—Unicamp, Campinas, São Paulo, Brazil

Kathlyn A. Parker (51), Department of Chemistry, Stony Brook University, Stony Brook, New York, USA

Félix Rodríguez (33), Instituto Universitario de Química Organometálica “Enrique Moles,” Universidad de Oviedo, Julián Clavería, Oviedo, Spain

Jared T. Shaw (225), Department of Chemistry, University of California, Davis, California, USA

Arash Soheili (131), Department of Biochemistry, The University of Texas Southwestern Medical Center at Dallas, Dallas, Texas, USA

Corey R.J. Stephenson (207), Department of Chemistry, University of Michigan, Ann Arbor, Michigan, USA

Uttam K. Tambar (131), Department of Biochemistry, The University of Texas Southwestern Medical Center at Dallas, Dallas, Texas, USA

Michael D. Van Heyst (155), Department of Pharmaceutical Sciences, and Department of Chemistry, University of Connecticut, Storrs, Connecticut, USA

Craig M. Williams (249), School of Chemistry and Molecular Biosciences, University of Queensland, Brisbane, Queensland, Australia

Dennis L. Wright (155), Department of Pharmaceutical Sciences, and Department of Chemistry, University of Connecticut, Storrs, Connecticut, USA

Preface

I write this a bit more than 4 months after my father died. He was a complicated man, just like any other, unknown in many aspects, even to those close to him. Perhaps due to The Depression or The War or just Life, he was not as formally educated as he could have been, but he wanted more for his children (he got it) and he was quite clever in his own right. If you wanted anything that involved pipes or ductwork, he could design it and install it, a real engineer. He also did some basic research. I recall one experiment with a series of cups in our garage. He decided to test the effects of different liquids on the setting of cement: everything from water, milk, juice, and alcohol, all the way to gasoline. Ahh . . . curiosity-driven, basic research. . . I still like it. He was, however, not as happy when I used the hydrolysis of calcium carbide to generate acetylene (in our basement) so that it could be bubbled through a solution of copper sulfate. So it smelled a bit; what's the big deal, Dad?

As we continue to lose members of "The Greatest Generation," we should recall that we are their legacy. They lived their lives with concepts of duty, pride, and honor that we would all do well to remember, whether practicing science or just simply living. I miss my Father, but he lives on in me and I do my best to honor him through how I live my life. Mistakes are included, however. But Dad always said, "The man who makes no mistakes, makes nothing."

And so we move on to chemistry. Here we present a collection of stories that are part of the very human exercise of science and, as I think many would agree, that of art. Design, invention, struggle, tenacity; these are all aspects of the practice of synthesis. It is always a pleasure to delve into such stories, as they are mysteries, written by the chemists who had to confront the realities of Mother Nature directly, deal with the lady who always has the final word, and hope that they could find at least one path that allowed them passage to their goal. Synthesis at both the level of methodology and target-oriented synthesis is an exercise in science, art, engineering, philosophy, and probably sometimes religion (though praying that a reaction will work never has an effect, at least not for me). My thanks go out to all of the authors who took the time to share a part of their lives with other members of the scientific community.

Finally, I would like to thank Elsevier for their continued commitment to this series, in spite of some obstacles. In particular, I want to express my gratitude to Derek Coleman and Susan Dennis for their support over the years.

There is much more to be done. Let's do it!

MICHAEL HARMATA

Substrate-Directed Heck–Matsuda Arylations: From Curiosity to a Valuable Synthetic Tool

Caio Costa Oliveira and Carlos Roque Duarte Correia¹

Chemistry Institute, State University of Campinas—Unicamp, Campinas, São Paulo, Brazil

¹Corresponding author: roque@iqm.unicamp.br

Chapter Outline

1. Introduction and Overview	1	3.2. Stereoselective Arylation of N-Protected Allylic Amine Derivatives	11
2. Substrate-Directed Heck–Matsuda Reaction	4	3.3. Stereoselective Arylation of Cyclopentene Scaffolds	21
2.1. Some Preliminary Results	4	4. Conclusion	30
3. Development and Synthetic Applications of the Substrate-Directed Heck–Matsuda Reaction	6	Acknowledgments	30
3.1. Stereoselective Arylation of Allylic Esters	6	References	31

1 INTRODUCTION AND OVERVIEW

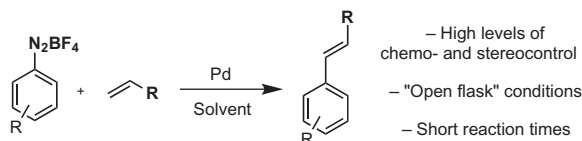
The availability of efficient synthetic methods is a critical aspect in the synthesis of complex organic molecules. After careful planning, the designed synthesis should be achieved in a regio- and stereoselective way, beginning from simple and readily accessible starting materials, if possible under mild reaction conditions.¹ With this objective in mind, we have been working on the development of new methodologies for the short and efficient total synthesis of aryl-containing molecules of pharmacological and functional interest.²

Aiming at this important goal, we have been investigating the Pd-catalyzed arylation of olefins with arenediazonium salts, known as

Heck–Matsuda reaction. This reaction was first described in 1977 by Tsutomu Matsuda, who pointed out the unique reactivity of the arenediazonium salts in the Heck reaction, allowing a fast and direct generation of cationic aryl-palladium species in the reaction medium.³ Indeed, the high levels of chemo- and stereocontrol observed in these reactions usually do not depend on the use of halide scavengers (such Ag^+ or Ti^+ salts), dry solvents, inert atmosphere, or phosphane ligands (Scheme 1).^{2,4}

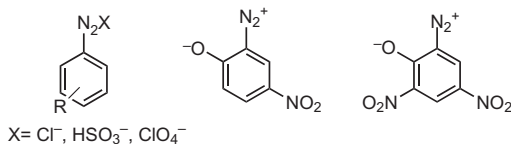
In spite of these advantages, the Heck–Matsuda reaction was overlooked by the chemical community for more than two decades, probably due to the high reactivity of the arenediazonium salts and their potential instability, if possessed of the appropriate counterion. Another reason might be the fact that the extremely successful development of Heck reactions (more specifically arylations) employing aryl halides and aryl triflates, together with the design of a variety of phosphane ligands (chiral and achiral), contributed to the decline of arenediazonium salts as viable starting materials for the Heck arylation. Another important factor that might have retarded the routine use of the Heck–Matsuda in organic synthesis is the incompatibility of most phosphane ligands with arenediazonium salts. Arenediazonium salts tend to react with strong bases and nucleophiles. These limitations also help to explain the late development of the enantioselective version of the Heck–Matsuda reaction, which was achieved only in 2012.⁵

Arenediazonium salts are considered by some researchers as hazardous materials due to their high reactivity⁶ and the low thermostability of some members of this family of compounds. There are two main structural requirements to classify aryl diazonium salt as potential hazardous or explosive: (i) the presence of small oxidizable or high oxygenated counteranions, such as Cl^- , HSO_3^- , and ClO_4^- ; and (ii) zwitterionic diazophenols containing nitro groups as substituents in the aromatic ring.⁷ To overcome these problems, one can use arenediazonium salts bearing nonoxidizable counteranions, such as BF_4^- , PF_6^- , or even tosylate as electrophiles in the Heck–Matsuda reaction. The large majority of these compounds are obtained as fluffy solids after the diazotation of anilines in water, followed by recrystallization in acetone by the addition of cold ethyl ether. The diazotation reactions can be carried out on large scale—from decagrams to kilos—with good to high overall yields (70–90%). Most of these salts can be stored in a refrigerator or freezer for several days or weeks without significant decomposition (Figure 1). Additionally, for critical cases, one can carry out thermal analysis such as DSC (differential scanning calorimetry) and TGA (thermo gravimetric analysis) to obtain

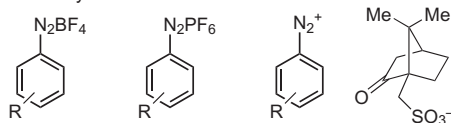
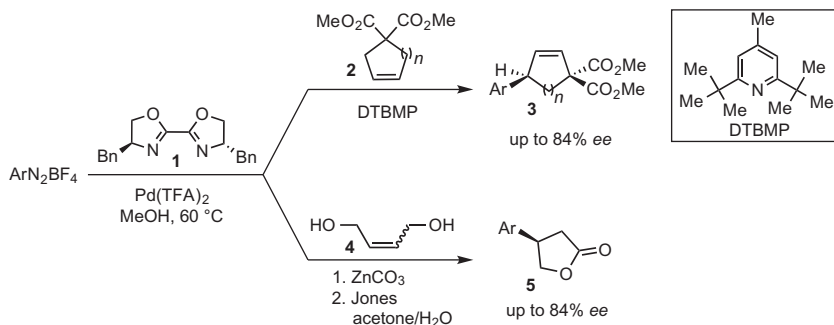


SCHEME 1 An overview of Heck–Matsuda reaction.

Thermounstable aryldiazonium salts



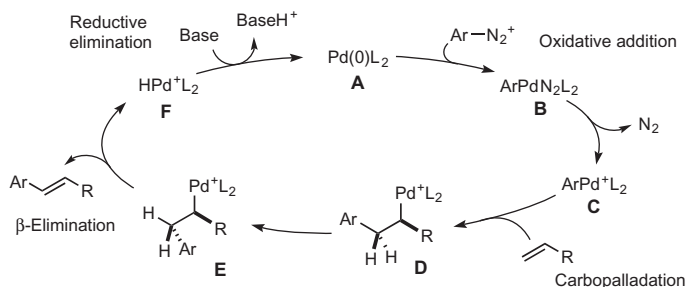
Thermostable aryldiazonium salts

**FIGURE 1** Some examples of aryldiazonium salts.**SCHEME 2** Enantioselective Heck–Matsuda reaction.

valuable information about the stability of the arenediazonium salt one is planning to use in the laboratory. Another viable alternative is the *in situ* generation of the arenediazonium salt.⁸ Indeed, there are several examples of this strategy in industrial applications of the aryldiazonium tetrafluoroborates for the Heck–Matsuda, Sandmeyer, and Meerwein reactions on the kilo scales.⁹

Another aspect that probably contributed to the limited interest in the Heck–Matsuda reaction in organic synthesis for many years was the absence of its enantioselective version. In 2012, we described the first enantioselective Heck–Matsuda arylation of olefins using the chiral bisoxazoline **1** as the ligand for this transformation.⁹ This opened the door for the application of this reaction in more challenging transformations such as the enantioselective arylation of acyclic olefins in good yields with enantiocontrol (Scheme 2).¹⁰ Initial studies were carried out aiming at the desymmetrization of cyclic olefins (**2**), and arylation of more challenging acyclic olefins (**4**).

The general catalytic cycle for the Heck–Matsuda reaction using acyclic olefins starts with the oxidative addition of the Pd(0) catalyst **A** to the aryldiazonium salt and sequential elimination of nitrogen to produce the cationic palladium species **C**. This intermediate is very electrophilic and it promptly



SCHEME 3 General catalytic cycle for the Heck–Matsuda reaction.

binds to the olefin to produce the alkyl-palladium **D**. As both the carbopalladation and β -elimination steps occur in a *syn*-stereospecific way, the intermediate **D** undergoes rotation to align one of the hydrogens with palladium, as shown in **E**. Usually, the conformer in which the aryl group and R substituent are *anti* is the most favored one to minimize steric repulsion. After that, β -elimination affords the olefin with *E* configuration. Next, the acidic palladium hydride **F** reacts with a base to regenerate the $\text{Pd}(0)$ catalyst (Scheme 3).

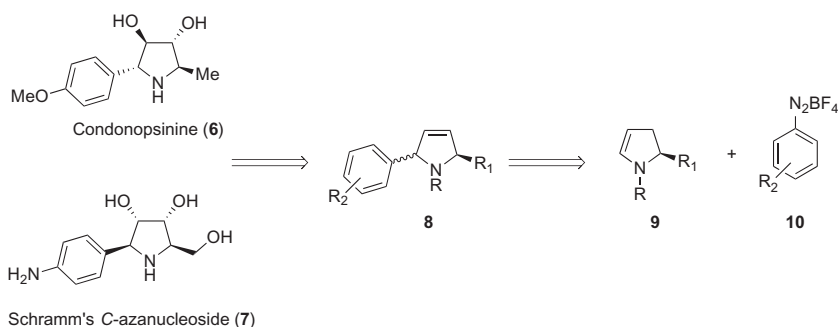
As the Heck–Matsuda reaction does not require the use of phosphanes, the cationic palladium species shown in the catalytic cycle (Scheme 3) are stabilized only by weak ligands such as the solvent or by the base. This fact led us to realize that we could modulate and control the reactivity of the palladium species by substrates possessing chelating groups such as the carbonyl groups. Indeed, this approach has been very productive in the development of new and efficient methodologies for the stereoselective arylation of olefins under mild reaction conditions.^{11–14} Inspired by the seminal review of Evans *et al.*, we described these reactions as the *Substrate-Directed Heck–Matsuda Reaction*. This term is defined as a preassociative interaction of the reagent with polar functional groups neighboring the reaction center that directly influence the stereoselectivity of the overall process.¹⁵

2 SUBSTRATE-DIRECTED HECK–MATSUDA REACTION

2.1 Some Preliminary Results

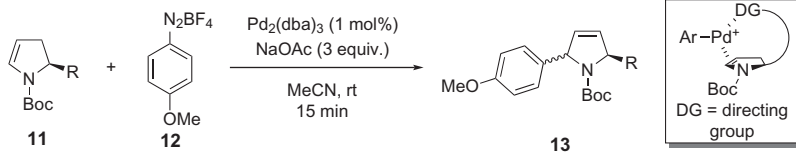
We reported our first results with the Heck–Matsuda reaction in the late 1990s for the arylation of chiral, nonracemic, endocyclic enecarbamates **9** to produce the aryl pyrrolidines **8**.¹⁶ These interesting intermediates were further applied in the total synthesis of several fully substituted *N*-heterocycles with pharmacologically active compounds such as the antibiotic and hypertensive pyrrolidine alkaloid codonopsin **6**, and the antitrypanosomal Schramm's *C*-azanucleoside **7** (Scheme 4).¹⁷

The initial objective in these early studies was the synthesis of the *trans*-substituted aryl pyrrolidines. Therefore, the Heck–Matsuda reactions were

**SCHEME 4** Heck–Matsuda reaction of endocyclic enecarbamates.**TABLE 1** Stereoselective Heck–Matsuda with the Enecarbamate **11**

Entry	R	Conditions	<i>trans/cis</i> ratio	Yield (%)
1	CO ₂ Me (11a)	Pd(OAc) ₂ (10 mol%) 2,6-Di- <i>t</i> -butyl-4-methylpyridine EtOH, 55 °C, 10 min	88/12	85
2	CO ₂ Me (11a)	Pd ₂ (dba) ₃ (1 mol%) NaOAc (3 equiv.) MeCN, rt, 5 min	90/10	95
3	Boc (11c)	Pd ₂ (dba) ₃ (1 mol%) NaOAc (3 equiv.) MeCN, rt, 15 min	90/10	96

performed with the high hindered enecarbamate **11** substituted at C₅ with a trityl ether. The first reported reaction was carried out in methanol at 55 °C with 10 mol% of Pd(OAc)₂ as the catalyst and 2,6-di-*t*-butyl-4-methylpyridine as the base to provide the Heck adduct in 85% yield with a stereoselectivity of 88/12 in favor of the desired *trans* isomer (Table 1, entry 1).¹⁶ The conditions were further optimized, and the palladium source, the base, and the solvent were replaced, respectively, by Pd₂(dba)₃, NaOAc, and MeCN (Table 1, entry 2).¹⁷ Although this new methodology increased the yield to 95%, the stereoselectivity was almost the same. To check if the size of the protective group on the nitrogen would exercise any stereocontrol, the carbomethoxy

TABLE 2 The Influence of the Directing Group in the Arylation of **11**


Entry	R	<i>trans</i> / <i>cis</i> ratio	Yield (%)
1	CH ₂ OTr (11c)	90/10	96
2	CO ₂ Me (11d)	86/14	90
3	CON(Me)OMe (11e)	49/51	92
4	CH ₂ OH (11f)	42/58	95

group was replaced by a more hindered Boc group, but the same levels of stereocontrol were observed (Table 1, entry 3).¹⁸ For this reason, the reaction conditions shown in entry 2 were chosen as the best for the arylation of **11**.

However, replacement of the trityl ether by coordinating groups, such as esters and alcohols, led to considerable decrease in the stereoselectivity of the Heck arylation (Table 2). These results were rationalized as a consequence of a preassociative interaction of the directing groups (DGs) with the cationic aryl-palladium species leading to an increase in the *cis* isomer. As shown in Table 2, the electronic nature of the groups had significant influence on the stereoselectivity of the reaction. With the coordinating methyl ester (**11d**), a slight increment in favor of the *cis* isomer was observed (Table 2, entries 1 and 2). Moreover, more electron-rich groups such as the Weinreb amide (**11e**) or the hydroxymethyl (**11f**) made the reaction completely unselective (Table 2, entry 3) or slightly favoring the *cis* isomer (Table 2, entry 4). These intriguing results were actually our first contact with this potentially useful strategy to direct the Heck–Matsuda reaction.

3 DEVELOPMENT AND SYNTHETIC APPLICATIONS OF THE SUBSTRATE-DIRECTED HECK–MATSUDA REACTION

3.1 Stereoselective Arylation of Allylic Esters


Allylic esters are among the most versatile substrate in organic synthesis. They are popular substrates for many transition metal-catalyzed reactions, such as dihydroxylation, the Tsuji–Trost reaction, hydrogenation, and isomerization, *inter alia*.¹⁹ In this context, the Heck arylation can be considered a privileged reaction for the formation of such esters in a regio- and stereoselective way. However, this transformation has been a challenging one due to the

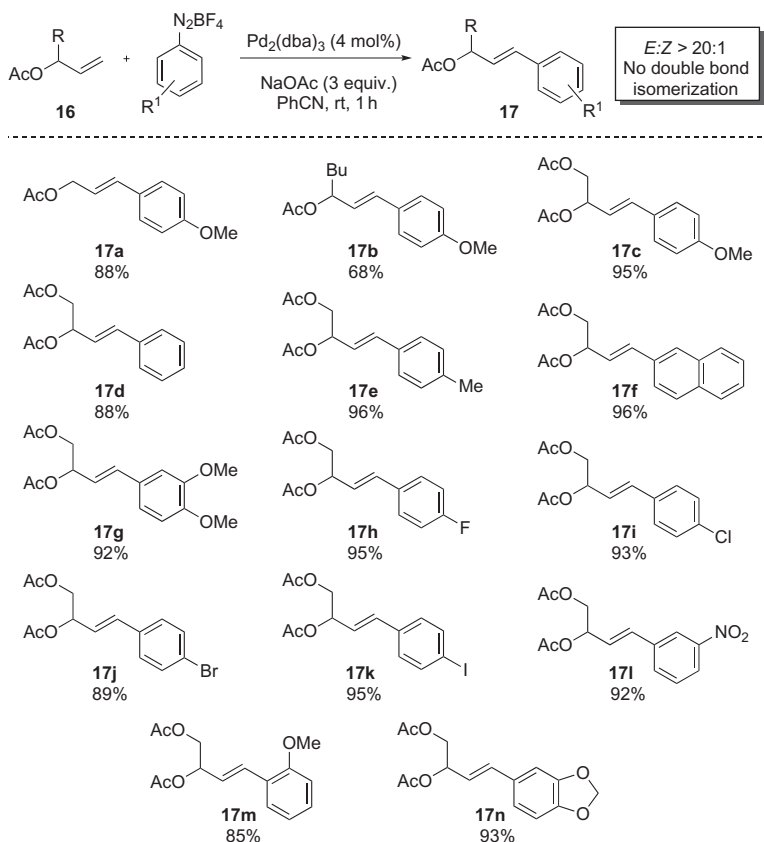
low chemo-, regio-, and stereoselectivities displayed in the process. A glimpse of the most general methodologies for the *E*-selective γ -arylation of allylic esters is shown in Table 3. The regioselectivity does not seem to be a major issue, but a careful analysis indicates that the reaction conditions are usually harsh, requiring high temperatures, somewhat long reaction times, and stoichiometric amounts of additives (Table 3).^{20–22}

Faced with this scenario, we decided to investigate the Heck arylation of allylic esters with diazonium salts to make it a more practical transformation. In 2009, we then described the arylation of allylic esters with aryldiazonium salts using $\text{Pd}_2(\text{dba})_3$ (4 mol%) as catalyst, NaOAc (3 equiv.) as base, and benzonitrile as solvent (Scheme 5).¹¹ These reactions were carried out at room temperature for only 1 h in an open flask. To our satisfaction, all products were obtained with almost perfect regio- and stereocontrol in favor of the *E*-cinnamyl acetates **17**. It is worth pointing out that in all cases double-bond isomerization or OAc elimination was not observed. The isolated yields were excellent, including for those reactions using aryldiazonium salts containing halides (**17i–k**), which are also likely to promote competitive Heck reactions. Electron deficient (**17l**) as well as *ortho* substituents (**17m**) were well tolerated. These results make this methodology one of the mildest alternatives for the stereoselective Heck arylation of allylic esters (Scheme 5). The library of products obtained constitutes potential substrates for organic synthesis.

The proposed general catalytic cycle for this reaction encompasses a mix of conventional intermediates with unconventional ones. The process presumably starts with the oxidative addition of the aryldiazonium salt to produce the cationic aryl palladium **B**. As the substrate has two coordinating

TABLE 3 Stereoselective Arylation of Allylic Acetates

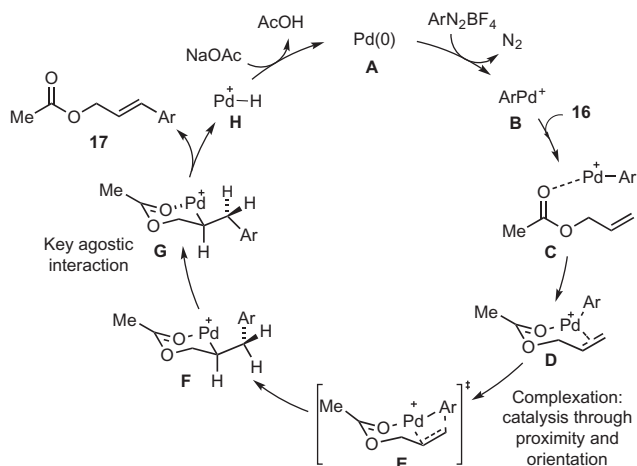
					
Entry	Group (year)	X	Conditions	Selectivities	Yields (%)
1	Jiao (2008)	I	$\text{Pd}(\text{OAc})_2$ (2.5 mol%), Ag_2CO_3 (0.6 equiv.), benzene, reflux, 10 h	>20:1	55–94
2	Jiao (2009)	$\text{B}(\text{OR})_2$	$\text{Pd}(\text{OAc})_2$ (5 mol%), AgOAc (2 equiv.), CuF_2 (2 equiv.), KHF_2 (2 equiv.), acetone, 85 °C, 5 h	6:1 to >20:1	37–92
3	Deng (2012)	$\text{B}(\text{OH})_2$	$\text{Pd}(\text{OAc})_2$ (10 mol%), $(n\text{-Bu})_4\text{NCl}$ (1.5 equiv.), KH_2PO_4 (2 equiv.), DMF, 120 °C, 6–16 h	>20:1	54–84



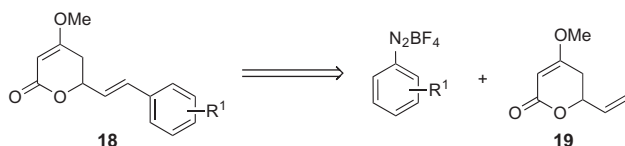
SCHEME 5 Regio- and stereoselective arylation of allyl acetates.

sites in close proximity, the cationic aryl-palladium ends up forming a complex (**Scheme 6**), which undergoes the carbopalladation through transition structure **E**, thus transferring the aryl group to the terminal carbon while the cationic palladium gets involved in a six-membered oxapalladacycle as in **F**. This structure restricts the conformational mobility of the intermediate and precludes the possibility of double-bond migration because the only hydrogens that can undergo a *syn*- β -elimination are the ones presented at the newly created benzylic carbon. For steric reasons, the conformer **G** is the one most favored to undergo β -elimination, thus providing the *E*-cinnamyl acetate **17**. The resulting palladium hydride **H** is consumed by the NaOAc to regenerate the Pd(0) catalyst, which restarts the catalytic cycle (**Scheme 6**).

This synthetic strategy brings into account interesting aspects of the Heck–Matsuda arylations. As it does not rely on external ligands, the substrates behave as such, not only stabilizing the cationic δ -aryl-palladium complex but also providing structural bias that controls the regio- and stereoselectivity



SCHEME 6 Proposed catalytic cycle for the Heck–Matsuda reaction with allyl acetates.

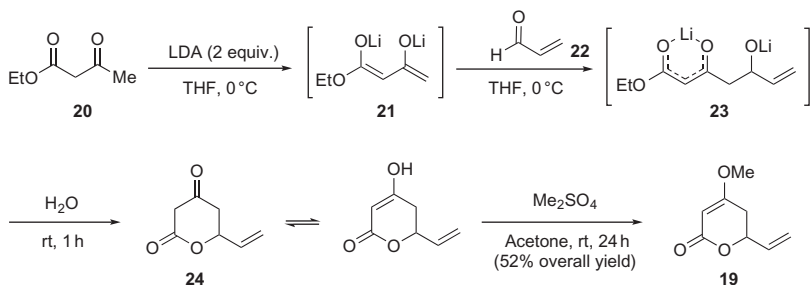
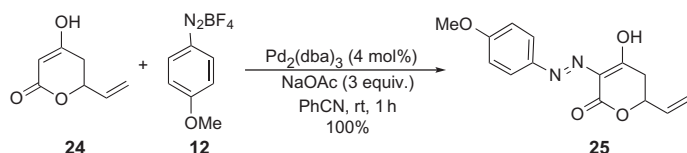
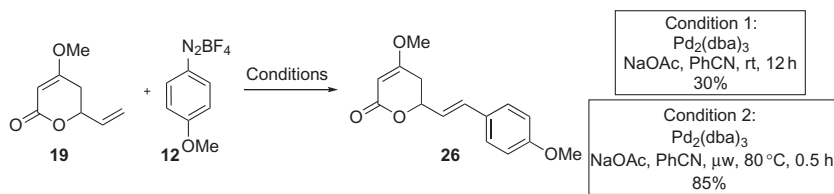


SCHEME 7 Retrosynthetic analyses for the synthesis of structure 18.

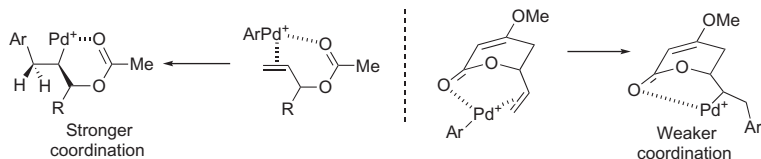
of the overall process. This principle has been an important aspect of many Heck–Matsuda reactions of bi- and multifunctional substrates, as will also be illustrated in the examples below.

Once we realized that the substrate-directed arylation strategy could promote a rapid increase in the structural complexity of the allylic acetates, we decided to apply it in the total synthesis of biologically active kavalactones, represented by compound 18 in Scheme 7. The key step would be the stereoselective arylation of the substrate 19, which would lead us directly to the core skeleton of these natural products.

The synthesis of the vinyl-substituted lactone 19 started with the reaction of ethylacetoacetate 20 with 2 equiv. of LDA. The interesting bis-enolate 21 was then trapped with freshly distilled acrolein 22 to produce the intermediate 23. The regioselectivity of this reaction can be explained by product development control, because this intermediate retains the more stable conjugated enolate. Upon hydrolyses, intermediate 23 spontaneously cyclizes to the β-keto lactone 24, whose enol tautomer underwent direct O-alkylation with dimethyl sulfate. This sequence could be carried out in multigram scale with isolated overall yields of 52% (Scheme 8).

SCHEME 8 Synthesis of the lactone **19**.SCHEME 9 Japp-Klingemann reaction of the enol from **24**.

Pd complexation with cyclic and acyclic allyl acetates:

SCHEME 10 Heck-Matsuda reaction with **19**.

It should be mentioned that O-methylation of the ketone in **24** was necessary to avoid competition between the Heck-Matsuda arylation and the nucleophilic addition of the enol to the aryldiazonium salt, a process known as the Japp-Klingemann reaction. Indeed, when **24** was submitted to the standard Heck-Matsuda reaction conditions, the azo compound **25** was obtained in quantitative yield (Scheme 9). Azo compounds are easily detected due to the formation of highly colored products via this reaction.

Preliminary attempts to perform the Heck-Matsuda arylation of **19** with the aryldiazonium salt **12** led to a 30% yield of the desired styrenyl lactone **26** after 12 h at room temperature (Scheme 10). After some optimization,

we found out that heating under microwave conditions (80 °C) could increase the yield of **26** to 85%. The unexpected lower reactivity of olefin **19** under standard conditions can be explained by the conformational restriction of the allylic acetate moiety present in the structure that hinders the directing ability of the carbonyl to the cationic aryl palladium during the carbopalladation step (Scheme 10).

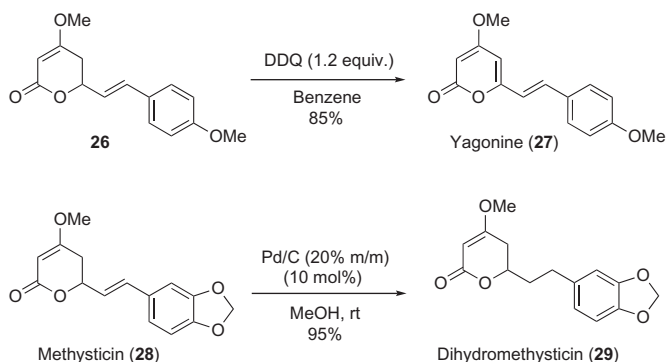
These substrate-directed Heck reactions allowed the synthesis of pharmacologically active compounds in a very straightforward way. For example, compound **26** was oxidized with DDQ to provide the natural product yagonine **27**. Additionally, methysticin **28** was obtained in 59% yield (95% based on recovered starting material) directly from the Heck–Matsuda reaction. The chemoselective reduction of the least hindered double bond of **28**, using Pd/C as catalyst, provided dehydromethysticine **29** in 95% yield (Scheme 11).

These reports were the first to describe the use of this type of strategy. The mild reaction conditions and the rapid increase in the structural complexity allowed the synthesis of bioactive natural products in a straightforward way.¹¹

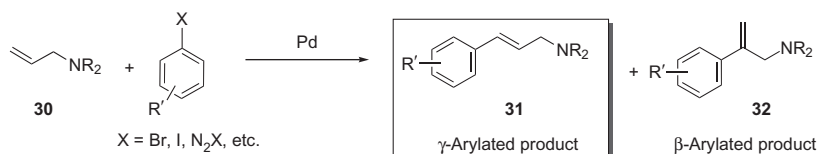
3.2 Stereoselective Arylation of *N*-Protected Allylic Amine Derivatives

γ -Arylated allylic amines, represented here by compound **31**, are common structural motifs in many pharmacological active molecules, such as the CP-724-714 (**33**), used for the treatment of ovarian cancer, and flunarizine **34**, which is used to reduce headache frequency in both adults and children (Scheme 12). Because both the β - and γ -regioisomers are usually obtained through conventional Heck arylations, the regioselective arylation of allyl amines has become a challenging transformation in the last few years.

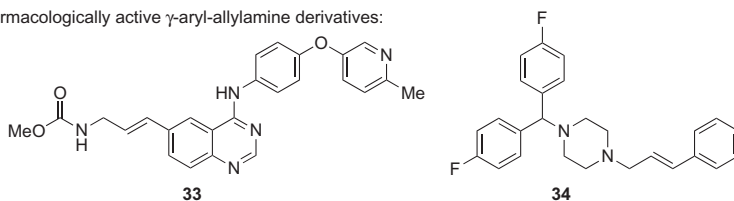
A common strategy to control the regioselectivity of the Heck reaction of an unactivated (alkyl-substituted) olefin is to select the type of mechanism under which the Heck reaction will be operating. With aryl halides, after oxidative addition the halogen atom stays bonded to palladium and the Heck



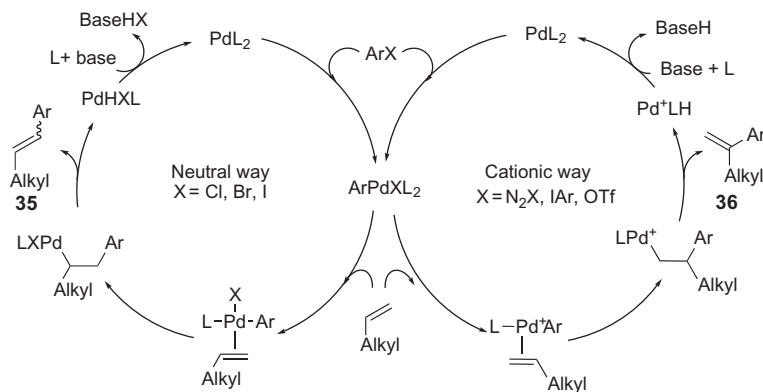
SCHEME 11 Synthesis of biologically active kavalactones.



Pharmacologically active γ -aryl-allylamine derivatives:



SCHEME 12 γ -Arylated allylic amines.

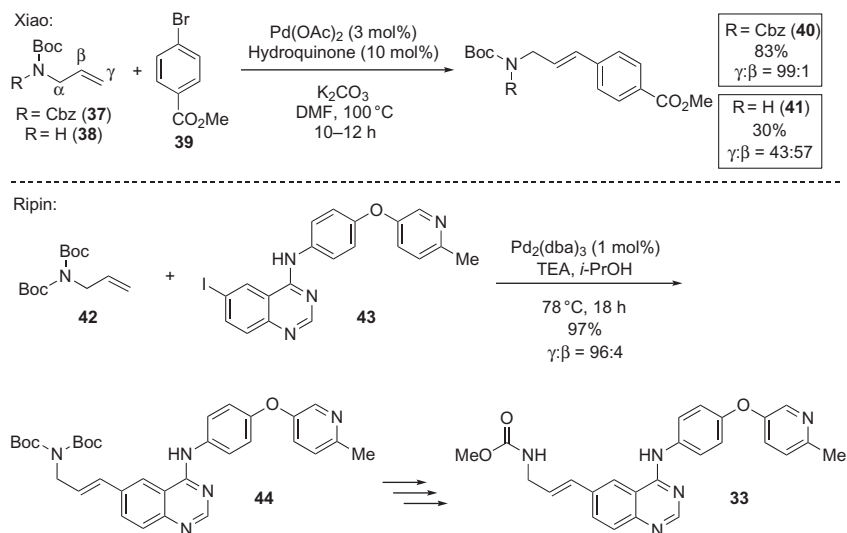


SCHEME 13 Heck mechanisms with unactivated olefins.

reaction follows a “neutral” pathway (Scheme 13). On the other hand, when the arylating partners (the electrophile) are aryldiazonium salts, iodonium salts, or aryl triflates, noncoordinating species or anions are generated after the oxidative addition step. Upon dissociation of those species, cationic organopalladium intermediates are formed and a polar mechanistic pathway will operate. In the neutral pathway, the carbopalladation step is usually controlled by steric factors, and the aryl group is normally transferred by less-hindered carbon of the olefin, yielding the 1,2-disubstituted Heck adduct **35**. As expected, for the cationic pathway some charge distribution is observed with palladium binding to the more nucleophilic carbon and the aryl group transferred to the more electrophilic one—the internal carbon. This regioselectivity can also be explained by a better stabilization of the partial positive charge developed during carbopalladation by the more substituted carbon (Scheme 13).

In spite of the similarity between allylic esters, amides, and carbamates, their reactivities in palladium-catalyzed reactions are distinct. For instance, allylamine derivatives are unsuitable substrates for the Tsuji–Trost reaction and the somewhat bulky *N*-substituted derivatives have very limited complexation capabilities toward the metal. Therefore, the arylation of these compounds via Heck reactions follows two major strategies: (i) the use of *N*-substituted allyl amides/carbamates in a neutral pathway to obtain the γ -arylated product; or (ii) the application of the cationic pathway to achieve the synthesis of the β -arylated isomer. For example, Xiao⁶ reported the γ -selective arylation of *N*-substituted allylcarbamates **37** in high yields using Pd(OAc)₂/hydroquinone. However, when the unsubstituted carbamate **38** was the substrate, the Heck product was obtained in only 30% yield and the regioselectivity was insignificant. Another very interesting result was obtained by Ripin and coworkers during the total synthesis of the CP-724-714 (**33**).²³ The Heck reaction between the *N,N*-Boc-allylamine **42** and the aryl iodide **43** furnished the γ -arylated product **44** in high yield and regioselectivity. The authors pointed out that the two Boc groups were essential to obtain the desired regioselectivity (Scheme 14).

While aryl halides are the substrates of choice for the neutral Heck arylations of allylamine derivatives, aryl triflates are the most used for the cationic mode. However, as oxidative addition of Pd(0) to aryl triflates is usually slower than that with aryl bromides and iodides, bidentate ligands are commonly used to increase the stability and nucleophilicity of the Pd(0) catalyst, thus preventing the formation of “Pd black” (an inactive form of Pd(0)).

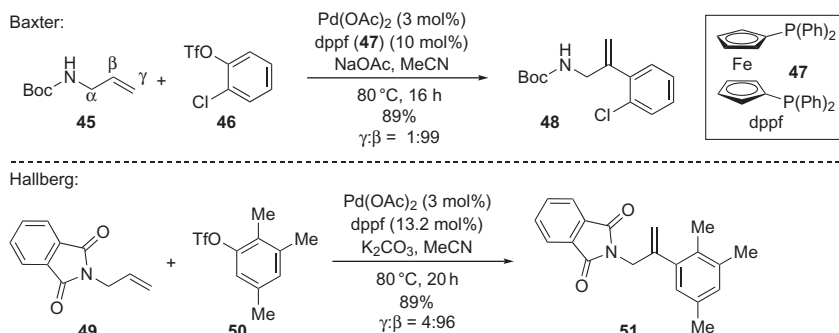


SCHEME 14 Arylation of allylamine derivatives under neutral conditions.

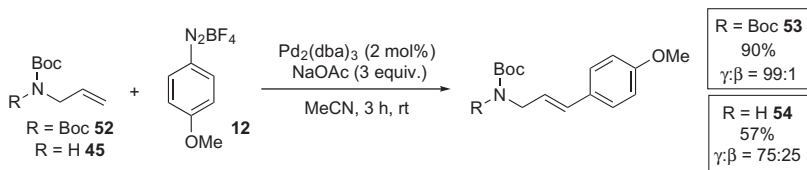
Furthermore, bidentate ligands preclude the anchimeric assistance of the coordinating groups because during carbopalladation all four coordinating sites of the Pd(II) are occupied. As a result of the cationic mechanism, the β -arylated products are the major Heck adduct when using aryl triflates. This strategy was successfully applied by Baxter and Hallberg for the arylation of the *N*-Boc-allylamine **45**²⁴ and the *N*-allylphthalimide **49**,²⁵ respectively. In both cases, the catalytic system employed consisted of Pd(OAc)₂ and the ligand dppf [1,10-bis(diphenylphosphino)ferrocene] (**47**) (Scheme 15). It is worth pointing out that high β -selectivity was observed in both cases.

These results pose some interesting questions concerning the development of a general method for the synthesis of γ -arylated allylamine derivatives using aryldiazonium salts. Could this reaction be applied for the regioselective arylation of both *N*-substituted or *N,N*-disubstituted allyl amine substrates? Although Cacchi and coworkers had demonstrated that this reaction was indeed possible, a major limitation of their methodology was the use of *N,N*-protected allylamines to obtain the desired γ -arylated product **53** (Scheme 16). Indeed, when the monoprotected allylamine **45** was used as substrate, a mixture of the β and γ isomers was obtained in a 75:25 ratio. These results indicate that besides the operation of a cationic mechanism, the regioselectivities can also be governed by steric effects.²⁶

In spite of this unfavorable scenario, we were able to demonstrate that a wide range of *N*-substituted allylamines could be arylated in a regioselective



SCHEME 15 Arylation of *N*-substituted allylamine under cationic conditions.



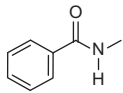
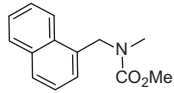
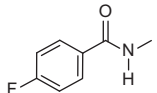
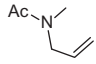
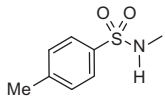
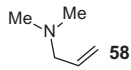
SCHEME 16 Cacchi's methodology.

fashion using conditions similar to those applied for the allylic acetates (Scheme 5). The substrate-directable Heck–Matsuda reaction was successfully applied to the arylation of both *N*-mono and disubstituted substrates, as can be seen in Table 4. All reactions were carried out at room temperature, using 1.2 equiv. of the olefin and 4 mol% of Pd₂(dba)₃. The regioselectivity was very high for all examples, including for allyl formamide (entry 5), the smallest possible *N*-substituted amide derivative. This last result strongly indicated that the regiocontrol derives from direction by the carbonyl group, and not from the steric hindrance of the nitrogen substituents. Amines proved unreactive, probably because they inactivated the Pd catalyst. For example, substrate **58** was inert under the standard conditions (entry 14). Finally, the γ -isomer with a *Z* configuration was observed only in a few cases in very small amounts.

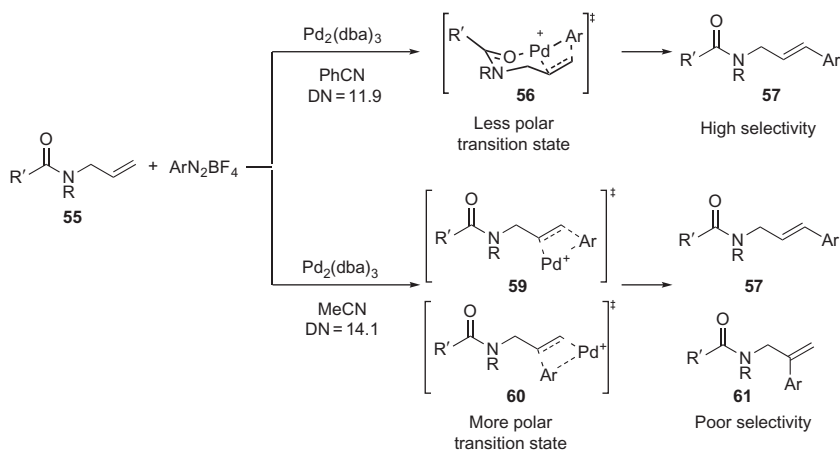
An interesting observation in this process concerns the influence of the solvent. We used benzonitrile as the solvent, whereas Cacchi's method uses acetonitrile. With benzonitrile electronic factors rule the selectivity, while with acetonitrile the steric aspects seem to predominate. A plausible explanation is based on the difference of polarity between the two solvents as well as their donicity number (a tendency of the solvent to interact with a Lewis acid).²⁷ As acetonitrile is more polar than the benzonitrile, transition states without the interaction between the palladium and the carbonyl such as **59** and **60** are favored. The opposite phenomenon is expected for the benzonitrile, with its lower donicity. The cationic palladium intermediate is internally solvated by the carbonyl oxygen, thus favoring the cyclic intermediate. With decreased solvation of the cationic palladium, a closer contact of the carbonyl moiety to the metal is facilitated (Scheme 17). These data suggest that these parameters explain the key role of the benzonitrile in the Heck–Matsuda reaction.

To further demonstrate the utility of the Heck–Matsuda reaction with allylamine derivatives, we carried out concise total syntheses of several biologically active molecules. As part of our philosophy, a synthesis should be accomplished in a practical manner using straightforward routes under mild reaction conditions. Our first target, the antifungal naftifine **68**, was obtained in four steps in 53% overall yield (Scheme 18). The initial steps were the alkylation of allylamine **62** with 1-(chloromethyl)naphthalene **63** and the protection of the newly formed secondary amine with methyl chloroformate to furnish **65** with 96% yield in each step. The carbamate **65** was then applied in the key Heck–Matsuda reaction using phenyldiazonium tetrafluoroborate to provide the unsaturated carbamate **67** in 85% yield with both regio- and stereocontrol greater than 95:5. Due to the bulkiness of the *N*-substituents, the reaction was slow at room temperature, but it could be carried out in 1 h at 80 °C. Finally, reduction of the carbamate moiety with LiAlH₄ yielded the desired naftifine **68** in 87% yield.

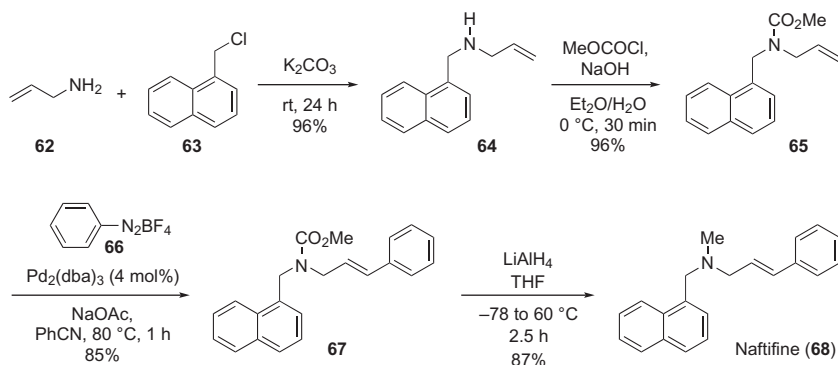
For the total synthesis of the phytohormones abamine (**75**) and abamine SG (**77**), the amide **70**, obtained from 4-fluorobenzoic acid **69**, was arylated

9		1 (60%), >95:5	12		1 (85%), >95:5
10		7 (72–95%), >95:5	13		2 (60–85%), >95:5
11		4 (63–98%), >93:7	14		1 (–)

^aWhen present, the *Z* isomer of the γ -arylated Heck adduct was observed in very small amounts (<5%).



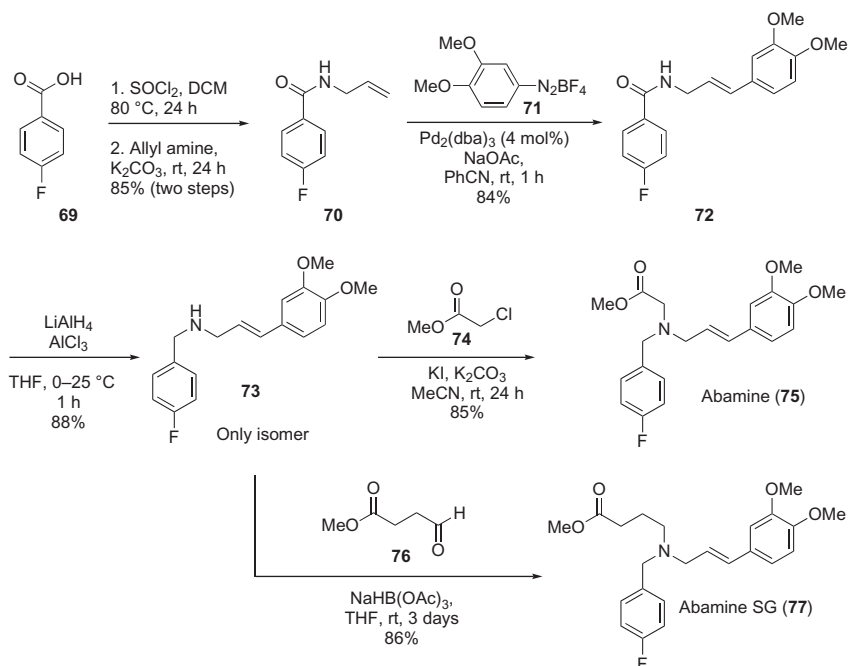
SCHEME 17 The role of benzonitrile and acetonitrile in the Heck–Matsuda reaction.



SCHEME 18 Total synthesis of the antifungal naftifine (**68**).

with the electron-rich aryldiazonium salt **71** with total selectivity in favor of the *E* product in 85% yield (Scheme 19). Next, reduction of the amide group was accomplished in 88% yield by alane (AlH_3 , generated *in situ*) prepared using AlCl_3 and 3 equiv. of LiAlH_4 . The secondary amine **73** was used as a common precursor of abamine (**75**) and abamine SG (**77**). In the first case, the total synthesis was finished by a Finkelstein-like $\text{S}_{\text{N}}2$ reaction between **73** and methyl 2-chloroacetate **74**, whereas reductive amination of amine **73** and methyl 4-oxobutanoate **76** was performed to conclude the synthesis of abamine SG **77**.

Cinacalcet (**85**) is an orally active drug that decreases the secretion of the parathyroid hormone, and for this reason, it is indicated for the treatment of hypercalcemia.²³ For its total synthesis, we started with the alkylation of the

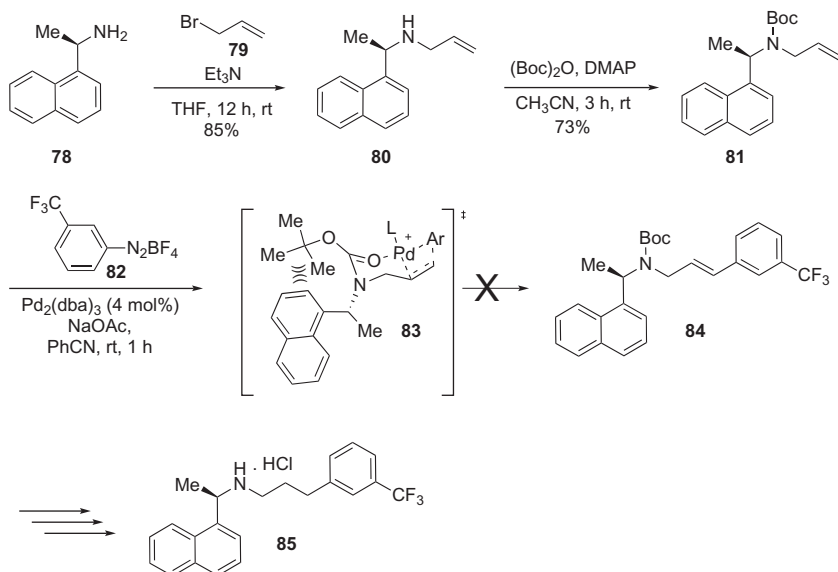


SCHEME 19 Total synthesis of the abamines.

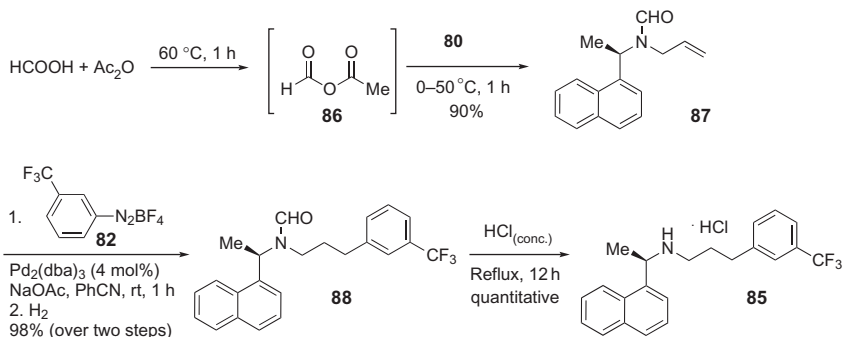
enantiopure amine **78** with allyl bromide (**79**), followed by protection of the secondary amine **80** with $(\text{Boc})_2\text{O}$. Despite the good yields for these steps, the Heck–Matsuda reaction with **81** was totally ineffective for the synthesis of **84**, only the starting material being recovered (Scheme 20). A plausible explanation is the steric hindrance of both the naphthyl ring and the *tert*-butyl groups, preventing the formation of the pivotal cyclic transition state **83** during the carbopalladation step (Scheme 20).

To circumvent this steric problem, the Boc group was replaced by a formyl group, which was installed on amine **80** by the *in situ* generated mixed anhydride **86** (Scheme 22). The newly formed formamide **87** was successfully used for the Heck–Matsuda reaction. This was followed by a reduction of the styrenic double bond by simply adding a balloon of hydrogen to the reaction flask (98% yield over two steps). Next, the *N*-formyl moiety of **88** was hydrolyzed in concentrated HCl to furnish cinacalcet hydrochloride in quantitative yield.

Finally, for the synthesis of the muscle relaxant alverine (**91**), *N*-acetyl-diallylamine **89** was successfully applied in a double Heck–Matsuda reaction, followed by *in situ* hydrogenation to give secondary amide **90** in 72% yield over two steps (Scheme 21). Next, reduction of the carbonyl amide with AlH_3 furnished the alverine (**91**) in 96% yield. It is worth pointing out



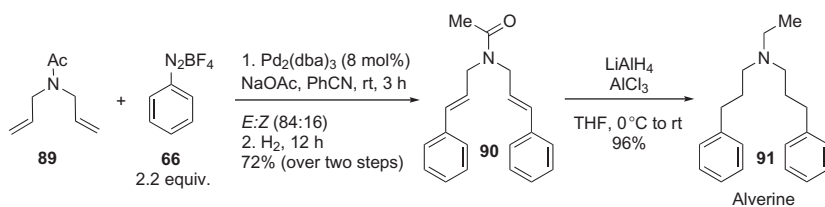
SCHEME 20 Initial attempts of the total synthesis of the cinacalcet.



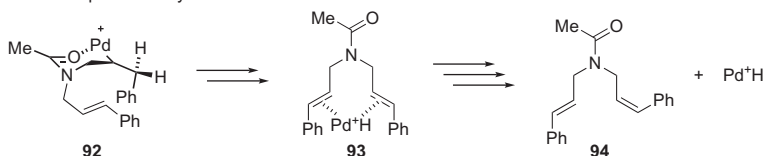
SCHEME 21 Total synthesis of cinacalcet (**85**).

that besides the perfect regiocontrol, the *E*:*Z* ratio (84:16) of this Heck–Matsuda reaction was the worst among all the examples with allylamine derivatives evaluated so far. As for the formation of the *Z* isomer **94**, it likely occurs by a reinsertion of the palladium hydride to the previously formed *E* product. This process might be favored by an intramolecular transfer of the palladium hydride after the β -elimination and before its decomplexation from the Heck adduct **93** (Scheme 22).

In summary, the stereoselective arylation of allylamine derivatives was accomplished by a substrate-directed Heck–Matsuda strategy. The data we obtained from these studies suggest that the origin for the regiocontrol in favor



Intramolecular palladium hydride transfer:



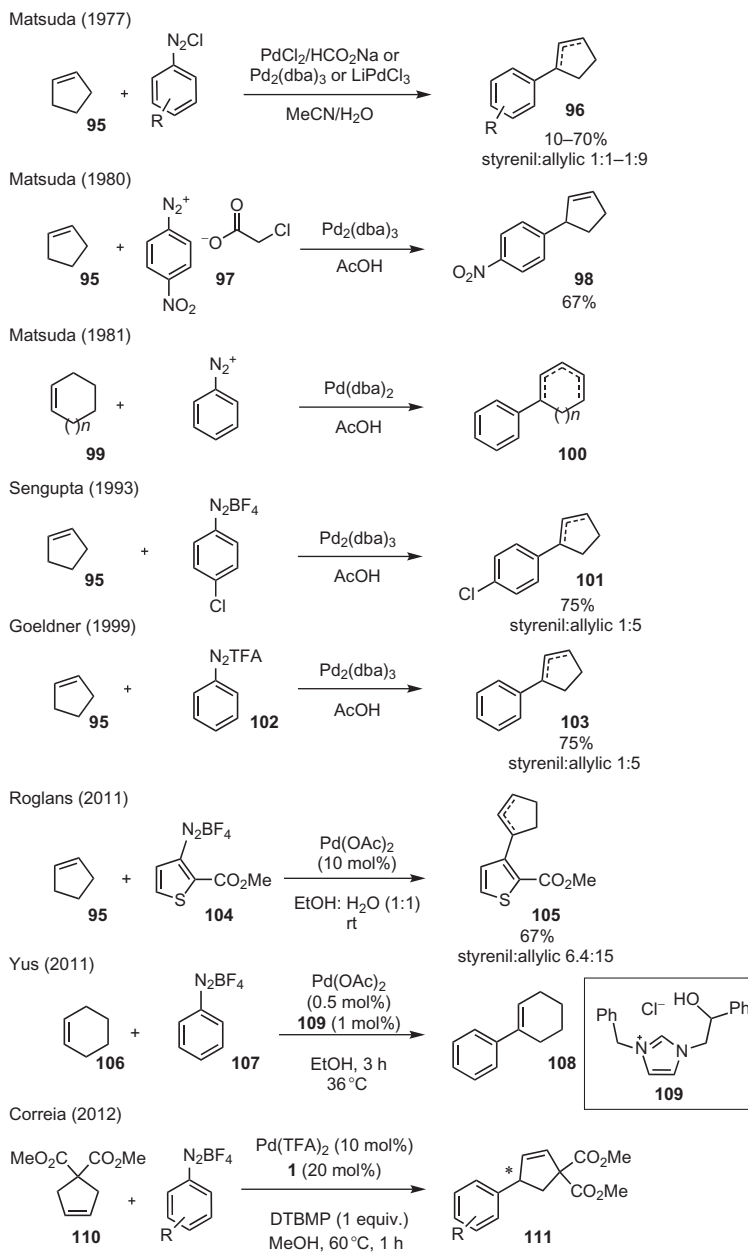
SCHEME 22 Total synthesis of the alverine (**91**).

of the γ -arylation resides in the chelation of a carbonyl moiety in the substrates with the cationic δ -aryl-palladium species. Additionally, the steric hindrance of the substituents does not seem to have strong influence on the regioselectivity of the arylating process as mono *N*-substituted amides and carbamates were successfully arylated. Finally, aryldiazonium salts with both electron-donating or -withdrawing groups could be used, as demonstrated in the total synthesis of the biologically active compounds naftifine (**68**), abamine (**75**), abamine SG (**77**), cinacalcet hydrochloride (**85**), and alverine (**91**).^{12,14}

3.3 Stereoselective Arylation of Cyclopentene Scaffolds

The Heck reaction of nonconjugated cycloalkenes is a topic of great interest in organic synthesis, not only because aryl cycloalkanes are common structural motifs in natural products or bioactive compounds, but also because they are challenging targets.²⁸ In the case of the Heck–Matsuda reaction, cycloalkenes have been used as substrates, but a complex mixture of the styrenil and allylic products is often observed (Scheme 23).^{3,29–34} When in 2012 our group reported the enantioselective arylation of the dimethylcyclopentenedicarboxylate **110**,⁵ there were only two examples of the selective arylations: one reported in 1980 by Matsuda favoring the allylic product using the aryldiazonium chloroacetate salt **97**,²⁹ and another reported recently by Yus for the synthesis of the styrenil product **108** in the presence of the *N*-heterocyclic carbene **109**.³⁴

We realized that DGs could be attached to cyclopentenes to control the stereoselectivity of the process, thus allowing the syntheses of fully functionalized arylcyclopentenes. To evaluate this concept, we first chose the readily available olefins **112** and **113** as substrates for the substrate-directed Heck–Matsuda reaction. The presence of two potential DGs posed interesting questions concerning the facial selectivity of the Heck–Matsuda reaction (Scheme 24).

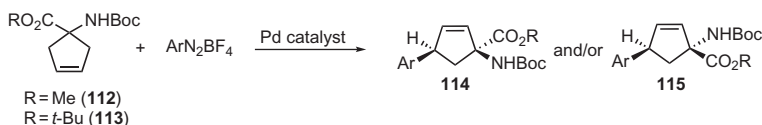


SCHEME 23 Overview of the Heck–Matsuda reaction with cyclic olefins. Asterisk in compound **111** indicates the presence of a stereogenic center of unknown absolute configuration.

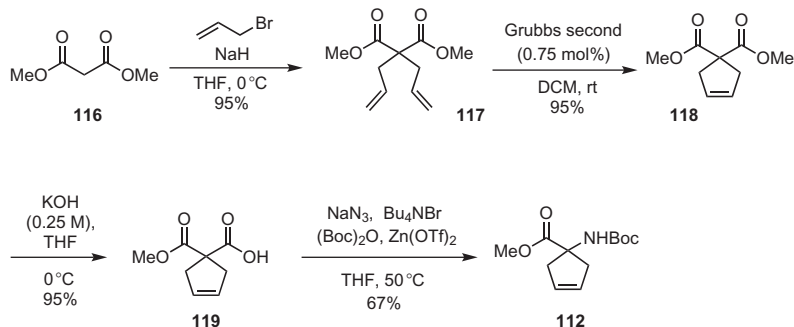
A 60 g synthesis of the starting material **112** began with the double alkylation of the dimethyl malonate (**116**) with allyl bromide (**79**), followed by ring-closing metathesis catalyzed by 0.75 mol% of the Grubbs catalyst (second generation) in 95% yield for each step (Scheme 25). Next, the critical monohydrolysis of diester **118** was carried out by the addition of a cold solution of KOH into a solution of **118** in THF. A strict control of the temperature was very important during the hydrolysis process to avoid the formation of the corresponding diacid. Finally, Curtius degradation of acid **119** was achieved by the one-pot methodology developed by Lebel, providing the desired carbamate **112** in 67% yield.³⁵

The mechanism proposed for the Curtius degradation starts with the activation of carboxylic acid **119** by the (Boc)₂O, catalyzed by Zn(OTf)₂, to generate carbonic anhydride **120**, which is attacked by the azide ion to provide the unstable acyl azide **121** and sodium *t*-butoxide as a byproduct (Scheme 26). Next, isocyanate **122** is obtained by the decomposition of intermediate **121** with extrusion of N₂. Reaction with sodium *t*-butoxide provides the desired carbamate **112**.

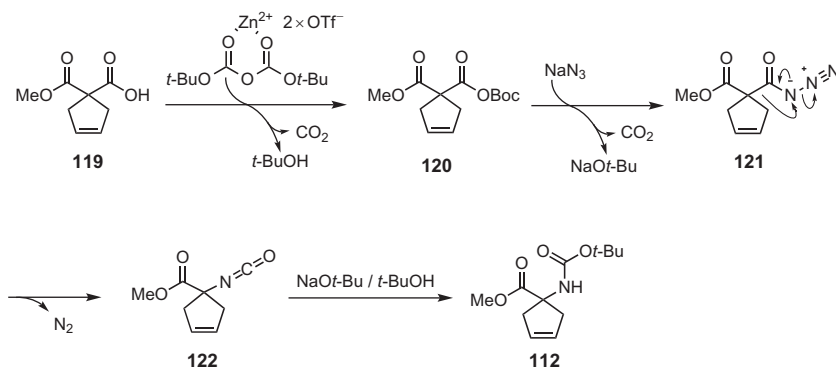
With the starting olefins in hand, the initial attempts for the substrate-directed Heck–Matsuda reaction were performed under conditions similar to those applied for the arylation of allylic esters (1.2 equiv. of the aryldiazonium salt). Disappointingly, the desired product **123a** was obtained in less than 10% yield, together with 38% yield of the isomerized starting material **124**. Gratifyingly, when olefin **112** was used in slight excess, the



SCHEME 24 Heck–Matsuda reaction of cyclic olefins **112** and **113**.



SCHEME 25 Synthesis of the carbamate **112**.



SCHEME 26 Mechanistic proposal for the Curtius degradation.

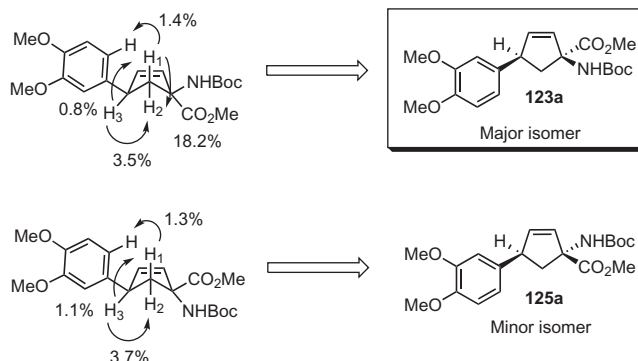
TABLE 5 Synthesis of the Arylcyclopentene **123a**

Entry	112 (equiv.)	71 (equiv.)	123a Yield (%)	124 Yield (%)
1	1	1.2	>10	38
2	1.2	1	90	<5

arylcyclopentene **123a** was isolated in 90% yield in a diastereomeric ratio of 87/13 with almost total suppression of isomerization of olefin **112** (Table 5).

The relative stereochemistry of compounds *syn*-**123a** (with respect to the *t*-butoxy carbamate) and *anti*-**123a** were assigned by NMR using nuclear Overhauser effect (NOE) experiments of the isolated diastereoisomers (Scheme 27). Irradiation of H_1 (*syn* to the NHBoc group) of the major isomer led to a 1.4% NOE enhancement of the *ortho* aromatic hydrogens. Furthermore, irradiation of the benzylic hydrogen (H_3) induced an NOE increment of 0.8% in H_1 and 3.5% in H_2 , indicating a greater proximity between H_2 and H_3 . On the other hand, for the minor isomer the NOE enhancement between (H_1) and the *ortho* aromatic hydrogens was 1.3%, whereas irradiation of the benzylic hydrogen (H_3) induced an NOE enhancement of 1.1% in H_1 and 3.7% in H_2 . Precedents for this critical assignment of H_1 and H_2 in both isomers can be found in the literature, which indicate the hydrogen *syn* to the ester group as the more deshielded hydrogen.^{36,37}

Using the optimized conditions for the arylation of olefin **112**, the scope of the method was then evaluated with a number of aryldiazonium salts bearing

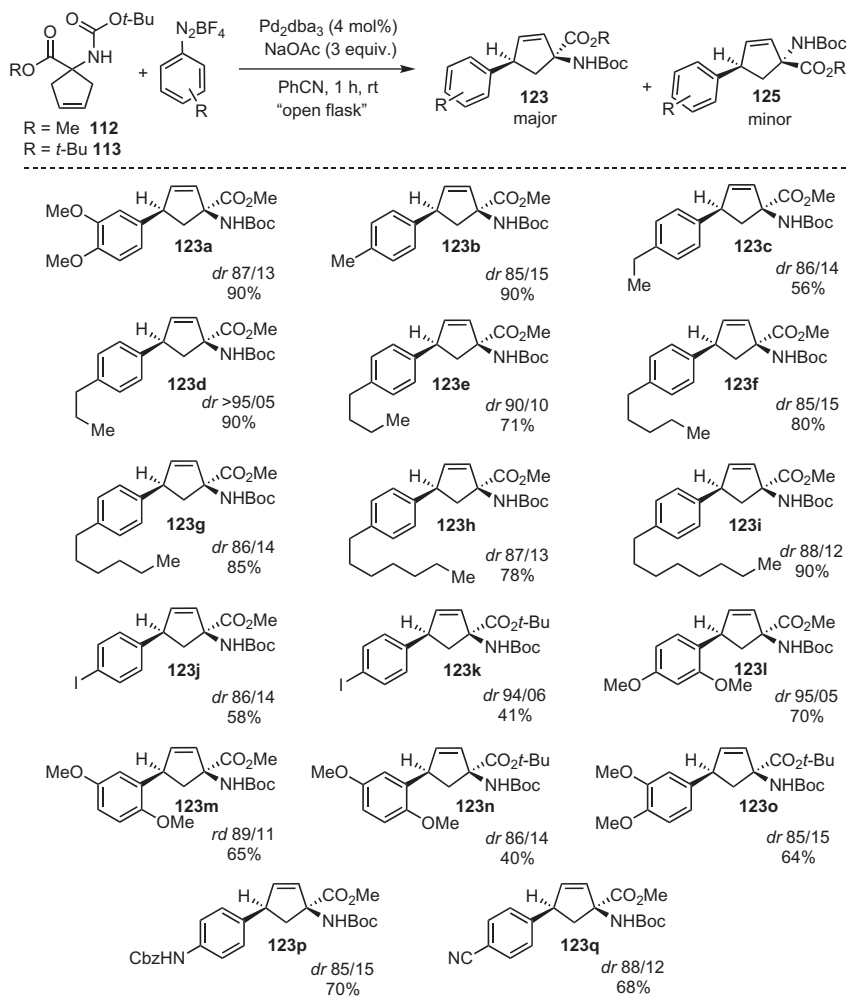


SCHEME 27 Assignment of the relative stereochemistry of *syn*- and *anti*-123a.

both an electron-rich (**123a–p**) or an electron-poor substituent (**123q**). In all instances, the Heck arylation gave the *syn* adduct as the main stereoisomer. Once again, the Heck–Matsuda reaction proved totally chemoselective when 4-iodobenzenediazonium tetrafluoroborate was applied (**123j,k**). The lower yields observed for the arylation of the more hindered olefin **113** can be explained as a result of the congestion created by geminal bulky groups, thus affecting the complexation of the cationic aryl palladium to the carbamate carbonyl group. Finally, aiming at future synthetic applications, the *p*-alkylaryl-substituted Heck products were obtained with good levels of stereochemical control (**123b–j**) (Scheme 28). An important detail observed during the development of this method was the physical condition of the base NaOAc. As this base has limited solubility in benzonitrile, it must be used as a fine powder to attain good yields in the Heck–Matsuda reactions.

A common feature of the Heck–Matsuda reactions involving cyclic unactivated olefins is the formation of mixtures of allylic and styrenil adducts due to isomerization of the double bond. It is worth pointing out that the potential Heck adduct **128** (Scheme 29) was not observed in any case. A possible explanation for this is the presence of a slight excess of starting olefin **112**, which might act as a scavenger of palladium hydride **126** to form intermediate **129**. This step would prevent palladium hydride transfer to the kinetic Heck adduct **114** onto its less-hindered face, *syn* to the ester group, resulting in the formation of **127**, which in turn would generate the styrenic isomer **128** after β -elimination. The less-hindered olefin **112** also acts as a more powerful Pd–H scavenger because of its more electron-rich carbamate carbonyl group (Scheme 29).

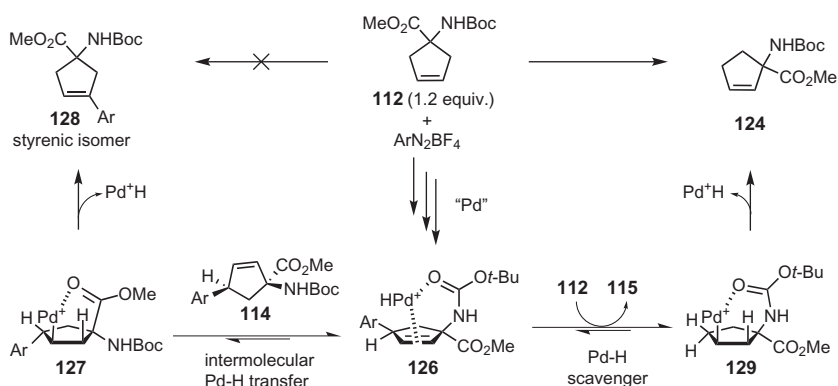
Based on these observations, a catalytic cycle was proposed starting with the oxidative addition of Pd(0) to the aryldiazonium salt to generate the cationic aryl-palladium intermediate **B**, which complexes preferentially to the more electron-rich carbonyl group of carbamate group (**C**) (Scheme 30). Moreover, this configuration seems less strained than the alternative complex



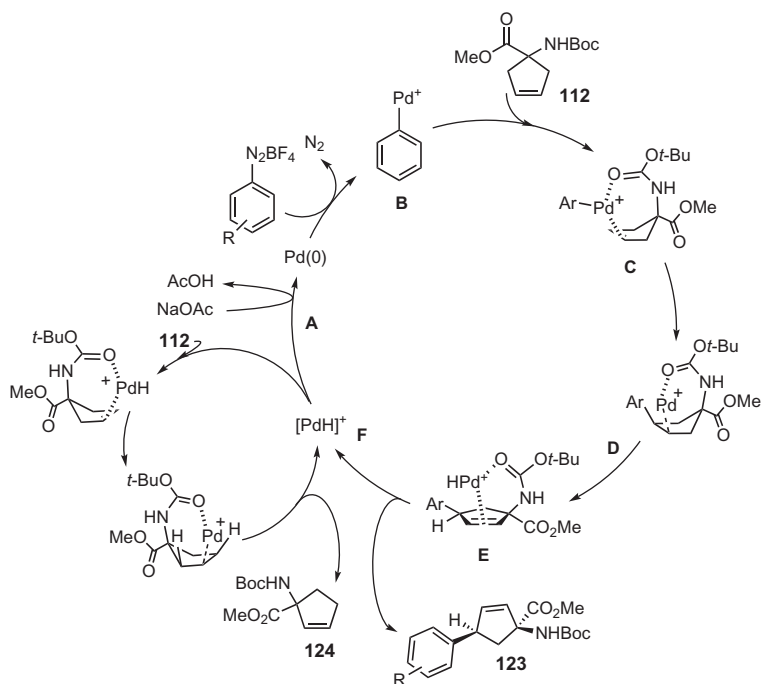
SCHEME 28 Substrate-directed Heck–Matsuda reaction of olefins **112** and **113**.

involving interaction of the aryl palladium **B** with the ester moiety. This leads to carbopalladation from the same face of the carbamate group (**C**). Next, β -elimination produces the Heck–Matsuda adduct still bound to palladium hydride. At this point, this Pd-hydride can be decomposed by the base or trapped by another molecule of the substrate to form the isomerized product **124**, which is inactive for further Heck–Matsuda arylation.

These mechanistic insights made the method an effective tool to be explored in organic synthesis. To illustrate its utility, we performed the total synthesis of VPC01091 (**130**), an agonist of the sphingosine 1-phosphate (S1P, **131**) cellular receptor. Among the important biological functions of



SCHEME 29 Rationale for the formation of isomerized olefin **124** and the lack of formation of the styrenic adduct **128**.



SCHEME 30 Rationale for the diastereoselectivity and formation of **124**.

S1P is the sequestration of lymphocytes, thus attenuating the autoimmune response. The development of selective agonists for the S1P receptor has been a topic of great interest in both academia and pharmaceutical industry. For example, fingolimod (Gilenya[®], **132**) is the first orally active drug for the treatment of multiple sclerosis (Figure 2).

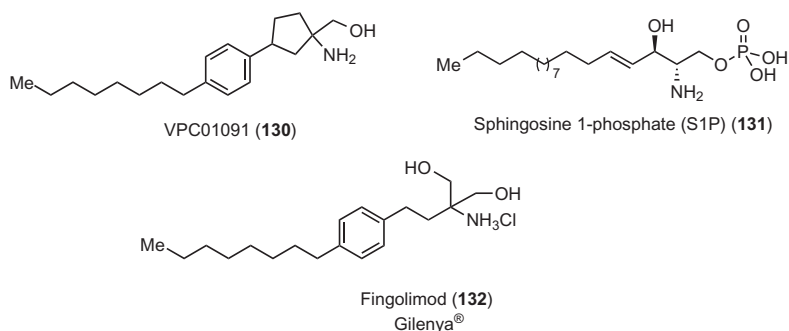
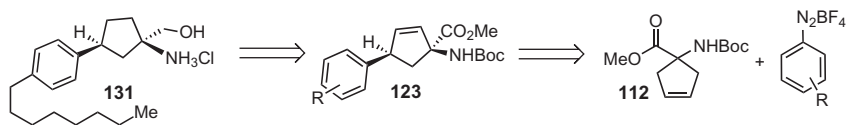


FIGURE 2 Structures of the VPC01091 (**130**), S1P (**131**), and fingolimod (**132**).



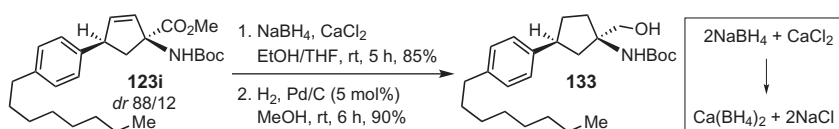
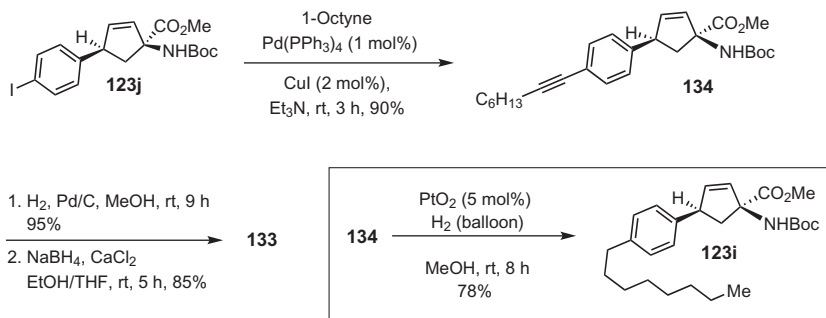
SCHEME 31 Retrosynthetic analysis for the total synthesis of the VPC01091 (**131**).

One of the drawbacks in the use of the fingolimod (**132**) is that it does not show selectivity between S1P receptors and interacts with S1P₁, S1P₃, S1P₄, and S1P₅ indiscriminately. Interaction with receptor subtypes 4 and 5 does not cause any significant side effects. However, interaction with the S1P₃ receptor causes disturbances in the cardiovascular system, such as bradycardia and hypertension.

In the search for more selective drugs, in 2006 a group of researchers at Abbott discovered that the mixture of the four stereoisomers of the VPC01091 (**130**) showed the *in vivo* ability of decreasing the concentration of T lymphocytes in the bloodstream without changing heart rate.^{38–41} These results indicated that **130** is a selective agonist for the S1P₁ receptor, thus making it an excellent drug candidate for the treatment of multiple sclerosis.

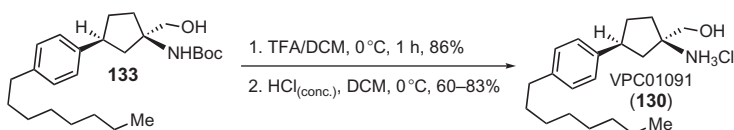
As the substrate-directed Heck–Matsuda reaction promoted a significant increase in structural complexity, we envisioned that VPC01091 (**131**) could be synthesized in a straightforward manner starting from the Heck adducts of the reaction between **112** and the corresponding aryldiazonium salt (Scheme 31).

Our first approach started with the reduction of the methyl ester moiety of **123i** (85% yield) using a mixture of NaBH₄ and CaCl₂ to generate *in situ* the stronger reducing agent Ca(BH₄)₂ (Scheme 32). To avoid problems with the Boc group, the work-up was performed under basic conditions, using K₂CO₃ and NaHCO₃. At this point, the diastereomeric alcohols could be easily separated by column chromatography and the major isomer was then submitted to catalytic hydrogenation to furnish alcohol **133** in 90% yield.

SCHEME 32 Synthesis of the alcohol **133**.SCHEME 33 Synthesis of alcohol **133** starting from **123j**.

Another interesting approach to intermediate **133** was based on the Sonogashira reaction of arylcyclopentene **123j**, obtained chemoselectively by the arylation of olefin **112** with the corresponding iodine-substituted aryl diazonium salt. Although many authors consider aryl iodides as the best substrates for the Heck reactions, oxidative addition to aryl diazonium salt is a very fast process, keeping intact the aryl iodide moiety that is instrumental for the Sonogashira reaction (90% yield). After the attachment of the side chain, the alkyne and olefin moieties of **134** were fully hydrogenated under Pd/C catalysis (95% yield), followed by reduction of the methyl ester with $\text{NaBH}_4/\text{CaCl}_2$ to provide the desired alcohol **133** in 85% yield. As previously observed, the diastereomeric alcohols could be easily separated by column chromatography at this point (Scheme 33). Additionally, after some experimentation, it was discovered that the use of PtO_2 as catalyst promotes the chemoselective reduction of the alkyne moiety in **134** leaving the double bond intact. These studies were designed to develop a reliable method for the introduction of alkyl chains of any length or for incorporation of extra functional groups using the Sonogashira cross-coupling reaction.

The final steps of the synthesis were the removal of the Boc group in **133** with trifluoroacetic acid in dichloromethane at 0°C (85% yield), followed by formation of hydrochloride salt of VPC01091 (**130**) by addition of concentrated HCl in dichloromethane (Scheme 34). Curiously, although the NMR data of intermediate **123i** was identical to those reported in the literature, after removal of the Boc group, we observed slight differences in the NMR spectra of our final product **130** and those reported for VPC01091.⁴⁰ However, it is a well-known fact that NMR chemical shifts for aminoalcohols change depending on the water



SCHEME 34 Final steps for the synthesis of the VPC01091 (**130**).

content of the sample and due to variations in temperature.⁴¹ The total synthesis of VPC01091 (**130**) was accomplished by a concise and practical route involving only five steps in 40% overall yield under mild conditions.

In summary, the substrate-directed Heck–Matsuda reaction was successfully applied for the synthesis of polyfunctionalized cyclopentenenes under very mild conditions. The method is very robust, and aryldiazonium salts with distinct electronic or steric properties were well tolerated. The power of this methodology was demonstrated by the total synthesis of the VPC01091 (**130**), an agonist of the S1P₁ receptor, a potential new drug for the treatment of multiple sclerosis.¹³

4 CONCLUSION

In this review, we described the development of the substrate-directed Heck–Matsuda reaction from its detection as an unplanned result, which stimulated our imagination and curiosity, leading to its realization as a valuable tool in organic synthesis.

Our first applications of this new method have allowed the successful regio- and stereoselective arylation of acyclic allylic esters and *N*-protected allylamine derivatives. As a consequence of the high synthetic value of the arylated products, they were applied in the total synthesis of several bioactive compounds. Starting from allylic esters, the synthesis of kavalactones such as the yagonine (**27**), methysticin (**28**), and dehydromethysticine (**29**) was accomplished in a straightforward way. Additionally, the γ -arylated allylamine derivatives were applied to the total synthesis of the bioactive compounds naftifine (**68**), abamine (**75**), abamine SG (**77**), cinacalcet hydrochloride (**85**), and alverine (**91**).

This methodology was also applied to the stereoselective arylation of substituted cyclic compounds to provide highly complex aryl-substituted cyclopentene scaffolds with total control of the double bond position. This unique substrate-directed Heck–Matsuda reaction was applied in the total synthesis of the S1P₁ agonist VPC01091 (**130**).

ACKNOWLEDGMENTS

The authors specially thank the many past and present members of the research group involved in the development of the Heck–Matsuda reaction whose names appear in the references. The authors also thank the Brazilian funding agencies, in particular to the State

of São Paulo Research Foundation Agency (FAPESP), the Brazilian National Research Council (CNPq), and the Coordination for the Improvement of Higher Education Level Personnel (Capes) for financial support and fellowships.

REFERENCES

1. Hudlicky, T.; Reed, J. *The Way of Synthesis*. Wiley-VCH: Weinheim, 2007.
2. Taylor, J. G.; Moro, A. V.; Correia, C. R. D. *Eur. J. Org. Chem.* **2011**, 1403–1428.
3. Kikukawa, K.; Matsuda, T. *Chem. Lett.* **1977**, 159–162.
4. Roglans, A.; Pla-Quintana, A.; Moreno-Manas, M. *Chem. Rev.* **2006**, *106*, 4622–4643.
5. Correia, C. R. D.; Oliveira, C. C.; Salles, A. G., Jr.; dos Santos, E. A. F. *Tetrahedron Lett.* **2012**, *53*, 3325–3328.
6. Jiang, Z.; Zhang, L.; Dong, C.; Ma, B.; Tang, W.; Xu, L.; Fan, Q.; Xiao, J. *Tetrahedron* **2012**, *68*, 4919–4926.
7. Agrawal, J. P.; Hodgson, R. D. *Organic Chemistry of Explosives*. Wiley: West Sussex, 2007.
8. Norris, T.; Bezze, C.; Franz, S. Z.; Stivanello, M. *Org. Process Res. Dev.* **2009**, *13*, 354–357.
9. Molinaro, C.; Mowat, J.; Gosselin, F.; O'Shea, P. D.; Marcoux, J.-F.; Angelaud, R.; Davies, I. W. J. *Org. Chem.* **2007**, *72*, 1856–1858.
10. Oliveira, C. C.; Angnes, R. A.; Correia, C. R. D. *J. Org. Chem.* **2013**, *78*, 4373–4385.
11. Moro, A. V.; Cardoso, F. S. P.; Correia, C. R. D. *Org. Lett.* **2009**, *11*, 3642–3645.
12. Prediger, P.; Barbosa, L. F.; Génisson, Y.; Correia, C. R. D. *J. Org. Chem.* **2011**, *76*, 7737–7749.
13. Oliveira, C. C.; dos Santos, E. A. F.; Nunes, J. H. B.; Correia, C. R. D. *J. Org. Chem.* **2012**, *77*, 8182–8190.
14. Prediger, P.; da Silva, A. R.; Correia, C. R. D. *Tetrahedron* **2014**, *70*, 3333–3341.
15. Hoveyda, A. H.; Evans, D. A.; Fu, G. C. *Chem. Rev.* **1993**, *93*, 1307–1370.
16. Oliveira, D. F.; Severino, E. A.; Correia, C. R. D. *C. Tetrahedron Lett.* **1999**, *40*, 2083–2086.
17. Severino, E. A.; Correia, C. R. D. *C. Org. Lett.* **2000**, *2*, 3039–3042.
18. Severino, E. A.; Costenaro, E. R.; Garcia, A. L. L.; Correia, C. R. D. *C. Org. Lett.* **2003**, *5*, 305–308.
19. Lumbroso, A.; Cooke, M. L.; Breit, B. *Angew. Chem. Int. Ed. Engl.* **2013**, *52*, 1890–1932.
20. Pan, D.; Chen, A.; Su, Y.; Zhou, W.; Li, S.; Jia, W.; Xiao, J.; Liu, Q.; Zhang, L.; Jiao, N. *Angew. Chem. Int. Ed. Engl.* **2008**, *47*, 4729–4732.
21. Su, Y.; Jiao, N. *Org. Lett.* **2009**, *11*, 2980–2983.
22. Yao, B.; Liu, Y.; Wang, M.-K.; Li, J.-H.; Tang, R.-Y.; Zhang, X.-G.; Deng, C.-L. *Adv. Synth. Catal.* **2012**, *354*, 1069–1076.
23. Ripin, D. H.; Bourassa, D. E.; Brandt, T.; Heather, N. F.; Castaldi, M. J.; Hawkins, J.; Johnson, P. J.; Massett, S. S.; Neumsnn, K.; Phillips, J.; Raggon, J. W.; Rose, P. R.; Rutherford, J. L.; Sitter, B.; Stewart, A. M.; Vetelino, M. G.; Wei, L. *Org. Process Res. Dev.* **2005**, *9*, 440–450.
24. Baxter, C. A.; Cleator, E.; Alam, M.; Davies, A. J.; Goodyear, A.; O'Hagan, M. *Org. Lett.* **2010**, *12*, 668–671.
25. Olofsson, K.; Sahlin, H.; Larhed, M.; Hallberg, A. *J. Org. Chem.* **2001**, *66*, 544–549.
26. Cacchi, S.; Fabrizi, G.; Goggiani, A.; Sferrazza, A. *Org. Biomol. Chem.* **2011**, *9*, 1727–1730.
27. Reichardt, C.; Welton, T. *Solvents and Solvent Effects in Organic Chemistry*. Wiley-VCH: Weinheim, 2010.
28. Oestreich, M. *The Mizoroki–Heck Reaction*. Wiley: Chichester, 2009.

29. Kikukawa, K.; Maemura, K.; Nagira, K.; Wada, F.; Matsuda, T. *Chem. Lett.* **1980**, 551–552.
30. Kikukawa, K.; Nagira, K.; Wada, F.; Matsuda, T. *Tetrahedron* **1981**, 37, 31–36.
31. Sengupta, S.; Bhattacharya, S. *J. Chem. Soc., Perkin Trans. 1* **1993**, 1943–1944.
32. Colas, C.; Goeldner, M. *Eur. J. Org. Chem.* **1999**, 1357–1366.
33. Pla-Quintana, A.; Parella, T.; Roglans, A. *Adv. Synth. Catal.* **2011**, 353, 2003–2012.
34. Peñafiel, I.; Pastor, I. M.; Yus, M. *Eur. J. Org. Chem.* **2012**, 2012, 3151–3156.
35. Lebel, H.; Leogane, O. *Org. Lett.* **2006**, 7, 4107–4110.
36. Larue, V.; Gharbi-Benarous, J.; Acher, F.; Valle, G.; Crisma, M.; Toniolo, C.; Azerad, R.; Girault, J.-P. *J. Chem. Soc., Perkin Trans. 2* **1995**, 1111–1126.
37. Ung, A. T.; Pyne, S. G.; Batenburg-Nguyen, U.; Davis, A. S.; Sherif, A.; Biscoff, F.; Lesage, A. S. *J. Tetrahedron* **2005**, 61, 1803–1812.
38. Lynch, K. R.; Macdonald, T. L. Sphingosine 1-Phosphate Agonists Comprising Cycloalkanes and 5-Membered Heterocycles Substituted by Amino and Phenyl Groups. WO Patent 2006088944, 2006.
39. Zhu, R.; Snyder, A. H.; Kharel, Y.; Schaffter, L.; Sun, Q.; Kennedy, P. C.; Lynch, K. R.; Macdonald, T. L. *J. Med. Chem.* **2007**, 50, 6428–6435.
40. Fix-Stenzel, S. R.; Hayes, M. E.; Zhang, X.; Wallace, G. A.; Grongsaard, P.; Schaffter, L. M.; Hannick, S. M.; Franczyk, T. S.; Stoffel, R. H.; Cusack, K. P. *Tetrahedron Lett.* **2009**, 50, 4081–4083.
41. Denmark, S. E.; Thorarensen, A.; Middleton, D. S. *J. Am. Chem. Soc.* **1996**, 118, 8266–8277.

(–)-Berkelic Acid: Lessons Learned From Our Investigations on a Scalable Total Synthesis

Tamara Arto, Abraham Mendoza², Francisco J. Fañanás¹, and Félix Rodríguez¹

Instituto Universitario de Química Organometálica “Enrique Moles,” Universidad de Oviedo, Julián Clavería, Oviedo, Spain

¹Corresponding authors: fjfv@uniovi.es; frodriguez@uniovi.es

Chapter Outline

1. Introduction: Isolation and Interest on Berkelic Acid	33	4. Retrosynthetic Analysis	42
2. Structural Assignment and Previous Total Syntheses of (–)-Berkelic Acid	35	5. Our Synthesis of (–)-Berkelic Acid	43
3. Our Approach to Berkelic Acid from Research on New Methodology: Model Studies	37	6. Conclusions	48
		Acknowledgments	49
		References	49

1 INTRODUCTION: ISOLATION AND INTEREST ON BERKELIC ACID

Bioactive secondary metabolites (natural products) have proven to be a rich source of drugs and they have also served as an inspiration for the development of analogues with enhanced bioactivities.¹ These natural products are usually isolated from organisms living in conventional environments. However, in recent years, a high priority has been placed on obtaining natural products from

²Current address: Department of Organic Chemistry, Arrhenius Laboratory, Stockholm University, SE-106 91 Stockholm, Sweden.

organisms that survive extraordinary environments (extreme-tolerant microorganisms and extremophiles).² Organisms capable of growing under extreme conditions have evolved developing unique metabolic pathways that provide singular compounds with structures different from those produced by conventional life forms. This has made extremophiles treasure troves for natural product chemists and biotechnology/pharmaceutical industries.

Berkeley Pit Lake is a clear example of an extreme environment (Figure 1). This lake, near the town of Butte in the US state of Montana, was formed when an abandoned open-pit copper mine, shut down in the 1980s, was flooded with infiltrating ground water. This has resulted in the formation of a highly acidic (pH 2.5) and metal-contaminated pool. Nowadays, Berkeley Pit Lake is a dangerous place at risk of a serious ecological disaster and in evident need of remediation. However, this polluted lake has proven to be an appropriate ecosystem for the growth of different bacteria, algae, and protozoans. Several unknown natural products have been isolated from these extremophiles.³ One of them, (–)-berkelic acid, was isolated in 2006 by Stierle and coworkers from a *Penicillium* species collected from the surface of Berkeley Pit Lake.⁴ This novel chroman spiroacetal derivative was found to effectively inhibit the matrix metalloproteinase-3 in the micromolar range ($GI_{50}=1.87\text{ }\mu\text{M}$) and caspase-1 in the millimolar range ($GI_{50}=0.098\text{ mM}$). The isolation team also reported that (–)-berkelic acid exhibited selective activity toward the ovarian cancer cell line OVCAR-3 ($GI_{50}=91\text{ nM}$). However, the cytotoxicity against these specific tumor cells has been subject of some controversy because a synthetic sample of material obtained by Snider and coworkers did not show significant activity.⁵ This fact reinforces the need for a deeper study on the bioactivity of this natural product and its analogues.

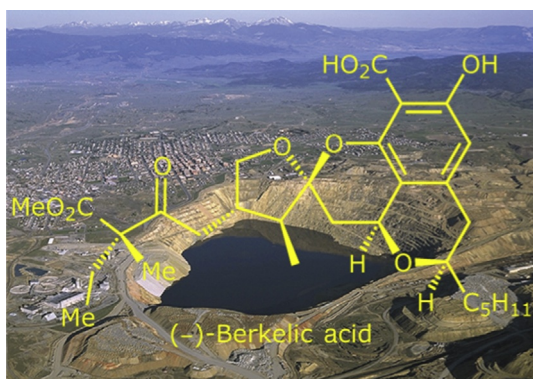


FIGURE 1 Berkeley Pit Lake in Butte (Montana, US) and structure of (–)-berkelic acid.

2 STRUCTURAL ASSIGNATION AND PREVIOUS TOTAL SYNTHESSES OF (–)-BERKELIC ACID

In 2008, just 2 years after the isolation of the natural product, Fürstner and coworkers reported the synthesis of the enantiomer of the methyl ester of berkelic acid.⁶ The extensive NMR work and crystallographic experiments performed served to revise the originally proposed structure of the natural product by reassigning the relative stereochemistry at C18 and C19 (Figure 2). However, the relative configuration of the lateral quaternary stereocenter at C22 and the absolute stereochemistry of the natural product were unresolved at this time. Although the authors could not access the natural product because they reached a compound just one step away from the target, this pioneering work may be considered as the first far-reaching synthetic approach to berkelic acid.

Snider and coworkers published the first complete total synthesis of (–)-berkelic acid **1** in 2009, confirming the reassignments made by Fürstner and establishing the stereochemistry at C22 and the absolute configuration of the natural product.⁷ The key step of this synthesis was an oxa-Pictet–Spengler reaction between intermediates **4** and **5** that delivered the tetracyclic core **3** in basically one step (Scheme 1). Elongation of the lateral chain was achieved by creating the C21–C22 bond through an aldol reaction between trimethylsilyl

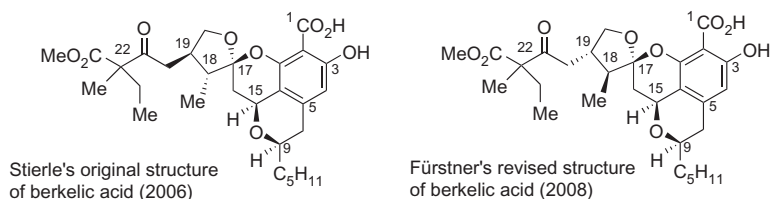
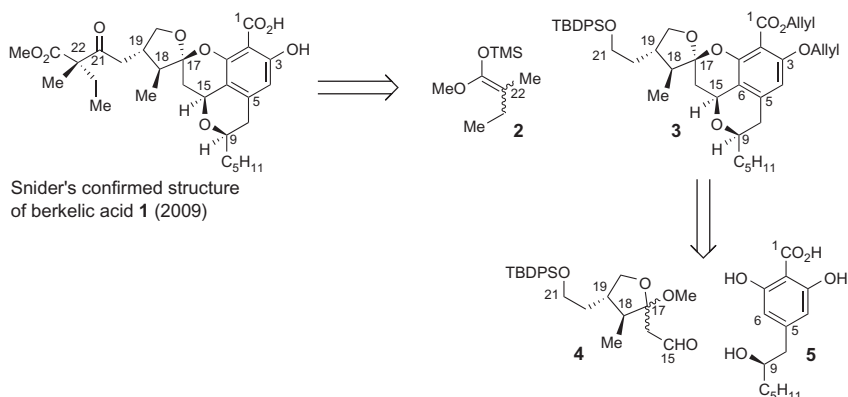


FIGURE 2 Stierle's original and Fürstner's revised structures of (–)-berkelic acid.

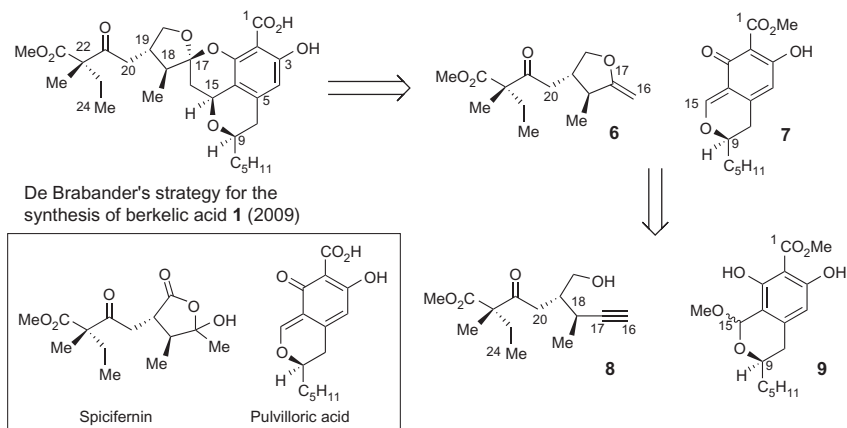


SCHEME 1 Snider's synthesis of (–)-berkelic acid.

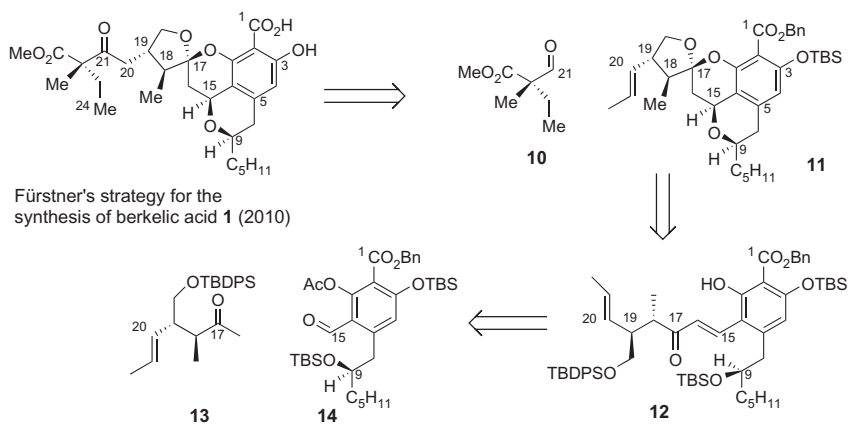
ketene acetal **2** and the C21-aldehyde derived from **3** followed by oxidation of the resulting aldol product to the 1,3-ketoester derivative. The synthesis proceeded with a longest linear sequence of 13 steps (no less than 20 global steps considering available starting materials) in 2% global yield allowing the final isolation of 11.1 mg of synthetic (–)-berkelic acid **1** for the first time.

Soon after Snider's synthesis appeared, De Brabander and coworkers published a different approach to berkelic acid based on the coupling of the two natural product-inspired fragments **6** (related to spicifernin) and **7** (related to pulvilloric acid) (Scheme 2).⁸ The key step of the synthesis relied on the *in situ* formation of the exocyclic enol ether **6** by cycloisomerization of alkynol derivative **8** and further formal [4+2]-cycloaddition reaction with heterodiene **7** (formed *in situ*) from acetal **9**. As a difference with respect to all other total syntheses of (–)-berkelic acid published to this point, in this strategy the C20–C24 lateral chain was incorporated into fragment **6** at an early stage and before the construction of the central polycyclic core. Although this approach is original in its biosynthetic basis, it is somewhat less convergent and modular than the others. The synthesis proceeded with a longest linear sequence of 10 steps (no less than 17 global steps considering available starting materials) in 10% global yield (improved by recycling some intermediates). However, the efficiency of the strategy was compromised by the need for using two equivalents of the advanced intermediate **8** in the key step of the synthesis. Nonetheless, 3.7 mg of (–)-berkelic acid could be finally obtained.

Following their initial studies on the real structure of (–)-berkelic acid previously mentioned, Fürstner and coworkers published in 2010 a total synthesis of this natural product.⁹ The successful route was based on an aldol reaction between methyl ketone **13** and benzaldehyde derivative **14** to give enone derivative **12** (Scheme 3). A subsequent deprotection/1,4-addition/spiroacetalization cascade reaction delivered the tetracyclic core **11**. Installation of the lateral chain was achieved by oxidative rupture, reduction, and



SCHEME 2 De Brabander's synthesis of (–)-berkelic acid.



SCHEME 3 Fürstner's synthesis of (–)-berkelic acid.

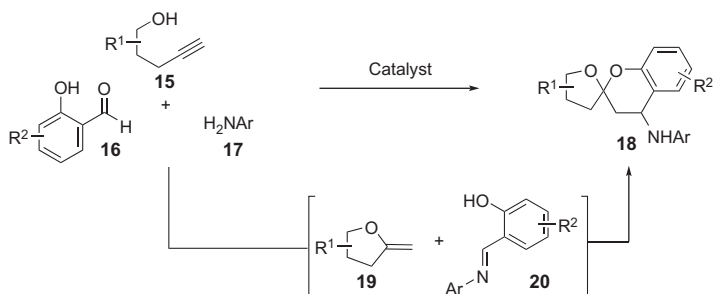
iodination of the alkene of **11** to obtain the corresponding C20-iodide. An iodine–lithium exchange followed by addition of the formed organolithium compound to aldehyde **10** and further oxidation of the alcohol obtained afforded (–)-berkelic acid **1** after a hydrogenolysis of the benzyl ester. The synthesis proceeded with a longest linear sequence of 19 steps (no less than 26 global steps considering available starting materials) in 5% global yield allowing the final isolation of 4.7 mg of (–)-berkelic acid.

While the three reported total syntheses of (–)-berkelic acid allowed access to synthetic samples of the natural product, achieving a scalable and modular synthesis of this target remained, for various reasons, an unmet challenge. It should also be noted that Pettus¹⁰ and Brimble's¹¹ groups have also reported formal total syntheses of (–)-berkelic acid.

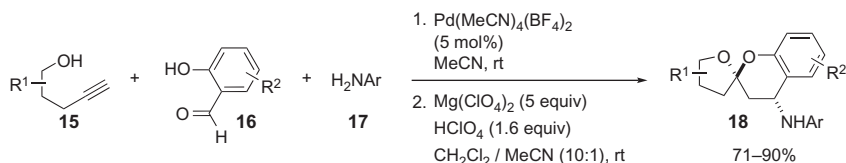
3 OUR APPROACH TO BERKELIC ACID FROM RESEARCH ON NEW METHODOLOGY: MODEL STUDIES

Our interest on the synthesis of (–)-berkelic acid stemmed from our work on multicomponent coupling reactions involving alkynol derivatives.¹² We and others have demonstrated that the metal-catalyzed cycloisomerization reaction of alkynol derivatives is a powerful strategy to synthesize cyclic enol ethers.¹³ While working on this project we realized that chroman spiroacetals, the core structure of (–)-berkelic acid, could be available through a one-pot, three-component coupling reaction of a pentynol derivative **15**, a salicylaldehyde **16**, and an aniline **17** (Scheme 4).¹⁴ We thought that under appropriate conditions an exocyclic enol ether **19** and an imine **20** should be formed. Further reaction of these two reagents should proceed through the formation of the desired chroman spiroacetals through a formal Mannich-type reaction followed by spiroacetalization.

After some optimization studies, it was found that the palladium(II) complex $\text{Pd}(\text{MeCN})_4(\text{BF}_4)_2$ was the best catalyst to perform the multicomponent



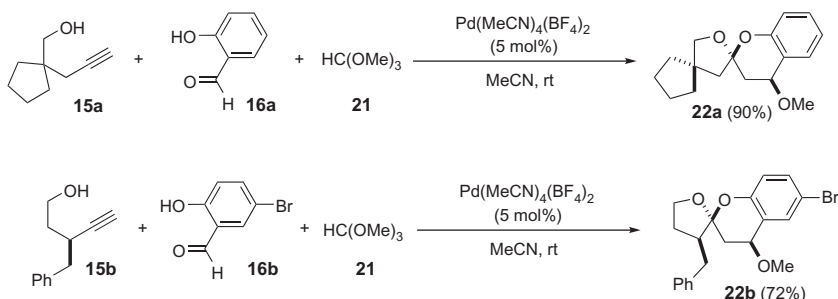
SCHEME 4 Our initial proposal for the synthesis of chroman spiroacetals.



SCHEME 5 Three-component coupling reaction for the synthesis of amino-substituted chroman spiroacetals.

reaction proposed for the synthesis of chroman spiroacetal derivatives.¹⁴ Thus, a series of pentynol derivatives **15**, salicylaldehydes **16**, and anilines **17** were reacted in the presence of 5 mol% of $\text{Pd}(\text{MeCN})_4(\text{BF}_4)_2$ in acetonitrile at room temperature to prepare the amine-substituted chroman spiroacetal derivatives **18** as an equimolecular mixture of diastereoisomers. Treatment of the crude of the reaction with $\text{Mg}(\text{ClO}_4)_2$ and HClO_4 in dichloromethane/acetonitrile (10:1) allowed the clean conversion of the mixture of two diastereoisomers into a single one (Scheme 5).

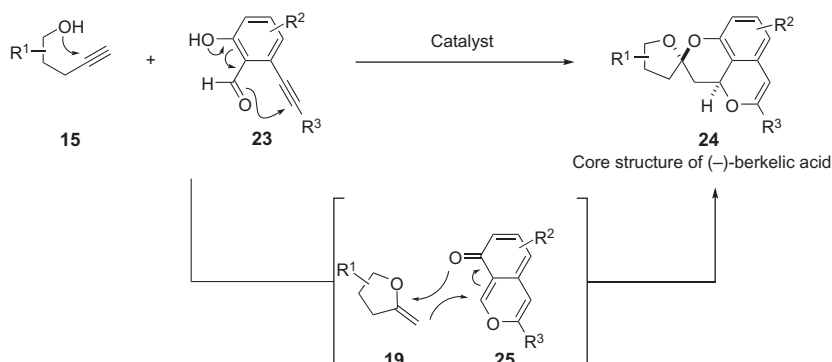
Although this reaction was interesting from the synthetic point of view, its potential application to the total synthesis of berkelic acid was not yet obvious. To this end, the developed multicomponent reaction would need to be adapted to get oxygen-substituted chroman spiroacetals instead of the nitrogen-substituted spiroacetals **18** obtained. To access these compounds, it was evident that a reagent that would provide the oxygen function should replace the third component of the reaction, the aniline **17**. In this sense, we thought that orthoesters could be the ideal reagents to provide the desired oxygenated-functionality because we supposed that, under the reaction conditions, a transesterification reaction between the orthoester and the salicylaldehyde should occur and then, the intermediate formed would react with the enol ether generated *in situ*. As a proof of concept, we reacted pentynol derivative **15a**, salicylaldehyde **16a**, and trimethyl orthoformate **21** with 5 mol% of $\text{Pd}(\text{MeCN})_4(\text{BF}_4)_2$ in acetonitrile at room temperature and, to our delight, the desired oxygen-substituted spiroacetal **22a** was isolated in high yield and as a single diastereoisomer (Scheme 6).¹⁴ Interestingly, it was not necessary to perform an equilibration reaction, as required in the synthesis



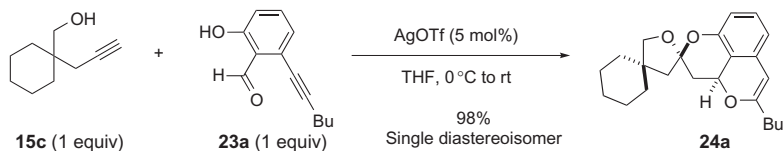
SCHEME 6 Diastereoselective synthesis of oxygen-substituted chroman spiroacetals.

nitrogen-substituted spiroacetals **18**, and a single diastereoisomer was directly obtained. Another remarkable feature of this reaction was that the relative configuration of the carbon atom carrying the alkoxy-group in **22a** was opposite to that observed in the nitrogen-substituted spiroacetals **18** and fortunately, this configuration is similar to that observed in the natural product (–)-berkelic acid. In an attempt to go further with these model experiments, we performed a reaction with the chiral (racemic) pentynol derivative **15b** with a substituent at the propargylic position (Scheme 6). We selected this pentynol thinking of the possibility of using this reaction for a new total synthesis of (–)-berkelic acid. Looking at the structure of the natural product, we realized that its total synthesis would require the use of a pentynol derivative substituted at the propargylic position (similar to **15b**). Thus, we wanted to know the influence of the substitution at the propargylic position on the stereoselectivity of the reaction. It was a pleasure to find that the product **22b** was obtained as a single diastereoisomer and, more interestingly, that the relative configuration of all three stereocenters corresponded to those observed in (–)-berkelic acid. In other words, the stereocenter of **15b** directed the formation of the other two in the desired way.

All these results seemed to indicate that this reaction was ideal for the construction of the (–)-berkelic acid skeleton. However, a serious problem was still unresolved at this point: how to construct the additional pyran ring contained in the natural product. Nevertheless, our experience on cycloisomerization reactions led us to speculate on the possibility that a unique metal complex could promote the cycloisomerization of alkynol **15** to give the exocyclic enol ether **19** and also that the cycloisomerization of an alkynyl-substituted salicylaldehyde **23** would give **25**. Thus, activation of the alkyne of **15** should promote a hydroalkoxylation reaction to give the exocyclic enol ether **19**. On the other hand, activation of the alkyne in **23** should promote a cascade cyclization process to finally give the 8*H*-isochromen-8-one derivative **25**. The formal [4+2]-cycloaddition reaction between intermediates **19** and **25** would result in the formation of the core structure of (–)-berkelic acid **24** in a very simple way (Scheme 7).



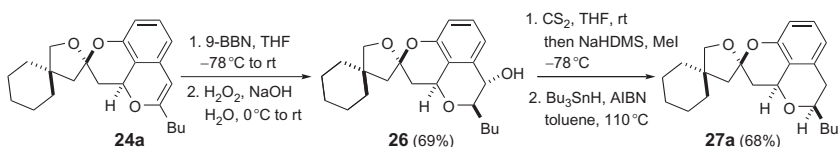
SCHEME 7 Our initial proposal for the synthesis of the tetracyclic core of (–)-berkelic acid.



SCHEME 8 Proof of concept. Silver-catalyzed synthesis of a chroman spiroacetal similar to (–)-berkelic acid.

To quickly assess the viability of our proposed key reaction, we explored a model system employing readily available alkynol **15c** and salicylaldehyde derivative **23a**. In this simplified case, we intentionally selected an alkynol without stereogenic centers and a simplified version of the required aldehyde. As previously mentioned, it was our intention that the same metal catalyst would activate the alkyne of both reagents **15** and **23**. After a short optimization study, it was found that this model reaction proceeded in the presence of 5 mol% of silver triflate (AgOTf) to give the desired polycyclic chroman spiroacetal derivative **24a** basically in a quantitative yield as a single diastereoisomer (Scheme 8). It should be noted that this reaction proceeds without the need of an excess of either of the starting materials **15c** or **23a**.

This remarkable result demonstrated that it could be possible to assemble the skeleton of berkelic acid in just one reaction from two simple starting molecules. Also, the efficiency of the reaction and the known functional group tolerance of the catalyst encouraged us to carry on with our planned strategy. However, we were fully aware that we still had to address a challenging goal: the diastereoselective reduction of the carbon–carbon double bond of the isochromene. This process was studied using the model compound **24a** and two strategies were devised: (i) the obvious direct hydrogenation reaction of the alkene and (ii) an indirect method based on a hydroboration/oxidation/deoxygenation sequence. As will be shown later, the direct hydrogenation reaction proved problematic in our first attempts,



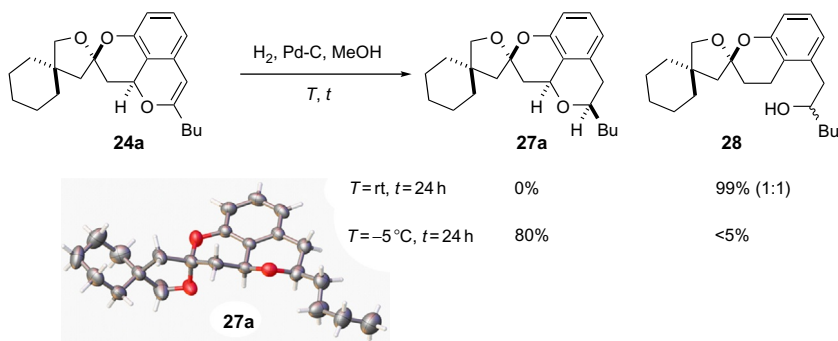
SCHEME 9 Model studies for the selective reduction of the alkene.

so the indirect strategy was evaluated. Thus, treatment of **24a** with 9-borabicyclo[3.3.1]nonane (9-BBN) followed by oxidation with hydrogen peroxide rendered the alcohol **26** in good yield as a single diastereoisomer (Scheme 9). It was pleasant to find that the hydroboration reaction selectively occurred by the desired face of the alkene. For the deoxygenation reaction, we followed the Barton–McCombie protocol based on the formation of a xanthate derivative followed by treatment with tributyltin hydride. This sequence allowed us to get compound **27a** in good yield as a single diastereoisomer and with all stereocenters mimicking those of (–)-berkelic acid.

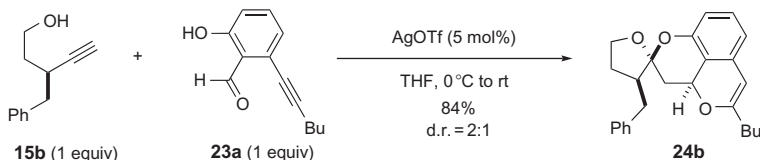
At this time, we had found the way to fully construct the skeleton of berkelic acid. However, we felt that the last reduction of the double bond of the enol ether through a three steps sequence (hydroboration, oxidation, and deoxygenation) was not the most elegant strategy for an efficient construction of the natural product. As previously pointed out, the best way to perform the desired reduction of the carbon–carbon double bond was a simple hydrogenation reaction. However, considering that the polycyclic core of berkelic acid contains a benzylic ether, we were concerned about the possibility of a hydrogenolysis process under the standard hydrogenation conditions. In fact, when the model compound **24a** was reacted with hydrogen (1 atm) in methanol in the presence of palladium on carbon at room temperature for 24 h, we isolated alcohol **28** in quantitative yield. In an attempt to avoid this undesired process, we tried the reaction with different catalysts and reaction conditions. Finally, the solution to this problem turned to be as easy as reducing the temperature of the reaction to -5°C . Under these conditions, we could obtain our desired product **27a** in high yield. This reaction was totally diastereoselective, indicating that the hydrogenation occurred exclusively on one face of the carbon–carbon double bond. To our delight, the X-ray structure of **27a** showed that the relative configuration of all stereocenters was identical to those of the central core of berkelic acid (Scheme 10).

Before facing the total synthesis of (–)-berkelic acid, we still needed to know about the diastereoselectivity of the reaction when a chiral alkynol derivative such as **15b** was reacted with the simple alkynyl-substituted salicylaldehyde derivative **23a** (Scheme 11). This study would serve to tell us if the stereocenter of **15b** could direct the formation of the other two in the desired way.

As shown, under the optimized reaction conditions found before, product **24b** was obtained as a 2:1 mixture of two diastereoisomers, but fortunately,



SCHEME 10 Direct hydrogenation of the alkene on a model substrate.

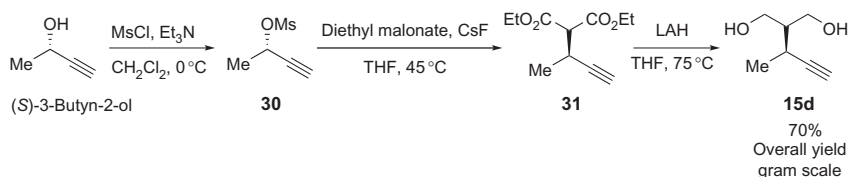


SCHEME 11 Diastereoselectivity of the reaction when a chiral alkynol is used as starting material.

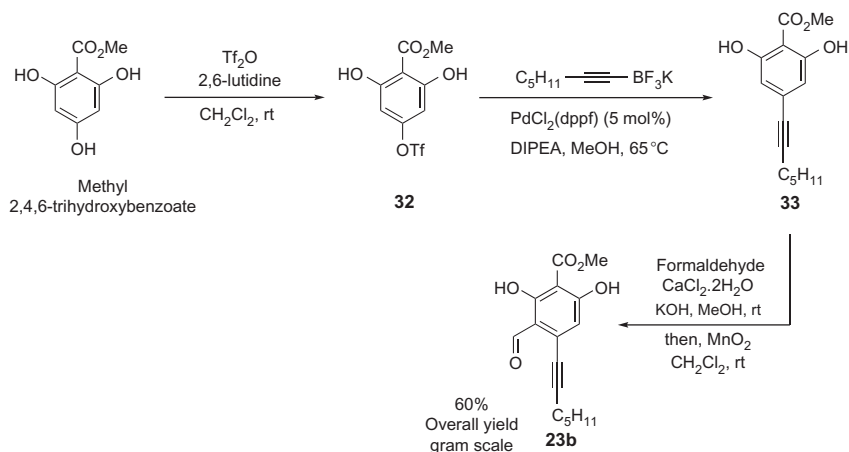
the relative configuration of all three stereocenters in the major isomer corresponded to those observed in berkelic acid.

4 RETROSYNTHETIC ANALYSIS

After all these studies with model molecules, we were confident that we would be able to synthesize (–)-berkelic acid. Thus, with our thinking biased toward a key step involving a coupling reaction between appropriate derivatives of pentyn-1-ol and salicylaldehyde, it was not difficult to unravel (–)-berkelic acid in a retrosynthetic sense (Scheme 12). Thus, we envisioned that the tetracyclic motif of (–)-berkelic acid **24c** could be constructed from alkynyldiol **15d** [available from commercially available (*S*)-3-butyn-2-ol] and fully decorated aldehyde **23b** (easily traced to methyl 2,4,6-trihydroxybenzoate) through a silver-catalyzed *in situ* formation of exocyclic enol ether **19a** and 8*H*-isochromen-8-one **25a** and subsequent formal cycloaddition reaction between these two intermediates. This reaction was risky in terms of stereoselectivity, because just one chiral center (that of alkynyldiol **15d**) would induce the selective formation of the other three newly formed ones in **24c** (including a desymmetrization in **15d**). However, the process was very attractive from the synthetic point of view, as it avoided the synthesis of starting materials with multiple stereocenters. Finally, to introduce the lateral chain, we devised a strategy based on an umpolung alkylation reaction



SCHEME 13 Scalable synthesis of the alkynyldiol fragment.



SCHEME 14 Scalable synthesis of the alkynyl-substituted aldehyde fragment.

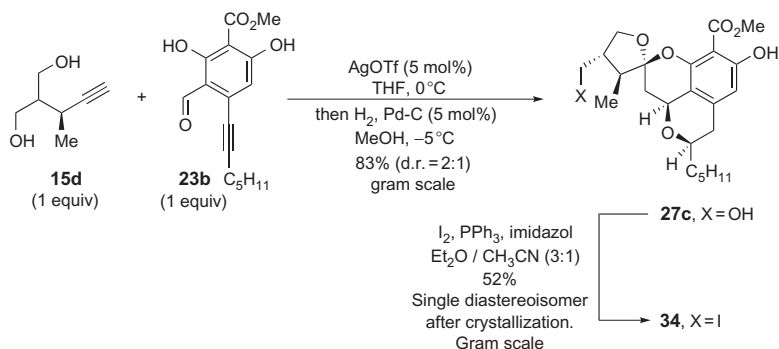
and subsequent drying with magnesium sulfate was much more satisfactory than classic work-up procedures involving treatments with sodium sulfate decahydrate or Rochelle salts.

Aldehyde **23b** was constructed starting from commercially available methyl 2,4,6-trihydroxybenzoate in just three steps (Scheme 14). Namely, triflic anhydride reacted selectively with the hydroxy group in *para*-position leading to compound **32**, which is a suitable substrate for a Sonogashira coupling needed to introduce the alkyne functionality. Attempts to accomplish a conventional Sonogashira reaction with 1-heptyne afforded poor yields. However, the efficiency of the process was highly improved when the coupling partner was changed from the simple alkyne to its corresponding alkynyltrifluoroborate salt derivative. By using this reagent, the desired coupling product **33** was obtained in 88% yield. The next step was the formylation of the aromatic ring. Attempts to perform a direct formylation of the aromatic ring with magnesium chloride and paraformaldehyde under the conditions reported for similar materials evolved to mixtures of undefined products. The classical Vilsmeier–Hack formylation reaction with dimethylformamide and phosphorous oxychloride was also ineffective. Subsequently, we decided to introduce the aldehyde functionality through a two-step sequence involving an initial

hydroxymethylation with aqueous formaldehyde in the presence of CaCl_2 and subsequent oxidation with manganese oxide. This sequence was performed in a one-pot process without purification of the hydroxymethyl intermediate. This strategy allowed us to obtain the desired aldehyde **23b** at multigram scale (4.8 g) and with a 60% global yield.

We next turned our attention to driving the cascade reaction necessary to assemble the (–)-berkelic acid core from diol **15d** and aldehyde **23b**. Our previous studies on model systems indicated that AgOTf was the best catalyst to perform the key step of our synthesis. Thus, under similar conditions, we observed that an equimolecular mixture of these components readily reacted in tetrahydrofuran as solvent and 5 mol% of AgOTf as catalyst (Scheme 15). This reaction led to the corresponding tetracyclic product **24c** (see Scheme 12). However, in order to avoid any decomposition of this relatively sensitive product, we directly performed the subsequent hydrogenation of the carbon–carbon double bond of the pyran ring without isolation of **24c** following the optimal conditions found in our model studies. Thus, the crude product of the reaction was dissolved in methanol and allowed to stand under 1 atm of hydrogen in the presence of palladium on carbon (5 mol%) at -5°C for 48 h (Scheme 15). This one-pot, two-step reaction allowed us to obtain compound **27c** in 83% yield on a multigram scale (2.4 g of this material was synthesized). Globally, this transformation is outstanding owing to its efficiency and stereoselectivity. Compound **27c** contains five chiral centers, one of them comes from the starting alkynyldiol **15d** but all the other four are formed during the reaction. It was a pleasure for us to find only two diastereoisomers in the crude of the reaction (d.r. = 2:1) and even more pleasant was to see that the structure of the major diastereoisomer corresponded to that of compound **27c** with all chiral centers resembling those of the natural product.

Considering our proposed retrosynthetic analysis, incorporation of the lateral chain would be performed through a coupling reaction between an acyl anion equivalent derived from aldehyde **10** and an electrophilic counterpart derived from alcohol **27c** obtained from **24c** (see Scheme 12). Thus, alcohol

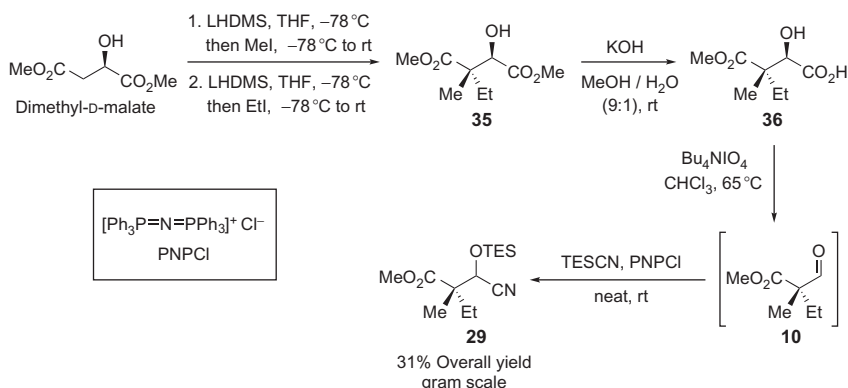


SCHEME 15 Scalable synthesis of the tetracyclic core of (–)-berkelic acid.

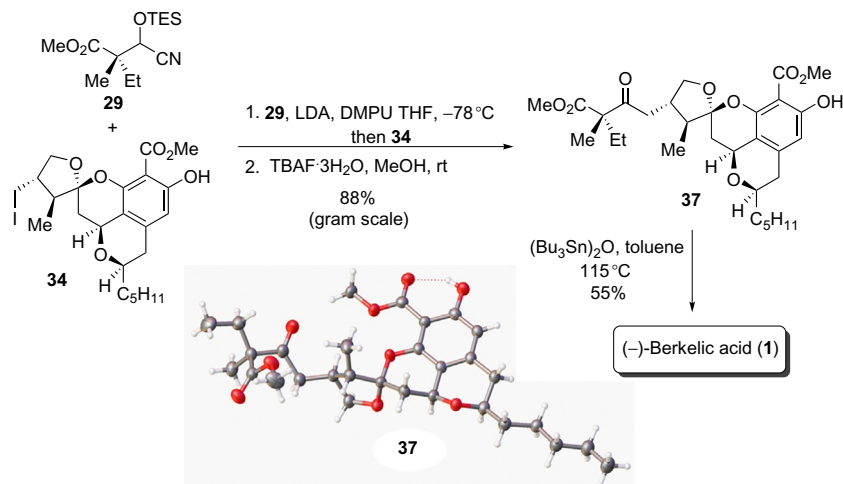
27c was transformed into iodide **34** by treatment with PPh_3 and iodine under standard conditions (Scheme 15). At this point, the minor diastereoisomer formed in the previous step was removed after a single recrystallization from a mixture of dichloromethane and ethanol. This protocol allowed the isolation of iodide **34** on a multigram scale (1.6 g) in 52% yield and enantiomerically pure form.

With iodide **34** in hand, we turned our attention to making an appropriate acyl anion equivalent derived from aldehyde **10** (see Scheme 12). Initially, this aldehyde was synthesized following a known procedure that involved a successive double alkylation of dimethyl-(D)-malate with methyl iodide, and ethyl iodide using lithium bis(trimethylsilyl)amide as base to give hydroxyester **35**.¹⁵ Obviously, the order of introduction of the alkyl groups, first methyl and then ethyl, marks the absolute configuration of the new quaternary stereocenter formed. The next step involved the selective hydrolysis of the less-hindered methyl ester with potassium hydroxide to give carboxylic acid **36** in essentially quantitative yield. This sequence, double alkylation of (D)-malate followed by selective hydrolysis of the ester functionality, could be performed on a multigram scale and allowed the isolation of 1.5 g of hydroxyacid **36**. Transformation of this hydroxyacid into the desired aldehyde **10** was initially performed by an electrochemical reaction as described by Seebach and coworkers.¹⁵ This reaction was performed by subjecting a solution of hydroxyacid **36** and triethylamine in methanol to electrolysis at 0 °C using platinum electrodes. Although this reaction gave good results when attempted at small scale (0.1 g per batch), it was not appropriate for our goal of getting enough material to achieve a scalable synthesis of the natural product. Thus, a more practical method to transform the hydroxyacid **36** into the desired aldehyde **10** became essential. A simple literature search on oxidation methods with potential application to our desired transformation led us to Santiello's work published in 1980.¹⁶ In this report, several uses of tetrabutylammonium periodate, including the oxidative rupture of α -hydroxyacids, are described. Fortunately, when we applied this protocol, treating hydroxyacid **36** with tetrabutylammonium periodate in chloroform at reflux for 2 h, we were able to get the aldehyde **10** without problems. At least in our hands, this method turned out to be much more efficient than the alternative electrochemical reaction. The new strategy allowed the synthesis of aldehyde **10** in high, reproducible yields and, more importantly, the reaction could be perfectly performed on a gram scale (Scheme 16).

With aldehyde **10** in hand, we just needed to transform it into the cyanohydrin derivative **29** (see Scheme 12). In this sense, we found that this cyanohydrin derivative could be obtained without purification and isolation of aldehyde **10**. More precisely, our desired cyanohydrin **29** was obtained by applying the method recently developed by Taillefer and coworkers for the cyanosilylation of aldehydes and ketones catalyzed by bis(triphenylphosphoranylidene)ammonium chloride (PNPCI).¹⁷ Thus, the



SCHEME 16 Scalable synthesis of the cyanohydrin fragment.



SCHEME 17 Final steps. Isolation of (–)-berkelic acid.

crude product of the reaction of oxidation of hydroxyacid **36** was reacted in neat triethylsilyl cyanide in the presence of a catalytic amount of PNPCI to give, after 1 h at room temperature, the cyanohydrin derivative **29** as an inconsequential mixture of isomers at the cyanohydrin center. Consequently, our desired cyanohydrin derivative **29** could be readily synthesized from dimethyl-(D)-malate in 31% global yield following a sequence in which all steps could be performed on a gram scale (1.0 g of the cyanohydrin derivative **29** was prepared).

With gram quantities of the iodide **34** and cyanohydrin **29** in hand, we tackled the final steps of our planned sequence (Scheme 17). For the coupling of these two fragments, we adopted the method described by Rychnovsky and Swenson for the alkylation of anions derived from cyanohydrins.¹⁸ Thus, cyanohydrin **29** was deprotonated with lithium diisopropylamide (LDA) in the

presence of 1,3-dimethyl-3,4,5,6-tetrahydro-2(1*H*)-pyrimidinone (DMPU) at -78°C . Further addition of iodide **34**, previously treated with LDA to deprotonate the phenol, led to the corresponding coupling product after 2.5 h at -60°C . The careful control of the temperature was crucial in affording good results in this coupling reaction. Final treatment of the crude of this reaction with tetrabutylammonium fluoride (TBAF) led to the diester **37** in 88% yield. Again, this sequence could be performed on a gram scale and it allowed the synthesis of 1.2 g of **37** in one batch. X-ray crystallographic analysis of **37** confirmed it as the (–)-berkelic acid methyl ester. At this point, with more than 1 g of diester **37** in hand, we were just one step away from our target. We only needed to accomplish a selective saponification of the aromatic methyl ester. It should be noted that diester **37** is a very stable compound and no decomposition was observed when stored for long periods. However, we were very concerned about Fürstner's statement about the stability of (–)-berkelic acid: *"we encountered problems in the purification, handling, and storage of (–)-berkelic acid such that oxidative degradation was a common frustration."*⁹ Thus, we thought that it would be very imprudent to risk all 1.2 g of diester **37** to get grams of a product that would decompose in short order. The last step of our synthesis was thus performed on a small scale (50 mg of **37** were used) following the protocol described by De Brabander that calls for treatment of diester **37** with an excess of tributyltin oxide in toluene at reflux for 10 h.⁸ It should be noted that this protocol was the only one of several methods attempted that allowed the selective hydrolysis of the aromatic ester. However, our main problem when we performed this reaction was the removal of the excess of tin-containing species and their separation from the final, precious product. This led us to develop a liquid–liquid extraction protocol in two stages that proved very effective. Thus, the crude of the reaction was diluted with acetonitrile and aqueous HCl (1 M) and stirred for 15 min. The aqueous phase was discarded and the acetonitrile organic phase was carefully extracted with hexane. The hexane phases mostly containing the tin species were discarded and the acetonitrile phase was concentrated and the residue further purified by conventional silica gel column chromatography. It was really a pleasure to see that the product coming off the column was pure (–)-berkelic acid (25 mg, 55% yield). A short communication on this successful scalable synthesis of (–)-berkelic acid was quickly sent for publication just before Christmas 2011 and the paper appeared on the Web on April 4, 2012.¹⁹ This work was highlighted in *Synfacts* in an article written by Ley and Frost.²⁰

6 CONCLUSIONS

In summary, starting with the discovery of a new catalytic method for the synthesis of chroman spiroacetals, we have been able to synthesize the relatively complex natural product (–)-berkelic acid. Thus, a topic (the multicomponent catalytic coupling reactions) that initially did not promise any short-term

revenue in terms of applicability, turned to be a powerful tool to get a relatively complex natural product. We believe that this example showcases how important the work on basic synthetic chemistry is to provide new methods to efficiently construct complex structures in a few steps.²¹ The synthesis of (–)-berkelic acid here described was easily accomplished from three commercial materials (methyl 2,4,6-trihydroxybenzoate, (*S*)-(–)-3-butyn-2-ol, and dimethyl-(*D*)-malate). Notably, from (*S*)-(–)-3-butyn-2-ol, containing just one stereocenter, we obtained the central core of the natural product, containing five stereocenters, without the need of any other chiral reagent or catalyst. This was achieved by a new silver-catalyzed reaction that allowed the construction of this central core in just one step. All but the last step were conducted on a gram scale and thus, we believe that the (–)-berkelic acid supply issue should be considered solved. Finally, the modular strategy followed should allow the easy production of several analogues of the natural product for biological activity studies.

ACKNOWLEDGMENTS

Financial support for this work was provided by MICINN (grant CTQ2010-16790), FICYT of Principado de Asturias (Severo Ochoa grant to T. A.), and MEC (FPU grant to A. M.). We particularly thank Dr. Baris Temelli (Hacettepe University of Ankara-Turkey) his contribution to the success of this project.

REFERENCES

1. A good example on the utility of natural products and their analogues is ingenol. See: Jørgensen, L.; McKerrall, S. J.; Kuttruff, C. A.; Ungeheuer, F.; Felding, J.; Baran, P. S. *Science* **2013**, *341*, 878–882. See also references therein.
2. Wilson, Z. E.; Brimble, M. A. *Nat. Prod. Rep.* **2009**, *26*, 44–71.
3. Stierle, D. B.; Stierle, A. A. Atta-ur-Rahman, Ed.; *Studies in Natural Products Chemistry*; Vol. 39; Elsevier Science: Amsterdam, 2013; pp 1–45.
4. Stierle, A. A.; Stierle, D. B.; Kelly, K. *J. Org. Chem.* **2006**, *71*, 5357–5360.
5. Wu, X.; Zhou, J.; Snider, B. B. *J. Org. Chem.* **2009**, *74*, 6245–6252.
6. Buchgraber, P.; Snaddon, T. N.; Wirtz, C.; Mynott, R.; Goddard, R.; Fürstner, A. *Angew. Chem. Int. Ed.* **2008**, *47*, 8450–8454.
7. Wu, X.; Zhou, J.; Snider, B. B. *Angew. Chem. Int. Ed.* **2009**, *48*, 1283–1286.
8. Bender, C. F.; Yoshimoto, F. K.; Paradise, C. L.; De Brabander, J. K. *J. Am. Chem. Soc.* **2009**, *131*, 11350–11352.
9. Snaddon, T. N.; Buchgraber, P.; Schulthoff, S.; Wirtz, C.; Mynott, R.; Fürstner, A. *Chem. Eur. J.* **2010**, *16*, 12133–12140.
10. Wenderski, T. A.; Marsini, M. A.; Pettus, T. R. *Org. Lett.* **2011**, *13*, 118–121.
11. (a) McLeod, M. C.; Wilson, Z. E.; Brimble, M. A. *Org. Lett.* **2011**, *13*, 5382–5385; (b) McLeod, M. C.; Wilson, Z. E.; Brimble, M. A. *J. Org. Chem.* **2012**, *77*, 400–406.
12. Rodríguez, F.; Fañanás, F. J. *Synlett* **2013**, *24*, 1757–1771.

13. (a) Alcaide, B.; Almendros, P.; Alonso, J. M. *Org. Biomol. Chem.* **2011**, 9, 4405–4416;
(b) Rudolph, M.; Hashmi, A. S. K. *Chem. Commun.* **2011**, 47, 6536–6544;
(c) Rodríguez, F.; Fañanás, F. J. Attanasi, O. A.; Spinelli, D., Eds.; Targets in Heterocyclic Systems, Chemistry and Properties; Vol. 13; Società Chimica Italiana: Rome, 2009; pp 273–302; (d) Patil, N. T.; Yamamoto, Y. *Chem. Rev.* **2008**, 108, 3395–3442.
14. Barluenga, J.; Mendoza, A.; Rodríguez, F.; Fañanás, F. J. *Angew. Chem. Int. Ed.* **2009**, 48, 1644–1647.
15. Renaud, P.; Hürzeler, M.; Seebach, D. *Helv. Chim. Acta* **1987**, 70, 292–298.
16. Santiello, E.; Manzocchi, A.; Farachi, C. *Synthesis* **1980**, 563–565.
17. Lacour, M.-A.; Rahier, N. J.; Taillefer, M. *Chem. Eur. J.* **2011**, 17, 12276–12279.
18. Rychnovsky, S. D.; Swenson, S. S. *J. Org. Chem.* **1997**, 62, 1333–1340.
19. Fañanás, F. J.; Mendoza, A.; Arto, T.; Temelli, B.; Rodríguez, F. *Angew. Chem. Int. Ed.* **2012**, 51, 4930–4933.
20. Ley, S. V.; Frost, J. R. *Synfacts* **2012**, 8, 813.
21. Fürstner, A. *Angew. Chem. Int. Ed.* **2014**, 53, 8–9.

The Mysterious Case of the Kingianins

Kathlyn A. Parker¹ and Hee Nam Lim²

Department of Chemistry, Stony Brook University, Stony Brook, New York, USA

¹Corresponding author: kathlyn.parker@stonybrook.edu

Chapter Outline

1. Introduction—What's Going on Here?	52	6. Pursuit of the Intramolecular RCDA Approach	61
1.1. The Structure of Kingianin A—Diels–Alder Origins?	52	6.1. Selection of an RCDA Substrate	61
1.2. The Kingianin Series—Structures and Biological Activities	52	6.2. Observations	63
2. Analysis of the Problem—Regio- and Stereochemical Issues	53	6.3. A Digression	64
3. Preliminaries: Tests of the RCDA Approach with Model Compounds	55	7. Synthesis of Kingianin A	65
3.1. Preparation of a Simple Model System	56	8. “Go Fish”—Pursuit of the Intermolecular RCDA Approach	66
3.2. Feasibility of the Key RCDA Step	57	9. Formal Synthesis of Kingianin A and Synthesis of Kingianins D, F, H, and J	68
4. Selecting a Strategy for the Total Synthesis of Kingianin A	59	10. NCI 60 Test Results for Kingianins A (NSC#D-768505/1) and H (NSC#D-768506/1)	70
5. Getting Started: Synthesis of a Pre-Kingianin A Equivalent	60	11. Reconsidering the Biosynthesis	71
		12. Conclusions	71
		Acknowledgments	77
		References	77

2. Current address: Department of Chemistry, University of Texas, Austin, TX 78712-1224, USA

1 INTRODUCTION—WHAT'S GOING ON HERE?

1.1 The Structure of Kingianin A—Diels–Alder Origins?

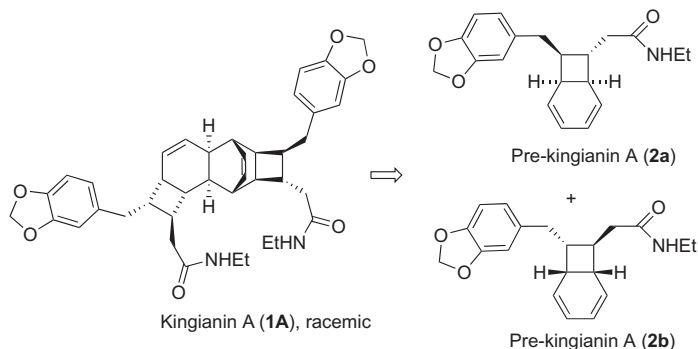
In July of 2010, the structure of kingianin A (**1A**),¹ a secondary metabolite isolated from the Malaysian tree *Endiandra kingiana* Gamble, appeared in the ASAP of *Organic Letters*. For us at that moment, the disclosure of this molecule was very stimulating. It certainly looked like a Diels–Alder dimer (Scheme 1) of two identical enantiomers of bicyclooctadiene **2**, a molecule that has been termed pre-kingianin A.² The recognition that the structure of kingianin A corresponds to a Diels–Alder product was not missed by the isolation team. Yet kingianin A cannot be the product of a thermal Diels–Alder reaction. Cyclohexadienes (unlike cyclopentadienes) do not readily undergo thermal dimerization,³ and this reaction would not be expected to take place in a tree or in a symbiont. Furthermore, an enzymatic construction of the pentacyclic ring system is unlikely because the natural product itself is racemic.

Solving the riddle of the presumably nonenzymatic, Diels–Alder-based biosynthesis of kingianin A might provide us with the key step for its total synthesis. Conversely, a synthetic method that effected the critical Diels–Alder cycloaddition could give us a hint as to the mechanism of this step in the biosynthesis.

One of us remembered (! no kidding, actually remembered !) the remarkable 1981 publication from Bauld and coworkers in the *Journal of the American Chemical Society* in which the radical cation Diels–Alder (RCDA) dimerization of cyclohexadiene was reported.⁴ Revisiting the paper after almost 30 years, the senior author noted the preference of the dimerization for formation of the *endo* product. The RCDA reaction of appropriate bicyclooctadienes therefore appeared to be a promising method for construction of the pentacyclic core of kingianin A, which corresponds to an *endo* Diels–Alder transition state.

1.2 The Kingianin Series—Structures and Biological Activities

At the time, there was a second mystery in the kingianin story. The isolation and structure determination of kingianin A were reported by a binational



SCHEME 1 Retrosynthesis and retrobiosynthesis: the Diels–Alder approach presents itself.

isolation team consisting of researchers from the Institute of the Chemistry of Natural Products at the French National Center for Research (CNRS) outside Paris and from the University of Malaya at Kuala Lumpur. We assumed that the isolation team followed the fractionation of their natural product extracts by means of an activity-based assay. However, their communication did not reveal the screen(s) that was (were) employed. It did allude to the isolation of 13 other “derivatives” and noted that some of these had “interesting biological properties.” We were eager to know the activities that the kingianins exhibited.

Consequently, we wrote to Dr. Marc Litaudon at the CNRS, asking for information on the additional structures and on the biological tests that had been performed. We also offered to supply synthetic materials, possibly including chiral materials, for his bioassay. However, Dr. Litaudon already had a collaboration in place for the total synthesis of kingianin A and analogues and for biological studies.

With no further information on the series of compounds or their activities, we nonetheless began the pursuit of model compounds and of intermediates for our synthesis. We thought that the structure of kingianin A alone justified its synthesis—but we were hopeful that the biological activity would be equally provocative.

Approximately 10 months after the appearance of the kingianin A structure, the Litaudon team published the structures of the 13 additional kingianins.⁵ Among the naturally occurring kingianins isolated are eight (A–F, H, and J, [Figure 1](#)) that appear to be derived from pairs of bicyclooctadienes in which the side chains are identical. The carbon skeleton of kingianin H is homologous to that of kingianin A and the carbon skeleton of kingianin J is homologous to that of kingianin F.

The second Litaudon report described the methods required to separate each of the racemic compounds from the others as well as the specifications for a chiral high-pressure liquid chromatography (HPLC) method that separated some pairs of enantiomers.

The second kingianin paper also tabulated the activities of the kingianins in an affinity displacement assay with the Bcl-xL protein, a member of the Bcl family that is involved in the regulation of apoptosis.⁶ Inhibitors of the antiapoptotic Bcl proteins are of significant interest in the search for anticancer drugs with new mechanisms of action.⁷

2 ANALYSIS OF THE PROBLEM—REGIO- AND STEREOCHEMICAL ISSUES

We examined the architecture of the naturally occurring kingianins and the stereochemical features of the Diels–Alder transition states that would lead to each of them. In every case, the pentacyclic core was invariant; that is, the relative stereochemistry at carbons 2, 5, 6, 7, 2', 3', 6', and 7' was identical. Furthermore, although the stereochemistry of the substituents at carbons

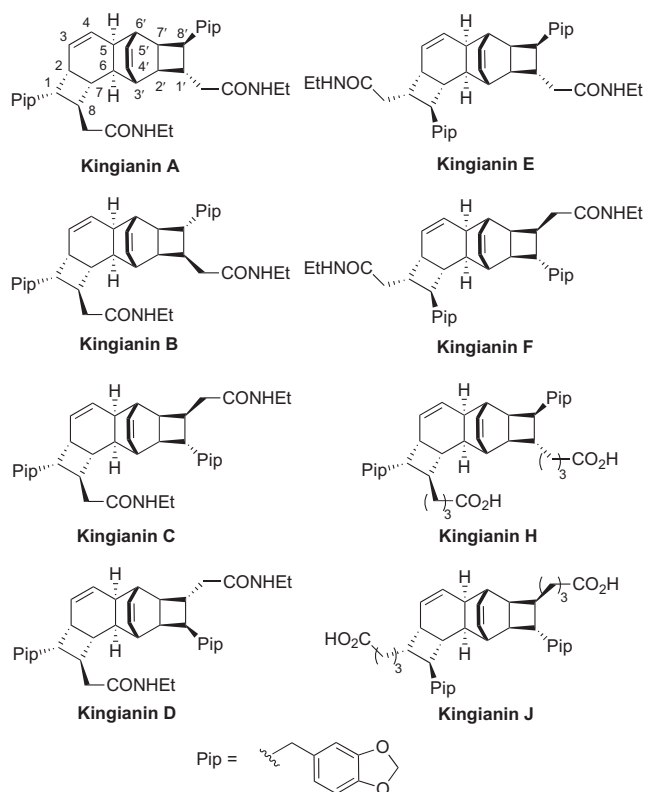


FIGURE 1 Kingianins A, H; B, C, D, E, F, and J.

1' and 8' varied (always *trans* but 1' α , 8' β or 1' β , 8' α), it was always constant at carbons 1 and 8 (1 α and 8 β).

Our observations led us to propose a general model for the RCDA cycloadditions of pre-kingianins with themselves or with each other. This model is based on a sterically least hindered *endo* transition state and utilizes the olefin adjacent to the *exo* substituent as the dienophile.⁸ Applied to pre-kingianin A (**2a** or its enantiomer **2b**), our model predicts that two molecules of one enantiomer would undergo the RCDA reaction to provide one enantiomer of kingianin A. Racemic pre-kingianin A, on the other hand, would give racemic kingianin A and a racemic isomer (Figures 2 and 3). This racemic compound was later reported as a congener of kingianin A; it is known as kingianin D.⁵

At this point, we should note that transition states for the cycloadditions leading to all of the kingianins fit the stereochemical model. In particular, kingianin F appears to be the Diels–Alder product of two identical *exo* isomers of a monomer that we designate here as pre-kingianin F, **3a** and its

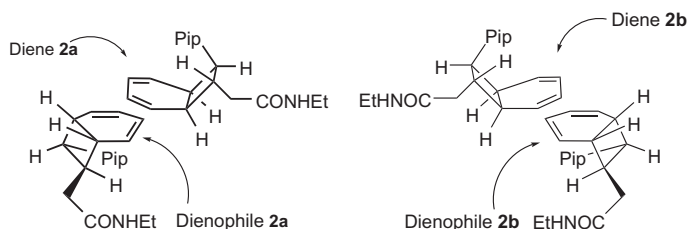


FIGURE 2 Left: Cycloaddition of one molecule of pre-kingianin A with an identical molecule. This arrangement corresponds to formation of one enantiomer of racemic kingianin A. Right: Same event as that on the left, but with the enantiomeric pre-kingianin A, leading to the second enantiomer present in racemic kingianin A.

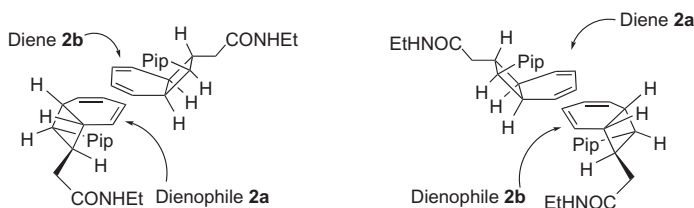


FIGURE 3 Left: Cycloaddition of one molecule of pre-kingianin A with a molecule of its enantiomer. This arrangement corresponds to formation of kingianin D. Right: Same event as that on the left but with the opposite enantiomers assuming the roles of diene and dienophile.

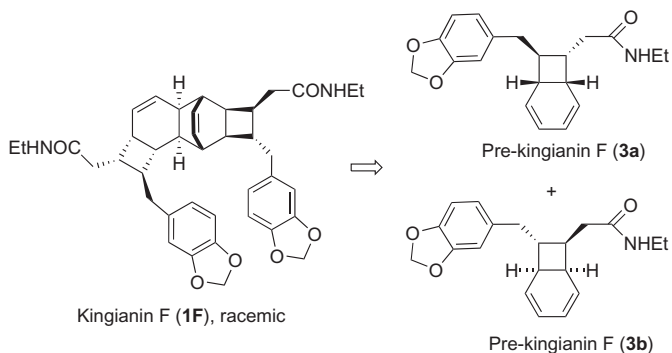
enantiomer **3b** (Scheme 2; Figure 4). Each of the kingianins B, C, and E appears to be a cycloadduct of an *endo* bicyclooctadiene **2** and an *exo* bicyclooctadiene **3**.

Representatives of only six of the eight apparently favored isomers in the kingianin series (those derived from an *endo* transition state, dienophilic olefin adjacent to the *exo* substituent) have been isolated. A kingianin that would be the cycloaddition product of two enantiomeric *exo* isomers of pre-kingianin F (i.e., **3a** and **3b**) has not been reported. Likewise, kingianin corresponding to a cycloaddition of a dienophile **3a** and a diene **2b** (and the enantiomeric pair) is not known. We here designate the prototypes for these two series as kingianins Y and Z (Figure 5).

3 PRELIMINARIES: TESTS OF THE RCDA APPROACH WITH MODEL COMPOUNDS

Inspired by what appeared to be an excellent match between method and target, we reproduced the RCDA dimerization of 1,3-cyclohexadiene⁴ and began to test preparations of substituted cyclohexadiene monomers that might serve as potentially useful intermediates in a total synthesis.

Meanwhile, our suspicion that pre-kingianin structures did not undergo thermal dimerization was confirmed by a report from Moses *et al.*² This group



SCHEME 2 Kingianin F appears to be the dimer of two identical enantiomers of bicyclocloctadiene **3**, that is, **3a** with **3a** and **3b** with **3b** (Figure 4).

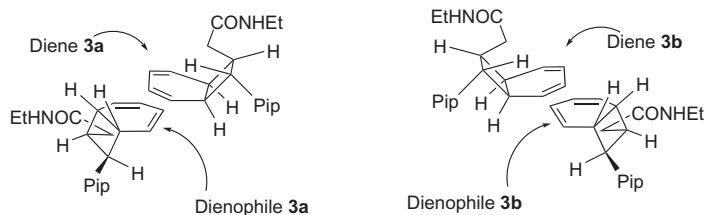


FIGURE 4 Cycloadditions to give racemic kingianin F.

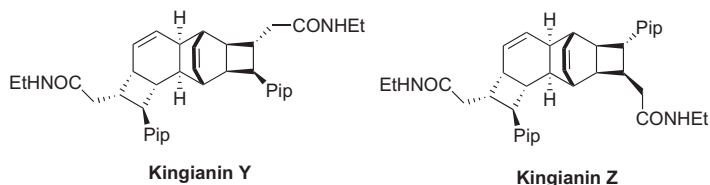
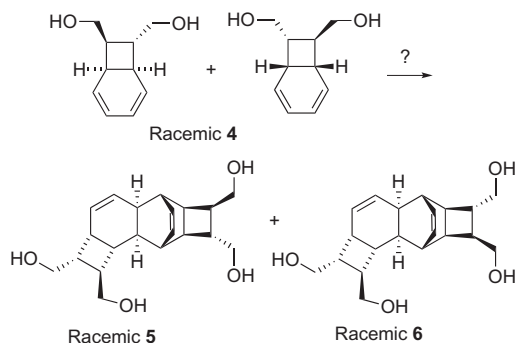


FIGURE 5 Unknown (to date) kingianins as ethyl amides.

considered, as we did, that thermal dimerization of pre-kingianins was unlikely. They prepared isomers **2** and **3** and demonstrated their stabilities, seeing only interconversion of these two compounds (by cycloreversion/cyclization) when they were heated to 195 °C.

3.1 Preparation of a Simple Model System

We planned to test the RCDA reaction on the known diol **4** (an intermediate in Nicolaou's endiandric acid synthesis)⁹ or a derivative thereof (Scheme 3). These model compounds have substituents at the relevant positions on the cyclobutane ring. However, unlike the pre-kingianin isomeric pairs, which have the potential to afford eight racemic *endo* Diels–Alder products,



SCHEME 3 Planned model study.

dimerization of a racemic mixture of a substrate **4** can give only two *endo* cycloadducts **5** and **6**; therefore, our analysis of this product mixture would be relatively simple.

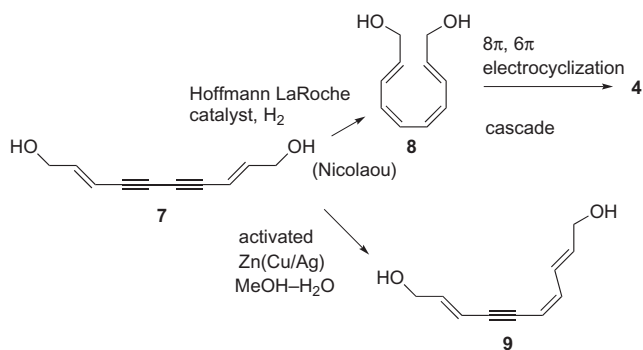
Diol **4** had been prepared from diol **7** by a cascade initiated by semi-hydrogenation; presumably intermediate diol **8** undergoes *in situ* $8\pi/6\pi$ tandem electrocyclicization. We prepared diol **7** in one step as described and planned to repeat this conversion.

We noted that the Nicolaou group had used a Lindlar catalyst that was a “gift from Hoffmann LaRoche . . . , courtesy of Dr. John Partridge [and that this] gave superior results to those obtained with commercial catalysts.” As time had passed and my (Parker’s) good friend John Partridge was no longer with Hoffmann LaRoche, we gave this reaction our best shot with the commercially available Lindlar catalyst (Aldrich). However, despite numerous attempts, we did not obtain the reported bicycldiol **4**. We examined other reductive methods with P2-Ni,¹⁰ activated Zn,¹¹ and Zn–Cu catalysts,¹² obtaining mixtures of the fully or partially hydrogenated products. One notably selective reaction with the activated Zn–Cu catalyst gave alkyne **9** as a major product—interesting but not useful for our purpose (Scheme 4).

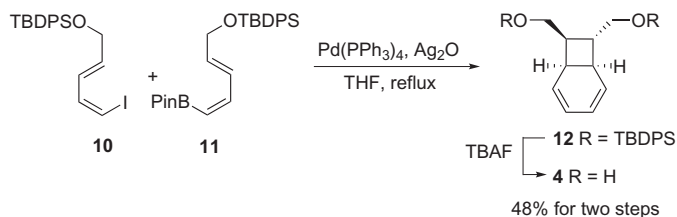
Modifying our strategy, we used a conventional coupling/tandem electrocyclicization method to obtain diol **4**. Thus, we prepared (*E,Z*)-iododiene **10**¹³ and (*E,Z*)-boronate **11** and subjected these intermediates to Suzuki conditions to obtain bicyclooctadiene **12**. Deprotection released diol **4** (Scheme 5).

3.2 Feasibility of the Key RCDA Step

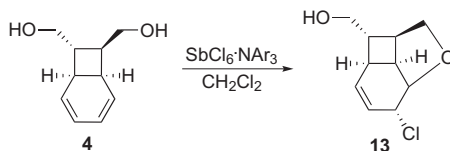
When we tested diol **4** under RCDA conditions, we recovered only chloroether **13** (Scheme 6). However, the corresponding diacetate **14** and the corresponding bis *p*-nitrobenzoate **15** gave mixtures (Scheme 7) that proved to be very interesting.



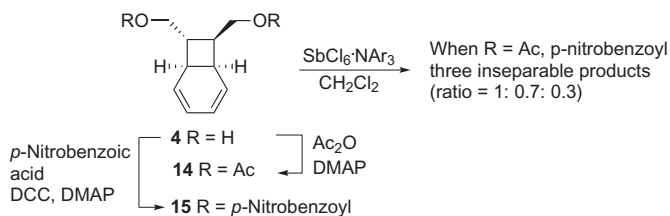
SCHEME 4 The semi-hydrogenation conditions of the diacetylene **7**.



SCHEME 5 Synthesis of the model diol **4** by Suzuki coupling.



SCHEME 6 Radical cation reaction of bicyclooctadiene diol **4**.



SCHEME 7 RCDA reactions of bicyclooctadienes diesters.

Although we were unable to separate the components of these mixtures, we could see signals in the NMR spectra that we believed to be characteristic of the kingianin core. While we had not isolated clean products, we now had additional confidence in the RCDA approach to kingianins. We therefore needed to select a plan that would get us to the end of the synthesis.

4 SELECTING A STRATEGY FOR THE TOTAL SYNTHESIS OF KINGIANIN A

Knowing that the RCDA reaction proceeded with bicyclooctadiene substrates, we projected four possible approaches to the total synthesis of kingianin A from racemic pre-kingianin A. (1) We could prepare chiral pre-kingianin A (or a synthetic equivalent) and accomplish the desired cycloaddition (as in [Figure 1](#)). (2) We could prepare racemic pre-kingianin A (or a synthetic equivalent), effect the intermolecular cycloaddition, and separate the kingianin A and kingianin D products by a chromatographic method. (3) We could find a trick that would facilitate separation of the desired kingianin A series product from its kingianin D series isomer. (4) We could find a trick that would allow selective reaction of pre-kingianin A through the transition state leading to the desired product (i.e., the transition state leading to the kingianin D series would be disfavored). Of course, each of these approaches has potential advantages and disadvantages.

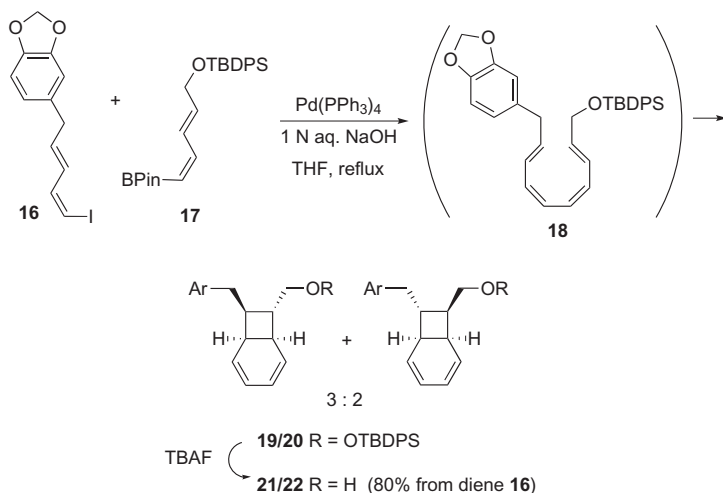
1. This would certainly work if we could prepare enantiomerically pure pre-kingianin A (i.e., **2a** or **2b**). Although there are a few examples of asymmetric induction in the preparation of similar cyclooctadiene derivatives, these have been tested with a more substituted tetraene precursor, which yields almost exclusively the two *endo* diastereomeric products. The best of these gives only moderate diastereomeric excesses, and it does require a bit of work.¹⁴ Furthermore, none of these methods has been applied to the preparation of cyclooctadienes that are only monosubstituted at the tetraene termini.
2. This would presumably work if we could reproduce the separation technology used by the isolation team. However, we really wanted to devise a synthesis that could be carried out without resorting to HPLC. In the preparation of pharmaceuticals, chromatography is an undesirable operation; HPLC is particularly bad because it is subject to limits of scale.
3. As we had no precedent for such a separation, we considered this approach to be “a fishing expedition.” Such excursions are occasionally successful but generally are not considered justifiable.
4. This approach was attractive because it relied on our ability to design a system in which the relative regio- and stereochemistry of the monomer

moieties would influence the accessibility of the transition state for reaction. In other words, thinking might help. Therefore, we found this approach intriguing and we pursued it.

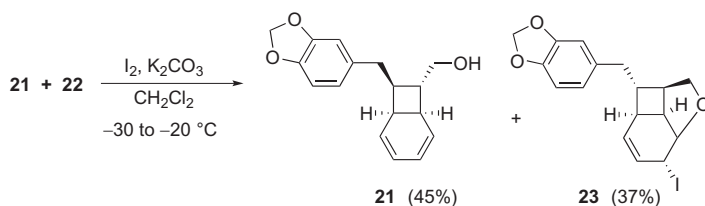
5 GETTING STARTED: SYNTHESIS OF A PRE-KINGIANIN A EQUIVALENT

We have had a fairly long-term interest in the synthesis of bicyclooctadiene natural products. Like others who have pursued these structures, we have used the Stille coupling as the standard method for preparing the linear *E,Z,Z,E*-tetraenes that undergo thermal $8\pi/6\pi$ cyclizations. Although this method had served its purpose admirably, we were eager to abandon the use of tin reagents. We screened conditions for the Suzuki reaction of vinyl iodide **16** and boronate **17**. Among the protocols examined in our system, that based on the tetrakis(triphenylphosphine) palladium reagent in aqueous NaOH and THF was superior to others, giving, after protecting group removal, a clean mixture of two bicyclic alcohols **21** and **22** in good yield (Scheme 8).

Carrying out the coupling on the allylic alcohol equivalent **17** offered a special advantage for our synthesis. We were aware of the trick used by Nicolaou for the differentiation of the *endo*- and *exo* alcohols in diol **4**. This involved treatment with I_2 and K_2CO_3 to effect iodoetherification in which the *endo* alcohol took part. By extension, we imagined that when the inseparable mixture of alcohols **21** and **22** was treated with iodine in the presence



SCHEME 8 Synthesis of bicyclooctadienes.



SCHEME 9 Removal of the *exo* alcohol **23** by iodoetherification.

of potassium carbonate, only isomer **22** would undergo iodoetherification. Indeed, this was the case and iodoether **23** and alcohol **21** were easily separated by chromatography (Scheme 9).

6 PURSUIT OF THE INTRAMOLECULAR RCDA APPROACH

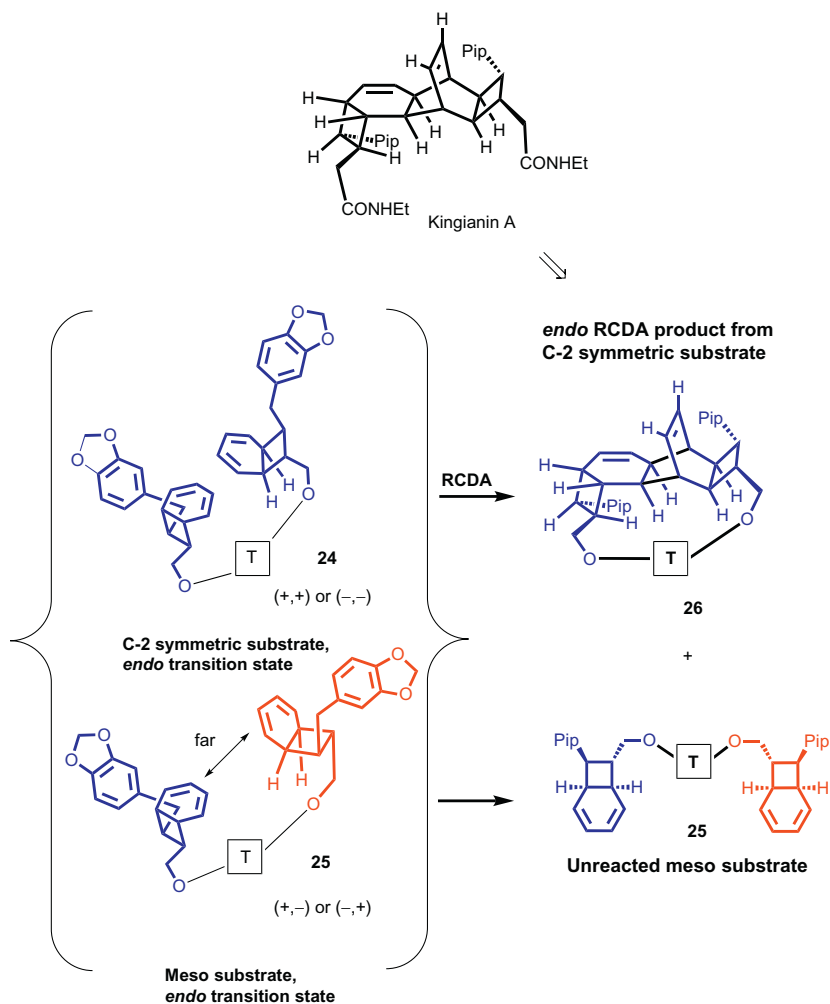
6.1 Selection of an RCDA Substrate

With easy access to clean alcohol **21**, we were prepared to examine the potential of our approach (4), that is, we would look for a trick. Our goal was to convert a racemic pre-kingianin A structure to a racemic kingianin A that did not contain a kingianin D-type isomer.

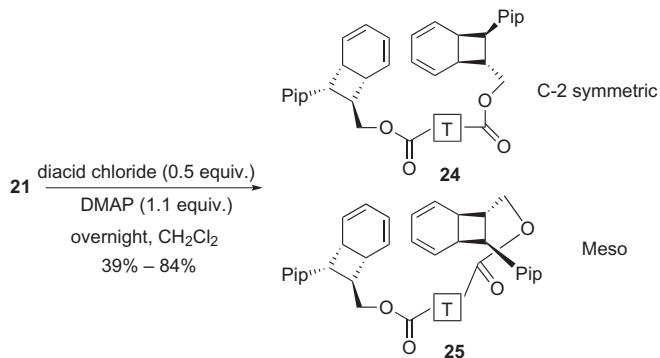
Our thought was that a C-2 symmetric dimer derived from alcohol **21** (e.g., **24a–e**) might easily adopt the transition state conformation required for dimerization of the cyclohexadiene moieties but that a meso dimer (**25**) derived from this alcohol would not be able to adopt a transition state that would lead to dimerization of its cyclohexadiene moieties (Scheme 10). We expected the cycloadduct from substrate **24** and recovered meso dimer **25** to be chromatographically distinct. This approach, if it proceeded as anticipated, had the advantage of allowing the recycling of alcohol **21**, which could be recovered from the unreacted meso dimer **25**. Therefore, we prepared a series of diester mixtures from racemic alcohol **21** (Scheme 11; Table 1). We were then ready to examine the hypothesis.

When tested, each of the ester mixtures **24/25a–e** gave two products, and in each case, the two were separable by preparative thin layer chromatography. We focused on the products from **24c/25c** (Scheme 12) because of the relatively high yields of both the substrate preparation and the RCDA reaction and the particularly easy separation of the RCDA products.

Detailed analysis of the NMR spectra of these two compounds showed that one was the anticipated dimer **26c** from the C-2 symmetric substrate and that the second was the *exo* cycloadduct **27** from the meso substrate. Removal of the tether from dimer **26c** gave diol **28**, which we considered a key intermediate on the route to kingianin A.

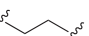
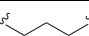
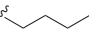
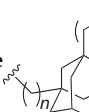


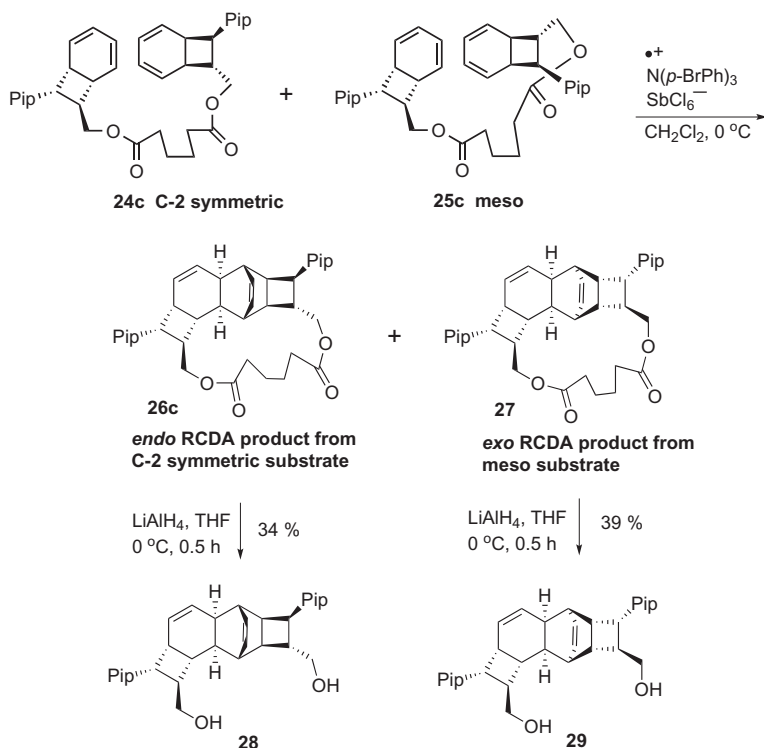
SCHEME 10 Anticipated selective dimerization of C-2 symmetric substrate.



SCHEME 11 Preparation of tethered substrates.

TABLE 1 Yields of Mixtures of Diastereoisomeric RCDA Substrates

Tether		Yield (%) 24 + 25
a 	Succinyl	72
b 	Glutaryl	84
c 	Adipoyl	75
de 	$n = 0$ Adamantyldicarboxyl	30
	$n = 1$ Adamantanediacyl	62

**SCHEME 12** Actual dimerization of the C-2 symmetric and meso substrates **24/25c** and liberation of free diols from the tethered products.

6.2 Observations

We also removed the tether from the second product to obtain diol **29**. Characterization of diols **28** and **29** revealed that they had potentially usefully different

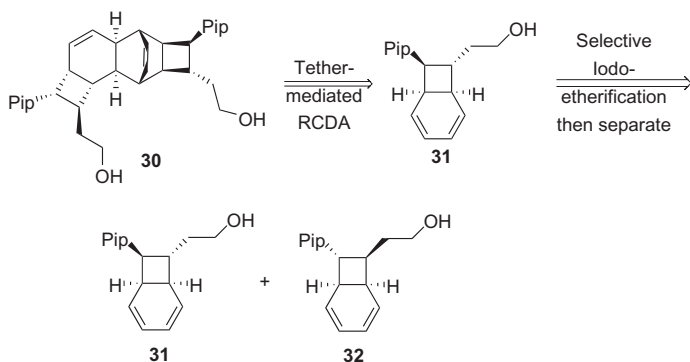
R_f values on a preparative TLC plate; diol **28** had an R_f value of 0.4 in 1:1 hex/-EtOAc, whereas diol **29** (from the tethered *exo* compound **25c**) had an R_f value of 0.60 under the same conditions. This was the first indication that diols in the kingianin series might be separable without resorting to HPLC methods.

Focusing on completion of the synthesis, we examined one-carbon chain lengthening strategies based on masked acyl cyanides¹⁵ and on modified Petersen olefinations.¹⁶ Preliminary experiments were not promising, and we considered the modification of our scheme in order to bypass the need for homologation.

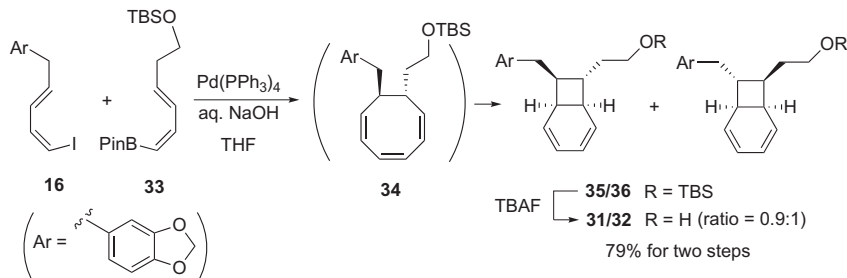
6.3 A Digression

We thought that the diol **30** might be available from *endo* alcohol **31** by a tether-mediated RCDA reaction as in the preparation of the diol **28**. A mixture of alcohol **31** and alcohol **32** should be available by the coupling/electrocyclization strategy, and the *exo* alcohol **32** would be removed by iodoetherification and chromatography (Scheme 13).

Following a conventional tandem coupling and electrocyclization strategy, we obtained a mixture of *endo*- and *exo* alcohols **31** and **32** (Scheme 14). These isomers were inseparable on TLC.



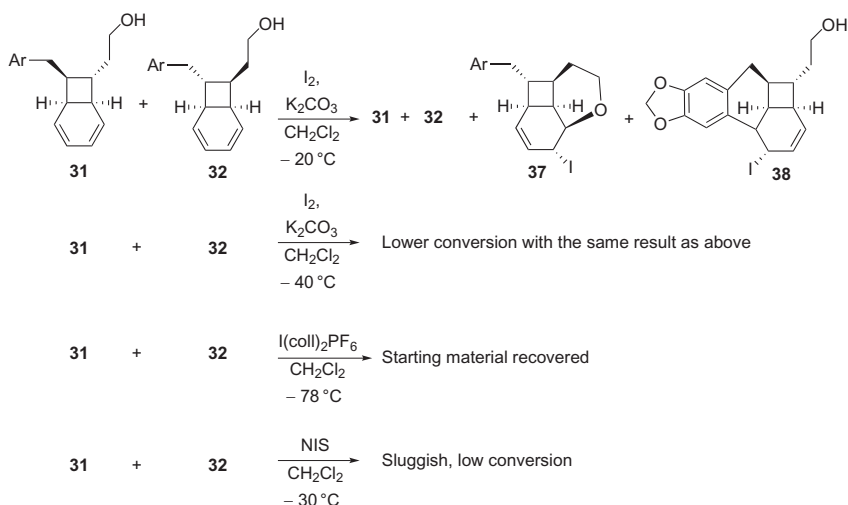
SCHEME 13 An alternative strategy to prehomologated diol **31**.



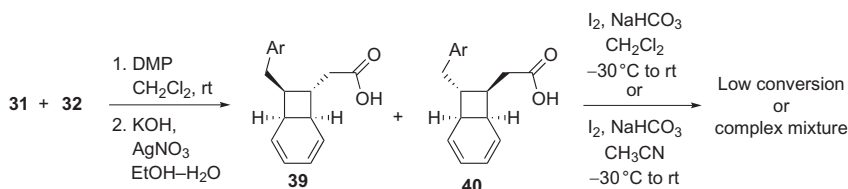
SCHEME 14 Synthesis of a mixture of the *endo*- and *exo*-alcohols **31** and **32**.

Thinking that we would be able to separate iodoether **37** from unreacted *endo* isomer **31**, we next carried out the iodoetherification procedure. However, in contrast to our expectation, the iodoetherification protocol gave a mixture that contained the Friedel–Crafts product **38** along with iodoether **37** and unreacted starting materials. Lowering the temperature or changing the iodine electrophile gave product mixtures that did not advance the synthesis (Scheme 15).

In addition, when we tuned the nucleophilicity of the side chain functionality by converting the alcohols to carboxylic acids, iodolactonization, when it occurred, appeared to be accompanied by the Friedel–Crafts alkylation (Scheme 16).



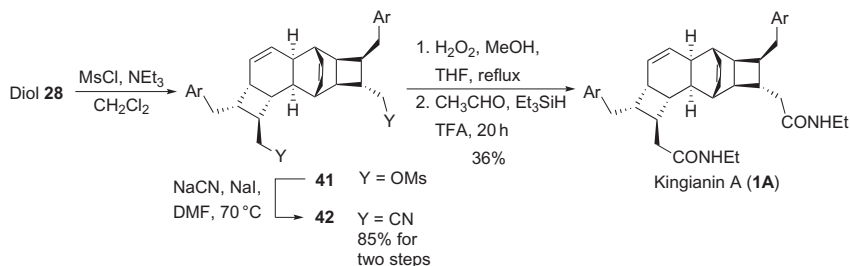
SCHEME 15 Iodoetherification of the *endo*- and *exo* alcohols **31** and **32**.



SCHEME 16 Preparation and attempted selective iodolactonization of the acids **39** and **40**.

7 SYNTHESIS OF KINGIANIN A

At this point, we returned to the one-carbon homologation strategy, adapting the procedure used by Moses *et al.* in the synthesis of pre-kingianin A. With the more complex diol **28**, this methodology proved efficient, completing the synthesis of the racemic natural product (Scheme 17) in a total of 12 steps from commercially available starting materials.



SCHEME 17 Double homologation: completion of the total synthesis of kingianin A.

In October 2012, we submitted a manuscript describing this total synthesis and we were subsequently pleased to see our work published in *Organic Letters*. We were happily surprised by what happened next. Shortly after the appearance of our communication online, we were contacted by Sabine Heller, an editor who had abstracted our paper for *Synfacts*.¹⁷ Then we learned that *Nature Chemical Biology* would feature it in the section on Research Highlights.¹⁸ And then Karl Hale wrote to tell us that the paper would be featured in the *Organic Letters/JOC/JACS* virtual issue on “Terpenoid- and Shikimate-Derived Natural Products Total Synthesis.”¹⁹ All of this led to tweets on the Stony Brook Chemistry Department webpage. Thus, we were introduced to the modern practice of publication highlighting and publication tweeting.

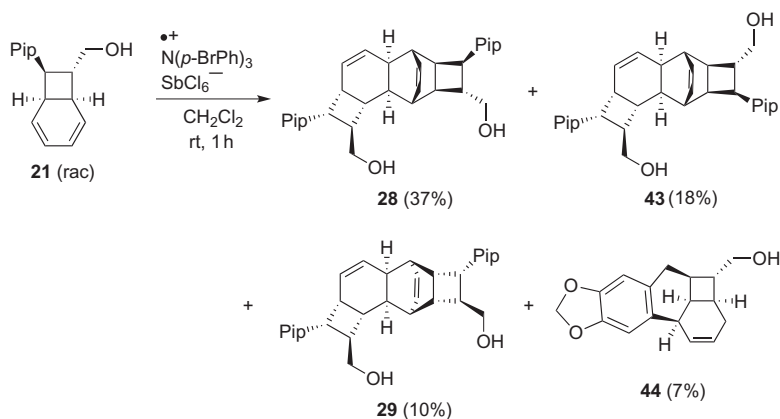
8 “GO FISH”—PURSUIT OF THE INTERMOLECULAR RCDA APPROACH

The observation that diols **28** and **29** were easily separated suggested to us that regio- and stereoisomeric diols corresponding to different kingianins might also differ significantly in their chromatographic properties. Indeed, if diols in the kingianin series were separable on standard chromatography (without the need to resort to HPLC), we would reconsider Approach #3 to the regio- and stereodiverse synthesis of multiple kingianins.

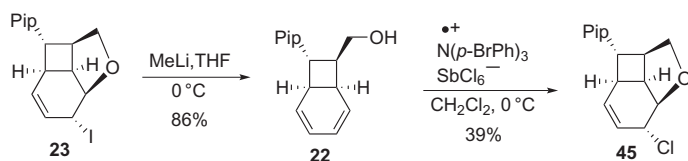
Indeed, when we examined the RCDA product mixture from alcohol **21**, we found that three RCDA products, isomeric diols **28**, **29**, and **43** and a non-Diels–Alder product **44** could be separated by preparative TLC (Scheme 18). Alcohol **28** corresponds in structure to kingianins A and H, and alcohol **43** corresponds to kingianin D.

We also examined the RCDA reaction of bicyclooctadienes derived from alcohol **22**. Alcohol **22** could be recovered from iodoether **23** by a simple reduction procedure. However, not surprisingly (see Scheme 6), this compound did not undergo the RCDA; rather it underwent cyclization, affording chloroether **45** when subjected to the electron transfer catalyst (Scheme 19).

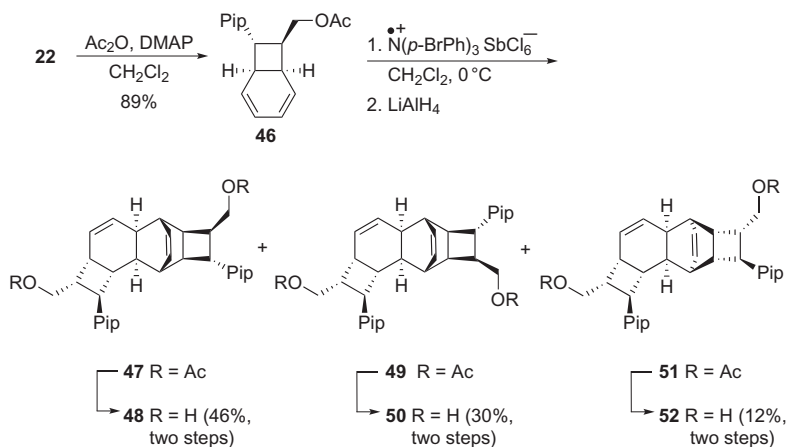
On the other hand, derivatization of alcohol **22** as the corresponding acetate gave a substrate that gave a mixture of three (two *endo* and one *exo*)



SCHEME 18 The intermolecular RCDA reaction of *endo* bicyclooctadienol **21**.



SCHEME 19 Recovery of alcohol **22** from iodoether **23** and its reaction with the electron transfer catalyst.



SCHEME 20 The intermolecular RCDA reaction of *exo* bicyclooctadiene.

RCDA products. Although these dimers were not easily separable, the lithium aluminum hydride reduction gave a mixture of diols **48**, **50**, and **52** that separated nicely on preparative TLC. Diol **48** corresponds in structure to kingianin F, and diol **50** corresponds to the hypothetical kingianin Z (Scheme 20).

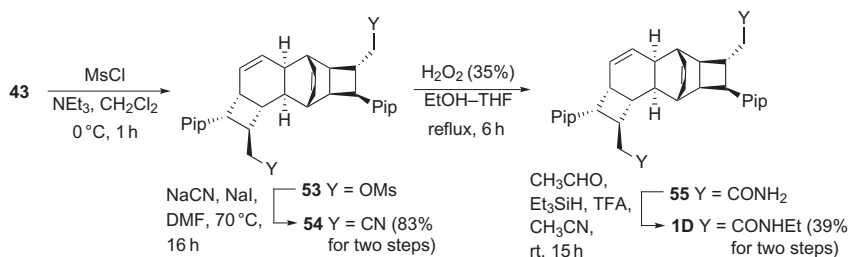
9 FORMAL SYNTHESIS OF KINGIANIN A AND SYNTHESIS OF KINGIANINS D, F, H, AND J

With diol **28** isolated from the intermolecular approach, we had completed a formal synthesis of kingianin A. With clean diol **43** in hand, we were able to apply the four-step double homologation to obtain kingianin D (Scheme 21). There were no surprises here.

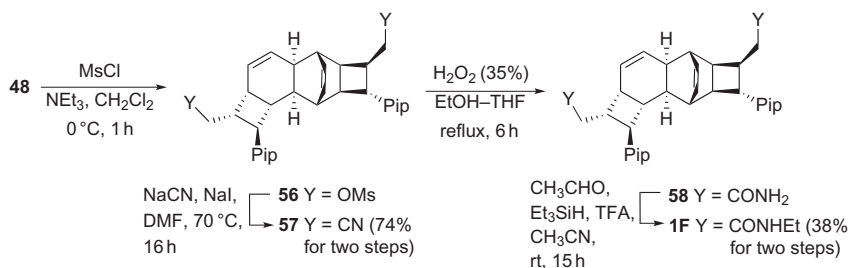
Likewise, the four-step double homologation nicely converted diol **48** to kingianin F in a straightforward fashion (Scheme 22).

Of the pseudosymmetric kingianins, the diacid kingianin H was reported to have the best activity in the Bcl-xL affinity displacement assay. Kingianin H was a particularly attractive synthetic target as we imagined that its synthesis might be particularly efficient. We required a three-carbon homologation of each of the side chains of diol **28**. For this, the reductive nickel-mediated conjugate addition of Manchand²⁰ proved to be excellent, converting diiodide **59** to diester **60**. Hydrolysis then completed the synthesis in a total of 9 steps from commercially available starting materials (Scheme 23).

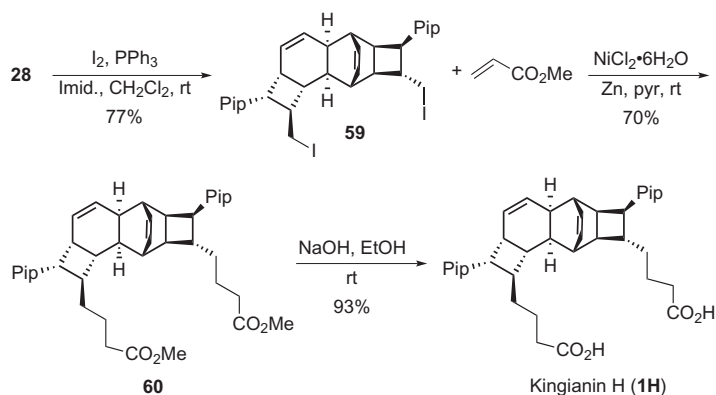
At about this time, the online *Angewandte* manuscript of Drew, Lawrence, and Sherburn appeared.²¹ This reported an intermolecular RCDA approach to a mixture of kingianins and the HPLC isolation of kingianins A, D, and F. This paper demonstrated the feasibility of preparing pre-kingianins by



SCHEME 21 Synthesis of kingianin D.



SCHEME 22 Synthesis of kingianin F.



SCHEME 23 Synthesis of kingianin H.

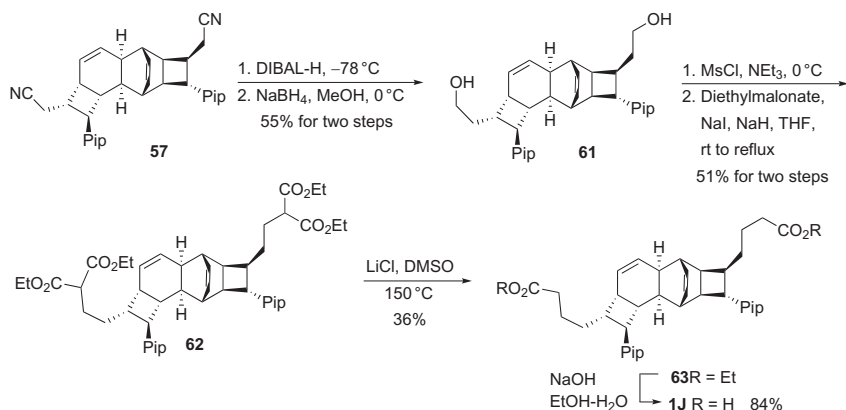
reduction of tetraynes to (*Z,Z,Z,Z*)-tetraene precursors and subsequent $8\pi/6\pi$ electrocyclicization. However, the latter reaction required heating to 100 °C, confirming the assumption that the (*Z,Z,Z,Z*)-tetraene is not a biosynthetic intermediate.

Noting the differences in emphasis and methods of preparation as well as the particularly efficient synthesis of kingianin H from our approach, we decided to complete the series of pseudosymmetric kingianins by preparing kingianin J.

We expected the synthesis of kingianin J to parallel that of kingianin H. However, when we applied Manchand reaction to the diiodide derived from diol **48**, we obtained products that appeared to have lost the Δ -3,4 olefin. Likewise, the reductive cobalt-mediated procedure of Cheng²² did not show the anticipated olefinic protons in the NMR spectrum of the crude product. We concluded that the C-1 side chain in compounds in the J series is situated very close to the double bond between carbons 3 and 4 and that reactive intermediates at this position may participate in intramolecular reactions with that double bond.

We knew, however, that we could do S_N2 chemistry at this position because we had converted diol **48** to dinitrile **57**. Therefore, we capitalized on this conversion, elaborating dinitrile **57** kingianin J by a series of sterically undemanding reactions. Thus, reduction to the dialdehyde and then to the diol **62** was followed by mesylation, malonic ester alkylation, dealkylative decarboxylation, and hydrolysis (Scheme 24).

This completed the total syntheses of the naturally occurring pseudosymmetric kingianins, A (formal synthesis), D, F, H, and J, by the intermolecular RCDA approach. Although the strategy required the separation of isomeric intermediates, separations were facile—either by selective conversion followed by chromatography or by preparative TLC. A full account of this work has now appeared.²³



SCHEME 24 Synthesis of kingianin J.

10 NCI 60 TEST RESULTS FOR KINGIANINS A (NSC#D-768505/1) AND H (NSC#D-768506/1)

Leverrier *et al.* had carried out activity-guided fractionation of the *E. kingiana* Gamble extract by means of an established competition bioassay method.²⁴ They then used this assay to measure the inhibition of the binding of the fluorescently labeled BH3 domain of Bak to Bcl-xL by each of the kingianins. Leverrier *et al.* noted that the kingianins with two acidic side chains were more active in the *in vitro* assay than those with only one acidic side chain and that those with no acid side chain were least active. They reported K_i values of 2 to $>300\ \mu\text{M}$ for the racemic compounds.

Acquisition of synthetic compounds allowed us to obtain activity data on racemic kingianins A and H in cell growth assays. In the one-dose test against the NCI60 panel, kingianin A showed detectable cell growth inhibition at $10^{-5}\ \text{M}$ ($10\ \mu\text{M}$); however, kingianin H showed no detectable activity at that dose. The complete NCI60 data for kingianin A (NSC#D-768505/1) and for kingianin H (NSC#D-768506/1) appear at the end of this chapter.

The biochemical and *in vitro* data appear inconsistent; however, the differences in structure may provide an explanation. In the competition assay, racemic kingianin H was active at $18 \pm 7\ \mu\text{M}$, whereas racemic kingianin A was <10 times as active. Presumably, there are barriers to passage across cell membranes for both compounds in the cell growth assays. It may be that this effect is more significant for the diacid kingianin H than for the diamide kingianin A. Although it is intriguing to note that the observed activity for kingianin A is clustered in the leukemia cell line panel,²⁵ kingianins A and H did not display exceptional activities at the concentrations tested in the NCI60 protocol.

In any event, the disruption of a protein-protein interaction with a small molecule is noteworthy.²⁶ In particular, the modulation of the Bcl

protein interactions with nonpeptide small molecules is an area of active research.²⁷

11 RECONSIDERING THE BIOSYNTHESIS

Returning to the question of the biosynthesis, we find that, although we have clues about the apparent nonenzymatic and nonthermal dimerization of pre-kingianin structures, we have discovered new questions that are not answered by results to date.

First, Drew, Lawrence, and Sherburn reported RCDA catalysis did not lead to the dimerization of pre-kingianin A (**2**).²¹ This certainly implies that pre-kingianin A is not the immediate biogenetic precursor of kingianin A by a nonenzymatic RCDA mechanism. Functional group modification after the dimerization is an obvious supposition.

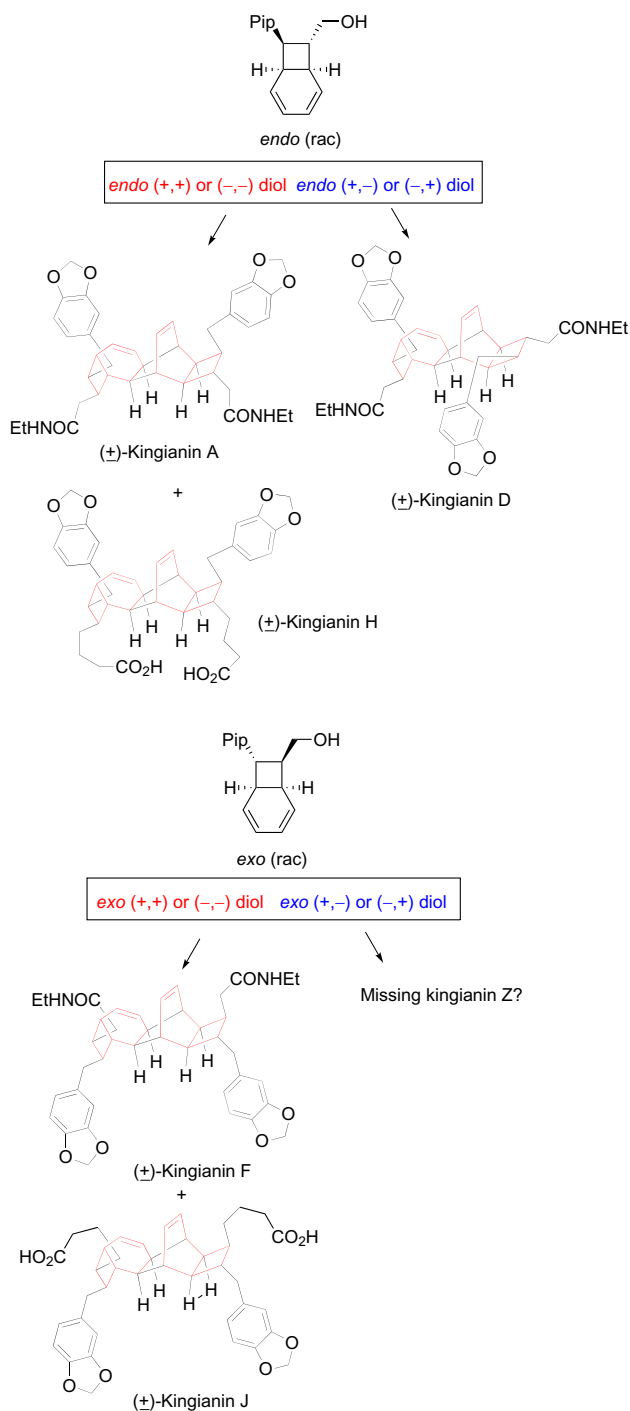
In addition, there is the broad question of why only six of the eight possible stereoisomeric pseudosymmetric dimers have been found in nature. Our laboratory approach, which is based on the reaction of a single racemic stereoisomer can, in principle, give only four of the possible products. Thus, it is interesting that the laboratory dimerization of cyclooctadiene **2** gives two *endo* kingianin structures that correspond to the natural products **1A** and **1D** and a minor amount of one *exo* Diels–Alder product. On the other hand, the intermolecular RCDA of cyclooctadiene **3** gives an *endo* kingianin structure corresponding to kingianin F and the *endo* kingianin structure corresponding to the as yet undiscovered kingianin Z. Of course, it is possible that kingianins Y and/or Z are natural products but that their activity in the isolation bioassay was negligible.

12 CONCLUSIONS

The structures of the products of nature continue to intrigue organic chemists. What are the mechanisms by which they are produced and how has evolution influenced their persistence? How can we take advantage of these compounds and their functions? In particular, can we use these natural products and the chemistry that we learn from them to improve human and veterinary health?

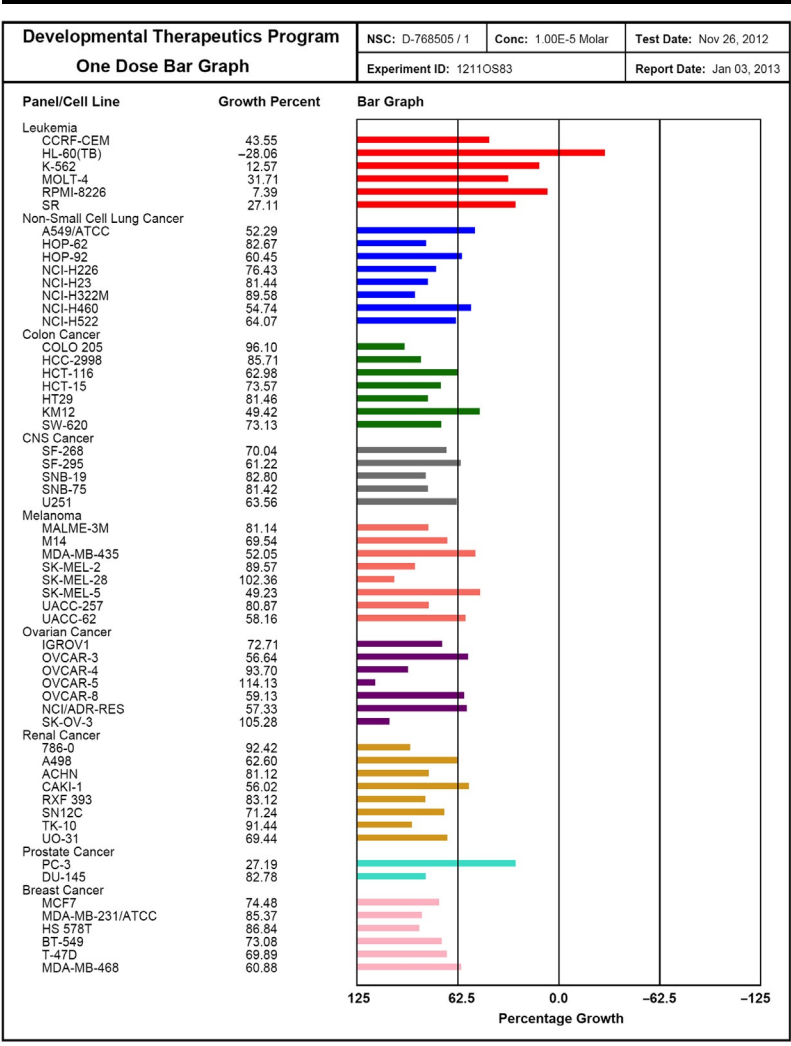
By developing what we believe to be a biomimetic approach to the kingianins, we have established the feasibility of a radical cation biosynthesis, and we have used this key reaction to develop a short chemical synthesis of five of the natural products (Scheme 25).

In addition, we discovered at least one general stereochemical influence on the key dimerization step. Finally, acquisition of kingianins from synthesis allowed us to obtain activity data for cell-based assays. The results of the NCI60 tests of kingianins A and H are given in Tables 2–5.



SCHEME 25 Summary of Kingianin synthesis by the intermolecular RCDA approach.

TABLE 2 One-Dose Test for Racemic Kingianin A (NSC# D-76805/1)



Growth % at 10⁻⁵ M.

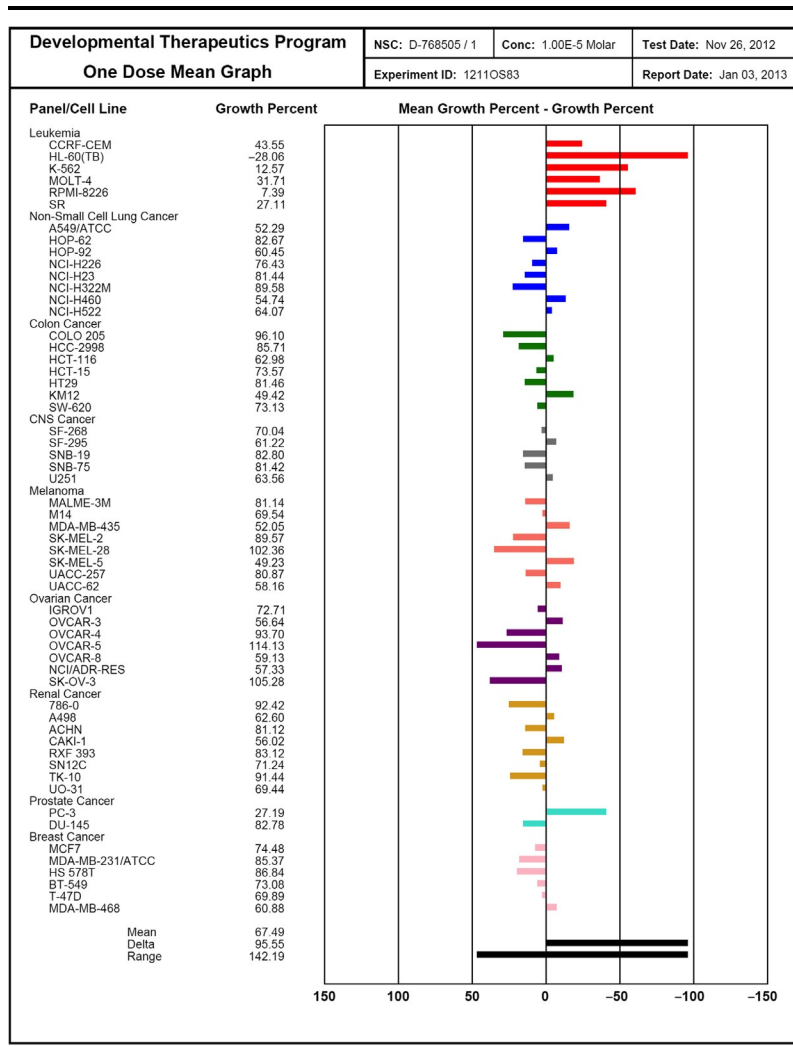
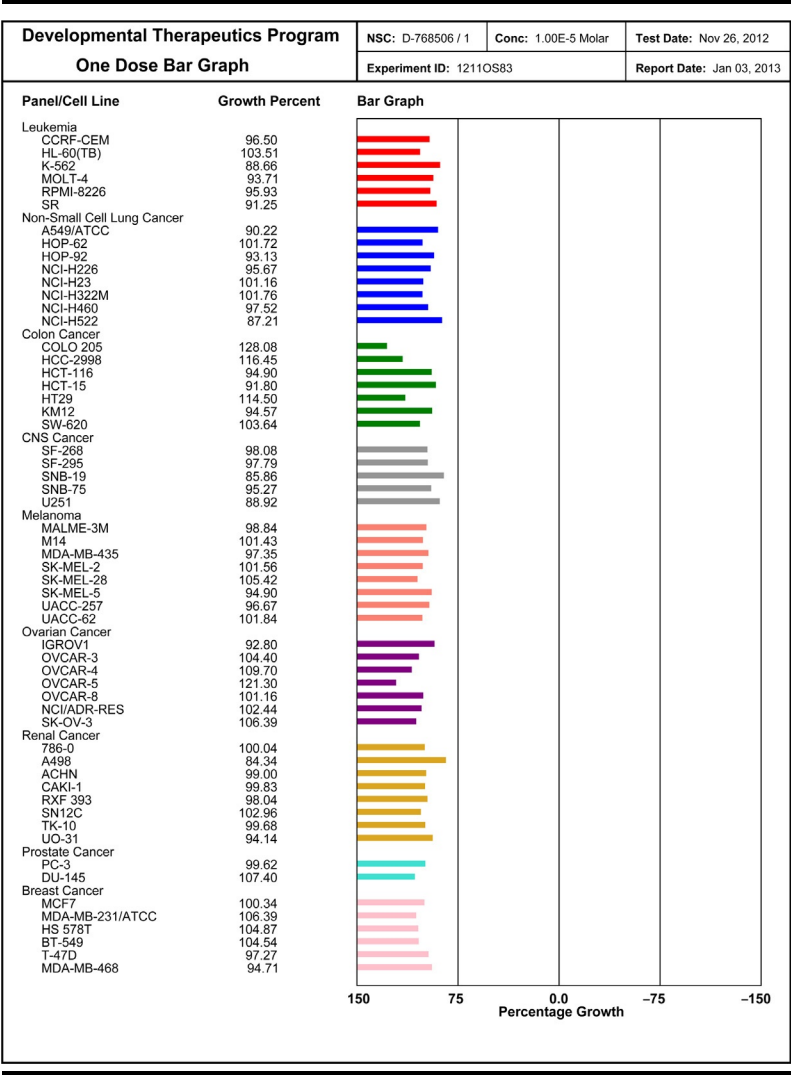
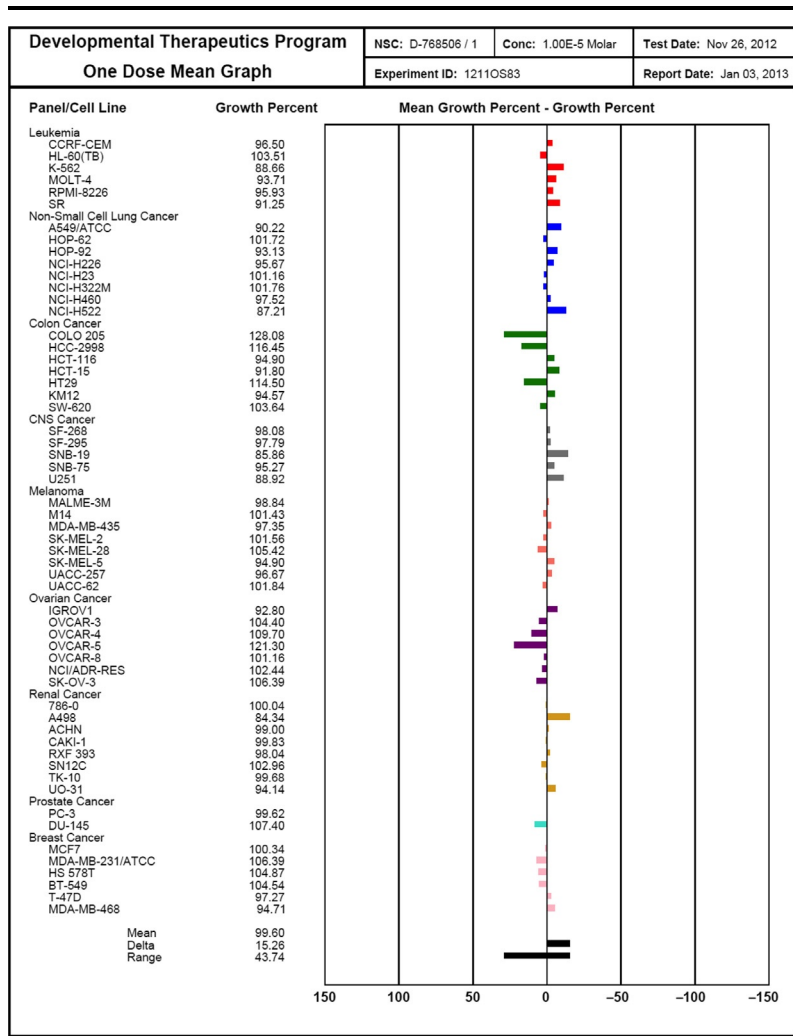
TABLE 3 One-Dose Test for Racemic Kingianin A (NSC# D-76805/1)Mean growth %—growth % at 10^{-5} M.

TABLE 4 One-Dose Test for Racemic Kingianin H (NSC# D-76806/1)



Growth % at 10⁻⁵ M.

TABLE 5 One-Dose Test for Racemic Kingianin H (NSC# D-76806/1)Mean growth %–Growth % at 10^{-5} M.

ACKNOWLEDGMENTS

We are grateful to the National Institutes of Health (GM 74776) and to the Targeted Research Opportunity (TRO) Program of the Carol M. Baldwin Breast Cancer Fund (Stony Brook University) for financial support of this work. In addition, we thank Te-Jung Hsu, Bo Liu, Daniel Resch, and Professor Joseph Lauher (Stony Brook University) for the X-ray crystallographic structure determination, Francis Picart (Stony Brook University) for expert assistance with NMR studies, and Yeongnam Choi for assistance with the graphics. We are grateful to Dr. John Beutler at the National Cancer Institute for facilitating the testing of our compounds and for helpful comments.

REFERENCES

1. Leverrier, A.; Dau, M. E. T. H.; Retaillieu, P.; Awang, K.; Gueritte, F.; Litaudon, M. *Org. Lett.* **2010**, *12*, 3638–3641.
2. Sharma, P.; Ritson, D. J.; Burnley, J.; Moses, J. E. *Chem. Commun.* **2011**, *47*, 10605–10607.
3. Valentine, D.; Turro, N. J., Jr.; Hammond, G. S. *J. Am. Chem. Soc.* **1964**, *86*, 5202–5208.
4. Bellville, D. J.; Wirth, D. W.; Bauld, N. L. *J. Am. Chem. Soc.* **1981**, *103*, 718–720.
5. Leverrier, A.; Awang, K.; Gueritte, F.; Litaudon, M. *Phytochemistry* **2011**, *72*, 1443–1452.
6. Youle, R. J.; Strasser, A. *Nat. Rev. Mol. Cell Biol.* **2008**, *9*, 47–60.
7. (a) Fais, F.; Tenca, C.; Ghiotto, F.; Bruno, S. *Int. J. Hematol. Oncol.* **2013**, *2*, 397–407; (b) Balakrishnan, K.; Gandhi, V. *Invest. New Drugs* **2013**, *31*, 1384–1394.
8. Lim, H. N.; Parker, K. A. *Org. Lett.* **2013**, *15*, 398–401.
9. Nicolaou, K. C.; Petasis, N. A.; Zipkin, R. E.; Uenishi, J. *J. Am. Chem. Soc.* **1982**, *104*, 5555–5557.
10. Oger, C.; Bultel-Poncé, V.; Guy, A.; Balas, L.; Rossi, J.-C.; Durand, T.; Galano, J.-M. *Chem. Eur. J.* **2010**, *16*, 13976–13980.
11. Mulzer, J.; Berger, M. *J. Org. Chem.* **2004**, *6*, 891–898.
12. Bolad, W.; Schroer, N.; Sieler, C. *Helv. Chim. Acta* **1987**, *70*, 1025–1040.
13. Gao, D.; O'Doherty, G. A. *Org. Lett.* **2010**, *12*, 3752–3755.
14. (a) Kim, K.; Lauher, J. W.; Parker, K. A. *Org. Lett.* **2012**, *14*, 138–141; Parker, K. A.; Wang, Z. *Org. Lett.* **2006**, *8*, 3553–3556, and references therein.
15. Nemoto, H.; Li, X.; Ma, R.; Suzuki, I.; Shibuya, M. *Tetrahedron Lett.* **2003**, *44*, 73–75.
16. Hackett, S.; Livinghouse, T. *J. Org. Chem.* **1986**, *51*, 879–885.
17. Carreira, E. M.; Huwyler, N. *Synfacts* **2013**, *9*, 356.
18. Goodman, C. *Nat. Chem. Biol.* **2013**, *9*, 138.
19. Hale, K. J. *Org. Lett.* **2013**, *1*, 3181–3198.
20. Manchand, P. S.; Yiannikouros, G. P.; Belica, P. S.; Madan, P. *J. Org. Chem.* **1995**, *60*, 6574–6581.
21. Drew, S. L.; Lawrence, A. L.; Sherburn, M. S. *Angew. Chem., Int. Ed.* **2013**, *52*, 4221–4224.
22. Shukla, P.; Hsu, Y.-C.; Cheng, C.-H. *J. Org. Chem.* **2006**, *71*, 655–658.
23. Lim, H. N.; Parker, K. A. *J. Org. Chem.* **2014**, *79*, 919–926.
24. Qian, J.; Voorbach, M. J.; Huth, J. R.; Coen, M. L.; Zhang, H.; Ng, S. C.; Comess, K. M.; Petros, A. M.; Rosenberg, S. H.; Warrior, U.; Burns, D. J. *Anal. Biochem.* **2004**, *328*, 131–138.

25. Placzek, W. J.; Wei, J.; Kitada, S.; Zhai, D.; Reed, J. C.; Pellecchia, M. *Cell Death and Disease* **2010**, *1*, e40.
26. (a) Thompson, A. D.; Dugan, A.; Gestwicki, J. E.; Mapp, A. K. *ACS Chem. Biol.* **2012**, *7*, 1311–1320; (b) Voet, A.; Banwell, E. F.; Sahu, K. K.; Heddle, J. G.; Zhang, K. Y. J. *Curr. Top. Med. Chem.* **2013**, *13*, 989–1001.
27. Brady, R. M.; Vom, A.; Roy, M. J.; Toovey, N.; Smith, B. J.; Moss, R. M.; Hatzis, E.; Huang, D. C. S.; Parisot, J. P.; Yang, H.; Street, I. P.; Colman, P. M.; Czabotar, P. E.; Baell, J. B.; Lessene, G. *J. Med. Chem.* **2014**, *57*, 1323–1343.

Total Synthesis of Chinensiolid B: An Exercise in Functional Group Selectivity with the Help of a Fortuitous Side Product and a Good Nose

Tim G. Elford* and Dennis G. Hall^{†,1}

*Gilead Alberta ULC, Edmonton, Alberta, Canada

[†]Department of Chemistry, University of Alberta, Edmonton, Alberta, Canada

¹Corresponding author: dennis.hall@ualberta.ca

Chapter Outline

1. Introduction	80	3.2. Synthesis of Disubstituted Allylboronate 7	91
1.1. Chinensiolid and Other α -Methylene γ -Lactones in Nature	80	4. Synthesis of the Cyclopentyl Aldehyde Substrate	91
1.2. Traditional Methods for the Synthesis of α -Methylene γ -Lactones	81	4.1. Literature Precedent	91
1.3. Use of 2-Alkoxy carbonyl Allylboronates to Access α -Methylene γ -Lactones	85	4.2. Preparation of Aldehyde 6	93
2. Model Studies and Retrosynthetic Analysis	86	5. Critical Moment—The Key Aldehyde Allylboration Step	95
2.1. Retrosynthetic Analysis	86	5.1. History and Theory of the Carbonyl Allylboration Reaction	95
2.2. Model Studies	88	5.2. Optimization of the Key Allylboration Step	96
3. Design and Synthesis of the Key Allylboronate	90	6. Seven-Membered Ring Generation	99
3.1. Selection of the Protecting Group	90	6.1. Unmasking the Terminal Alkene	99

6.2. Serendipitous Crystallinity Makes for a Useful Side Product	101	7.3. Final Push to Access Chinensiolide B	106
6.3. Closing the Ring with RCM	102	7.4. A Comparison of Our Spectral Data with the Literature	106
7. Installation of the Tertiary Alcohol and Final Steps	102	7.5. Do You Trust Your Nose or the Label?	107
7.1. Epoxidation Versus Oxymercuration	102	8. Conclusions	109
7.2. Redox Juggling for a Roundabout Epoxide Reduction	104	Acknowledgments	110
		References	110

1 INTRODUCTION

1.1 Chinensiolide and Other α -Methylene γ -Lactones in Nature

The α -methylene γ -lactone ring is a key structural motif in many natural products, most notably the sesquiterpene lactones (Figure 1). In 1985, it was estimated that approximately 10% of the known 30,000 natural products contained this α -methylene γ -lactone functionality.¹ As the number of known natural products that contain an α -methylene γ -lactone group keeps increasing, more and more interest is being shown in this class of compounds due to their unique biological properties. In many cases, the high bioactivity of these compounds is due to the presence of the electrophilic exocyclic enoate moiety, which can trap nucleophilic residues present in the active site of target enzymes. These natural products have shown to be quite useful as DNA

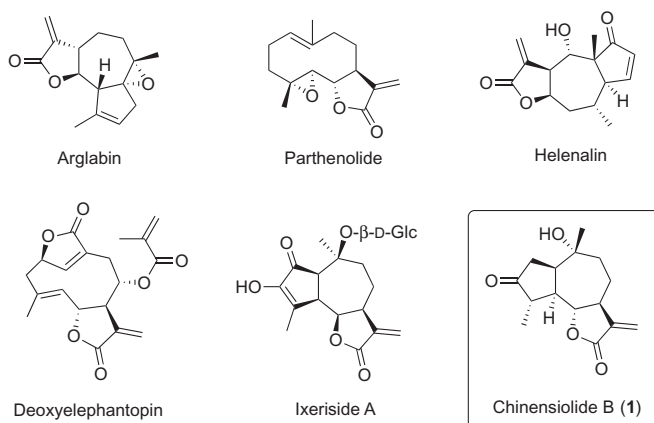


FIGURE 1 Selected natural products containing an α -methylene γ -lactone.

polymerase inhibitors, nuclear vitamin D receptor inhibitors, cellular steroidal inhibitors, blockers of tumor necrosis factor- α production, and have many other uses.² The wide inhibitory action of these natural products makes them potential drug candidates due to their cytotoxic, antiallergenic, anti-inflammatory, phytotoxic, and antimicrobial properties.³ In fact, arglabin (Figure 1) has been used successfully in Kazakhstan for the treatment of breast, colon, ovarian, and lung cancers.⁴ Chinensiolid B (**1**, Figure 1) constitutes another fascinating example of a natural product containing the α -methylene γ -lactone unit as part of a tricyclic 5-7-5-ring structure. There are five members of this family of sesquiterpenes that have been isolated and characterized to date,^{5,6} and the structure of chinensiolid B is shown in Figure 1. The chinensiolid natural products are isolated from rabbit milkweed (*Ixeris chinensis* Nakai), a perennial plant that grows in various parts of China.^{5,6} The plant is used in Chinese folk medicine for the treatment of bronchitis, pneumonia, pharyngitis, dysentery, and poisonous indigestion on the basis of its antifebrile, antidotal, and analgesic effects.

1.2 Traditional Methods for the Synthesis of α -Methylene γ -Lactones

As a result of the biological importance of these natural products, the synthesis of polysubstituted α -methylene γ -lactones has been of interest to synthetic chemists for several decades. Several routes have been devised to access the α -methylene γ -lactone ring; however, they tend to be lengthy and cumbersome if the lactone contains any sort of substitution.⁷ A review by Hoffmann and Rabe in 1985 discussed some of the methods developed up to that day for the preparation of α -methylene γ -lactones (Figure 2).¹

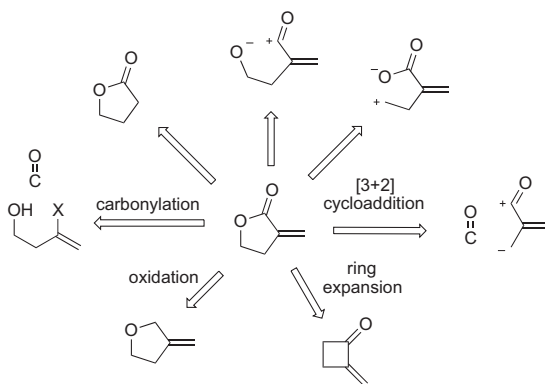
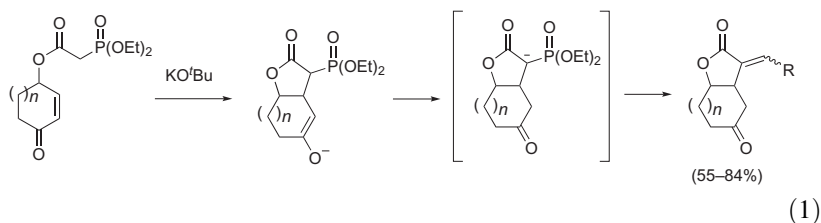
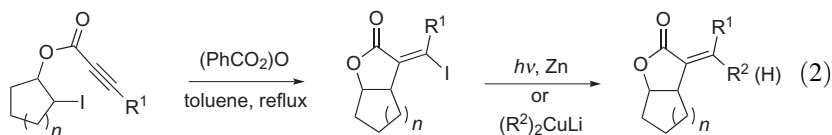


FIGURE 2 Various retrosynthetic routes to α -methylene γ -lactones discussed by Hoffmann and Rabe.¹

Since that time, there have been a number of other direct and indirect methods developed for the synthesis of this key structure.⁸ A few selected examples will be discussed in the next paragraphs so as to provide an overview of the different possibilities to access substituted α -methylene γ -lactones. To begin, Wittig–Horner–Emmons–Wadsworth olefinations utilizing cyclic phosphonate precursors can lead to both α -methylene and α -alkylidene γ -lactone products.⁹ Using such an approach to access bicyclic α -alkylidene γ -lactones, Taylor and co-workers developed a “one-pot” process initiated by the conjugate addition of tethered phosphonate-stabilized anions (Equation 1).¹⁰ The resulting enolate intermediate undergoes a proton transfer to provide a second phosphonate substituted carbanion that can condense with various aldehydes (RCHO).

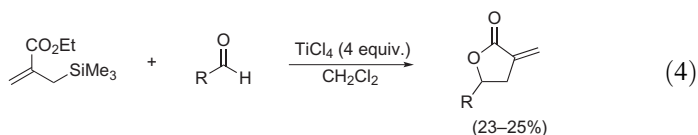
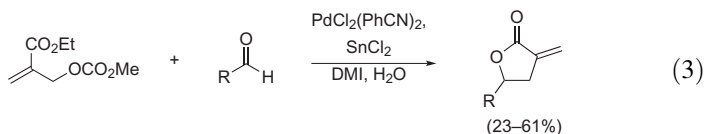


Another approach to bicyclic α -alkylidene γ -lactones requires the preparation of iodinated alkynoate precursors that can undergo a radical cyclization (Equation 2).¹¹ The resulting alkenyl iodide can be reduced with zinc to provide the trisubstituted alkene or can be further substituted with organocopper reagents to produce the desired γ -lactones embedding a tetrasubstituted alkene.

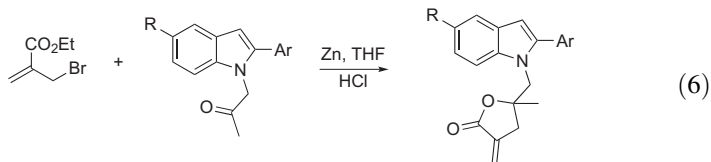
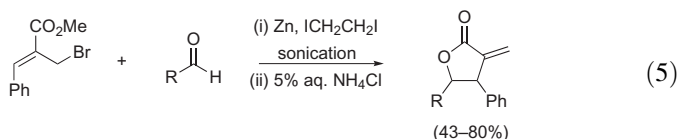


Other more direct methods make use of reagents that already have the *exo*-methylene preinstalled or established during the cyclization process. Traditional carbonyl allylation chemistry based on silicon and tin reagents has long been used to access α -methylene γ -lactones. Tin-based reagents add to aldehydes readily at low temperatures but require an excess amount of a strong Lewis acid.¹² Masuyama and co-workers developed an indirect, *in situ* method to prepare allylic tin reagents from the corresponding allylic carbonates, as shown in Equation (3).¹³ Under palladium catalysis, the transient allylic palladium complex that is generated transmetalates to tin to make a new allylic tin reagent, which subsequently adds to the aldehyde to provide

γ -lactones in modest yields. Not surprisingly, the analogous silicon reagents are much less reactive and require higher reaction temperatures (Equation 4).¹⁴ Even under these conditions, reactions with aldehydes provide low yields of lactone products.



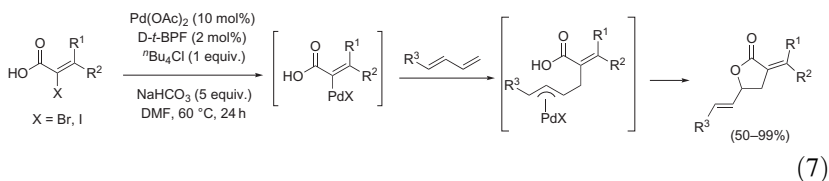
Barbier-type additions are attractive methods because the required allylic halide precursors are often commercially available, and are more stable than a preformed organometallic reagent (Equation 5). The required 2-alkoxycarbonyl allylic zinc reagents can be prepared from zinc powder.¹⁵ Lactonization tends to occur under the reaction conditions; however, the diastereoselectivity of the reactions tends to be poor with 3-substituted reagents. Zinc-mediated Barbier-type allylations are mild enough for use with functionalized substrates and can utilize both aldehydes and ketones as substrates.



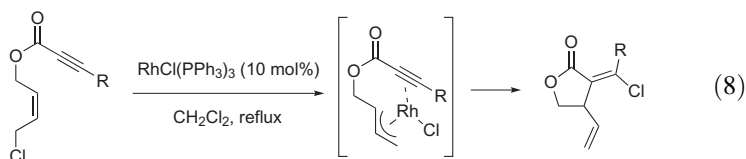
For example, Yang and co-workers employed a zinc-mediated Barbier reaction with either aldehydes or methyl ketones to form α -methylene γ -lactones containing novel indole substituents that were tested as inhibitors of kinase enzymes (Equation 6).¹⁶ Indium has also been exploited in Barbier-type additions and it has the advantage of being compatible with aqueous conditions and the reactions occur readily at room temperature.¹⁷

With the rise of cross-coupling chemistry mediated by various transition metals, new methods for the preparation of α -alkylidene γ -lactones are appearing. Gagnier and Larock developed a heteroannulation method

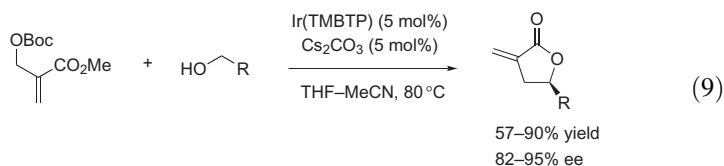
mediated by palladium utilizing α -halo alkenoic acids and substituted butadienes (Equation 7).¹⁸ Under palladium catalysis in the presence of a bulky phosphine, (di-*t*-butylphosphino)ferrocene, a cascade process leads to α -alkylidene γ -lactones in moderate to high yields.

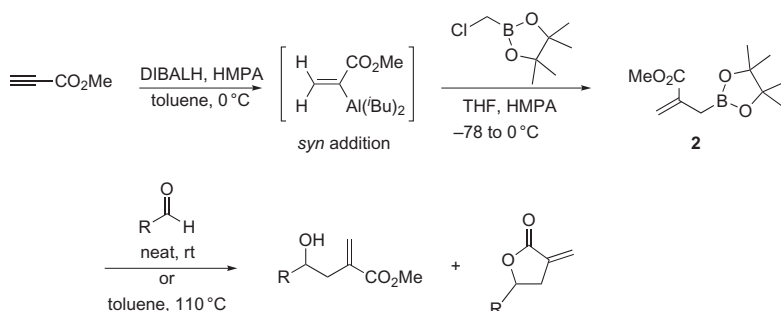


In a similar fashion, Zhang and co-workers have made use of a rhodium-catalyzed cycloisomerization protocol utilizing tethered 1,6-enynes as an efficient route to α -alkylidene γ -lactones containing a β -vinyl group and various substituents on the α -*exo*-alkene.¹⁹ In the presence of a cationic rhodium catalyst, a rhodium π -allyl species is formed that coordinates to the pendant alkyne (Equation 8). Subsequent carboration forms the γ -lactone ring of the final product and this is followed by reductive elimination to generate the alkenyl chloride. This process can also consume allylic alcohols instead of allylic chlorides and by subjecting them to an intramolecular rhodium-catalyzed Alder ene reaction it can thus produce α -alkylidene γ -lactones containing a formyl substituent in the β -position.²⁰



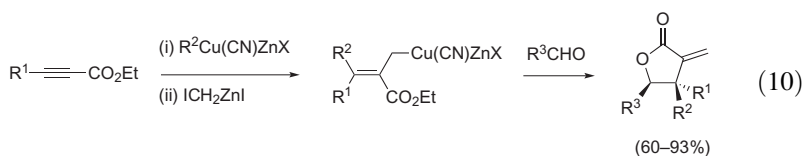
Krische and co-workers have taken the cross-coupling approach one step further to employ Morita–Baylis–Hillman adducts as substrates in an iridium-catalyzed transfer hydrogenation reaction (Equation 9).²¹ By using a chiral iridium-based catalyst, chiral α -methylene γ -lactones can be accessed in moderate to high yields and with enantiomeric excesses as high as 95%. The advantage of this approach is that it makes use of simple primary alcohols as one coupling partner, and it generates the chiral allyl metal reagent *in situ* from a precursor that can be synthesized in two simple chemical steps.





SCHEME 1 Synthesis and reactivity of 2-alkoxycarbonyl allylboronate **2** with aldehydes.

One approach that was influential in our research on the synthesis and applications of allylboronates to access α -methylene γ -lactones, which was reported by Sidduri and Knochel, utilize a mixed zinc–copper reagent that allowed for the one-pot preparation of α -methylene γ -lactones (Equation 10).²² The desired copper-based allylation reagents are formed with high selectivity through a *cis*-carbocupration, and the diastereoselectivity of aldehyde addition is high, which suggests a Type I chair-like transition state similar to allylboration reactions (see Section 5.1).

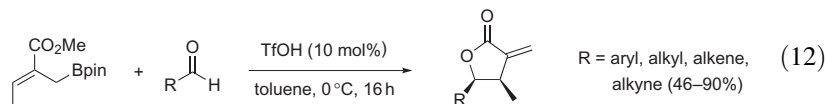
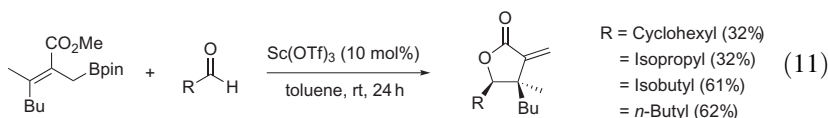


1.3 Use of 2-Alkoxycarbonyl Allylboronates to Access α -Methylene γ -Lactones

Allylic boronates containing a carboxyl group in the β -position are known as 2-alkoxycarbonyl (or 2-carboalkoxy) allylboronates. The first report describing the preparation of unsubstituted 2-alkoxycarbonyl allylboronate reagents, and their subsequent addition to aldehydes to form α -methylene γ -lactones, was disclosed by Villiéras and co-workers in 1993.²³ The desired 2-alkoxycarbonyl allylboronate **2** was prepared via a regioselective hydroalumination of methyl propiolate followed by trapping of the resulting alkenyl aluminum species with highly electrophilic halomethylboronic esters (Scheme 1). The resulting 2-alkoxycarbonyl allylboronate **2** was combined with various aldehydes to provide the expected alcohols after a reaction time of 1–2 weeks at room temperature. When the reactions were performed in toluene at reflux, the reaction time was slightly decreased and a significant proportion of lactonized product was

isolated. It should be noted that allylboronates containing substituents at the γ -position can also be synthesized in the same fashion. These 3-substituted allylboronates show reduced reactivity due to increased steric interactions with the incoming aldehyde but they react in a diastereospecific fashion whereby the alkene geometry in the allylboronate dictates which diastereomeric lactone is produced. More information on the stereochemical outcome of aldehyde allylboration reactions will be discussed in [Section 5.1](#).

More recent work in our^{24,25} and other²⁶ groups has shown that the use of Lewis (Equation 11) and Brønsted acid (Equation 12) catalysts can significantly reduce the reaction times for these allylboration reactions. Furthermore, the reaction temperature can be lowered, which allows for sensitive functional groups to be present on the aldehyde and allylboronate. It is also important to mention that even in the presence of the catalyst, the diastereospecificity of the reaction is maintained.



Before this total synthesis project began, we had just completed a diversity-oriented synthesis project that made use of the allylboration reaction to access simple substituted α -methylene γ -lactones, which were further functionalized using a variety of transition metal-catalyzed reactions.²⁷ We were now interested in applying this allylboration methodology to pursue a target-oriented synthetic problem that would demonstrate its suitability toward a complex natural product. Chinensiolide B presented this sort of challenge.

2 MODEL STUDIES AND RETROSYNTHETIC ANALYSIS

2.1 Retrosynthetic Analysis

When inspecting the structure of chinensiolide B and visualizing a possible retrosynthesis, the initially daunting feature from an organic synthesis standpoint is the presence of five contiguous tertiary and quaternary stereogenic centers along the central seven-membered ring ([Scheme 2](#)). The sixth stereocenter also stands out as a challenge since it is subject to epimerization due to its adjacency to a ketone. Third, the α -methylene γ -lactone itself is a very reactive electrophilic center, and all reactions to be performed after installation of this moiety must be carefully planned and chosen to avoid possible side reactions. Finally, installation of a tertiary alcohol in a diastereoselective fashion is not

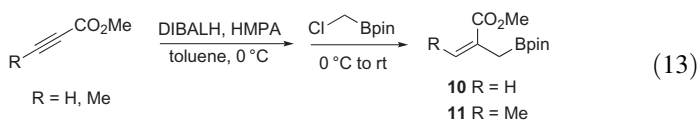
such that the rate of RCM is much greater than intermolecular CM. Although RCMs to form seven-membered rings are known in the literature,²⁸ they are not straightforward due to competing side reactions such as alkene migration and reductions.²⁹ For a successful epoxidation, we were relying on finding an electrophilic epoxidizing agent (assuming that nucleophilic epoxidizing agents would preferentially react, in an undesired fashion, with the electrophilic α -methylene group of the γ -lactone) that would react preferentially from the bottom face. Upon inspection of a handheld molecular model of the alkene intermediate, it was not clear to us which side of the molecule was less sterically blocked due to the flexibility and planarity of the molecule. Again putting this concern aside for the moment, triene intermediate **4** was envisioned to be accessible via a selective deprotection of the primary alcohol that would be followed by an elimination reaction. A Grieco elimination seemed ideal for this purpose.

Continuing with the retrosynthesis, protected diol **5** would directly arise from the tandem allylboration/lactonization methodology that had been a focus of our group's research for a number of years and would utilize two highly functionalized coupling partners: aldehyde **6** and allylboronate **7**. Introduction of the reactive α -methylene γ -lactone this early in the synthetic strategy allowed for a highly convergent approach; however, it could be seen as unwise due to severe chemoselectivity issues in the later stage of the synthetic sequence as already pointed out. Regardless, it was imagined that aldehyde **6** could be accessed from ketone **8** through the use of a Favorskii rearrangement.³⁰ Similar reactions had been demonstrated in the literature, so we were confident in being able to access the desired aldehyde from ketone **8**. Going further back, this ketone would ultimately arise from the use of a chiral pool reagent, (*R*)-carvone, which again had been demonstrated on similar compounds in the literature.³¹ We saw no point in replacing or even improving well-established chemistry, so access to key aldehyde **6** was planned based on this short, practical, and generally feasible route. Synthesis of the other key fragment, allylboronate **7**, was straightforward and relied on standard synthetic chemistry.²³ It could be synthesized directly from alkyne **9**, which is made in two simple steps from 4-pentyn-1-ol. With our synthetic plan now in hand, work was undertaken starting on July 14, 2008, to investigate the key allylboration reaction.

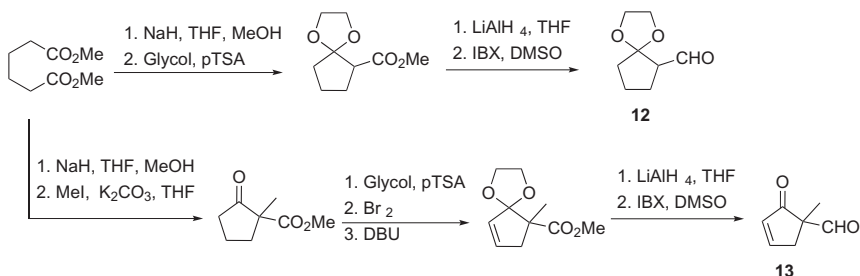
2.2 Model Studies

Before embarking on a total synthesis of chinensiolide B, we thought it would be prudent of us to briefly assess the feasibility of our synthetic plan. We outlined a series of model studies to determine whether there were any intrinsic limitations to the allylboronate or aldehyde substrates (reactivity, protecting group compatibility, etc.) that would be difficult to resolve at a later stage. In addition, we wondered whether our key allylboration step would provide

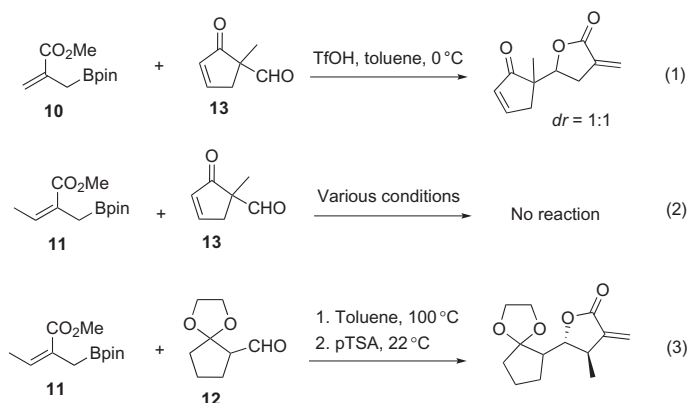
a useful level of diastereoselectivity, and, if it did, whether the major product was the desired diastereomer. In order to evaluate these questions, we began with the synthesis of two model allylboronates, **10** and **11** (Equation 13), and two cyclic aldehydes **12**³² and **13**³³ (Scheme 3).



Examination of the allylboration reaction with cyclic aldehydes **12** and **13** did provide us with useful additional information. Reaction of unsubstituted allylboronate **10** with aldehyde **13** under acid-catalyzed conditions was successful in generating the α -methylene γ -lactone product (Scheme 4, Equation 1) but, unfortunately, there was no diastereoselectivity. Furthermore, when the more substituted allylboronate **11** was used, there was no reaction at all (Scheme 4, Equation 2). Attempts with other reaction conditions (thermal, Lewis acid-catalyzed) also proved unsuccessful. Although our planned



SCHEME 3 Synthesis of model cyclic aldehydes **12** and **13**.



SCHEME 4 Model allylboration studies with cyclic aldehydes **12** and **13**.

synthesis did not use an aldehyde containing an adjacent quaternary center, it made us realize that we were beginning to push the steric boundaries for the aldehyde partner in these additions of electronically deactivated allylboronates. When switching to the less substituted aldehyde **12**, we were pleased to see that allylboronate **11** could now successfully react to generate the desired γ -lactone products (Scheme 4, Equation 3). However, the diastereoselectivity of the reaction could not be determined as all of the diagnostic peaks in the ^1H NMR spectrum overlapped and we were unsuccessful in separating the diastereomers.

By this point, we felt that we had expended enough effort on model reactions. We had established that cyclic aldehydes containing an α -tertiary center were suitable substrates with the 2-alkoxycarbonyl 3-substituted allylboronates. This realization provided enough assurance to undertake the total synthesis with optimism.

3 DESIGN AND SYNTHESIS OF THE KEY ALLYLBORONATE

3.1 Selection of the Protecting Group

In preparing for the synthesis of the required allylboronate **7**, we first had to choose the protecting group for the primary alcohol. The requirements that we laid out in choosing the protecting group were (a) it would have to first of all withstand all the conditions necessary to prepare the allylboronate reagent (basic and reducing conditions), (b) it had to withstand the allylboration/lactonization conditions (elevated temperature or strong acidic conditions), and (c) it had to be cleaved selectively in the presence of the protected secondary alcohol. It should be noted that the second requirement is not an absolute necessity since the step following the key allylboration/lactonization is deprotection of this primary alcohol. If deprotection did occur cleanly during the allylboration/lactonization, then the requirement would change to the concomitant deprotection having a negligible effect on the allylboration/lactonization reaction. In looking at the list of possibilities, a large number of protecting groups come to mind but we ultimately limited it down to a tetrahydropyran (THP) group, a tosylate (Ts) group, a *t*-butyl-dimethylsilyl (TBS) group, and a *t*-butyl-diphenylsilyl (TBDPS) group. The THP group was chosen since it should be stable to all of the reaction conditions proposed; however, it would produce diastereomers during the allylboration/lactonization step, which would complicate product analysis. The Ts was chosen as it was simple to install and uses rather orthogonal deprotecting methods (e.g., light, dissolved metal, mild reducing agents). The TBS and TBDPS groups were chosen as they are relatively stable to basic conditions and can be cleaved in the presence of most secondary silyl protecting groups (at the planning stage, we were leaning toward the use of a silyl protecting group for the secondary alcohol on the aldehyde coupling partner).

The TBS group had the additional advantage in that it could possibly be removed during the allylboration/lactonization step if strong acidic conditions were used.

3.2 Synthesis of Disubstituted Allylboronate 7

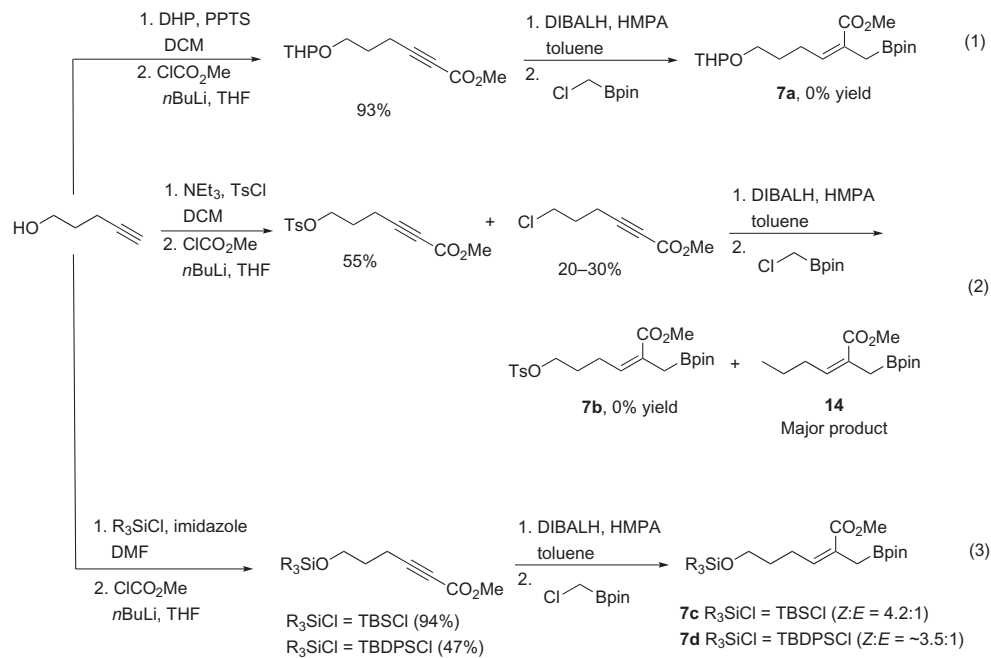
Once we had selected a few options for the protecting group, we then set out to synthesize four different allylboronates (Scheme 5). Starting from 4-pentyn-1-ol, protection of the primary alcohol was performed to install the THP, Ts, TBS, or TBDPS groups using standard conditions. Installation of the ester to make the α,β -unsaturated ester was achieved by treating the terminal alkyne with *n*-butyllithium followed immediately by methyl chloroformate. This reaction proceeded well for the alkynes containing the THP group (Equation 1) and the silyl protecting groups (Equation 3). However, for the Ts-protected alcohol (Equation 2), a competing side reaction where chloride had displaced the OTs group was noted during the preparation of the acetylenic ester and accounted for up to 30% of the reaction outcome. Interestingly, no 5-chloropent-1-yne was observed during the installation of the OTs group due to displacement of the primary tosylate by chloride, which is often observed as a side reaction.

The next step in the allylboronate synthesis involved treatment of the acetylenic esters with DIBALH to generate a vinyl aluminum species *in situ* followed by quenching with chloromethyl pinacolboronate.²³ Unfortunately, this is where we began to run into unexpected issues. For the THP-protected alcohol, none of the desired allylboronate was isolated (Equation 1). ¹H-NMR analysis of the crude mixture indicated a complex mixture of products that was not examined further. The substrate containing the Ts group also shared a similar fate in that none of the desired product was obtained (Equation 2). Instead, the OTs group had been displaced by hydrogen to generate ester **14**. On the other hand, the TBS- and TBDPS-substituted substrates behaved well and the desired allylboronates **7c** and **7d** were isolated in acceptable yields (Equation 3). However, both substrates led to a mixture of isomeric *Z/E* diastereomers that could not be separated by chromatography. We decided to carry the mixture of allylboronates forward in hope that the different diastereomers could either be separated in the next step or that the undesired isomer would isomerize under the reaction conditions to the more stable, desired *Z*-diastereomer.

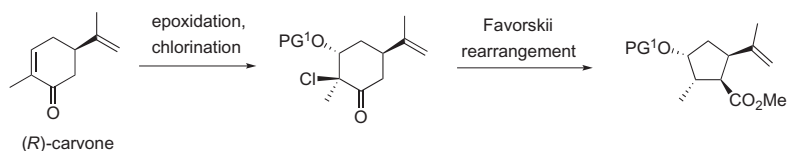
4 SYNTHESIS OF THE CYCLOPENTYL ALDEHYDE SUBSTRATE

4.1 Literature Precedent

In determining how to synthesize the desired aldehyde coupling partner **6**, a search of the literature made us aware of a number of total synthesis projects



SCHEME 5 Synthesis of allylboronates **7a–7d**.



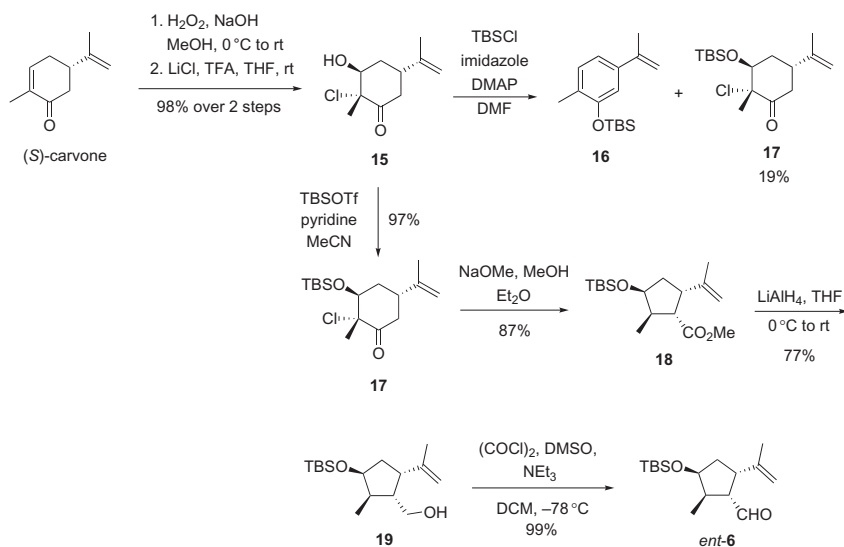
SCHEME 6 Preparation of polysubstituted cyclopentanes in total syntheses performed by the Ley research group.³¹

from the group of Prof. Steven Ley that had started with carvone and generated a similar intermediate structure as the one that we were seeking to assemble.³¹ In their synthesis, they relied on converting (*R*)-carvone into an α -chloroketone that was subjected to the Favorskii rearrangement (Scheme 6). This route provided quick access to a highly substituted cyclopentane ring, but more importantly, it contained a substitution pattern and the proper functional group handles that we required for the synthesis of our requisite aldehyde 6.

In reading the details of the Ley Group synthesis, they mentioned that both TBDPS and THP protecting groups were tested on the secondary alcohol and that the TBPDS group resulted in lower yields and selectivity during the Favorskii rearrangement. We were reluctant to consider a THP for this secondary alcohol as there was considerable concern that it would not survive acid-catalyzed allylboration conditions. We decided to investigate other protecting groups.

4.2 Preparation of Aldehyde 6

Once we had decided to follow the route described above, it was time to assemble the reagents. In searching our lab chemical database for carvone, it turned out that we did not have any of the (*R*)-carvone required to synthesize the natural enantiomer of chinensiolid B. However, we did have an old but nearly full 100-mL bottle of (*S*)-carvone that must have been obtained in years past from our departmental chemical recycling facility. The commercial bottle, which had a yellowed label that needed to be taped in place to keep it from peeling off, clearly stated the contents were (*S*)-carvone. A quick ¹H-NMR analysis confirmed that the integrity of this stock of carvone was fine, so rather than order a new bottle of (*R*)-carvone and wait for it to arrive, we decided that we would initiate the preliminary work with (*S*)-carvone. Eventually, we would order a bottle of (*R*)-carvone or just settle with synthesizing the antipode of chinensiolid B starting from (*S*)-carvone. Thus, we began our synthesis by following the conditions reported by Ley and co-workers, first forming the epoxide under nucleophilic conditions followed by regioselective epoxide opening with LiCl under acidic conditions (Scheme 7). These two reactions occurred without event, providing 15 in excellent yield and no purification of the intermediate epoxide was necessary.



SCHEME 7 Synthesis of key aldehyde *ent*-6.

However, the subsequent hydroxyl protection step provided us with our second reagent incident. In searching our chemical database for different protecting group reagents that would suit our purposes, we came across a situation where most of our supplies were insufficient toward the intended scale. The only reagent that we had plenty of was TBSCl, so we used it. The initial conditions employed to install the TBS protecting group turned out to not be ideal, as they led to a significant amount of a TBS-protected phenol derivative **16** resulting from multiple eliminations. But it provided us with ~ 2 g of desired ketone **17** with which to test the Favorskii rearrangement. In comparison with the study from the Ley group in which a TBDPS-protected substrate was used,³¹ the TBS-protected substrate **17** performed extremely well in the Favorskii rearrangement. We were unable to detect any other major side products and in fact, the crude NMR spectrum was surprisingly clean. Ultimately, after chromatography, the desired polysubstituted cyclopentane product **18** was obtained in 87% yield. Once the TBS protecting group was found to be suitable for the Favorskii rearrangement, we returned to examine and optimize the TBS protection step. Upon switching to more a reactive reagent, TBSOTf, the desired product **17** could now be obtained with ease in high yield.

Once we had our hands on reasonable quantities of cyclopentane **18**, we investigated the conversion of the ester into the requisite aldehyde moiety. We resorted to a two-step process using LiAlH₄ to fully reduce the ester to the alcohol and then reoxidize the alcohol to the aldehyde under Swern conditions. The reduction step was somewhat messy as compared to the other reactions in the sequence but still provided **19** in reasonable yields. Due to the fact that most of the reactions were high yielding and quite clean by

^1H -NMR analysis, we also attempted performing the six-step sequence without any chromatography other than for isolating aldehyde *ent*-6. We found that the aldehyde product was somewhat difficult to purify (long-lasting column with low polarity solvent and closely eluting side products), which is most likely linked to impurities generated in the reduction step. Product *ent*-6 isolated via this sequence tended to decompose over time. Ultimately, we were successful in our attempt to limit the number of purification steps, and the first five steps of the sequence could be executed without purification steps. Column chromatography was only used to purify alcohol **19**. This purification was much easier to perform and allowed for clean aldehyde *ent*-6 to be generated from the oxidation step. Aldehyde *ent*-6 still had a tendency to decompose over time but this decomposition was much slower when *ent*-6 originated from purified **19**. The overall yield for the five-step sequence involving only two purifications was 61% as compared with 63% yield when performing purification steps after each reaction (other than the first). However, this sequence avoided three column chromatography steps and was thus our preferred strategy for accessing aldehyde *ent*-6 from (*S*)-carvone.

5 CRITICAL MOMENT—THE KEY ALDEHYDE ALLYLBORATION STEP

5.1 History and Theory of the Carbonyl Allylboration Reaction

Ever since the discovery that allylboranes could add in a nucleophilic fashion to aldehydes and ketones in 1964,³⁴ carbonyl allylboration reactions have been thoroughly utilized in organic chemistry. Modification of allylic boron reagents and the substrates with which they can react has been the focus of many research groups over the past three decades. The application of allylboronates in the context of aldehyde allylation, which results in the formation of homoallylic secondary alcohols via an allyl transfer reaction with aldehydes, has become an invaluable tool to synthetic chemists (Figure 3).³⁵

There are several excellent methodologies reported in the literature that make use of a variety of allylating reagents based on boron, silicon, tin, and titanium metals for carbonyl allylation reactions. In the early 1980s, Denmark and Weber developed a classification system for allylation reagents that takes into account their proposed mechanism of addition to the carbonyl moiety (Figure 4).³⁶

Allylic boronates belong to the Type I class of reagents and are involved in a closed, Zimmerman–Traxler chair-like transition state whereby

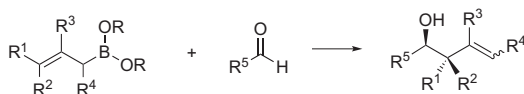


FIGURE 3 General structure of allylboronates and their stereoselective addition to aldehydes.

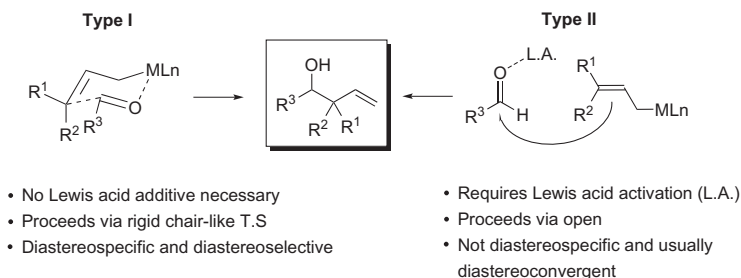
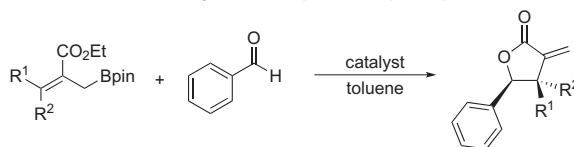


FIGURE 4 Classification system for Type I and Type II allylation reagents.³⁶

activation of the carbonyl group is achieved by the boron atom in the allylic boronate reagent.^{37,38} The stereochemistry present in the final product is dictated by the stereochemistry of the 3-substituted reagent. For example, *Z*-crotyl boronates lead to propionate products with *syn* stereochemistry, while *E*-crotyl boronates provide products with *anti* stereochemistry. In contrast, the popular trialkyl allylic silanes fall into the Type II class of reagents. These allylation reagents actually require that an additional Lewis acid be added to the reaction mixture in order for useful reaction rates to be obtained. Due to the compact transition state observed for Type I reagents, carbonyl allylation proceeds with a level of diastereoselectivity that is generally far superior to that of the Type II silicon and tin reagents. Many carbonyl allylation reactions with allylic tin and silicon reagents have been shown to proceed in the presence of various organic and metal catalysts in both stoichiometric and substoichiometric amounts.³⁹ However, by 2000, there had been no reports of allylboration reactions that make use of this type of catalysis. In this regard, our group made a remarkable discovery in 2002 when it was found that Lewis acids could catalyze an allylboration reaction.²⁴ Miyaoura and co-workers also published results in the same year describing the use of Lewis acids to increase aldehyde allylboration reaction rates.²⁶ One class of allylboronates that benefit greatly from this catalysis is the 2-alkoxycarbonyl allylboronates. These reagents react very slowly with aldehydes at room temperature (reaction times as long as 2 weeks) due to the deactivating effect of the electron-withdrawing 2-carboxyester group, however with the use of Lewis or Brønsted acid catalysis, the reaction times are reduced significantly to less than 1 day (Table 1).

5.2 Optimization of the Key Allylboration Step

As already mentioned, we had a number of options for reaction conditions at our disposal when we began looking at the key allylboration/lactonization step. Thermal conditions were the traditional way, either under standard or microwave-promoted heating. Furthermore, we could also make use of the

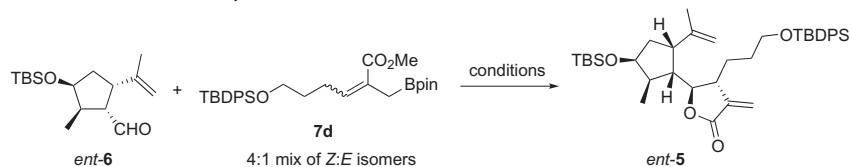
TABLE 1 Comparison of Catalyzed and Uncatalyzed Aldehyde Allylboration Reactions Using 2-Alkoxycarbonyl Allylboronates

Entry	R ¹ , R ²	Catalyst	Temperature (°C)	Time (h)	Yield (%)
1	Me, Me	None	22	24	0
2	Et, Me	Sc(OTf) ₃	22	24	93
3	Me, Me	Sc(OTf) ₃	0	16	<5
4	Me, Me	CF ₃ SO ₃ H	0	16	99

more recently developed Lewis acid-catalyzed or Brønsted acid-catalyzed conditions. We had already examined a few of these different experimental procedures for our model studies (see [Section 2.2](#)), but we returned to screen some of these reaction conditions with the actual substrates for this total synthesis, aldehyde *ent*-**6** and allylboronate **7d**. Initially, the thermal reaction was investigated but it was found to be sluggish and after 3½ days, the reaction had only reached 66% conversion (entry 1, [Table 2](#)). Triflic acid was investigated as a catalyst; however, only starting materials were isolated when the reaction was attempted at 0 °C (entry 2), and aldehyde *ent*-**6** decomposed when the reaction was performed at room temperature (entry 3). Scandium (III) triflate was also investigated with similarly poor results (entry 4). However, when BF₃·OEt₂ was used as the catalyst, the desired reaction occurred quite readily at room temperature (entry 5). Lowering the catalyst loading from 20 to 2.5 mol% and the reaction temperature from 23 to 0 °C provided conditions that maximized the yield while minimizing decomposition of *ent*-**6**, which resulted in clean reaction mixtures based on the analysis of the crude reaction mixture by ¹H NMR (entry 7).

Thus, when using 2.5 mol% of BF₃·OEt₂ at 0 °C for 48 h, the desired γ-lactone product *ent*-**5** was isolated in an exceptional yield of 87% (based on the amount of *Z*-**7d** used) and with complete diastereoselectivity. This observed selectivity (>95% dr) was an unexpected but welcome surprise, as four possible isomers could be expected from this reaction mixture. However, allylboronate *Z*-**7d** reacted in a completely diastereoselective fashion with aldehyde **6** to provide only one diastereomer. Furthermore, allylboronate *E*-**7d** proved to be essentially inert to the reaction conditions and could be recovered after the reaction. Thus, of four possible products, only one γ-lactone in a *trans* configuration was obtained. Analysis of the product by

TABLE 2 Screening of Conditions for the Allylboration/Lactonization Reaction



Entry	Catalyst	Loading (mol%)	Temperature (°C)	Time (h)	Conversion (%) ^a	Yield (%) ^b
1	None	n/a	90	84	66	n.d.
2	TfOH	20	0	16	0 ^c	n.d.
3	TfOH	20	23	16	0 ^c	n.d.
4	Sc(OTf) ₃	10	23	48	10	n.d.
5	BF ₃ ·OEt ₂	20	23	16	100	67
6	BF ₃ ·OEt ₂	5	0	48	100	65
7	BF ₃ ·OEt ₂	2.5	0	48	100	87

Allylboronate **7d** remained unreacted. n.d., not determined.

^aConversion based on comparison of **5** to **Z-7d** via ¹H NMR analysis of the crude reaction mixture.

^bYield is based on the amount of **Z-7d** used.

^cComplete decomposition of aldehyde **6** was observed by ¹H NMR.

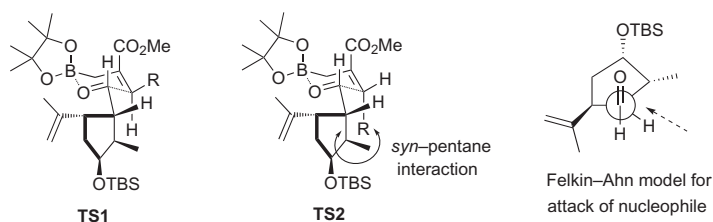


FIGURE 5 Rationale for observed stereoselectivity during the allylboration reaction.

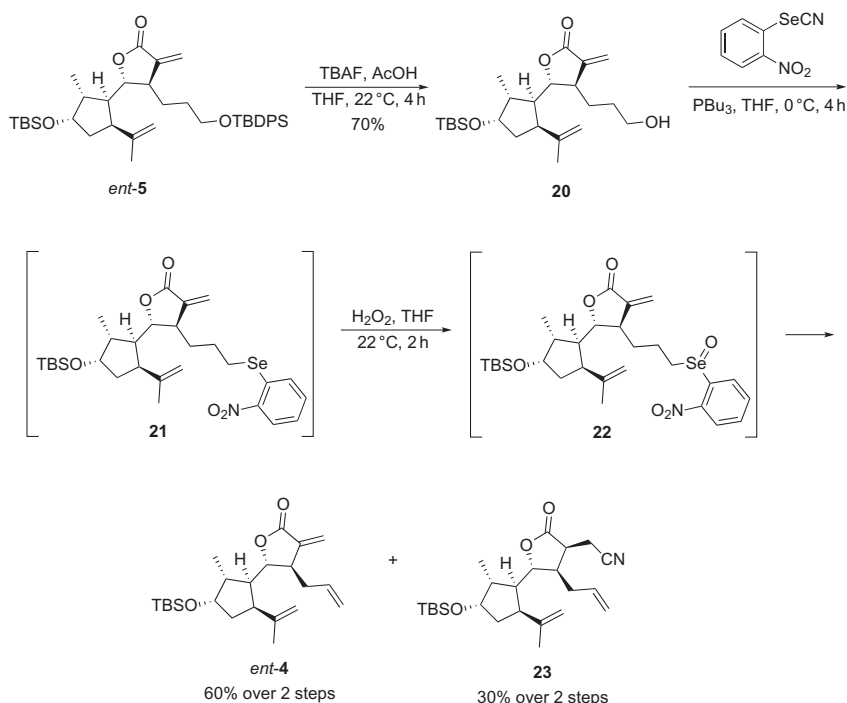
^1H NMR and by nOe experiments suggested that γ -lactone *ent*-**5** possessed the correct relative stereochemistry that is present in chinensiolid B, but this assignment could not be deemed conclusive (see Section 6.2 for a definitive proof of stereochemistry). The *trans* diastereoselectivity in the allylboration step can be explained with the usual six-membered chair-like transition state for this reaction (TS1, Figure 5). The chair-like transition state for this allylboration reaction also explains why *E*-**7d** is slower to react, since there is a significant *syn*-pentane interaction in the corresponding Zimmerman–Traxler transition state (TS2, Figure 5). The remarkable diastereofacial selectivity in the reaction of *Z*-**7d** with aldehyde *ent*-**6** can be rationalized according to the Felkin–Ahn model depicted in Figure 5, which places the large isopropylidene methine away from the reactive face of the carbonyl. Although the relatively high reactivity and the superb diastereoselectivity observed in the key allylboration step were quite surprising, the outcome was extremely satisfying and, in hindsight, it could be rationalized in simple terms.

6 SEVEN-MEMBERED RING GENERATION

6.1 Unmasking the Terminal Alkene

Once we had access to large amounts of allylboration product *ent*-**5**, we next had to perform the selective deprotection of the primary TBDPS group in the presence of the secondary TBS-protected alcohol. After searching through Greene's protecting group compendium,⁴⁰ we identified potentially suitable conditions and confirmed that this transformation could be accomplished by using 1.5 equiv. of TBAF buffered with 1.5 equiv. of acetic acid in THF.⁴¹ In this way, the monoprotected intermediate **20** was isolated in 70% yield (Scheme 8).

Once the primary alcohol was revealed, we prepared for the planned Grieco elimination⁴² to achieve the desired elimination. This pivotal reaction makes use of an activated selenium reagent that displaces the primary alcohol to generate a new selenium species **21**. Upon oxidation and heating, the resulting selenoxide intermediate **22** undergoes an intramolecular elimination reaction to generate triene *ent*-**4**. Preliminary experiments with the Grieco elimination, however, were frustrated by the fact that a significant amount



SCHEME 8 Selective deprotection of *ent-5* and Grieco elimination to form *ent-4*.

of a side product seemed to dominate the crude reaction mixture. After taking the time to isolate and characterize this main side product, it was clear what was happening. The Grieco elimination reaction is typically run at room temperature, and under these conditions, conjugate addition of cyanide (a by-product of the reaction that is generated from the selenium reagent) onto the α -methylene γ -lactone group of our substrate led to observed side product **23**. As mentioned earlier, the *exo*-methylene unit on the γ -lactone is a very reactive center for nucleophiles and here was a perfect example of how it could (and did) create problems in our synthesis. Lowering the temperature of the reaction to 0 °C helped to minimize this side reaction from occurring. We also had to reduce the number of equivalents of selenium reagent and tributylphosphine from 2.4 to 1.1 equiv. Thus, by carefully controlling the stoichiometry of the reaction and by performing the reaction at a lower temperature, the reaction could be completed within about 4 h and the amount of conjugate addition side product **23** was kept to about 30%. Unfortunately, the reaction also had to be performed as a two-step procedure. All attempts at performing the alcohol displacement and oxidation/elimination as a one-pot protocol led to higher amounts of the undesired conjugate addition product. We resorted to doing an aqueous work-up following the first step,

concentrating down the organic layer and then redissolving in THF and performing the oxidation/elimination step at room temperature. Although having to include a work-up in between the two steps was not ideal, it still allowed for *ent*-4 to be obtained in 60% yield over the two steps and it avoided the use of chromatography for the selenium intermediate.

6.2 Serendipitous Crystallinity Makes for a Useful Side Product

At this stage of our endeavor, the stereochemical assignment of *ent*-6, and thus *ent*-4, was still a concern. Product *ent*-4 was isolated as an oil, and NMR experiments aimed at assessing the stereochemistry proved to be inconclusive, much like the inconclusive NMR results observed for *ent*-6. Now a month or so after isolating and characterizing the conjugate addition side product **23**, it was noticed that an NMR tube that had contained this side product in ether had evaporated to dryness. Sitting at the bottom of the tube was a nice single, orange crystal! Thus, we immediately took the crystal to our X-ray Crystallography Laboratory and fortuitously, the crystal's quality was suitable for diffraction and allowed for an X-ray crystal structure to be obtained (Figure 6).

From this crystal structure, we were able to finally confirm the relative stereochemical outcome of the previous allylboration reaction. So in the end, although by-product **23** was undesired and could not be avoided, it did allow for conclusive proof that the allylboration reaction did indeed provide the desired diastereomer that was required for the total synthesis of chinensiolid B. This serendipitous result provided much encouragement for us as we were now nearing the end of the synthesis.

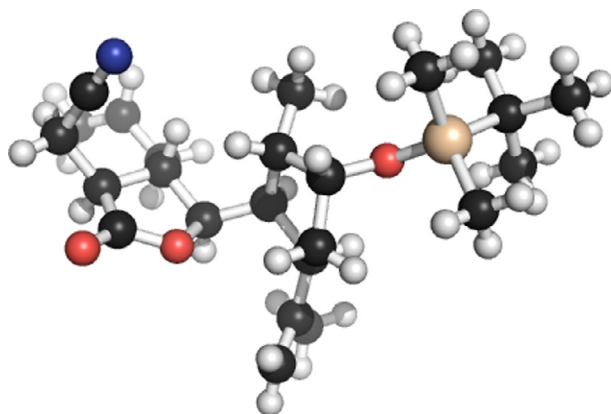


FIGURE 6 Crystal structure for side product **23**.

6.3 Closing the Ring with RCM

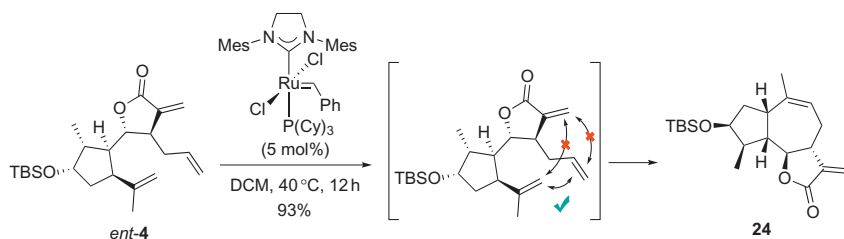
In principle, the planned RCM of intermediate **4** would furnish the seven-membered ring of chinensiolid B. Formation of medium-sized rings by RCM can be problematic especially when the resulting alkene product is tri- or tetrasubstituted²⁹; however, there are several examples where this chemistry has been successful in achieving this feat.⁴³ As described above, one additional issue of chemoselectivity that arises is the coupling of two different alkenes in the presence of a third alkene. In other words, RCM to form the requisite seven-membered ring of **24** must be chemoselective and avoid reaction with the α -methylene γ -lactone unit that could also participate to give four- or six-membered rings (Scheme 9). In spite of our apprehensions about this step, by using 10 mol% of the Grubbs II catalyst at a substrate concentration of 0.005 M, the desired RCM was successfully achieved in 12 h. The RCM was then attempted with only 5 mol% of catalyst, and this also provided desired tricycle **24** with an excellent yield of 93% (Scheme 9).

Most likely, the steric bulk around the α -methylene unit suppressed intermolecular CM and the unfavored formation of a tetrasubstituted bridgehead olefin suppressed intramolecular CM between this alkene and the propylidene group. Similarly, the formation of a tetrasubstituted alkene by intermolecular CM of the isopropenyl unit is disfavored. As a result, the desired RCM proceeded in an uncontested manner under moderately dilute conditions (0.005 M). Thus, this RCM strategy ultimately proved to be very effective for accessing the core structure of the chinensiolid family.

7 INSTALLATION OF THE TERTIARY ALCOHOL AND FINAL STEPS

7.1 Epoxidation Versus Oxymercuration

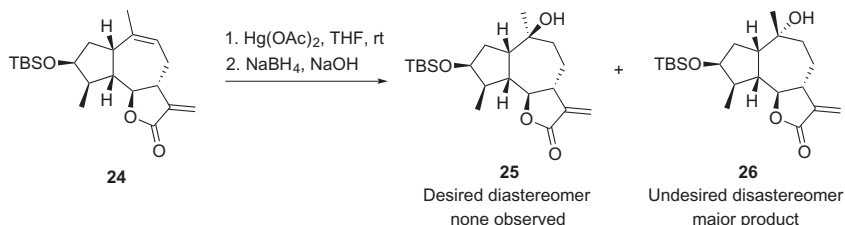
Now that we had built up the tricyclic core structure of chinensiolid B, all that was left to achieve was to install the tertiary alcohol and convert the protected secondary alcohol to a ketone. We decided to evaluate different methods to convert the trisubstituted alkene first into the tertiary alcohol and leave the deprotection and oxidation to the end. In looking at different options to



SCHEME 9 Ring-closing metathesis of *ent*-**4** to form tricycle **24**.

install the tertiary alcohol, we envisioned two possible methods to accomplish this feat. The first one involved oxymercuration of the double bond followed by reduction of the resultant mercury adduct. This route was appealing as oxymercuration is a textbook example of Markovnikov addition and usually results in high regioselectivities favoring the formation of the more substituted alcohol. The second option was to perform an epoxidation of the double bond and then use a nucleophilic hydride source to reductively open the epoxide on its least substituted side to form the tertiary alcohol. In comparing these two possible options on paper, oxymercuration/reduction was a two-step, one-pot process that would give us the desired regioselectivity. However, the diastereoselectivity outcome was unclear, as the oxymercuration step could occur from one of two faces. Building a handheld model of **24** was not that informative in terms of evaluating steric hindrance and directing effects, since both effects bore an opposing preference to which side the oxymercuration could occur from. Similarly, epoxidation of the alkene could be attempted, but again the facial selectivity was difficult to predict as opposing steric effects and directing group effects were also possible for this synthetic approach. Furthermore, the reductive opening of the epoxide would have to be both highly regioselective and, because of the highly reactive α -methylene γ -lactone unit still present, chemoselective too.

We initially chose to investigate the oxymercuration/reduction route as it posed the fewest questions and could be achieved in a one-pot fashion. The one-pot procedure was tested on a small scale (0.1 mmol) and only provided a few milligrams of material. However, switching to a two-step process (with an aqueous work-up to provide the crude mercury adduct) resulted in material that was relatively clean according to ^1H -NMR analysis of the crude reaction mixture (Scheme 10). In order to determine whether the correct stereochemistry had been formed, we rationalized that the chemical shifts of the protons around the newly formed stereocenter should be similar to those of the natural product if indeed the right diastereomer had been generated. Thus, a comparison of the chemical shifts of the nearby protons, unfortunately, showed that they were quite different when compared to the chemical shifts of the same protons in the natural product. We tried to convert the few milligrams that we had into chinensiolide B to confirm that the wrong diastereomer was



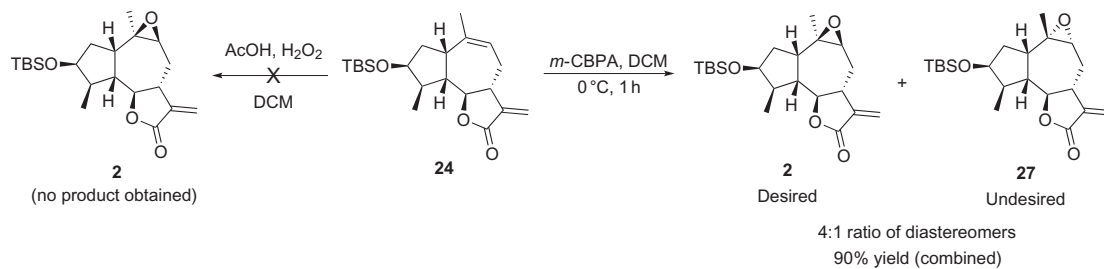
SCHEME 10 Oxymercuration approach to install the tertiary alcohol.

formed, but this attempt failed and we were unable to salvage any conclusive proof. However, since we had enough suspicions about the diastereoselectivity, we abandoned this route in favor of assessing the alternate approach of epoxidation followed by reductive opening.

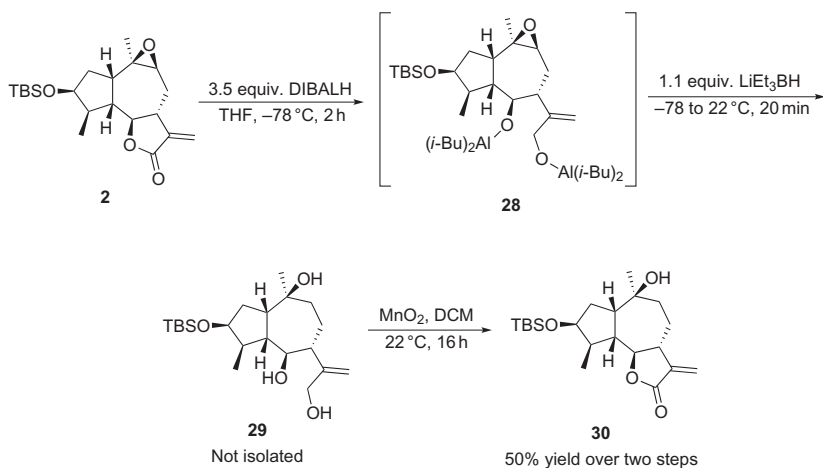
For the epoxidation and reduction approach, again the issue of chemoselectivity arose due to the presence of the α -methylene γ -lactone unit. Nucleophilic epoxidation conditions were not a viable option due to the electrophilic nature of the γ -lactone. Thus, only electrophilic epoxidizing agents were considered. A literature search identified a similar substrate devoid of the α -methylene unit on the γ -lactone ring, which had been epoxidized in a chemo- and diastereoselective fashion using AcOOH.⁴⁴ Our attempts at the epoxidation of **24** with AcOOH proved to be futile, as none of the desired epoxide was obtained and only starting materials were isolated after work-up. However, with *m*CPBA as the epoxidizing agent, the trisubstituted alkene in **24** could be successfully reacted to give **2** in a 4:1 mixture of diastereomers (Scheme 11). Based on comparing the chemical shifts of the protons near the epoxide in the two diastereomers with those reported for chimensiolide B and our previously synthesized alcohol **26**, we made an educated assessment and determined that the major diastereomer was indeed **2**. Unfortunately, all attempts to separate the desired product **2** from isomer **27** were unsuccessful, and thus the mixture was carried through to the next step.

7.2 Redox Juggling for a Roundabout Epoxide Reduction

Regioselective opening of epoxides to give Markovnikov products (i.e., the most substituted alcohol) is typically achieved through the use of nucleophilic hydride reagents such as LiAlH_4 or LiEt_3BH .⁴⁵ Use of these reagents, as one could have probably expected, was problematic as we ran into issues of over-reduction of the γ -lactone in **2**. With strong reducing agents like LiAlH_4 , competing side reactions occurred on the α -methylene γ -lactone unit of **2** (lactone reduction to give a diol with concurrent reduction of the *exo*-methylene double bond). To make matters worse, these reducing agents also gave poor selectivity for the epoxide opening. In contrast, we found that LiEt_3BH could provide good regioselectivity in the epoxide opening, but conjugate reduction of the α -methylene on the γ -lactone unit occurred at a faster rate. Many other reducing agents were screened for their ability to selectively open the epoxide, with no success. This proved to be a case where the electrophilicity and/or reactivity of the α -methylene γ -lactone was simply too high to overcome. We eventually settled on a one-pot, double reduction protocol whereby the γ -lactone was first selectively reduced with DIBALH *in situ* to generate intermediate **28**, and then LiEt_3BH was added to open the epoxide in a regio- and chemoselective manner (Scheme 12). Treatment of crude product **29** with MnO_2 allowed for reoxidation of the allylic diol to occur, thus easily reforming the α -methylene γ -lactone moiety to generate **30**. As an added



SCHEME 11 Diastereoselective epoxidation of **24**.



SCHEME 12 Redox manipulations for the reductive opening of epoxide **2**.

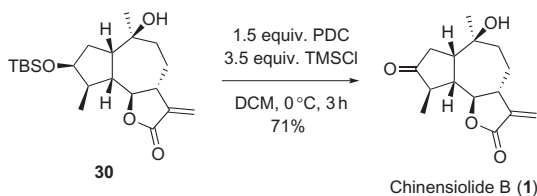
bonus, the two diastereomers present at the end of this reduction/oxidation sequence (arising from the mixture of **2** and **27** generated in the epoxidation step) could now be separated to provide the desired γ -lactone product. Although not ideal as far as step-count is concerned, this sequence shows that the indiscriminate reactivity of the α -methylene γ -lactone can be circumvented by temporarily altering its oxidation state in a carefully orchestrated manner.

7.3 Final Push to Access Chinensiolid B

All that remained to complete our synthesis of chinensiolid B was to cleave the TBS group on the secondary alcohol and oxidize it to generate the requisite ketone. We had little material available at this point and time was beginning to run out (it was late November 2009 and Tim's PhD defense was only 2 months away). As such, we were curious to test a procedure from the literature whereby oxidative cleavage of the secondary TBS protecting group would reveal the desired ketone functionality in one step.⁴⁶ Thus, on 15 mg of **30**, oxidative cleavage of the TBS group was performed with pyridinium dichromate and trimethylsilyl chloride in CH_2Cl_2 (Scheme 13). The reaction was uneventful and provided 4 mg of starting material, but more importantly, 5 mg (71% yield) of a product that, at a quick glance at the ^1H NMR data, looked like chinensiolid B (**1**).

7.4 A Comparison of Our Spectral Data with the Literature

After the initial excitement, a more thorough comparison of the ^1H and ^{13}C NMR peak listings was performed. It was at this point that we realized, with great distress to both of us, that the spectral data for our synthetic sample of putative chinensiolid B did not match that reported in the original isolation



SCHEME 13 Oxidative cleavage of silyl ether **30** to provide synthetic chinensiolide B (**1**).

paper.⁵ The ^1H NMR data showed that some of the peaks were close in chemical shift (within 0.1 ppm) to the reported values; however, others were quite different (up to 0.5 ppm difference). The ^{13}C NMR spectrum also had some peaks that were identical in chemical shift and others that were significantly different (>1 ppm difference). The HRMS and IR data for synthetic “chinensiolide B” confirmed that our sample had the correct molecular formula and functional groups, so we initially suspected that epimerization of one of the stereocenters had occurred to give a diastereomer of chinensiolide B. Tim was not fully convinced of this possibility and so we began to look at other sources that could explain the discrepancy in NMR data. We decided to contact the corresponding author of the isolation paper, Prof. Masayoshi Ando, and to our surprise, we learned that the solvent listed for the NMR analysis in the isolation paper was incorrect. Instead of the stated solvent (CDCl_3), according to Prof. Ando the NMR analysis had actually been performed in pyridine- d_5 ! After dissolving our synthetic sample of “chinensiolide B” in pyridine- d_5 and repeating the NMR analysis, the ^{13}C NMR spectrum was now a perfect match and the ^1H NMR spectrum was also a match except for one peak. The ^1H NMR peak listed at 2.27 ppm in the isolation paper was not present in the ^1H NMR spectra for our synthetic “chinensiolide B.” Instead, we observed two extra peaks, one at 2.76 ppm and the other at 1.84 ppm. However, upon looking at the actual copy of the ^1H NMR spectrum obtained from Prof. Ando for natural chinensiolide B, it was realized that the listing of peaks in the ^1H NMR description in the isolation paper was also partially incorrect! The ^1H NMR spectrum provided by Prof. Ando showed a peak at 2.76 ppm and no peak at 2.27 ppm as well as a peak at 1.84 ppm and not the two peaks listed at 1.36 ppm. Thus, there were in fact two errors in the isolation paper with regards to the listing of chemical shifts. In the end, to our great relief, the ^1H NMR spectra for natural and synthetic chinensiolide B were an unambiguous match once the same solvents for the NMR analysis were used and the errors in chemical shift were noted. Celebration time? Maybe not.

7.5 Do You Trust Your Nose or the Label?

Now that all of our data confirmed that we had synthesized chinensiolide B, all that was left to be accomplished was to obtain the optical rotation of our

synthetic material to meet journal requirements and ascertain that we had made the antipode of the natural product (recall that we started with (*S*)-carvone, not the (*R*) antipode). Upon standard routine subsection of a sample of synthetic chinensiolide B to the polarimeter, we were expecting to observe a negative optical rotation since the naturally occurring chinensiolide B has an optical rotation with a positive sign (lit.⁵: $[\alpha]_{\text{D}} = +2.6$, c 0.47, CHCl_3). Naturally, we were stunned when the optical rotation came back ($[\alpha]_{\text{D}} = +4.8$, c 0.12, CHCl_3) with a positive sign! This unexpected result indicated one of two things. Either the isolation paper had the wrong absolute stereochemistry for natural chinensiolide B or our synthesis was actually of the natural enantiomer. The latter explanation seemed outrageous at first, since the old bottle of starting carvone was labeled as (*S*)-carvone and the X-ray crystal structure of side product **23** from the Grieco elimination had confirmed the absolute stereochemistry. Well, that is not exactly true. A minor issue arose when the crystal structure was resolved. When we originally obtained the X-ray crystal structure of side product **23**, the crystallographer, Dr. Bob McDonald, mentioned that the resulting data pointed to an absolute stereochemistry that might be opposite to what we were proposing. The Flack parameter⁴⁷ obtained for our crystal structure was 0.95, which indicated that the absolute configuration is opposite to what we were proposing. However, there was a large enough amount of standard uncertainty in the X-ray data that it could not be used alone to confirm the absolute stereochemistry. After discussing this discrepancy with Bob, and since we were working under the realistic assumption that we had started from (*S*)-carvone, a decision was made to propose the absolute stereochemistry as shown in [Scheme 8](#). This matter was now proving to be very significant in that it indicated there might be a problem in our synthesis, not in the isolation paper. Could the bottle that was clearly labeled as (*S*)-carvone and was assumed to be (*S*)-carvone might actually contain (*R*)-carvone? Dennis, who makes students smell carvone samples in his undergraduate classes as a way to highlight and experience the different properties of enantiomers on protein receptors, remembered that (*S*)-carvone smells like caraway and (*R*)-carvone smells like spearmint. He hurried Tim to go smell the contents of the old bottle. Low and behold, the contents of the bottle shown in [Figure 7](#) smelled like spearmint! Furthermore, we obtained the optical rotation of a sample ($[\alpha]_{\text{D}} = -61$ (neat)), which confirmed that the bottle in fact contained (*R*)-carvone (literature value for $[\alpha]_{\text{D}} = -61$ (neat)). Thus, the label on the bottle was wrong! The starting material for the total synthesis was in actual fact (*R*)-carvone, which translated to a total synthesis of the natural enantiomer of chinensiolide B. Once this surprising realization was made, the sign of the observed optical rotation for synthetic chinensiolide B made sense and did indeed match the optical rotation for the natural product. So, 3 weeks before Christmas 2009, we finally had full confidence that we had indeed completed a total synthesis of the natural enantiomer of chinensiolide B and in the same way confirmed the absolute stereochemistry and structure of this natural product.

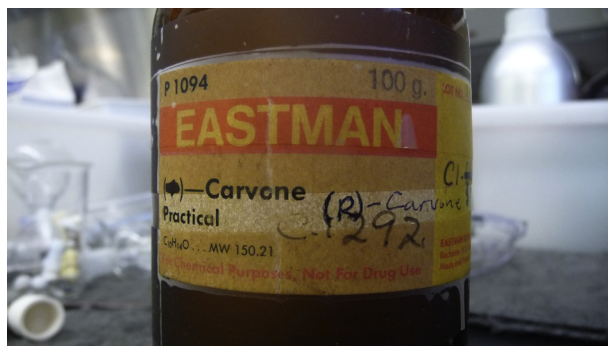


FIGURE 7 The infamous bottle of carvone, now inscribed with the right stereochemistry.

8 CONCLUSIONS

Our synthetic efforts that culminated in the total synthesis of chinensiolide B started with model studies of simpler systems. We investigated the limits of aldehyde allylboration chemistry with 2-alkoxycarbonyl allylboronates and created a basis from which we could cautiously approach a synthetic strategy to the desired target. We made use of literature precedent to access both key fragments needed for our synthetic approach, aldehyde **6** and allylboronate **7**. A switch in the protecting group from TBDPS or THP to TBS on a secondary alcohol allowed us to improve on the literature approach to key precursor **6** and also paved the way for a selective deprotection later on in the synthetic sequence. After optimization of the reaction conditions, the key aldehyde allylboration step unfolded extremely well and allowed us to access a single diastereomer in high yield despite the possibility of four isomers being generated. This transformation constitutes one of the most efficient carbonyl allylboration reactions ever reported both in terms of its stereoselectivity and also in terms of the level of complexity of both the aldehyde and the allylboronate. This transformation, however, unveiled a reactive α -methylene γ -lactone in the product. Soon thereafter, when performing the Grieco elimination to access the requisite terminal alkene, the high reactivity of the α -methylene γ -lactone raised its ugly head and formation of a conjugate addition side product of cyanide could not be avoided. Paradoxically, this was a rare situation where a side product proved very useful in that it was crystalline and suitable for X-ray diffraction, which led to a much needed confirmation of the stereochemistry of the key allylboration reaction. After closing the ring with RCM, epoxidation to position the oxygen atom followed by reductive epoxide opening proved to be less straightforward than initially planned. However, upon playing with the oxidation state of the α -methylene γ -lactone moiety *in situ*, we were able to circumvent a synthetic roadblock and install the tertiary alcohol on the desired carbon atom with the necessary

stereochemistry. Finishing off the synthetic effort was accomplished by a little known procedure that cleaved the secondary TBS group and oxidized the alcohol into the desired ketone in a single step. Conflicting analytical data between the synthetic material and that reported in the literature for the natural product created a great deal of stress, but through discussions with Prof. Ando, we uncovered the issue: the wrong NMR solvent was listed in the supporting information of his isolation paper along with two peak listing errors. Then, to top it all off, the measured optical rotation of the synthetic material matched that of the natural product when we expected the antipode. Again, human error was at the source of the problem, and we discovered that we had in fact used (*R*)-carvone even though the old bottle used had a label stating that it was (*S*)-carvone. So after a good deal of drama at the end, we received an early Christmas 2009 present in the form of a completed total synthesis of (+)-chinensiolid B. Several lessons were learned throughout this adventure, and none more important than the realization that no amount of planning can prevent the occurrence of setbacks and surprises, even when you least expect it.

ACKNOWLEDGMENTS

We are grateful to the Natural Sciences and Engineering Research Council (NSERC) of Canada and the Alberta Ingenuity Fund for providing funding for this project. We also wish to thank the University of Alberta for providing laboratory space and support services (NMR, IR, HRMS, optical rotation) and Dr. Robert McDonald for the X-ray crystallographic analysis and discussions regarding X-ray data that were collected.

REFERENCES

1. Hoffmann, H. M. R.; Rabe, J. *Angew. Chem. Int. Ed. Engl.* **1985**, *24*, 94–110.
2. Konaklieva, M. I.; Plotkin, B. J. *Mini Rev. Med. Chem.* **2005**, *5*, 73–95.
3. Janecki, T.; Blaszczyk, E.; Studzian, K.; Janecka, A.; Krajewska, U.; Rozalski, M. J. *Med. Chem.* **2005**, *48*, 3516–3521.
4. Zhangabylov, N. S.; Dederer, L. Y.; Gorbacheva, L. B.; Vasil'eva, S. V.; Terekhov, A. S.; Adekenov, S. M. *Pharm. Chem. J.* **2004**, *38*, 651–653.
5. Zhang, S.; Wang, J.; Xue, H.; Deng, Q.; Xing, F.; Ando, M. *J. Nat. Prod.* **2002**, *65*, 1927–1929.
6. Zhang, S.; Zhao, M.; Bai, L.; Hasegawa, T.; Wang, J.; Wang, L.; Xue, H.; Deng, Q.; Xing, F.; Bai, Y.; Sakai, J.; Bai, J.; Koyanagi, R.; Tsukumo, Y.; Kataoka, T.; Nagai, K.; Hirose, K.; Ando, M. *J. Nat. Prod.* **2006**, *69*, 1425–1428.
7. (a) Hughes, M. A.; McFadden, J. M.; Townsend, C. A. *Bioorg. Med. Chem. Lett.* **2005**, *15*, 3857–3859; (b) Tong, X.; Li, D.; Zhang, Z.; Zhang, X. *J. Am. Chem. Soc.* **2004**, *126*, 7601–7607; (c) Lei, A.; He, M.; Zhang, X. *J. Am. Chem. Soc.* **2002**, *124*, 8198–8199; (d) Lee, K.; Jackson, J. A.; Wiemer, D. F. *J. Org. Chem.* **1993**, *58*, 5967–5971.
8. For selected reviews on this topic, see: (a) Elford, T. G.; Hall, D. G. *Synthesis* **2010**, 893–907; (b) Janecki, T., Attanasi, O. A., Spinelli, D. (Eds.), *Targets in Heterocyclic Systems*, vol. 10, Springer: Royal Society for Chemistry and Italian Society of Chemistry, 2006, pp. 301–320; (c) Feray, L., Bertrand, M.P., Attanasi, O.A., Spinelli, D. (Eds.), *Targets in Heterocyclic*

- Systems, vol. 12, Springer: Royal Society for Chemistry and Italian Society of Chemistry, 2008, p. 31; (d) Kitson, R. R. A.; Millemaggi, A.; Taylor, R. J. K. *Angew. Chem. Int. Ed. Engl.* **2009**, *48*, 9426–9451.
9. Janecki, T.; Blaszczyk, E.; Studzian, K.; Janecka, A.; Krajewska, U.; Rózsalski, M. *J. Med. Chem.* **2005**, *48*, 3516–3521.
10. Edwards, M. G.; Kenworthy, M. N.; Kitson, R. R. A.; Scott, M. S.; Taylor, R. J. K. *Angew. Chem. Int. Ed. Engl.* **2008**, *47*, 1935–1937.
11. (a) Haaïma, G.; Weavers, R. T. *Tetrahedron Lett.* **1988**, *29*, 1085–1088; (b) Haaïma, G.; Lynch, M.-J.; Routledge, A.; Weavers, R. T. *Tetrahedron* **1991**, *47*, 5203–5214.
12. Baldwin, J. E.; Adlington, R. M.; Sweeney, J. B. *Tetrahedron Lett.* **1986**, *27*, 5423–5424.
13. Masuyama, Y.; Nimura, Y.; Kurusu, Y. *Tetrahedron Lett.* **1991**, *32*, 225–228.
14. Hosomi, A.; Hashimoto, H.; Sakurai, H. *Tetrahedron Lett.* **1980**, *21*, 951–954.
15. (a) Lambert, F.; Kirschleger, B.; Villiéras, J. J. *Organomet. Chem.* **1991**, *406*, 71–86; (b) Mattes, H.; Benezra, C. *Tetrahedron Lett.* **1985**, *26*, 5697–5698; (c) Lee, A. S.-Y.; Chang, Y.-Y.; Wang, S.-H.; Chu, S.-F. *Tetrahedron Lett.* **2002**, *43*, 8489–8492.
16. Ding, H.; Zhang, C.; Wu, X.; Yang, C.; Zhang, X.; Ding, J.; Xie, Y. *Bioorg. Med. Chem. Lett.* **2005**, *15*, 4799–4802.
17. Choudhury, P. K.; Foubelo, F.; Yus, M. *Tetrahedron Lett.* **1998**, *39*, 3581–3584.
18. Gagnier, S. V.; Larock, R. C. *J. Org. Chem.* **2000**, *65*, 1525–1529.
19. Yong, X.; Li, D.; Zhang, Z.; Zhang, X. *J. Am. Chem. Soc.* **2004**, *126*, 7601–7607.
20. Lei, A.; He, M.; Zhang, X. *J. Am. Chem. Soc.* **2002**, *124*, 8198–8199.
21. Montgomery, T. P.; Hassan, A.; Park, B. Y.; Krische, M. J. *J. Am. Chem. Soc.* **2012**, *134*, 11100–11103.
22. Sidduri, A. R.; Knochel, P. *J. Am. Chem. Soc.* **1992**, *114*, 7579–7581.
23. Nyzam, V.; Belaud, C.; Villiéras, J. *Tetrahedron Lett.* **1993**, *34*, 6899–6902.
24. Kennedy, J. W. J.; Hall, D. G. *J. Am. Chem. Soc.* **2002**, *124*, 11586–11587.
25. Elford, T. G.; Arimura, Y.; Yu, S. H.; Hall, D. G. *J. Org. Chem.* **2007**, *72*, 1276–1284, and references cited therein.
26. Ishiyama, T.; Ahiko, T.; Miyaura, N. *J. Am. Chem. Soc.* **2002**, *124*, 12414–12415.
27. Elford, T. G.; Ulaczyk-Lesanko, A.; De Pascale, G.; Wright, G. D.; Hall, D. G. *J. Comb. Chem.* **2009**, *11*, 155–168.
28. For example, see: (a) Nicolaou, K. C.; Bulger, P. G.; Sarlah, D. *Angew. Chem. Int. Ed. Engl.* **2005**, *44*, 4490–4527; (b) Paquette, L. A.; Arbit, R. M.; Funel, J.-A.; Bolshakov, S. *Synthesis* **2002**, *14*, 2105–2109; (c) Kalidindi, S.; Jeong, W. B.; Schall, A.; Bandichhor, R.; Nosse, B.; Reiser, O. *Angew. Chem. Int. Ed. Engl.* **2007**, *46*, 6361–6363.
29. For example, see: (a) Chatterjee, A. K.; Morgan, J. P.; Scholl, M.; Grubbs, R. H. *J. Am. Chem. Soc.* **2000**, *122*, 3783–3784; (b) Hekking, K. F. W.; van Delft, F. L.; Rutjes, F. P. J. T. *Tetrahedron* **2003**, *59*, 6751–6758.
30. (a) Favorskii, A. E. *J. Russ. Phys. Chem. Soc.* **1894**, *26*, 590; (b) Favorskii, A. E. *J. Russ. Phys. Chem. Soc.* **1905**, *37*, 643; (c) Favorskii, A. E. *J. Prakt. Chem.* **1913**, *88*, 658.
31. Oliver, S. F.; Hogenauer, K.; Simic, O.; Antonello, A.; Smith, M. D.; Ley, S. V. *Angew. Chem. Int. Ed. Engl.* **2003**, *42*, 5996–6000.
32. Jones, R. L.; Wilson, N. H. *J. Chem. Soc. Perkin Trans. I* **1978**, 209–214.
33. Lee, K.-H.; Mar, E.-C.; Okamoto, M.; Hall, I. H. *J. Med. Chem.* **1978**, *21*, 819–822.
34. Mikhailov, B. M.; Bubnov, Y. N. *Izv. Akad. Nauk SSSR Ser. Khim.* **1964**, 1874.
35. Lachance, H.; Hall, D. G. *Org. React.* **2008**, *73*, 1–574.
36. Denmark, S. E.; Weber, E. J. *Helv. Chim. Acta* **1983**, *66*, 1655–1660.
37. Omoto, K.; Fujimoto, J. *J. Org. Chem.* **1989**, *63*, 8331–8336.
38. Li, Y.; Houk, K. N. *J. Am. Chem. Soc.* **1989**, *111*, 1236–1240.

39. Denmark, S. E.; Fu, J. *Chem. Rev.* **2003**, *103*, 2763–2794.
40. Wutz, P. G. M.; Greene, T. W. *Greene's Protective Groups in Organic Synthesis*; 4th ed., John Wiley & Sons Inc.: Hoboken, New Jersey, 2007.
41. Crouch, R. D. *Tetrahedron* **2004**, *60*, 5833–5871.
42. Grieco, P. A.; Gilman, S.; Nishizawa, M. *J. Org. Chem.* **1976**, *41*, 1485–1486.
43. For example, see: (a) Paquette, L. A.; Arbit, R. M.; Funel, J.-A.; Bolshakov, S. *Synthesis* **2002**, *14*, 2105–2109; (b) Kalidindi, S.; Jeong, W. B.; Schall, A.; Bandichhor, R.; Nosse, B.; Reiser, O. *Angew. Chem. Int. Ed. Engl.* **2007**, *46*, 6361–6363.
44. Alves, J. C. F.; Fantini, E. C. *J. Braz. Chem. Soc.* **2005**, *16*, 749–755.
45. Brown, H. C.; Krishnamurthy, S. *Tetrahedron* **1979**, *35*, 567–607.
46. Cossio, F. P.; Aizpura, J. M.; Palomo, C. *Can. J. Chem.* **1986**, *64*, 225–231.
47. (a) Flack, H. D. *Acta Crystallogr.* **1983**, *A39*, 876–881; (b) Flack, H. D.; Bernardinelli, G. *Acta Crystallogr.* **1999**, *A55*, 908–915; (c) Flack, H. D.; Bernardinelli, G. *J. Acta Crystallogr.* **2000**, *33*, 1143–1148.

Syntheses of the Bisindole Alkaloids of the Genera *Borreria* and *Flindersia*

Jeremy A. May¹

Department of Chemistry, University of Houston, Houston, Texas, USA

¹Corresponding author: jmay@uh.edu

Chapter Outline

1. Introduction and Background	113	4. Biomimetic Synthesis of the Flinderoles and Borreverines in Three Steps	121
1.1. The Flinderoles	113	4.1. Borrerine Synthesis	121
1.2. The Borreverines	114	4.2. Effects of Acid on Borrerine Dimerization	122
1.3. Antimalarial Activity	115	4.3. Methylative Dimerization	125
2. Biosynthetic Proposals	116	5. Optical Activity	127
2.1. For the Borreverines	116	5.1. Reports of Flinderole Optical Activity	127
2.2. For the Flinderoles	118	5.2. Experimental Evaluation	128
3. Synthetic Approaches to the Flinderoles	119	6. Conclusion	129
3.1. The Dethe Group	119	References	129
3.2. The Toste Group	120		
3.3. The Xiao Group	121		

1 INTRODUCTION AND BACKGROUND

1.1 The Flinderoles

The disclosure of the structures of flinderoles A–C (1–3, Figure 1) in 2009¹ sparked a flurry of synthetic activity. In fact, their complexity drew our interest just as we were setting up our laboratory at the University of Houston. The bisindole alkaloids contain an intriguing central pyrrolidine ring with two stereogenic carbons. Each of these stereocenters presents a challenge to

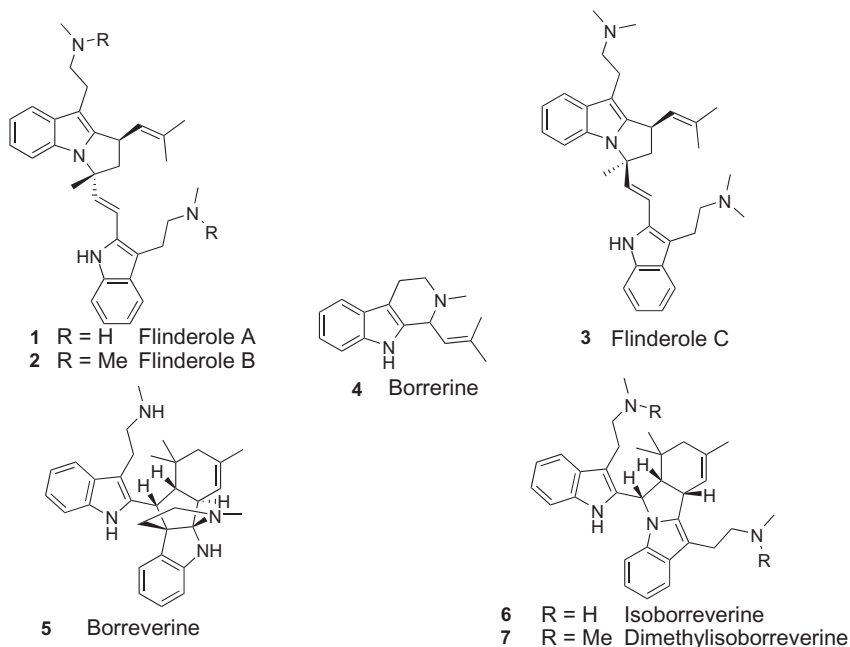


FIGURE 1 The flinderroles and borreverines.

synthetic chemists. The first, attached at the indole 2-position, is substituted with an *iso*-butylene group. While many enantioselective transformations have been developed for the formation of benzylic stereocenters, relatively few of these methods have been applicable to synthesize α -chiral indoles or α -chiral heterocycles generally. The second, connected to the indole nitrogen, is a tetrasubstituted carbon that again bears an alkenyl substituent. Several effective strategies have been proven to form carbamine centers enantioselectively through an iminium or imine intermediate. Most of these make use of chiral auxiliaries² to convey stereocontrol, though a few exceptions exist for imine allylation.³ Such intermediates are less applicable to the synthesis of the tertiary carbamine in the flinderroles, since an iminium that involves the indole nitrogen lone pair would result in a loss of aromatic stabilization in the indole ring. Such an intermediate would be much higher in energy than a standard iminium. Thus, novel approaches to these stereocenters would be needed for their synthesis, illustrating a problem that drew our attention as well as that of other synthetic chemists.

1.2 The Borreverines

Two known bisindole alkaloids of even greater structural complexity were also isolated from the *Flindersia* species: isoborreverine (**6**) and

dimethylisoborreverine (**7**).⁴ These compounds differ structurally from the flinderoles, since they contain a fused cyclohexenyl/pyrrolidine core. Borreverine (**5**), which was isolated from the genus *Borreria* in the 1970s,⁵ contains a similar core, but with a different indole connectivity that translates to a cyclohexenyl/cyclopentane core. As a result, the tryptamine side chain on that indole forms a bridged propellane ring system.

1.3 Antimalarial Activity

In addition to intriguing structures, flinderoles A–C, isoborreverine, and dimethylisoborreverine, have promising biological activities for the treatment of malaria (Table 1).^{1,6} In general, the dimethylamines (**2**, **3**, and **7**) were more potent than the monomethylamines (**1** and **6**) and have roughly similar efficacy to chloroquine. Dimethylisoborreverine's activity was particularly intriguing. Its lethality was not susceptible to resistance found in FCR3 or

TABLE 1 Antimalarial Activities of the Flindersial and Borrerial Alkaloids^{1,6}

Compound	IC ₅₀ (μM) ^a						
	<i>P. falciparum</i>					HEK 293	Selectivity index ^e
	3D7	FCR3 ^b	HB3 ^c	K1 ^d	HeLa		
Flinderole A (1)	0.75	0.92	1.16	1.61	19.93	19.97	12–26
Flinderole B (2)	0.21	0.11	0.64	0.08	2.79	2.13	3–27
Flinderole C (3)	1.10	0.36	1.17	0.33	19.21	9.75	8–29
Isoborreverine (6)	0.24	0.16	0.47	0.33	1.68	8.99	19–56
Dimethylisoborreverine (7)	0.22	0.02	0.81	0.06	5.37	4.09	5–205
Liriodenine	18.79	25.85	12.31	17.65	31.75	12.92	<1
Xylopinine	1.85	3.50	1.06	3.12	92.67	52.72	15–50
Voacamine	2.13	1.64	1.84	1.72	14.81	13.04	6–8
Chloroquine	0.02	0.09	0.02	0.30	103.35	26.96	300–1348
Artemisinin	0.02	0.02	0.02	0.01	>100	>100	>5000
Pyrimethamine	0.03	0.01	>1	>1	28.88	25.17	N/A
Puromycin	N/A	N/A	N/A	N/A	0.39	0.44	N/A

^aIC₅₀, 50% inhibitory concentration.

^bChloroquine-resistant strain.

^cPyrimethamine-resistant strain.

^dChloroquine-resistant and pyrimethamine-resistant strains.

^eRange of values calculated by IC₅₀(*P. falciparum*)/IC₅₀(HEK 293).

K1 strains of the parasite, which are resilient toward aminoquinolines such as chloroquine and mefloquin.⁷ Chloroquine has been found to interrupt the parasite's metabolism of hemoglobin.⁸ The aminoquinoline binds to free heme released from hemoglobin digestion and prevents it from being polymerized to hemozoin. Free heme builds to toxic levels in the parasite's food vacuole, in turn killing the parasite.⁸ A key study determined that while dimethylisoborreverine disrupts hemoglobin metabolism, it does not do so by binding free heme.^{6b} This observation, along with its lack of susceptibility to chloroquine resistance, suggests that it operates via a novel mode of action. We sought synthetic access to these alkaloids to aid in determination of the mechanism of action and as lead compounds for the development of new malaria therapies.

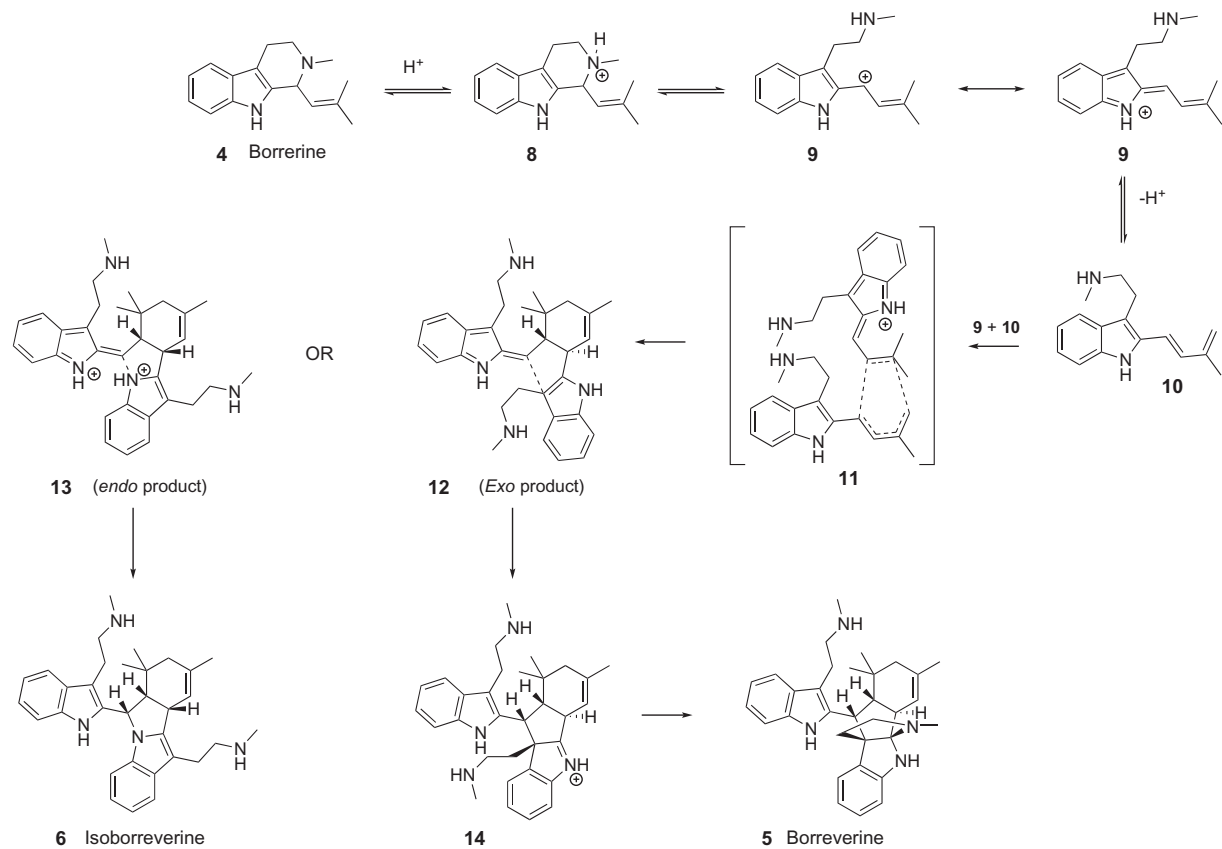
2 BIOSYNTHETIC PROPOSALS

Given the similarity in structural components between the flinderoles and the borreverines, multiple research groups postulated related biosyntheses for the two structural classes. Our initial impression was that they would be formed by the dimerization of two isoprenylated methyltryptamines in the presence of acid. A search in the chemical literature quickly turned up a study that postulated and validated that very idea for the borreverines.

2.1 For the Borreverines

2.1.1 Hypothesis

Koch and Cavé proposed that exposure of borrerine (**4**), itself a natural product produced by *Borreria* and *Flindersia*, to acid would cause protonation of the tertiary amine (Scheme 1), which in turn would lead to a reactive cationic intermediate **9**.^{4b} That intermediate would be stabilized by resonance through the proximal indole. The protons on the methyl groups in the cation **9** are acidic, and deprotonation would lead to the 2-isoprenylated tryptamine **10**. At this stage, the electron-rich diene in **10** can initiate a Diels–Alder reaction with the electron-deficient olefin in cation **9** (see transition state **11**). The functionalized-cyclohexene products **12** and **13** would still bear an electrophilic carbon within the alkylidene-2*H*-indolium ion (left indole ring in **12** and **13**). Either the nitrogen or C3 of the other indole may react with that nucleophilic center, forming the pyrrolidine or the cyclopentane found in isoborreverine or borreverine, respectively. In the latter case, the iminium group in **14** would react with the tryptamine side chain to form the propellane found in fully formed borreverine. The formation of borreverine versus isoborreverine is likely dependent on the Diels–Alder reaction. An *exo* transition state is needed to produce the *trans* cyclohexene **12**, which predisposes the indoles for C3 attack as found in borreverine formation.^{9b} On the other hand, if the Diels–Alder reaction proceeds through an *endo* transition state, then a *cis*



SCHEME 1 The biosynthesis of the borreverines.

cyclohexene **13** is produced, and the indole nitrogen acts as the nucleophile, producing isoborreverine. As the *endo* transition state for the Diels–Alder reaction is generally lower in energy, the formation of isoborreverine would be expected to be more prevalent relative to borreverine.

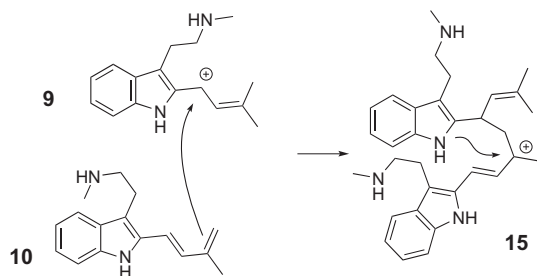
2.1.2 Experimental Support

The hypothesized biosynthesis of the borreverines was studied *in vitro* by Koch and Cavé. Testing proceeded by treatment of naturally produced borreverine with several acids. Their 1978 report reveals TFA in benzene at 55 °C provided the best results, with a 1:1 mixture of borreverine and isoborreverine being formed in 80% yield.^{4b} Prolonged reaction times enriched the mixture in isoborreverine, and pure borreverine could be converted to isoborreverine under those conditions. These latter observations indicate that interconversion between these compounds is possible and that isoborreverine is the thermodynamically preferred product.

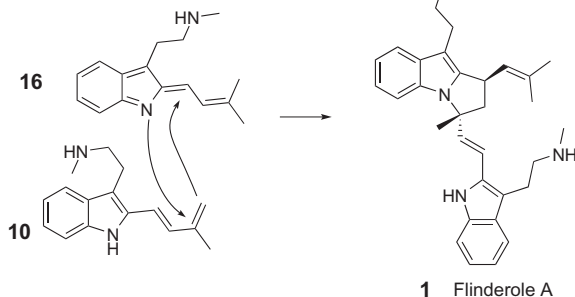
2.2 For the Flinderoles

Our group proposed a biosynthesis of the flinderoles that also proceeds via the intermediacy of cation **9** and isoprenylated indole **10** (Scheme 2).⁹ Cation **9** would

May *et al.*



Dethe *et al.*



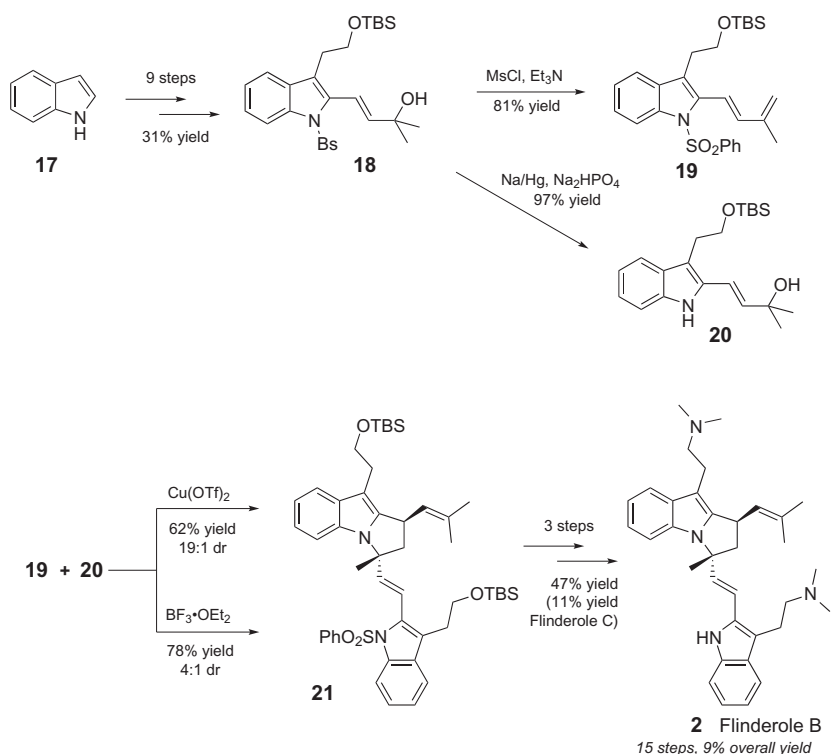
SCHEME 2 Biosynthesis proposals for the flinderoles.

be attacked at the benzylic position by the π -system of diene **10** instead of undergoing the Diels–Alder reaction that forms cyclohexenes **12** and **13**. Pyrrolidine ring closure would then proceed by indole nitrogen attack in the resonance-stabilized cation **15** to afford flinderole A (**1**). Dethe *et al.* had also proposed a nearly the identical sequence, with the pyrrolidine formed directly through a [2+3]-cycloaddition of dearomatized indole **16** and isoprenylated indole **10**.¹⁰

3 SYNTHETIC APPROACHES TO THE FLINDEROLES

3.1 The Dethe Group

Dethe and coworkers were the first to report a total synthesis of the flinderoles in 2011.^{10a} They initially studied model systems like 2-isoprenylskatole to demonstrate [2+3]-cycloadditions, but found that the acidic conditions resulted in polymerization of the dienes or very low yields of pyrrolidine product. To bring a synthesis inspired by their biosynthetic proposal to fruition, they incorporated a strategic benzenesulfonyl (SO_2Ph) protecting group on one of the reacting partners (see **19**, Scheme 3). This broke the symmetry of the dimerization and allowed the pyrrolidine product **21** to be formed in

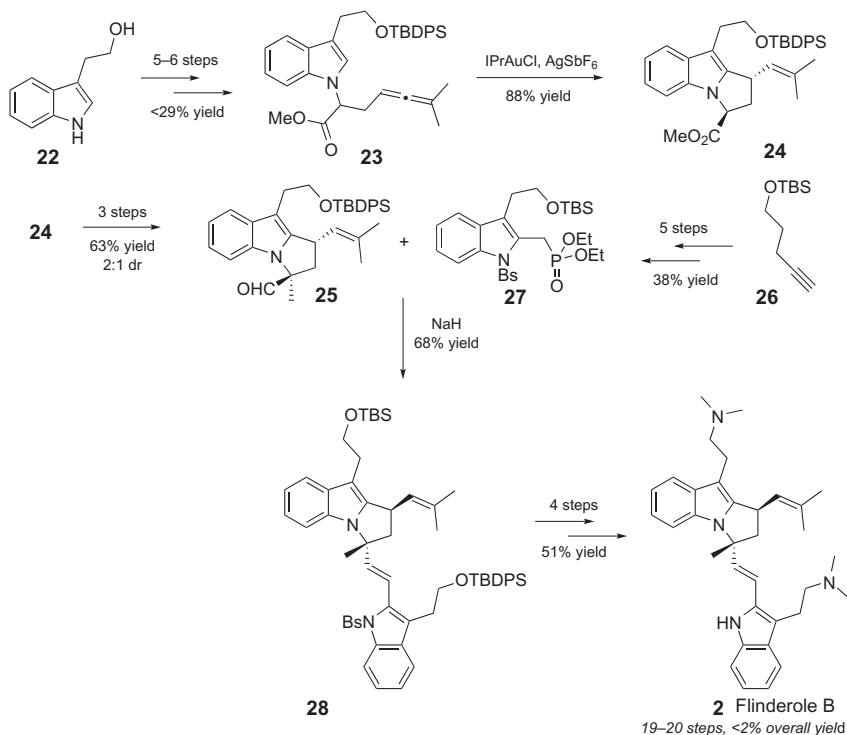


SCHEME 3 The Dethe group's synthesis of flinderole B.

62% yield and 19:1 dr with $\text{Cu}(\text{OTf})_2$ as a Lewis acid. In order to access the diastereomer related to flinderole C, the less diastereoselective $\text{BF}_3 \cdot \text{OEt}_2$ could be used to give pyrrolidine **21** in 78% yield and only 4:1 dr. Since these diastereomers could be chromatographically separated, that material was purified into its component diastereomers, and each was carried forward in the synthesis. The removal of protecting groups and incorporation of the tertiary amines proceeded without incident, resulting in a racemic synthesis of flinderole B in 15 total steps and 9% overall yield. Flinderole C, the minor diastereomer, was similarly produced in $\sim 2\%$ overall yield.

3.2 The Toste Group

Soon thereafter in 2011, Toste and coworkers reported a synthesis that differed from the biosynthetic proposals laid out by the May and Dethe groups (Scheme 4).¹¹ The Toste group's experience with cationic gold catalysis inspired an intramolecular Friedel–Crafts allylation reaction to form the flinderoles' pyrrolidine ring (see **24**) from *N*-functionalized indole **23**. Allene **23** was readily available from commercially available 3-hydroxyethylindole **22**, which could either be purchased or synthesized via reduction of



SCHEME 4 The Toste group's synthesis of flinderole B.

3-indoleacetic acid. α -Methylation of ester **24** afforded the diastereomeric relationship found in flinderole B in slight excess as shown in **25**. Phosphonate-mediated coupling with the protected indole **27** completed the flinderole core, and the use of Dethe *et al.*'s side chain amination provided the finished product in 19 total steps (20 if indole **22** is synthesized from 3-indoleacetic acid), 14 steps longest linear sequence, and ~2% overall yield for the major diastereomer.

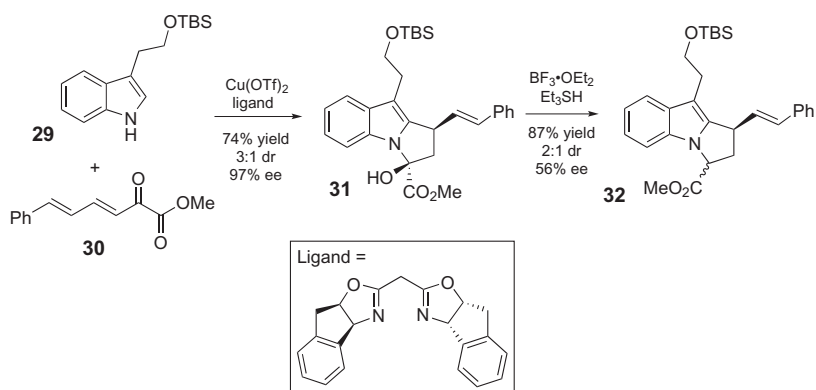
3.3 The Xiao Group

Very recently, an enantioselective pyrroloannulation has been disclosed, with the authors pointing out that it could potentially be used in an approach to the flinderoles or analogs thereof.¹² The copper-catalyzed annulation in the presence of a chiral bisoxazoline ligand forms pyrroloindole **31** from the simple 3-alkyl indole **29** through initial 2-functionalization of the indole ring followed by ring closure at the nitrogen (Scheme 5). Unfortunately, however, the reduction of hydroxyester **31** to ester **32**, which is reminiscent of pyrroloester **24** reported by Toste *et al.*, caused significant degradation of enantiopurity. It should also be noted that no examples without aryl substitution on the α,β -unsaturated ester **30** were demonstrated, so application of this approach to the flinderoles would require transformation of the styrenyl group in **32** to an *iso*-butylene.

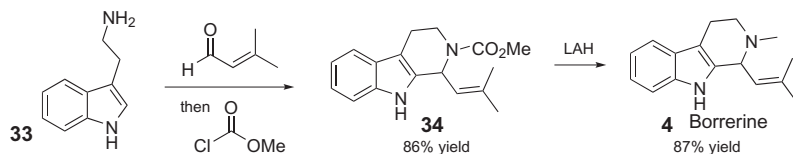
4 BIOMIMETIC SYNTHESIS OF THE FLINDEROLIS AND BORREVERINES IN THREE STEPS

4.1 Borrerine Synthesis

We reported a biomimetic synthesis of flinderoles A–C, desmethylflinderole C, isoborreverine, and dimethylisoborreverine in 2012.⁹ In that study, the dimerization of the fully elaborated borrerine, rather than a model system,



SCHEME 5 Enantioselective pyrrolidine formation from the Xiao group.



SCHEME 6 Borrerine synthesis.

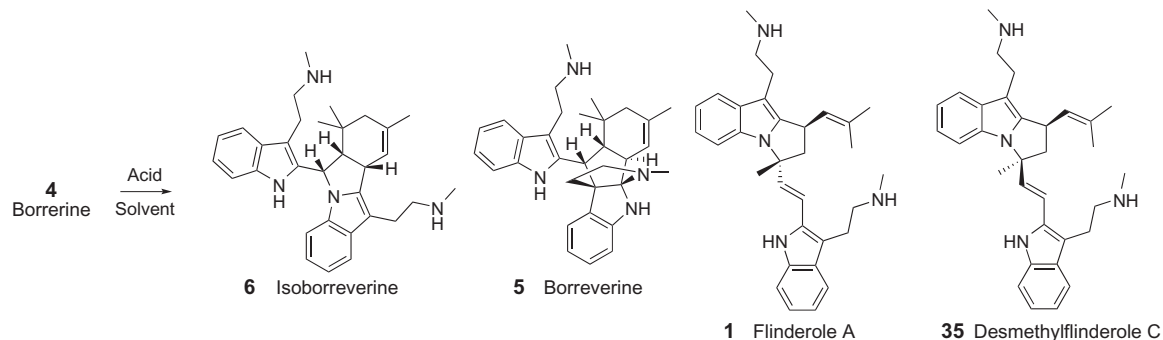
was targeted. Our experience in synthesis has been that model systems often fail to reproduce the reactivity of more complex molecules. Due to the lack of availability of naturally produced borreverine, it was synthesized from tryptamine in two steps through modification of Sakai's approach (Scheme 6).¹³ A significant increase in the yield of the first reaction was obtained by avoiding chromatography of the β -carboline. Purification via trituration resulted in $\sim 20\%$ increase in yield by avoiding silica-induced decomposition. Indeed, careful attention to the method of isolation and of purification of these indole alkaloids proved to be essential to successful experiments as detailed below. Subsequent reduction of the methyl carbamate generated the methylamine in borreverine (4).

4.2 Effects of Acid on Borrerine Dimerization

4.2.1 Neat TFA

Initially, we made an effort to reproduce the 1978 study by Koch and Cavé^{4b} to see if the flinderoles were produced in small amounts by those conditions but were overlooked at the time since their structure did not correspond to known natural products. Surprisingly, TFA in benzene at 55 °C did not produce any observable amounts of borreverine despite extensive efforts at purifying and isolating every product from the reaction. Instead, an equimolar mixture of each of the two flinderole diastereomers and isoborreverine was observed.⁹ Under a variety of TFA concentrations and with variations in solvents, we only observed trace amounts of borreverine. In fact, repeated experiments were needed to obtain enough of that material to obtain an analytically pure sample and fully characterize it to be sure that the product really was borreverine. A variety of alkaloid purification methods were sampled, but the best results were obtained through normal phase preparative TLC purification. Optimization of eluents was made, and then the improved conditions could be scaled for use with flash column chromatography. Given the similar R_F values and NMR spectra for borreverine and the flinderoles,^{9a} we cannot rule out that the flinderoles were produced in the 1978 experiments but were classified as borreverine.

In contrast to TFA in benzene, neat TFA greatly favored the formation of isoborreverine, with a 90:10 ratio to the flinderoles being observed after 30 min of reaction (Table 2). After extended time (>36 h), isoborreverine

TABLE 2 Conditions for the Dimerization of Borrerine^a

Acid	Equiv	Solvent	Temp	Time	Isoborreverine (%)	Borreverine (%)	Flinderole A (%)	Desmethyl-flinderole C (%)
TFA	2.0	None	65 °C	48 h	100	0	0	0
BF ₃ ·OEt ₂	2.0	PhH	22 °C	72 h	100	0	0	0
AlCl ₃	2.0	PhH	60 °C	40 m	40	0	0	0
Sc(OTf) ₃	2.0	PhH	60 °C	40 m	38	0	0	0
Tf ₂ O	2.0	PhH	0 °C	60 m	50	0	0	0
1 N HCl _(aq)	6.0	MeOH	55 °C	2 h	30	1	43	26
TFA	2.0	CHCl ₃	45 °C	1.2 h	5	1	38	33
AcOH	210	None	55 °C	18 h	21	31	24	24
TfOH	2.0	PhH	60 °C	40 m	Intractable mixture and decomposition			

^aProduct ratios determined from peak integration in the ¹H NMR of the crude product mixture.^{9a}

was the sole product observed. In fact, treatment of isolated samples of the flinderols under the same conditions also produced isoborreverine, again indicating the possibility for interconversion and the thermodynamic stability of isoborreverine. In neat TFA, the flinderols appear to be a minor, kinetically favored product. This biomimetic strategy generated this intriguing natural product in only three steps from tryptamine in 30% overall yield of the isolated product, allowing us to quickly synthesize substantial amounts of isoborreverine.

4.2.2 *Lewis Acids*

Generally, the use of Lewis acids produced isoborreverine (**6**) preferentially. Though all of the Lewis acids caused the dimerization of borrerine to proceed slowly, $\text{BF}_3 \cdot \text{OEt}_2$ proved to be the most reactive and gave nearly quantitative conversion to isoborreverine after 3 days. As the boron byproducts were easily removed, this acid proved to be convenient to synthesize hundreds of milligrams of isoborreverine of sufficient purity for further biological testing.

4.2.3 *1 N Anhydrous HCl in Methanol*

The first indication of conditions that would favor the formation of the pyrrolidine found in the flinderols resulted from the use of anhydrous HCl in methanol. These protic conditions resulted in a 2:1 bias in formal [2+3]-cycloaddition to Diels–Alder reaction products. Fewer than 6 equiv. of acid caused a sluggish reaction, and a higher concentration did not alter the ratio of products greatly. Nevertheless, this result provided hope that buffered or more weakly acidic conditions would avoid the interconversion of dimeric products that favors isoborreverine formation. We sought other conditions empirically that would provide the flinderols though kinetic reaction control.

4.2.4 *Dilute TFA*

Excitingly, the use of dilute TFA in CHCl_3 provided access to a flinderole-enhanced mixture. The lower concentration of acid in a moderately polar solvent seemed to favor the formation of the kinetic products and avoid alkaloid interconversion. Borrerine (**4**) was less reactive under these conditions, and the balance of the material was unreacted starting material. However, all components were readily purified via flash column chromatography. With these conditions, we could synthesize the flinderols as the major products directly from borrerine and in three steps from tryptamine.

4.2.5 *Acetic Acid*

Borreverine was not observed in any more than trace quantities unless a weaker acid was used. For example, neat acetic acid produced an equimolar mixture of each flinderole and borreverine. In this more weakly acidic

solvent, kinetic borreverine formation competes with flinderole formation. Studies are ongoing to further characterize the effects of pH on product formation, to reconcile the observed reactivity, and to identify conditions that favor borreverine formation.

4.2.6 Triflic Acid

Triflic acid was the only acid that caused extensive decomposition of borreverine and/or the dimeric products when used at elevated temperatures. Presumably, its strength was sufficient to allow for a variety of reaction pathways and resulted in an intractable mixture of dozens of compounds. If lower temperatures were used, then multiple products were still seen, but their formation occurred at a slower rate.

4.2.7 Reaction Outcome Correlated to Acid Strength

We have been seeking conditions that selectively form each of the dimeric compounds in [Figure 1](#) directly from borreverine. By identifying patterns in reactivity, we hope to build a predictive model that will inform those efforts. Though a comprehensive description of solvent and acid effects on the outcome of borreverine dimerization is still a work in progress, there appears to be a correlation between the strength of the acid and the distribution of bisindole alkaloid products.

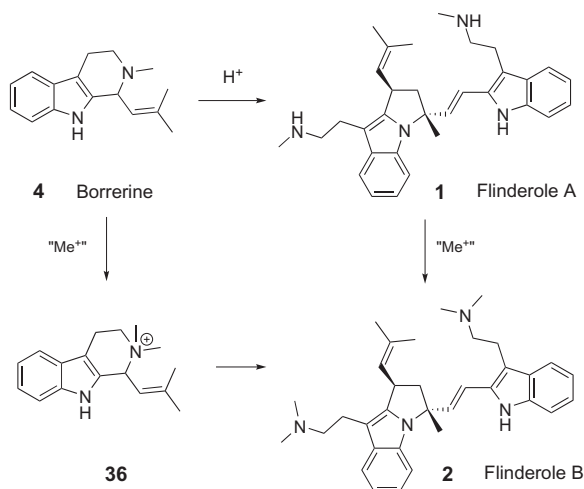
This variation occurs whether the modulation occurs through changing the acid to one with a higher or lower pK_a or if it occurs through variation in acid concentration. Stronger, more concentrated acid (e.g., neat TFA) allows for product equilibration to occur, eventually providing isoborreverine as the sole product. Since the product distribution at early time points is also biased toward isoborreverine, the *endo*-Diels–Alder reaction pathway appears to also be the most rapid under these conditions. As the acid concentration is lowered in a less-polar solvent (e.g., TFA in $CHCl_3$), the product equilibration is greatly slowed or stopped. At the same time, the pathway leading to pyrrolidine ring formation is found to be more rapid and the flinderoles are the major product. Similarly, in the presence of a weaker acid (e.g., AcOH), the formation of isoborreverine is minimized and the kinetically preferred flinderoles are again observed. Why borreverine (**5**) is only seen when AcOH is used to promote dimerization remains unclear, but ongoing experiments are expected to shed light on the matter. Our current hypothesis is that the nature of the solvent impacts the stability and therefore prevalence of ionic intermediates, which in turn alters the trajectory of the reaction.

4.3 Methylation Dimerization

Acidic dimerization of borreverine as described above provided only the monomethylamine natural products. The dimethylamine products were desirable

given their greater malarial potency. One could easily envision treating the dimeric products above under methylative conditions, which would provide those compounds in only four steps from tryptamine. We noticed that the species-specific methylation pattern for the natural products suggested another possibility. The *Flindersia* species *acuminata* only afforded the secondary amines **1** and **6**, whereas the species *amboinensis* only afforded the tertiary amines **2**, **3**, and **7**. It seems evident that the latter species produces a “methylase” that the former did not. Of course, the hypothetical methylase or methylases could act on flinderole A, desmethylflinderole C, or isoborreverine to produce their doubly methylated congeners (Scheme 7). On the other hand, this methylase could act directly on borreverine, producing a dimethyl ammonium **36** that initiates the cascade. The sequence, step count, and product ratios would be identical to those in Section 2.2, but the more biologically active compounds would be obtained. Given the abundance of electrophilic methylating reagents available to the synthetic chemist, we sought to test this possibility in the laboratory.

Treatment of borreverine with methyl triflate produced the ammonium **36**, which could be isolated and characterized.^{9a} Treatment of ammonium **36** with excess TFA initiated a dimerization sequence identical to that found for protonated borreverine, but in this case produced a mixture of the bis-tertiary amine products **2**, **3**, and **7** (Table 3). This reactivity mirrored that seen in the acid-promoted dimerization of borreverine to produce monomethylamines. In that case, 1 equiv. of acid produced no change in the starting material. Reaction was only seen in the presence of superstoichiometric amounts of acid. As before, extended reaction times and higher temperatures afforded exclusively the thermodynamically favored product, in this case dimethylisoborreverine.



SCHEME 7 Potential biosyntheses of flinderole B.

TABLE 3 Results of a Methylation-Initiated Dimerization Cascade

Time	Temp	Flinderole B (%)	Flinderole C (%)	Dimethylisoborrerverine (%)
15–20 min	0 °C	21 ^a	19 ^a	30 ^a
>2 h	Room temp	0	0	60 ^b

^aProduct ratios determined from peak integration in the ¹H NMR of the crude product mixture.^bIsolated yield.^{9a}

Thus, this alkaloid with promising novel antimalarial activity was synthesized in three steps from tryptamine and 45% overall yield. Flinderoles B and C were also produced for study, though conditions for their selective formation are still under development.

5 OPTICAL ACTIVITY

5.1 Reports of Flinderole Optical Activity

To this point, all of the experiments that we conducted have supported the biosynthetic hypothesis outlined at the top of [Scheme 2](#) (see [Section 2.2](#)). However, there remained a mildly vexing set of data from the 2009 report describing the flinderoles that on the surface seemed to contradict the possibility of an enzyme-free acid-promoted dimerization of borrerine. While the borreverines and related compounds like yuechukene were reported to be isolated as racemates, the flinderoles A–C were reported to have specific rotations of -6.4 , -7.3 , and -7.4 ($c=0.03$), respectively.¹ Since enantioenrichment implies an element of chiral control, and all acids studied in the dimerization produced racemic compounds, the report of optical activity in the natural samples suggested some biological involvement in their formation. Of note, however, is the low concentration used for the polarimetry experiments, which is not an extremely sensitive analytical technique. Furthermore, all three compounds exhibited similar specific rotations, even the two diastereomers. These

observations caused us to believe that the low absolute values of the rotations were not representative of that which would be found for an enantiomerically pure sample of a flinderole. If that were indeed the case, then our proposed enzyme-free dimerization remained entirely plausible, and, we would argue, highly likely given the studies for closely related compounds.

5.2 Experimental Evaluation

To support our belief that the original data may not have been reliable, we initiated a collaboration with the Armstrong analytical research group. Using the ample supply of compounds available from the three-step biomimetic synthesis, the latter group quickly developed HPLC-based assays to separate the enantiomers for **1**, **2**, **3**, **6**, and **7**.¹⁴ Key to the separation was the use of vancomycin-based stationary phases. In order to directly compare the rotations of enantiopure flinderole B to the literature value, the method was used on a prep-scale column to purify ≥ 14 mg of each enantiomer. The minus enantiomer gave a very low rotation at the same concentration ($c=0.03$) used for the natural sample (Table 4). In fact, the rotation was within the error range seen when using pure solvent in the solvent cell. The use of a 10-fold higher concentration afforded robust data, where equal but opposite specific rotations were obtained for the two enantiomers. The much larger specific rotation of -48.8 indicates that the highest enantioenrichment that the natural sample could have had when isolated was a 58:42 mixture of (–) and (+) enantiomers. However, the ambiguity at low concentration casts some doubt on the original data. Certainly, the *in vitro* work on flinderole formation demonstrates the possibility of enzyme-free dimerization of bornerine. Unfortunately, our collaborative effort was unable to locate an authentic natural sample of one of the flinderoles for the assay, and so conclusive evidence whether they are naturally produced racemically or enantioenriched remains to be obtained.

TABLE 4 Optical Rotations

Compound	Concentration	α	Standard deviation	$[\alpha]_D$ [24]
Natural flinderole B	0.03 g/100 mL	Not reported	N/A	-7.4
1st eluted from HPLC	0.028 g/100 mL	-0.006°	0.005	Not reliable
1st eluted from HPLC	1.400 g/100 mL	-0.342°	0.005	-48.8
2nd eluted from HPLC	0.325 g/100 mL	0.079	0.002	48.6

6 CONCLUSION

In conclusion, a significant body of work has resulted from the study of how the borreverines and flinderoles are synthesized, both *in vivo* and *in vitro*. The acid-mediated biosynthetic hypotheses have been validated in laboratory studies, resulting in a three-step synthesis of borreverine, isoborreverine, dimethylisoborreverine, and flinderoles A–C from tryptamine. Experiments that rely on the straightforward availability of these compounds are now underway to determine their mode of action and their biological targets, if any. Moreover, the rapid biomimetic synthesis lends itself to structure/activity relationship determination, medicinal chemistry approaches to improve the biological activity, and the synthesis of libraries based on the structures of these compounds.

REFERENCES

1. Fernandez, L. S.; Buchanan, M. S.; Carroll, A. R.; Feng, Y. J.; Quinn, R. J.; Avery, V. M. *Org. Lett.* **2009**, *11*, 329–332.
2. Charette, A. B. In: *Chiral Amine Synthesis: Methods, Developments and Applications*; Nugent, T. C., Ed.; Wiley-VCH: Weinheim, 2010; pp 1–49; (b) Cogan, D. A.; Ellman, J. A. *J. Am. Chem. Soc.* **1999**, *121*, 268–269; (c) Evans, J. W.; Ellman, J. A. *J. Org. Chem.* **2003**, *68*, 9948–9957; (d) Ding, H.; Friestad, G. K. *Synthesis* **2005**, *16*, 2815–2994; (e) Petrini, M.; Torregiani, E. *Synthesis* **2007**, *18*, 159–236; (f) Friestad, G. K.; Mathies, A. K. *Tetrahedron* **2007** *63*, 2541–2569.
3. (a) Ting, A.; Schaus, S. E. *Eur. J. Org. Chem.* **2007**, 5797–5815; (b) Lou, S.; Moquist, P. N.; Schaus, S. E. *J. Am. Chem. Soc.* **2007**, *129*, 15398–15404; (c) Lou, S.; Schaus, S. E. *J. Am. Chem. Soc.* **2008**, *130*, 6922–6923; (d) Luan, Y.; Schaus, S. E. *Org. Lett.* **2011**, *13*, 2510–2513; (e) Municipinto, G.; Moquist, P. N.; Schreiber, S. L.; Schaus, S. E. *Angew. Chem. Int. Ed.* **2011**, *50*, 8172–8175; (f) Riant, O.; Hannedouche, J. *Org. Biomol. Chem.* **2007**, *5*, 873–888; (g) Yin, B.; Zhang, Y.; Xu, L.-W. *Synthesis* **2010**, *21*, 3583–3595; (h) Yus, M.; González-Gómez, J. C.; Foubelo, F. *Chem. Rev.* **2011**, *111*, 7774–7854.
4. (a) Pousset, J.-L.; Cavé, A.; Chiaroni, A.; Riche, C. *J. Chem. Soc., Chem. Commun.* **1977**, 261–262; (b) Tillequin, F.; Koch, M.; Pousset, J.-L.; Cavé, A. *J. Chem. Soc., Chem. Commun.* **1978**, 826–828; (c) Tillequin, F.; Rousselet, R.; Koch, M.; Bert, M.; Sevenet, T. *Ann. Pharm. Fr.* **1979**, *37*, 543–548; (d) Tillequin, F.; Koch, M.; Bert, M.; Sevenet, T. *J. Nat. Prod.* **1979**, *42*, 92–95.
5. Pousset, J.-L.; Kerharo, J.; Maynard, G.; Monseur, X.; Cavé, A.; Goutarel, R. *Phytochemistry* **1973**, *12*, 2308–2310.
6. (a) Fernandez, L. S.; Jobling, M. F.; Andrews, K. T.; Avery, V. M. *Phytother. Res.* **2008**, *22*, 1409–1412; (b) Fernandez, L. S.; Sykes, M. L.; Andrews, K. T.; Avery, V. M. *Int. J. Antimicrob. Agents* **2010**, *36*, 275–279.
7. (a) Goldberg, D. E.; Sharma, V.; Oksman, A.; Gluzman, I. Y.; Welles, T. E.; Piwnicka-Worms, D. *J. Biol. Chem.* **1997**, *272*, 6567–6572; (b) Snow, R. W.; Guerra, C. A.; Noor, A. M.; Myint, H. Y.; Hay, S. I. *Nature* **2005**, *434*, 214–217; (c) Trouiller, P.; Battistella, C.; Pinel, J.; Pecoul, B. *Trop. Med. Int. Health* **1999**, *4*, 412–420.
8. (a) Goldberg, D. E. *Curr. Top. Microbiol. Immunol.* **2005**, *295*, 275–291; (b) Liu, J.; Istvan, E. S.; Gluzman, I. Y.; Gross, J.; Goldberg, D. E. *Proc. Natl. Acad. Sci.* **2006**, *103*, 8840–8845.

9. (a) Vallakati, R.; May, J. A. *J. Am. Chem. Soc.* **2012**, *134*, 6936–6939; (b) Vallakati, R.; May, J. *Synlett* **2012**, 23, 2577–2581.
10. (a) Dethe, D. H.; Erande, R. D.; Ranjan, A. *J. Am. Chem. Soc.* **2011**, *133*, 2864–2867; (b) Dethe, D. H.; Erande, R. D.; Ranjan, A. *J. Org. Chem.* **2013**, *78*, 10106–10120.
11. Teng, T.-M.; Das, A.; Huple, D. B.; Liu, R.-S. *J. Am. Chem. Soc.* **2010**, *132*, 12565–12567.
12. Cheng, H.-G.; Lu, L.-Q.; Wang, T.; Yang, Q.-Q.; Liu, X.-P.; Li, Y.; Deng, Q.-H.; Chen, J.-R.; Xiao, W.-J. *Angew. Chem. Int. Ed.* **2013**, *52*, 3250–3254.
13. Yamanaka, E.; Shibata, N.; Sakai, S.-I. *Heterocycles* **1984**, *22*, 371–374.
14. (a) Vallakati, R.; Smuts, J. P.; Armstrong, D. W.; May, J. A. *Tetrahedron Lett.* **2013**, *54*, 5892–5894; (b) Smuts, J. P.; Na, Y.-C.; Vallakati, R.; Přibylka, A.; May, J. A.; Armstrong, D. W. *Anal. Bioanal. Chem.* **2013**, *405*, 9169–9177.

Synthesis of (\pm)-Amathaspiramide F: Stereochemical Switch of a [2,3]-Stevens Rearrangement

Arash Soheili, Carrie Johnson, and Uttam K. Tambar¹

Department of Biochemistry, The University of Texas Southwestern Medical Center at Dallas, Dallas, Texas, USA

¹Corresponding author: uttam.tambar@utsouthwestern.edu

Chapter Outline

1 Introduction	131	4.1 [2,3]-Stevens	
2 Amathaspiramide Alkaloids	132	Rearrangement	
3 Previous Syntheses of Amathaspiramides	133	Methodologies	140
3.1 Trauner Synthesis of Amathaspiramide F	134	5 Initial Route to Amathaspiramide A	144
3.2 Sakaguchi Synthesis of Amathaspiramide F	136	6 Role of <i>ortho</i>-Substitution of Aromatic Carbonates	148
3.3 Fukuyama Syntheses of Amathaspiramides A–F	137	7 Formal Synthesis of Amathaspiramide F	148
4 Retrosynthetic Analysis of Amathaspiramides	139	8 Concluding Remarks	152
		Acknowledgments	152
		References	152

1 INTRODUCTION

Why is total synthesis still an important scientific endeavor? *Is* total synthesis still an important scientific endeavor? These were questions that my group and I pondered as we opened our lab doors in the fall of 2009. We had been students and practitioners of natural product total synthesis since our earliest days as chemists. We remembered learning about the most amazing total synthesis campaigns that defined the field of synthetic chemistry for decades.¹

We were eager to make this research area an important dimension of our newly formed group.

But we were also aware of the changing world of synthetic chemistry. We recognized that the motivation for future total synthesis projects was as important for the sustainability of the field as the actual chemistry involved in the completion of the syntheses. Natural product synthesis uniquely utilizes cutting-edge synthetic chemistry to impact science and society beyond the completion of the total synthesis.

There are two general reasons why our lab is interested in natural product synthesis. First, some natural products possess valuable properties (such as biological activity in the context of human disease). If these chemicals cannot be obtained easily in large amounts from their natural sources, the laboratory synthesis of natural products provides a unique opportunity to study their activity in more detail for the purpose of benefiting human society. Moreover, the potential to generate unnatural derivatives of these naturally occurring chemicals with more potent or unique biological activities can be realized most effectively through chemical synthesis.

Second, natural products provide an opportunity for learning new lessons in chemical reactivity, which drives the field of synthesis forward. Many fundamental principles of chemical reactivity were elucidated in the context of natural product syntheses. Some of the most memorable total syntheses over the past 100 years are valued for the journey as much as the destination. Arash Soheili, a postdoctoral fellow in our lab, was particularly interested in this motivation for natural product synthesis because of our group's focus on the development of new chemical reactions. Our earliest achievements as a research laboratory were mainly centered on the discovery of new stereoselective reactions, specifically metal-catalyzed [2,3]-rearrangements.² Arash believed that the application of our group's methods to natural product synthesis was an exciting opportunity to gain new insight into fundamental issues of reactivity in the context of [2,3]-rearrangements. While [3,3]-Claisen and Cope rearrangements are indispensable tools in the synthesis of complex natural products,³ [2,3]-rearrangements have been underutilized, presumably because the factors that govern their stereoselectivity are less understood.⁴ Arash thought that the elucidation of factors that control the diastereoselectivity of [2,3]-rearrangements in the context of a total synthesis would lead to the utilization of these reactions for natural product synthesis in a more predictable manner.

2 AMATHASPIRAMIDE ALKALOIDS

In early 2012, Arash came across the amathaspiramides (**1a–f**), a family of marine alkaloids that were isolated in 1999 by Prinsep and coworkers from a New Zealand collection of the bryozoan *Amathia wilsoni* (Figure 1).⁵ The structures were determined by detailed NMR analysis, including NOESY

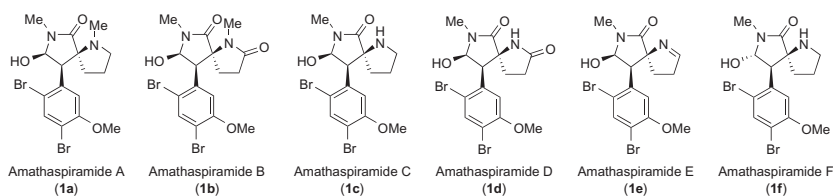


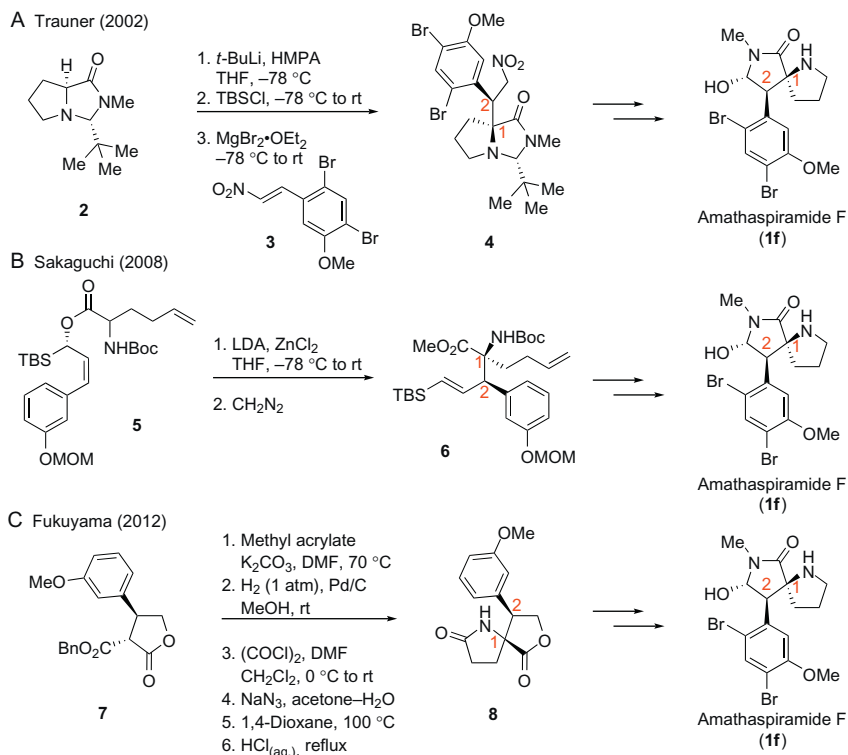
FIGURE 1 Structures of amathaspiramide alkaloids.

NMR experiments. A single-crystal X-ray diffraction study of amathaspiramide F (**1f**) supported the relative and absolute stereochemistry assignment for all six members of this alkaloid family. The amathaspiramides contain a highly dense diazaspirononane structure with three contiguous stereocenters. The pyrrolidinone portion of the molecule contains an unusual *N*-acyl hemiaminal and a benzylic center attached to a dibromomethoxyphenyl group. The various amathaspiramides differ in the alkylation and oxidation state of the pyrrolidine ring. Amathaspiramides A (**1a**) and E (**1e**) show moderate antiviral, antibacterial, and cytotoxicity activity. Due to their unique structure and biological activity, the amathaspiramides have attracted the attention of the synthetic chemistry community. Arash's interest in this family of compounds was strengthened by a desire to apply his recently developed palladium-catalyzed [2,3]-Stevens rearrangement in their synthesis,⁶ with the hope that we would discover something new about the stereochemistry of [2,3]-rearrangements in complex molecular settings.

3 PREVIOUS SYNTHESSES OF AMATHASPIRAMIDES

Since the isolation of the amathaspiramides in 1999, there have been efforts by various groups toward their total synthesis.⁷ In 2002, Trauner reported the first synthesis of a member of this alkaloid family, (–)-amathaspiramide F.⁸ The Sakaguchi group followed in 2008 with their own completed synthesis of (–)-amathaspiramide F.⁹ It was not until 2012 that other members of the amathaspiramide family were synthesized. The Fukuyama group completed the syntheses of the entire family (amathaspiramides A–F).¹⁰

These three synthetic efforts toward the amathaspiramides unveiled important stereocontrolling elements for the assembly of contiguous stereocenters in complex molecular settings (e.g., C1 and C2, [Scheme 1](#)). For example, Trauner's total synthesis of amathaspiramide F highlighted a diastereoselective conjugate addition of a functionalized *N,N*-acetal of proline (**2**) to nitrostyrene derivative **3** ([Scheme 1A](#)). Sakaguchi utilized a diastereoselective enolate Claisen rearrangement of α -acyloxy- α -alkenylsilane **5** to assemble the contiguous stereocenters of the natural product ([Scheme 1B](#)). More recently, Fukuyama reported the synthesis of all members of this alkaloid family, relying on a diastereoselective conjugate addition of β -ketoester **7** to methyl



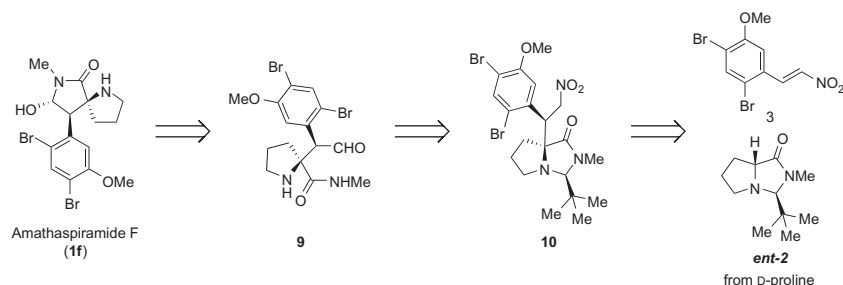
SCHEME 1 Previous approaches to the synthesis of C1 and C2 in the amathaspiramides.

acrylate and a Curtius rearrangement to generate the two contiguous stereo-centers at C1 and C2 (Scheme 1C).

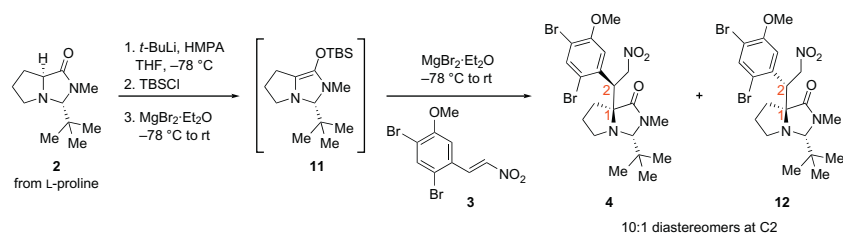
3.1 Trauner Synthesis of Amathaspiramide F

The Trauner retrosynthesis of amathaspiramide F commenced with a disconnection of the *N*-acyl hemiaminal group to amino aldehyde **9**, which could be derived from a Nef reaction of nitroalkyl **10** (Scheme 2). It was envisioned that Seebach's asymmetric alkylation of α -amino acids could be utilized in the conjugated addition of *N,N*-acetal **ent-2** with nitrostyrene **3**.¹¹ Trauner initially surmised that D-proline was required as the starting material, since previous work by Seebach had shown that alkylation occurs on the same face as the *t*-butyl group.

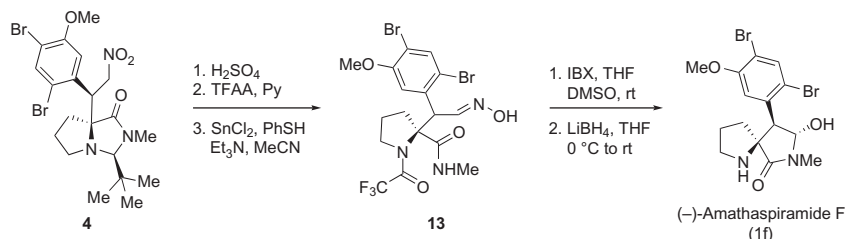
Since D-proline was expensive, the Trauner group chose to use L-proline for the synthesis of *ent*-amathaspiramide F (Scheme 3). The lithium enolate of *N,N*-acetal **2** was difficult to form, and it was ultimately determined that HMPA was required for successful deprotonation. Unfortunately, the conjugated addition to nitrostyrene with the lithium enolate did not provide any



SCHEME 2 Trauner's retrosynthetic analysis of amathaspiramide F.



SCHEME 3 Trauner's assembly of C1 and C2 of amathaspiramide F.



SCHEME 4 Completion of Trauner's synthesis of amathaspiramide F.

desired product. However, trapping of the enolate with TBSCl followed by conjugate addition using $\text{MgBr}_2 \cdot \text{Et}_2\text{O}$ resulted in a 10:1 mixture of diastereomers 4 and 12. The two diastereomeric products were epimeric at C2, and both compounds had the *S* configuration at C1, which was opposite of what was expected based on Seebach's precedent. Fortunately, the major diastereomer 4 possessed the desired stereochemistry at both C1 and C2 for natural amathaspiramide F. This stereoselectivity was attributed to the bulky silyl group in silylketene aminal 11, which directed the alkylation opposite the face of the *t*-butyl group and on the concave face in an open transition state.

With compound 4 in hand, the Trauner group developed a short sequence of five steps to the natural product (Scheme 4). The *N,N*-acetal was cleaved using sulfuric acid followed by protection of the pyrrolidine as the

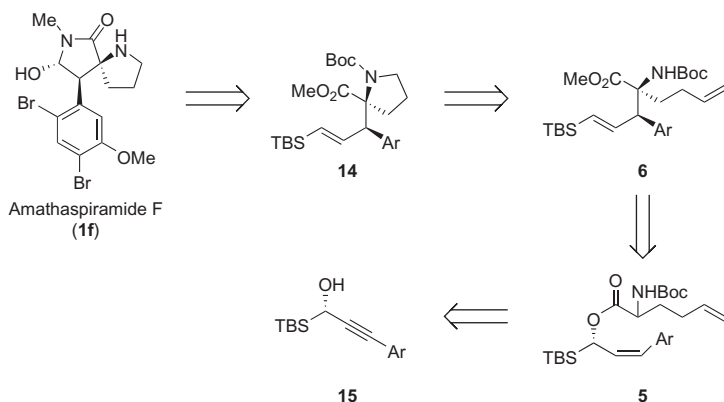
trifluoroacetamide. Attempts at direct reduction of the nitro group to the aldehyde were unsuccessful, and thus a two-step sequence was required. The nitro alkyl group was reduced in the presence of SnCl_2 to furnish oxime **13**. The oxime was then hydrolyzed using IBX to the corresponding aldehyde, which spontaneously formed the *N*-acyl hemiaminal as a single diastereomer. Reduction of the amide with lithium borohydride provided (–)-amathaspiramide F. This approach constituted a concise six-step enantioselective synthesis of amathaspiramide F starting from the known *N,N*-acetal **4**.

3.2 Sakaguchi Synthesis of Amathaspiramide F

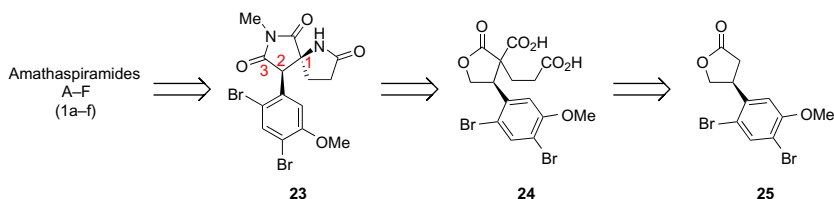
In the Sakaguchi group's total synthesis of (–)-amathaspiramide F, the key disconnection to generate the two contiguous stereocenters was based on an enolate Claisen rearrangement of aminoester **5**, which could be derived enantioselectively from arylpropargyl alcohol **15** (Scheme 5).

The Sakaguchi group began their synthesis from α -silyl propargyl alcohol **16**, which was converted in two steps using a Sonogashira coupling and oxidation into propargyl ketone **17** (Scheme 6). The ketone was reduced enantioselectively in the presence of DIP-Cl to propargyl alcohol **15** in greater than 95% ee. Selective *Z*-reduction of the alkyne followed by coupling with Boc-homoallylglycine provided compound **19**, which underwent the Claisen rearrangement after exposure to LDA and ZnCl_2 . Rearrangement product **6** was obtained as a 7:1 mixture of diastereomers favoring the desired stereochemistry for amathaspiramide F, which was later confirmed in an advanced intermediate.

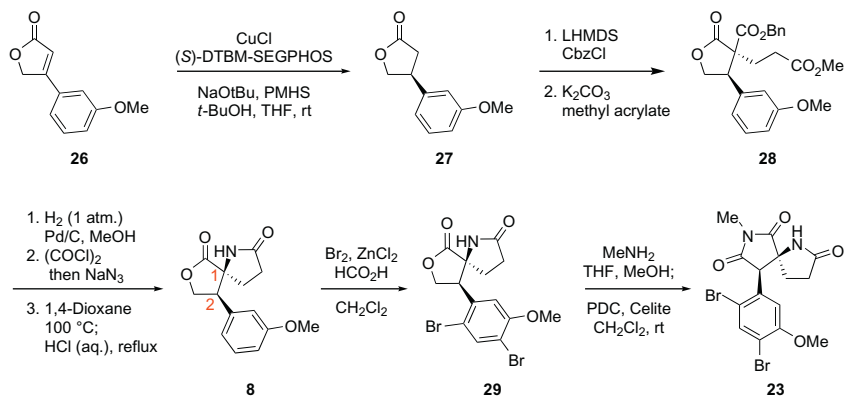
Through a six-step sequence, aminoester **6** was converted to aldehyde **20**, which included the pyrrolidine ring and was poised for the final ring formation (Scheme 7). Attempts at direct conversion of methyl ester **20** to the amide or aminal using methylamine led to low yields of the desired product **21a**.



SCHEME 5 Sakaguchi's retrosynthetic analysis of amathaspiramide F.



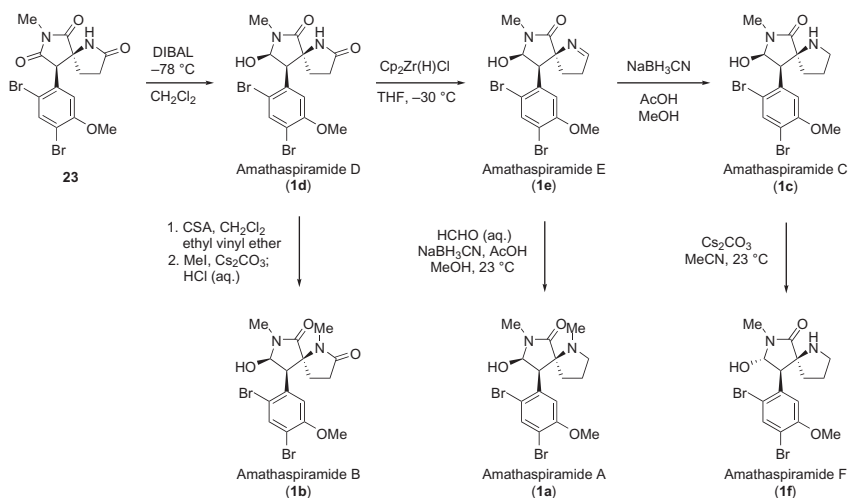
SCHEME 8 Fukuyama's retrosynthetic analysis of amathaspiramides A–F.



SCHEME 9 Fukuyama's assembly of C1 and C2 of amathaspiramides A–F.

The Fukuyama synthesis commenced with the copper-catalyzed asymmetric reduction of butenolide **26** to give lactone **27** in 98% enantiomeric excess (Scheme 9). Sequential alkylation with CbzCl followed by methyl acrylate provided lactone **28** and installed both of the required contiguous stereocenters. The key Curtius rearrangement was performed by conversion of the benzyl ester to the acyl azide followed by heating. Subsequent treatment with aqueous HCl provided cyclized lactam **8**. This compound was then dibrominated to lactam **29** using bromine, ZnCl_2 , and formic acid, which were the only conditions that were able to introduce the *ortho*-bromine. The fully elaborated aromatic compound **29** was treated with methylamine followed by PDC to obtain cyclic *N*-methylimide **23**.

Having cyclic imide **23** in hand, Fukuyama utilized a short number of steps to access all naturally occurring amathaspiramides (Scheme 10). After testing several reducing agents including NaBH_4 , L-selectride, and LiAlH_4 , it was found that DIBAL provided amathaspiramide D (**1d**) in 52% isolated yield. Amathaspiramide D was converted to amathaspiramide E (**13**) by reduction of the lactam to the imine using Schwartz's reagent ($\text{Cp}_2\text{Zr(H)Cl}$). Amathaspiramide E was reduced to provide amathaspiramide C (**1c**) or methylated under formylative conditions to provide amathaspiramide A (**1a**). Amathaspiramide C easily epimerized under basic conditions to yield

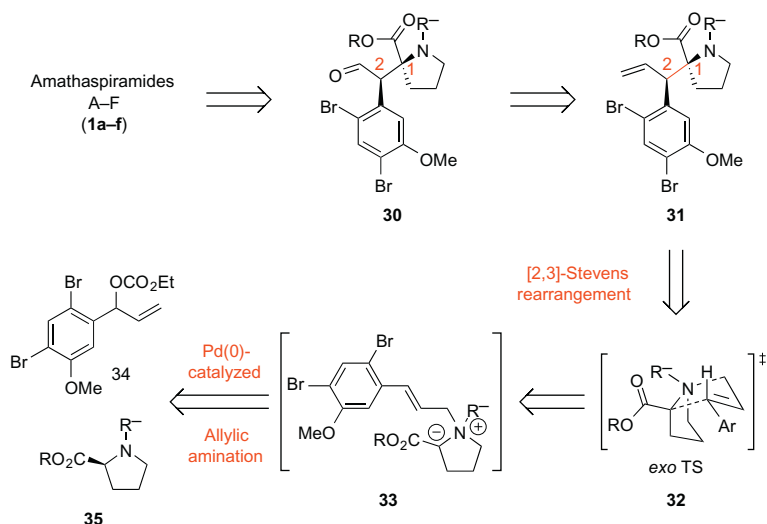


SCHEME 10 Completion of Fukuyama's synthesis of amathaspiramides A–F.

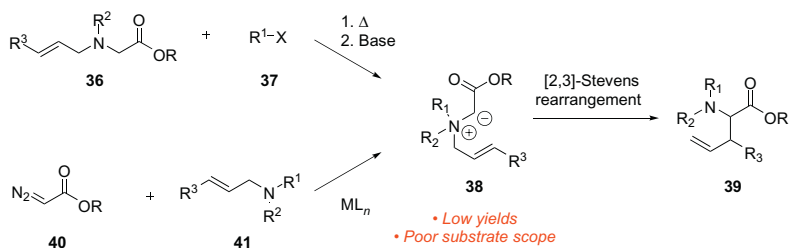
the more stable amathaspiramide F (**1f**). Amathaspiramide D was converted to amathaspiramide B (**1b**) using a two-step sequence of protecting the alcohol with ethyl vinyl ether followed by methylation of the lactam and subsequent deprotection with aqueous acid.

4 RETROSYNTHETIC ANALYSIS OF AMATHASPIRAMIDES

Similar to other synthetic approaches toward the amathaspiramides, Arash was interested in utilizing a stereoselective method to construct the two contiguous stereocenters at C1 and C2, while also assembling the core cyclic structure of this family of alkaloids. Our retrosynthesis was based on disconnecting at the *N*-acyl hemiaminal group to reveal aldehyde **30** (Scheme 11). The aldehyde could be obtained from γ,δ -unsaturated aminoester **31**, which Arash recognized as a retron for the [2,3]-Stevens rearrangement he recently developed in our group. The substrates for this rearrangement would be carbonate **34** and proline **35**, which would selectively couple to form ammonium ylide **33**. After the retrosynthesis was sketched on a piece of paper, Uttam Tambar remembers telling Arash, “We should be able to synthesize one of these natural products in less than a month!” In retrospect, this confidence was foolish, but at the time it seemed well-grounded. Based on everything that was known about the diastereoselectivity of [2,3]-Stevens rearrangements,¹² Uttam expected that the contiguous stereocenters at C1 and C2 would form stereoselectively through *exo* transition state **32** of the [2,3]-rearrangement. Once the key intermediate **31** was formed, Uttam believed the completion of the synthesis would be straightforward.



SCHEME 11 Our retrosynthetic analysis of amathaspiramides via a [2,3]-rearrangement.



SCHEME 12 Traditional approaches to the synthesis of ammonium ylides for [2,3]-Stevens rearrangements.

4.1 [2,3]-Stevens Rearrangement Methodologies

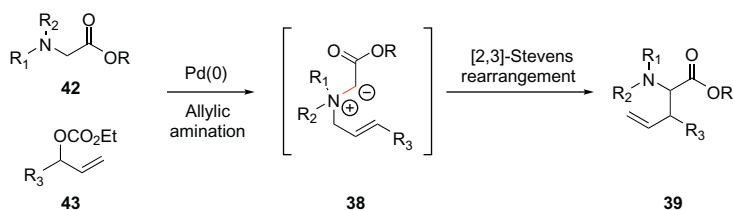
The [2,3]-Stevens rearrangement is a thermal sigmatropic rearrangement of an ammonium ylide (**38**) to form unnatural amino acid derivatives **39** (Scheme 12). Traditionally, the ammonium ylides have been formed through alkylation of aminoesters **36** with alkyl halides **37** to form quaternary salts followed by treatment with base.¹³ Although effective, the harsh conditions lead to side products and limited substrate scope. More recently, the coupling of diazoesters **40** and allylic amines **41** in the presence of metals like copper, rhodium, and palladium has been developed for the direct construction of ammonium ylides **38** via metal carbenoid intermediates.¹⁴ Although this approach represented an advance over the traditional alkylation chemistry, the use of diazoesters still limits the synthetic utility of these reactions.

Recently, our group was in pursuit of a milder and more versatile approach to form ammonium ylides that would allow a wider substrate scope for the

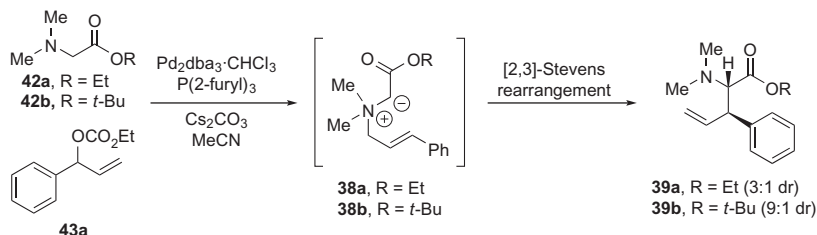
[2,3]-Stevens rearrangement. We envisioned that a palladium-catalyzed allylic amination of a tertiary aminoester **42** with an allylic carbonate **43** in the presence of base should directly provide ammonium ylide **38** and subsequent thermal rearrangement product **39** (Scheme 13). Although primary and secondary allylic amines have extensively been used in allylic amination chemistry,¹⁵ tertiary amines are not considered competent substrates for this mode of reactivity.¹⁶ Despite the lack of literature precedent, Arash was determined to develop this reaction.

We commenced our studies with dimethyl glycine ethyl ester **42a** and cinnamyl carbonate **43a** (Scheme 14). After screening various ligands and bases with palladium sources, we identified Pd₂dba₃·CHCl₃, trifurylphosphine, and cesium carbonate in acetonitrile as the optimal conditions. Glycine ethyl ester **42a** furnished product **39a** as a 3:1 mixture of diastereomers, which could be improved to 9:1 dr by utilizing glycine *t*-butyl ester **42b** for the synthesis of rearrangement product **39b**.

Using these optimal conditions, Arash determined that the substrate scope of the reaction was very general (Scheme 15). Aromatic rings with halogen substitution, including fluorine, bromine, and chlorine, participated in the reaction in good yield and diastereoselectivity. Substrates with electron-rich aromatic rings, such as *para*-methoxyphenyl and dimethoxyphenyl, gave good yields and stereoselectivities for the [2,3]-rearrangement product. Even heteroaromatic compounds like pyridine could be used in the reaction. A dimethylamino functional group was not required for the reaction, as



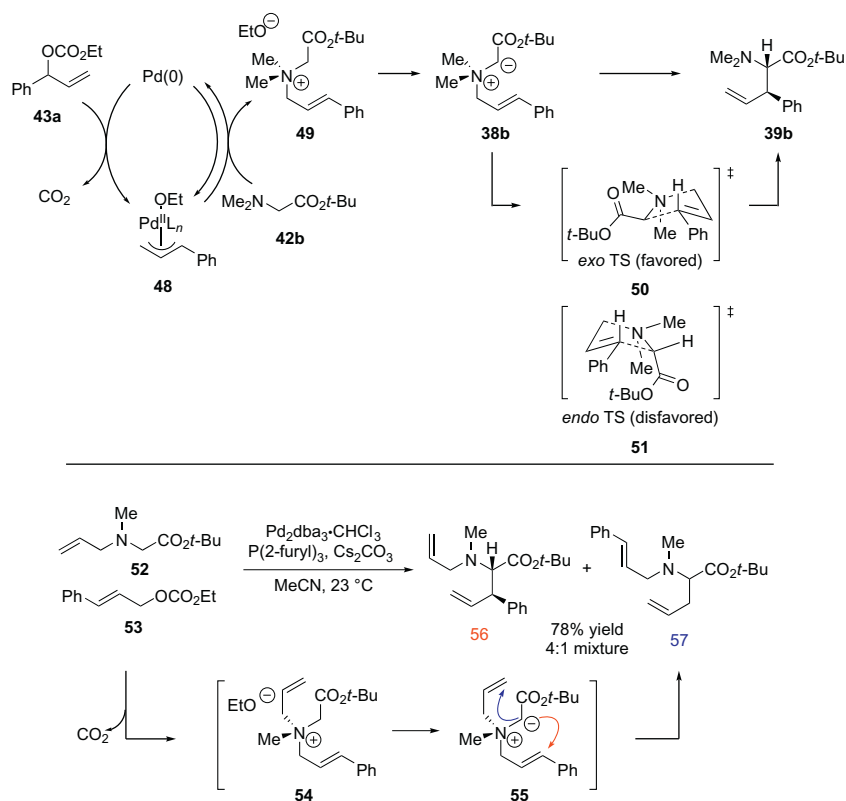
SCHEME 13 Our idea for the metal-catalyzed [2,3]-Stevens rearrangement.



SCHEME 14 Development of a diastereoselective palladium-catalyzed [2,3]-Stevens rearrangement.

substrates with tertiary amines like piperidine and pyridinone also reacted effectively. The [2,3]-Stevens rearrangement was also tolerant of amino ketones that were substituted with phenyl and *t*-butyl groups. Fully substituted carbon centers could be synthesized, along with enantiopure products using Oppolzer's camphorsultam chiral auxiliary. The stereochemical configurations of the products were determined by single X-ray crystallography and were consistent with an *exo*-selective [2,3]-rearrangement.

The overall mechanism of the reaction is similar to other allylic amination chemistry (Scheme 16). Carbonate **48** reacts with palladium(0) to form the π -allyl complex, which undergoes allylic amination with glycine ester **42b**. The ammonium salt **49** is then deprotonated with base to form the ammonium ylide **38b**, which undergoes thermal [2,3]-rearrangement to form product **39b** via *exo* transition state **50**. Interestingly, we never observed ammonium intermediates **49** and **38b**. To gain more insight into the mechanism, we designed a crossover experiment to further prove the formation of ammonium intermediates through allylic amination. Subjecting allylglycine ester **52** to our standard



SCHEME 16 Mechanism of the palladium-catalyzed [2,3]-Stevens rearrangement.

conditions with cinnamyl carbonate **53** yielded a 4:1 mixture of products **56** and **57**. The results can be easily explained by the allylic amination mechanism in which both the allyl and cinnamyl appendage can participate in the [2,3]-rearrangement through intermediate **55**. The ammonium intermediate is typically not observed in the reaction due to rapid deprotonation and rearrangement. Other evidence also suggests that the ammonium salt formation is under rapid equilibrium with the starting palladium π -allyl complex.

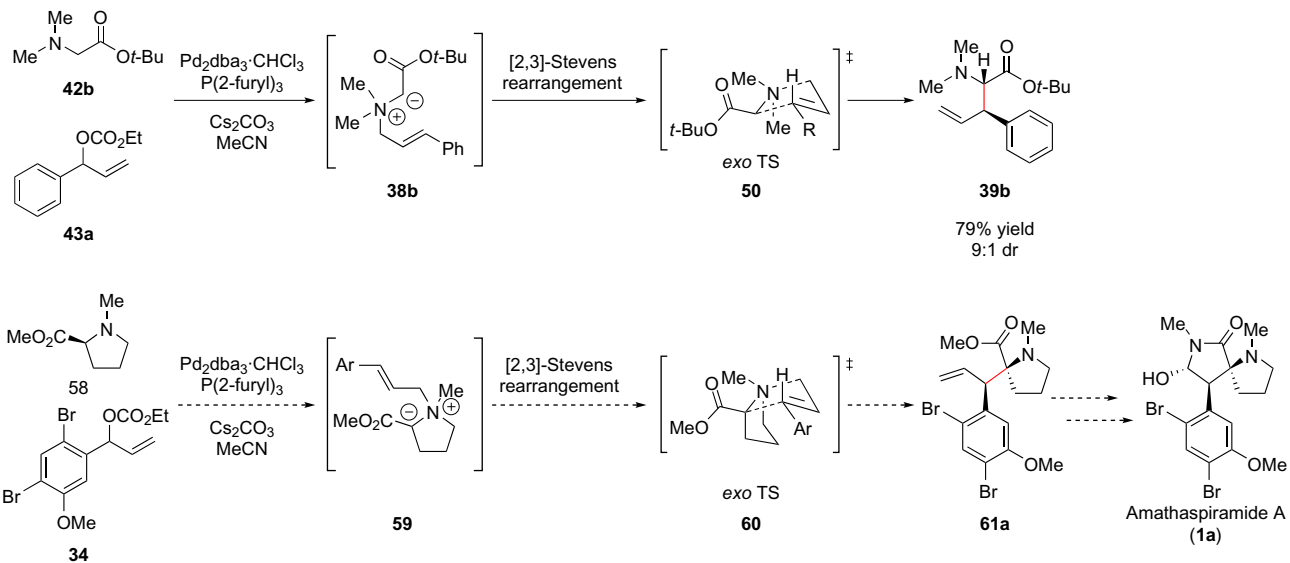
5 INITIAL ROUTE TO AMATHASPIRAMIDE A

Initially, Uttam and Arash decided to target amathaspiramide A, because it contained an *N*-methylpyrrolidine that was compatible with our tandem allylic amination/[2,3]-Stevens rearrangement (Scheme 17). We viewed the conversion of proline ester **58** and carbonate **34** to aminoester **61a** as a natural extension of our previously reported synthesis of aminoester **39b** from glycine ester **42b** and carbonate **43a**.¹⁷ Moreover, we expected to form the desired diastereomer of the [2,3]-rearrangement (**61a**) via a well-ordered *exo* transition state **60**, analogous to *exo* transition state **50** that was proposed for the rearrangement of simpler substrates. We also chose to start with the fully elaborated dibromomethoxyphenyl carbonate **34** to avoid the late-stage installation of aryl bromides.

We were able to quickly access the required carbonate **34** by addition of vinylmagnesium chloride to dibromomethoxy aldehyde **62** followed by capping with ethyl chloroformate (Scheme 18). We then subjected carbonate **34** to our standard palladium conditions with *N*-methylproline **58**. Gratifyingly, we obtained the rearrangement product **61** in a 73% yield as a 1:3 mixture of diastereomers.

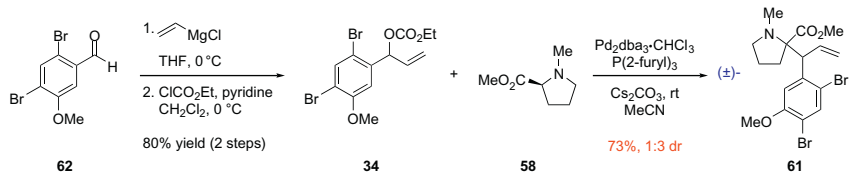
Although the synthesis of aminoester **61** was a significant achievement, two unexpected problems were revealed at this point in the synthesis. First, chiral HPLC analysis revealed that each diastereomer of the rearrangement product **61** was racemic, despite the use of enantiopure proline ester **58** as the starting material. We hypothesized that the racemization event occurred during either a nondiastereoselective allylic amination event (since the nitrogen in the ammonium intermediates **63** and **59** is a stereocenter) or a reversible allylic amination event prior to rearrangement, with a loss of the α -carbon stereocenter during formation of ammonium ylide **59** (Scheme 19). Since we were never able to address this racemization, we made the strategic decision to proceed with the development of a racemic synthesis of the amathaspiramides.

A second and more major problem with the formation of aminoester **61** was the relative stereochemistry of the major rearrangement product. Although we had not yet determined the relative stereochemistry of the major diastereomer, it was assumed to be the desired stereoisomer **61a** based on *exo* transition state **60**. Unfortunately, this analysis was incorrect, as we were able to eventually grow a single X-ray crystal of the major product, which revealed

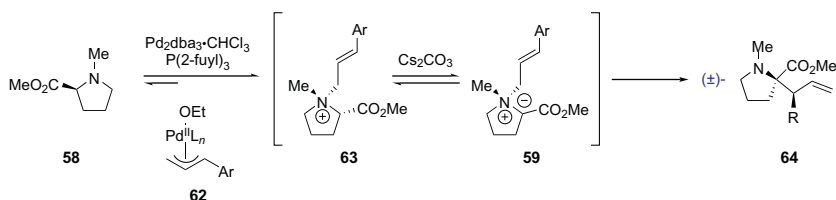


SCHEME 17 Proposed application of our palladium-catalyzed [2,3]-Stevens rearrangement to the synthesis of amathaspiramide A.

† transition states



SCHEME 18 Initial attempt to synthesize core structure of amathaspiramide A via a [2,3]-rearrangement.



SCHEME 19 Enantiopure proline ester furnishes racemic [2,3]-rearrangement product.

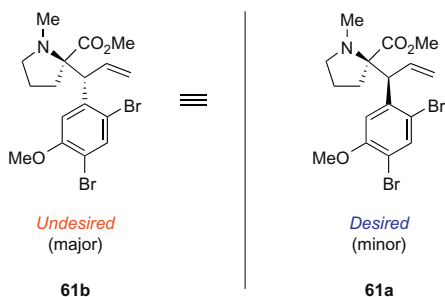
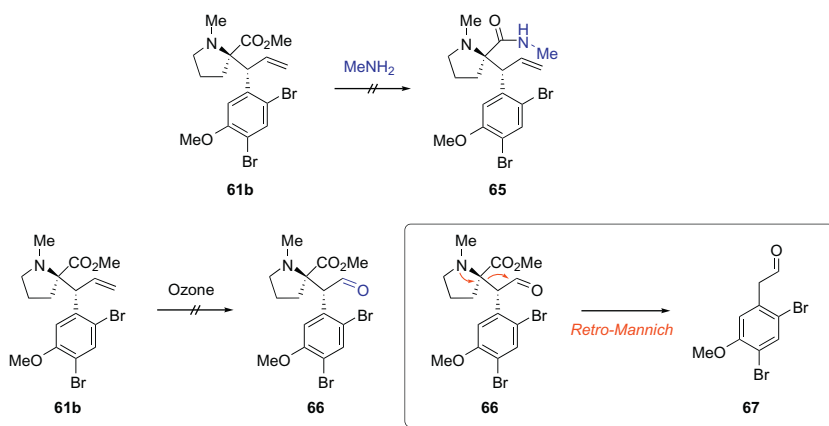


FIGURE 2 Undesired stereochemistry of [2,3]-Stevens rearrangement product.

the relative stereochemistry to be consistent with the undesired diastereomer **61b** (Figure 2).

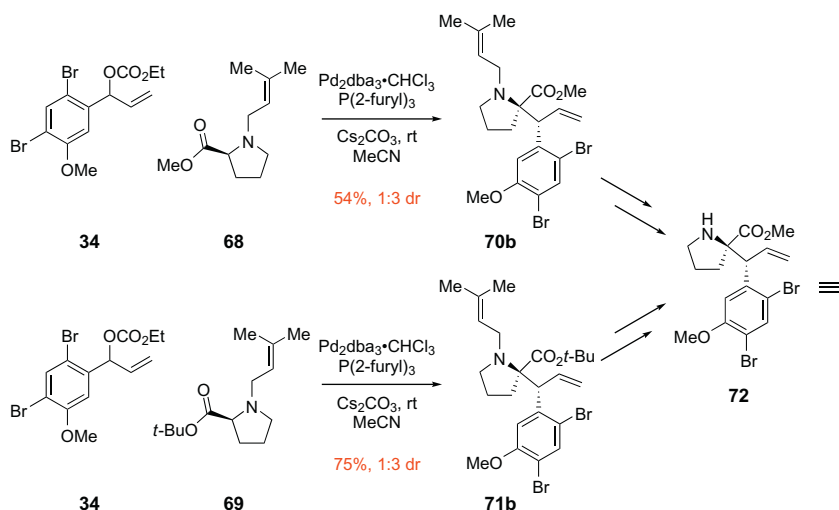
Although discouraged by the unexpected formation of the undesired diastereomer **61b**, we decided to explore the reactivity of aminoester **61b** in order to develop the remaining reactions necessary for the endgame of the total synthesis (Scheme 20). At this point, Carrie Johnson joined the project as a Summer Undergraduate Research Fellow. For 3 months, Carrie helped establish a detailed understanding of the reactivity of Stevens rearrangement products such as **61b**, which served as the foundation for our future endgame strategy. Initially, Carrie attempted to directly convert methyl ester **61b** to *N*-methyl amide **65** without any success under various conditions. This was attributed to the highly congested and sterically demanding environment surrounding the ester group. Carrie's next strategy was to convert the aminoester **61b** to aldehyde **66** via oxidation, which would facilitate the installation of



SCHEME 20 Failed attempts to advance [2,3]-rearrangement product.

methylamine. Surprisingly, numerous attempts at ozonolysis did not yield the desired product. After further investigation, we determined that although the starting material was being converted to the ozonolysis product, aldehyde **66** was undergoing a rapid retro-Mannich reaction to aldehyde **67**, presumably due to the electron-rich nitrogen group in **66**. All attempts at *in situ* trapping of the aldehyde of ozonolysis product **66** were unsuccessful. This prompted us to incorporate a functional group other than methyl on the proline nitrogen. This would potentially allow us to circumvent the retro-Mannich side reaction, address the diastereoselectivity problem of the [2,3]-rearrangement, and facilitate the synthesis of other members of amathaspiramide family that lack the *N*-methylproline (e.g., amathaspiramide F, Figure 1).

We chose to install a prenyl protecting group on the proline nitrogen, because it would be easier to remove and would also add steric bulk that might alter the diastereoselectivity of the [2,3]-Steven rearrangement (Scheme 21). We reacted both proline methyl ester **68** and proline *t*-butyl ester **69** with carbonate **34** under our standard palladium-catalyzed conditions. The reactions furnished the *N*-prenylated rearrangement products **70b** and **71b** in good to moderate yield. Unfortunately, conversion of these rearrangement products to aminoester **72** allowed for X-ray crystallographic confirmation that we were forming the undesired diastereomers as the major products in both reactions. At this point, all reactions with proline esters and dibromo-methoxyphenyl carbonate **34** were yielding the undesired diastereomer presumably through an *endo* transition state. This was contrary to previous observations of our group and other groups who have reported the typical *exo* selectivity of [2,3]-Stevens rearrangements. In light of this unusual stereochemical outcome, we sought to study this reaction more carefully in order to have a better understanding behind the switch in diastereoselectivity.



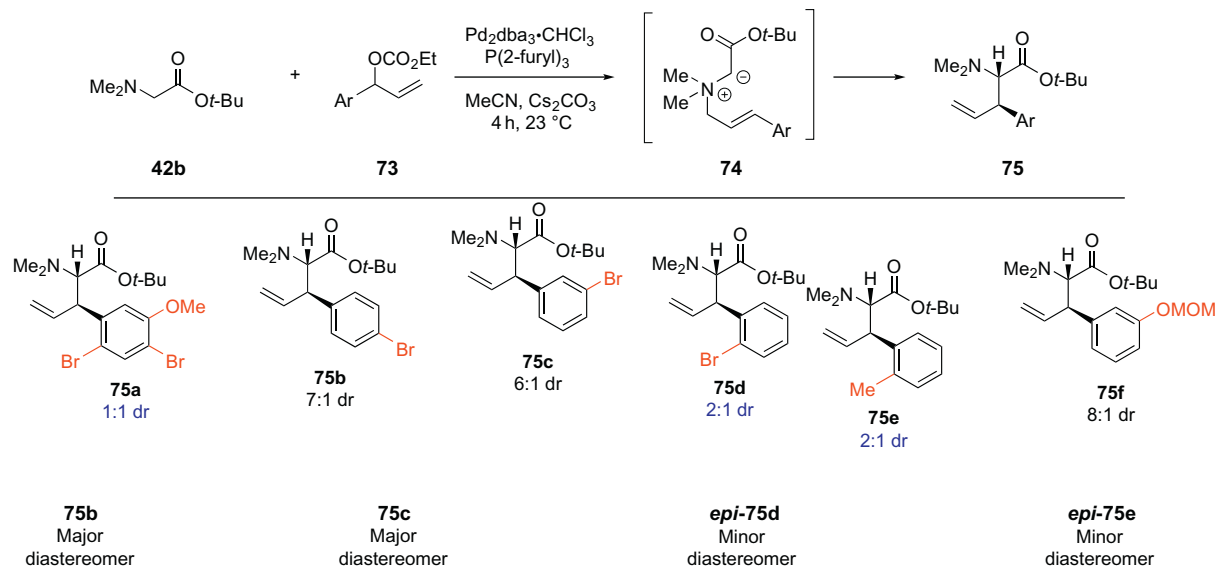
SCHEME 21 Undesired stereochemistry of more [2,3]-Stevens rearrangement products.

6 ROLE OF *ORTHO*-SUBSTITUTION OF AROMATIC CARBONATES

Arash's previous work on the palladium-catalyzed [2,3]-Stevens rearrangement had shown that the *exo* transition state was favored in all cases. He decided to test the dibromomethoxy phenyl carbonate that was used in the amathaspiramide synthesis with our previous acyclic glycine ester (Scheme 22). To his surprise, Arash found that this carbonate gave no selectivity and furnished the desired product in a 1:1 ratio of diastereomers. In contrast, the *para*-bromo and *meta*-bromo carbonates gave the desired *exo* product in 6:1 and 7:1 selectivity, respectively. Apparently, the substitution pattern of the dibromomethoxyphenyl was responsible for the low selectivity. This was further established with the reaction of *ortho*-bromophenyl carbonate, which gave the product in a low 2:1 dr favoring the *exo* product. This was a steric effect of the *ortho*-substituent, which was confirmed by the reaction of *ortho*-tolyl carbonate, which also gave a 2:1 ratio of isomers. It was clear from these results that in order to proceed with the amathaspiramide synthesis, we would have to perform our [2,3]-rearrangement without an *ortho*-bromo group. This would necessitate that we install the dibromo groups later in the synthesis. Luckily, a *meta*-OMOM phenyl group was well tolerated in our reaction and furnished the desired *exo* product as 8:1 ratio of diastereomers. Arash chose to proceed with this carbonate in our synthesis of the amathaspiramides.

7 FORMAL SYNTHESIS OF AMATHASPIRAMIDE F

Arash pursued the synthesis of amathaspiramide F by subjecting proline methyl ester **68** and *meta*-MOM phenyl carbonate **76** to our standard

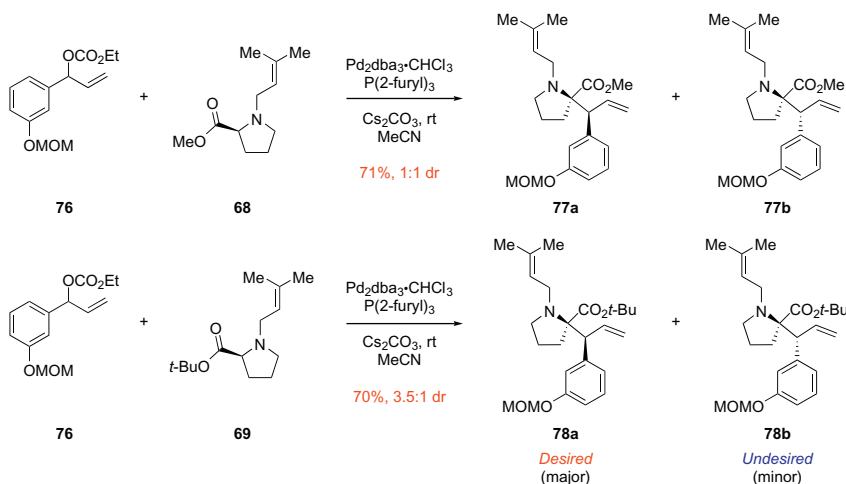


SCHEME 22 Effect of aryl substitution on the diastereoselectivity of the [2,3]-Stevens rearrangement.

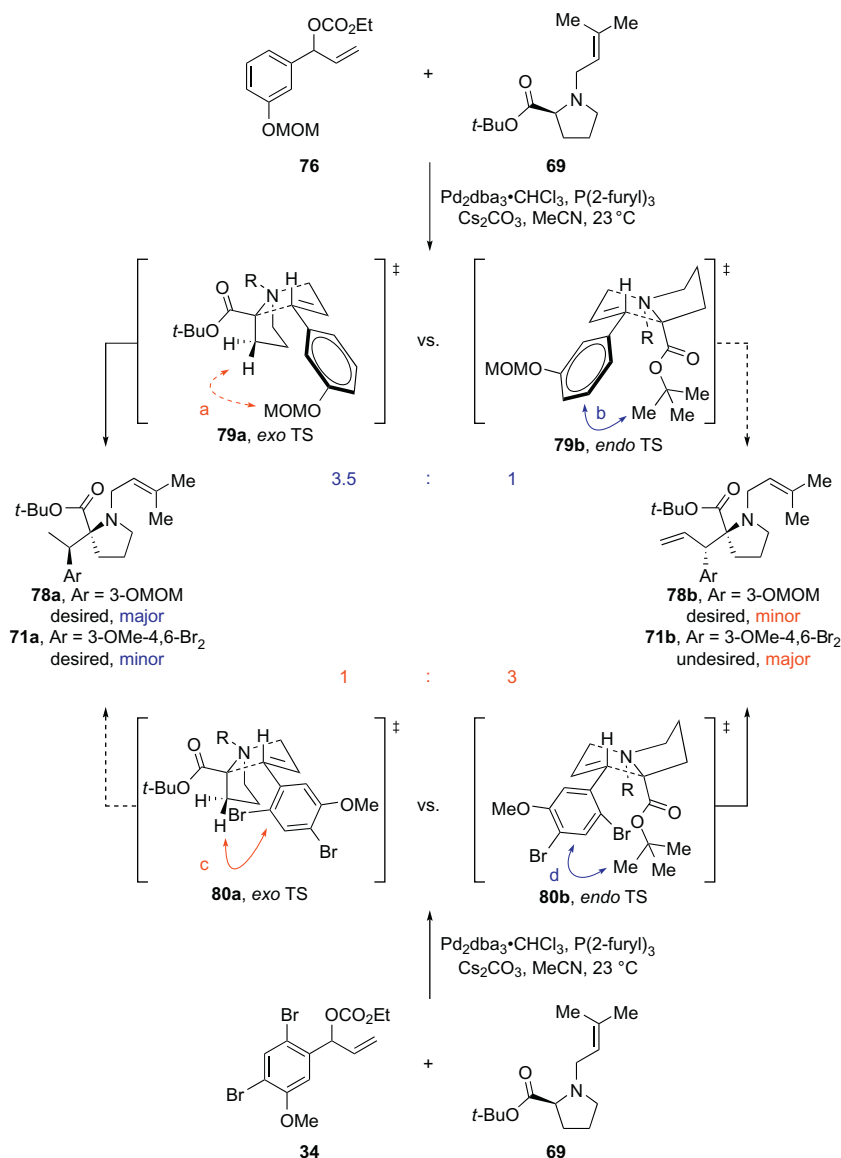
palladium conditions (Scheme 23). He obtained the rearrangement product in an unselective 1:1 ratio of diastereomers **77a** and **77b**. When he presented this result at a group meeting, Arash was actually very encouraged, because the *ortho*-bromo effect of the carbonate had been removed and the stereoselectivity appeared to be based on the ester group. Since the methyl ester was not bulky enough to impart selectivity, Arash coupled proline *t*-butyl ester **69** with carbonate **76**, which furnished a 3.5:1 mixture of diastereomers **78a** and **78b**. Gratifyingly, once the desired *exo* product **78a** was identified as the major rearrangement product; Arash and Uttam were elated!

We are preparing a detailed computational analysis of the origin of this switch in diastereoselectivity based on an *ortho*-substitution in the aromatic ring. In the meantime, we can speculate that this switch in diastereoselectivity is related to a torsional effect associated with the preference for *ortho*-substituted cinnamyl systems to adopt nonplanar conformations (Scheme 24).¹⁸ We surmise that proline derivative **69** and *meta*-substituted carbonate **76** form an ammonium ylide that lacks *ortho*-substitution in the aromatic ring. This ylide undergoes a [2,3]-rearrangement in which *exo* transition state **79a** is favored over *endo* transition state **79b**, because of the destabilizing interaction between the aromatic ring and the *t*-butyl ester in *endo* transition state **79b** (interaction b). This steric interaction is still relevant in *endo* transition state **80b**, when *ortho*-substituted carbonate **34** is coupled with aminoester **69** (interaction d). But the *exo* transition state **80a** is destabilized by the proximity of the β -proton of the aminoester and the nonplanar *ortho*-substituted aromatic ring (interaction c). These subtle effects in the conformation of substituted aromatic rings can account for the switch in diastereomeric ratio from 3.5:1 to 1:3.

Arash chose to proceed with the synthesis of amathaspiramide F, which would also confirm the stereochemistry of rearrangement product **78a**. The

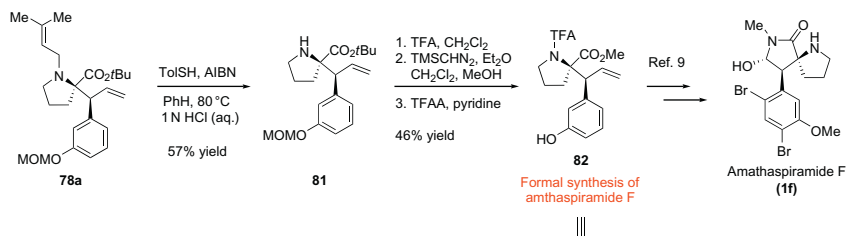


SCHEME 23 Desired stereochemistry of [2,3]-Stevens rearrangement product.



SCHEME 24 Rationale for switch in diastereoselectivity of [2,3]-Stevens rearrangement.

prenyl group of aminoester **78a** was easily deprotected using radical isomerization conditions (Scheme 25).¹⁹ In a three-step sequence, compound **81** was treated with trifluoroacetic acid to remove the MOM group and *t*-butyl ester group. The crude product was then treated with trimethylsilyldiazomethane to convert the acid to the methyl ester, followed by protection of the nitrogen



SCHEME 25 Formal synthesis of amathaspiramide F.

as the trifluoroacetamide. The spectral data for the resulting phenol **82** matched that for the same compound in Sakaguchi's synthesis of amathaspiramide F. Arash was also able to grow a single X-ray crystal structure, which confirmed the relative stereochemistry of phenol **82**. Our synthetic sequence therefore constituted a formal total synthesis of (\pm)-amathaspiramide F (**1f**) in 10 linear steps from carbonate **76** and proline ester **69**.²⁰

8 CONCLUDING REMARKS

Our retrosynthetic analysis for the amathaspiramides was one of the most straightforward strategies our group has ever proposed for the synthesis of a natural product. Based on everything we learned about the diastereoselectivity of [2,3]-Stevens rearrangements, we expected to obtain the desired diastereomer of the rearrangement product on our first attempt. But as is often the case with natural product synthesis, we uncovered an unusual stereochemical effect, which led us down an unexpected path to eventually solve the problem and complete the synthesis of amathaspiramide F. In addition to developing an efficient approach to a complex natural product, we hope that the discovery of this stereochemical switch, along with other factors that control the diastereoselectivity of [2,3]-rearrangements, will lead to the utilization of these reactions for natural product synthesis in a more predictable manner.

ACKNOWLEDGMENTS

Financial support was provided by the W.W. Caruth, Jr. Endowed Scholarship, the Robert A. Welch Foundation (Grant I-1748), the National Science Foundation (NSF CAREER 1150875), and the Sloan Research Fellowship. We thank Aaron Nash (University of Texas Southwestern Medical Center) for experimental assistance and Dr. Vincent Lynch (University of Texas at Austin) for X-ray structural analysis.

REFERENCES

1. (a) Corey, E. J.; Cheng, X.-M. *The Logic of Chemical Synthesis*, John Wiley & Sons, Inc.: New York, 1995; (b) Nicolaou, K. C.; Sorensen, E. J. *Classics in Total Synthesis: Targets, Strategies, Methods*; VCH: Weinheim, 1996.

2. (a) Bao, H.; Qi, X.; Tambar, U. K. *J. Am. Chem. Soc.* **2011**, *133*, 1206–1208; (b) Bao, H.; Qi, X.; Tambar, U. K. *Synlett* **2011**, 22, 1789–1792; (c) Bao, H.; Tambar, U. K. *J. Am. Chem. Soc.* **2012**, *134*, 18495–18498; (d) Bao, H.; Bayeh, L.; Tambar, U. K. *Synlett* **2013**, *24*, 2459–2463.
3. (a) Lutz, R. P. *Chem. Rev.* **1984**, *84*, 205–247; (b) Blechert, S. *Synthesis* **1989**, 71–82; (c) Paquette, L. A. *Tetrahedron* **1997**, *53*, 13971–14020; (d) Ito, H.; Taguchi, T. *Chem. Soc. Rev.* **1999**, *28*, 43–50; (e) Chai, Y. H.; Hong, S. P.; Lindsay, H. A.; McFarland, C.; McIntosh, M. C. *Tetrahedron* **2002**, *58*, 2905–2928; (f) Nubbemeyer, U. *Synthesis* **2003**, 961–1008; (g) Abraham, L.; Korner, M.; Schwab, P.; Hiersemann, M. *Adv. Synth. Catal.* **2004**, *346*, 1281–1294; (h) Castro, A. M. M. *Chem. Rev.* **2004**, *104*, 2939–3002; (i) Gonda, J. *Angew. Chem. Int. Ed. Engl.* **2004**, *43*, 3516–3524; (j) Nubbemeyer, U. In: Mulzer, J., Ed.; *Natural Products Synthesis II: Targets, Methods, Concepts*, Vol. 244; Springer Berlin Heidelberg: New York, 2005, pp 149–213; (k) Majumdar, K. C.; Alam, S.; Chattopadhyay, B. *Tetrahedron* **2008**, *64*, 597–643; (l) Ildardi, E. A.; Stivala, C. E.; Zakarian, A. *Chem. Soc. Rev.* **2009**, *38*, 3133–3148; (m) Majumdar, K. C.; Bhattacharyya, T.; Chattopadhyay, B.; Sinha, B. *Synthesis* **2009**, 2117–2142; (n) So, S. M.; Mui, L.; Kim, H.; Chin, J. *Acc. Chem. Res.* **2012**, *45*, 1345–1355; (o) Ziegler, F. E. *Chem. Rev.* **1988**, *88*, 1423–1452; (p) Davies, H. M. L. *Tetrahedron* **1993**, *49*, 5203–5223; (q) Enders, D.; Knopp, M.; Schiffrers, R. *Tetrahedron Asymmetry* **1996**, *7*, 1847–1882; (r) Ganem, B. *Angew. Chem. Int. Ed. Engl.* **1996**, *35*, 936–945; (s) Hiersemann, M.; Abraham, L. *Eur. J. Org. Chem.* **2002**, 1461–1471; (t) Hiersemann M.; Nubbemeyer U., (Eds.), *The Claisen Rearrangement*. Wiley-VCH: Weinheim, 2007.
4. (a) Honda, K.; Tabuchi, M.; Inoue, S. *Chem. Lett.* **1996**, 385–386; (b) Honda, K.; Yoshii, I.; Inoue, S. *Chem. Lett.* **1996**, 671–672; (c) Honda, K.; Igarashi, D.; Asami, M.; Inoue, S. *Synlett* **1998**, 685–687; (d) Li, W.-D. Z.; Wang, Y.-Q. *Org. Lett.* **2003**, *5*, 2931–2934; (e) Zhou, C.-Y.; Yu, W.-Y.; Chan, P. W. H.; Che, C.-M. *J. Org. Chem.* **2004**, *69*, 7072–7082; (f) Li, W.-D. Z.; Wang, X.-W. *Org. Lett.* **2007**, *9*, 1211–1214; (g) Sakaguchi, K.; Ayabe, M.; Watanabe, Y.; Okada, T.; Kawamura, K.; Shiada, T.; Ohfuné, Y. *Org. Lett.* **2008**, *10*, 5449–5452; (h) Sun, M.-r; Lu, H.-t; Wang, Y.-z; Yang, H.; Liu, H.-m *J. Org. Chem.* **2009**, *74*, 2213–2216.
5. Morris, B. D.; Prinsep, M.I.R. *J. Nat. Prod.* **1999**, *62*, 688–693.
6. (a) Soheili, A.; Tambar, U. K. *J. Am. Chem. Soc.* **2011**, *133*, 12956–12959; (b) Nash, A.; Soheili, A.; Tambar, U. K. *Org. Lett.* **2013**, *15*, 4770–4773.
7. Niu, D.; O'Doherty, G. A. *Chemtracts* **2009**, *22*, 81–88.
8. Hughes, C. C.; Trauner, D. *Angew. Chem. Int. Ed. Engl.* **2002**, *114*, 4556–4559.
9. Sakaguchi, K.; Ayabe, M.; Watanabe, Y.; Okada, T.; Kawamura, K.; Shiada, T.; Ohfuné, Y. *Org. Lett.* **2008**, *10*, 5449–5452; (b) Sakaguchi, K.; Ayabe, M.; Watanabe, Y.; Okada, T.; Kawamura, K.; Shinada, T.; Ohfuné, Y. *Tetrahedron* **2009**, *65*, 10355–10364.
10. Chiyoda, K.; Shimokawa, J.; Fukuyama, T. *Angew. Chem. Int. Ed. Engl.* **2012**, *51*, 2505–2508.
11. (a) Seebach, D.; Boes, M.; Naef, R.; Schweizer, W. B. *J. Am. Chem. Soc.* **1983**, *105*, 5390–5398; (b) Seebach, D.; Sting, A. R.; Hoffmann, M. *Angew. Chem. Int. Ed. Engl.* **1996**, *35*, 2708–2748.
12. (a) Stevens, T. S.; Creighton, E. M.; Gordon, A. B.; MacNicol, M. *J. Chem. Soc.* **1928**, 3193–3197; (b) Markó, I. E. In: Trost, B. M., Fleming, I., Eds.; *Comprehensive Organic Synthesis*, Vol. 3; Pergamon Press: New York, 1991; pp 913–974; (c) Brückner, R. In: Trost, B.M.; Fleming, I., Eds.; *Comprehensive Organic Synthesis*, Vol. 6; Pergamon Press: New York, 1991; pp 873–908; (d) Hoffmann, R. W. *Angew. Chem. Int. Ed. Engl.* **1979**, *18*,

- 563–640; (e) Honda, K.; Inoue, S.; Sato, K. *J. Am. Chem. Soc.* **1990**, *112*, 1999–2001; (f) Arboré, A. P. A.; Cane-Honeysett, D. J.; Coldham, I.; Middleton, M. L. *Synlett* **2000**, 236–238; (g) Moniz, G. A.; Wood, J. L. *J. Am. Chem. Soc.* **2001**, *123*, 5095–5097; (h) Workman, J. A.; Garrido, N. P.; Sançon, J.; Roberts, E.; Wessel, H. P.; Sweeney, J. B. *J. Am. Chem. Soc.* **2004**, *127*, 1066–1067; (i) Vanecko, J. A.; Wan, H.; West, F. G. *Tetrahedron* **2006**, *62*, 1043–1062; (j) Sweeney, J. B. *Chem. Soc. Rev.* **2009**, *38*, 1027–1038; (k) Mack, D. J.; Batory, L. A.; Njardarson, J. T. *Org. Lett.* **2011**, *14*, 378–381; (l) Strick, B. F.; Mundal, D. A.; Thomson, R. J. *J. Am. Chem. Soc.* **2011**, *133*, 14252–14255.
13. (a) Coldham, I.; Middleton, M. L.; Taylor, P. L. *J. Chem. Soc., Perkin Trans. 1* **1997**, 2951–2952; (b) Coldham, I.; Middleton, M. L.; Taylor, P. L. *J. Chem. Soc., Perkin Trans. 1* **1998**, 2817–2821; (c) Honda, K.; Tabuchi, M.; Kurokawa, H.; Asami, M.; Inoue, S. *J. Chem. Soc., Perkin Trans. 1* **2002**, 1387–1396; (d) Workman, J. A.; Garrido, N. P.; Sançon, J.; Roberts, E.; Wessel, H. P.; Sweeney, J. B. *J. Am. Chem. Soc.* **2005**, *127*, 1066–1067; (e) Gawley, R. E.; Moon, K. *Org. Lett.* **2007**, *9*, 3093–3096.
14. (a) Doyle, M. P.; Tamblin, W. H.; Bagheri, V. *J. Org. Chem.* **1981**, *46*, 5094–5102; (b) Del Zotto, A.; Baratta, W.; Miani, F.; Verardo, G.; Rigo, P. *Eur. J. Org. Chem.* **2000**, 3731–3735; (c) Padwa, A.; Beall, L. S.; Eidell, C. K.; Worsencroft, K. J. *J. Org. Chem.* **2001**, *66*, 2414–2421; (d) Clark, J. S.; Middleton, M. D. *Tetrahedron Lett.* **2003**, *44*, 7031–7034; (e) Glaeske, K. W.; Naidu, B. N.; West, F. G. *Tetrahedron Asymmetry* **2003**, *14*, 917–920; (f) Zhou, C.-Y.; Yu, W.-Y.; Chan, P. W. H.; Che, C.-M. *J. Org. Chem.* **2004**, *69*, 7072–7082; (g) Roberts, E.; Sançon, J. P.; Sweeney, J. B. *Org. Lett.* **2005**, *7*, 2075–2078; (h) Honda, K.; Shibuya, H.; Yasui, H.; Hoshino, Y.; Inoue, S. *Bull. Chem. Soc. Jpn.* **2008**, *81*, 142–147.
15. (a) Johannsen, M.; Jørgensen, K. A. *Chem. Rev.* **1998**, *98*, 1689–1708; (b) Hartwig, J. F.; Stanley, L. M. *Acc. Chem. Res.* **2010**, *43*, 1461–1475; (c) Trost, B. M.; Zhang, T.; Sieber, J. D. *Chem. Sci.* **2010**, *1*, 427–440.
16. For examples of intramolecular allylic amination with tertiary amines, see: (a) Grellier, M.; Pfeffer, M.; van Koten, G. *Tetrahedron Lett.* **1994**, *35*, 2877–2880. (b) van der Schaaf, P. A.; Sutter, J.-P.; Grellier, M.; van Mier, G. P. M.; Spek, A. L.; van Koten, G.; Pfeffer, M. *J. Am. Chem. Soc.* **1994**, *116*, 5134–5144.
17. For other examples of Stevens rearrangements with proline-derived ammonium ylides, see: (a) West, F. G.; Naidu, B. N. *J. Am. Chem. Soc.* **1994**, *116*, 8420–8421. (b) Naidu, B. N.; West, F. G. *Tetrahedron* **1997**, *53*, 16565–16574. (c) Glaeske, K. W.; West, F. G. *Org. Lett.* **1999**, *1*, 31–34. (d) Arboré, A. P. A.; Cane-Honeysett, D. J.; Coldham, I.; Middleton, M. L. *Synlett* **2000**, 236–238. (e) Clark, J. S.; Hodgson, P. B.; Goldsmith, M. D.; Blake, A. J.; Cooke, P. A.; Street, L. J. *J. Chem. Soc., Perkin Trans. 1* **2001**, 3325–3337. (f) Padwa, A.; Beall, L. S.; Eidell, C. K.; Worsencroft, K. J. *J. Org. Chem.* **2001**, *66*, 2414–2421. (g) Tayama, E.; Nanbara, S.; Nakai, T. *Chem. Lett.* **2006**, *35*, 478–479.
18. Shen, Q.; Kuhns, J.; Hagen, K.; Richardson, A. D. *J. Mol. Struct.* **2001**, 567–568, 73–83, and references therein.
19. Escoubet, S.; Gastaldi, S.; Timokhin, V. I.; Bertrand, M. P.; Siri, D. *J. Am. Chem. Soc.* **2004**, *126*, 12343–12352.
20. Soheili, A.; Tambar, U. K. *Org. Lett.* **2013**, *15*, 5138–5141.

Oxabicyclic Building Blocks as Key Intermediates in the Synthesis of the Natural Products (–)-Platensimycin and (+)-Frondosin A

Dennis L. Wright^{*,†,1}, Michael D. Van Heyst^{*}, and E. Zachary Oblak^{*,2}

^{*}Department of Pharmaceutical Sciences, University of Connecticut, Storrs, Connecticut, USA

[†]Department of Chemistry, University of Connecticut, Storrs, Connecticut, USA

¹Corresponding author: dennis.wright@uconn.edu

Chapter Outline

1. Introduction	156	3.1. Retrosynthetic Scheme	167
2. Formal Total Synthesis of (–)-Platensimycin	158	3.2. First Synthetic Plan and Initial Studies	168
2.1. Retrosynthetic Scheme	159	3.3. Lewis Acid Assisted Trialkylphosphine Ring Opening	172
2.2. TBCP Diels–Alder with Functionalized Furan	160	3.4. Carbonyl Transformation to Geminal Dimethyl Moiety	176
2.3. Model System to Study Intramolecular Alkylation Reaction	162	3.5. Completion of Total Synthesis	178
2.4. Formation of Caged Core Structure	163	4. Conclusion	179
2.5. Medicinal Chemistry Efforts	165	References	179
3. Asymmetric Total Synthesis of (+)-Frondosin A	167		

2. Current affiliation: Department of Chemistry, Princeton University, Princeton, New Jersey, USA.

1 INTRODUCTION

Since the initial report by Diels and Alder in 1928, the [4+2]-cycloaddition remains one of the most powerful and most frequently employed methods for the construction of six-membered ring systems, generating a high degree of structural complexity in a single synthetic transformation.¹ This cycloaddition process not only generates two new σ -bonds but also establishes up to four new contiguous stereocenters in the process, owing to the high regio- and stereoselectivities displayed by this pericyclic reaction. In the decades following its discovery, many versions of the Diels–Alder reaction were developed, including intramolecular [4+2]-cycloadditions, hetero-Diels–Alder reactions, and pressure and Lewis acid-accelerated Diels–Alder reactions.^{2,3}

Hoffmann⁴ and Noyori⁵ later developed and popularized the analogous higher order [4+3]-cycloaddition of an oxyallyl cation equivalent and 1,3-dienes as an attractive method for the formation of historically difficult-to-access seven-membered rings. The oxyallyl cations are typically generated from the reduction of α,α' -dihalo ketone derivatives, often generating symmetric cations.⁶ Subsequent addition to both cyclic and acyclic dienes produces the bicyclo[3.2.1]oct-6-en-3-ones, meso compounds that have found wide use in organic syntheses.⁷

One of the most successful variants of this higher-order process involves the use of furan as the cyclic diene partner which gives direct access to the 8-oxabicyclo-[3.2.1]-octane ring system. Many years ago, our research group became interested in the strategic use of these building blocks in the synthesis of biologically active natural products. These intermediates were attractive as the bridged bicyclic system could yield three distinct ring systems (cycloheptanoid, tetrahydropyranyl, and tetrahydrofuryl) upon cleavage of one of the three unique bridges contained within the bicyclic framework (Figure 1).

In our initial studies, begun at the University of Florida, we relied on the classic oxyallyl cation cycloaddition for the preparation of these intermediates, but quickly noticed some of the key limitations with this reaction, especially when highly substituted or annulated furans were employed as the diene

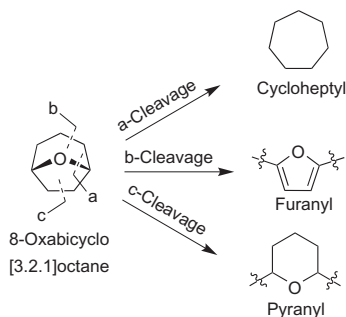


FIGURE 1 Synthetic goals of the Wright lab.

component where simple aromatic substitution products were frequently formed. During a typical evening chatting in Prof. Merle Batiste's office across the hall, he brought an interesting reaction to our attention that delivered a similar type of intermediate as the oxyallyl cation cycloaddition chemistry, but with an alternative array of functionality. The reaction had been known for several decades, and Merle had studied some of the mechanistic aspects in the early 1980s, but it had largely gone unnoticed for application as a key step in target-oriented synthesis.

In 1968, Tobey and Law reported on the intriguing reaction of furan, substituted furans, and cyclopentadiene with both tetrachloro- and tetrabromocyclopropene (TBCP).⁸ The two unsaturated systems reacted smoothly to directly produce cycloheptanoid systems, the products of a formal [4+3]-cycloaddition reaction. The authors proposed in their early manuscripts that the tetrahalocyclopropenes underwent an initial thermal Diels–Alder cycloaddition to produce the cyclopropyl norbornene derivatives **1a** and **1b** (Figure 2). However, these workers were unable to isolate or characterize the primary cycloadducts and instead observed a product which had spontaneously rearranged by way of a halogen atom migration to yield the bicyclo[3.2.1]octadiene nucleus **2a** and **2b**.

The majority of our group's research interest in this area has been focused on the development of the bridged bicyclic adducts derived from perhalocyclopropenes and furans as key intermediates for the synthesis of natural products. Of particular importance to our work was the early finding that the oxabicyclo[3.2.1]octane adducts derived in a single step through cyclocondensation of furans and TBCP could be readily converted into the versatile dibromoenone **3** through a high yielding, silver-mediated hydrolysis (Figure 3).⁹

These compounds serve as rigidified cycloheptenones with functional handles at each of the seven unique carbons of the ring that allows for excellent regio- and stereochemical control during subsequent synthetic elaboration of the core. The ability to effect cleavage, annulation, nucleophilic addition, and rearrangement of **3** has allowed the development of synthetic routes to a variety of natural products (Figure 3). Studies toward the eunicellin diterpene sclerophytin exposed the reactivity of dienophile (F) of **3** in cyclocondensation with dienes in constructing polycyclic structures.^{9a} Further elaboration of olefin (F) uncovered reactivity towards ring-opening cross-metathesis reactions to

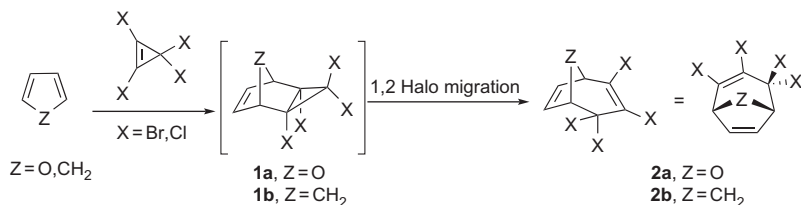


FIGURE 2 Tobey and Law's account of the Diels–Alder reaction between tetrahalocyclopropene and furan.

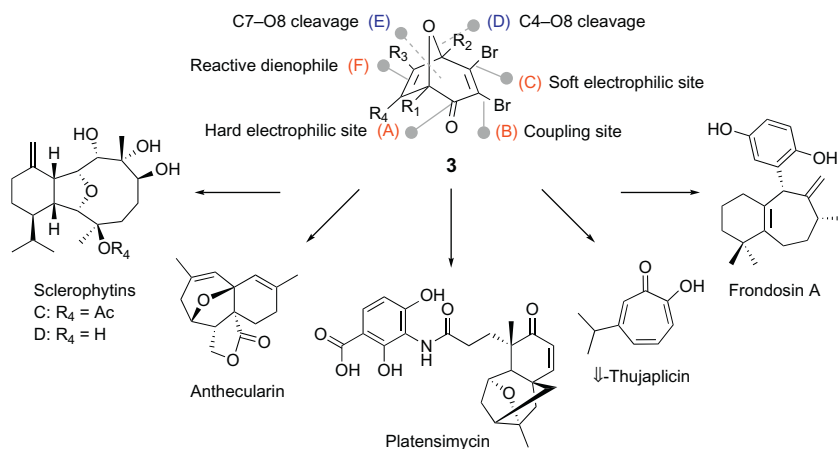


FIGURE 3 Oxabicyclo[3.2.1]octadiene versatility in the synthesis of natural products.

deconstructively form pyran intermediates, in synthetic efforts toward the potent antitumor agent pyranicin (not shown). Addition of nucleophilic functionality at the soft electrophilic site (C) of **3** along with novel samarium diiodide-promoted dehydrohalogenation effectively cleaving the C4–O8 (D) bond, provided an efficient four-step total synthesis of the non-benzenoid aromatic natural product β -thujaplicin.¹⁰ Most recently, the opportunity for substitutions at the C4–C7 array of **3** has allowed us to extend this cyclocondensation with TBCP to develop synthetic routes to the natural products (–)-platensimycin¹¹ and (+)-frondosin A.¹² In this chapter, we describe our approaches to these two target molecules that highlight the robust nature of the cycloaddition process and the synthetic versatility of the oxa-bridged intermediates.

2 FORMAL TOTAL SYNTHESIS OF (–)-PLATENSIMYCIN

In 2006, researchers at Merck elucidated the structure of the novel antibiotic platensimycin (Figure 4),¹³ attracting considerable attention from within the

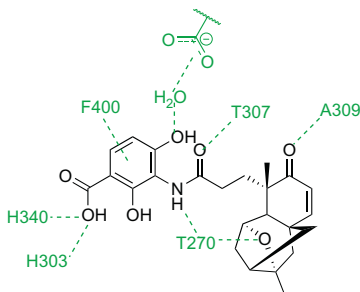
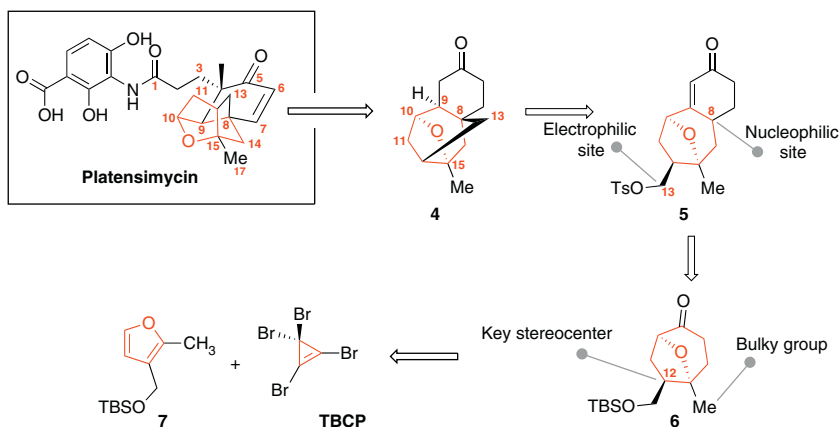


FIGURE 4 Platensimycin interactions with the mutated target enzyme ecFABF(C163Q).

scientific community due to its unprecedented molecular architecture and potent antibacterial activity against Gram-positive bacteria.¹⁴ Platensimycin's novel mode of action is trademarked by selective inhibition of the FabF enzyme, effectively blockading the biosynthesis of bacterial fatty acids. However, with a less than ideal pharmacokinetic profile, researchers have been focused on improving the drug's medicinal chemistry profile with structural modifications to the polar benzoic acid subunit and the tricyclic lipophilic cage.¹⁵ However, these efforts have thus far been disappointing, with all compounds showing attenuated activity compared to the natural product. An X-ray crystal structure of platensimycin in a complex with a mutant version of the FabF enzyme showed that these modified regions contained crucial drug–enzyme interactions.

2.1 Retrosynthetic Scheme

The presence of an embedded oxabicyclo[3.2.1]octane substructure suggested that a synthetic route could be constructed upon the TBCP:furan cycloaddition chemistry (Scheme 1). Retrosynthetic analysis of the caged structure **4** centered around a late-stage intramolecular alkylation to construct the C8–C13 bridge from a tricyclic intermediate such as **5** that was, in turn, envisioned to arise through annulation of a cyclohexenone onto a highly substituted oxabicyclo[3.2.1]octanone **6**. Central to the overall strategy would be an efficient preparation of **6** from TBCP and a simple 2,3-disubstituted furan **7**. We also hoped that this approach would allow us entry into analogs that were not accessible through the other disclosed approaches, namely those with significant alterations to the cyclohexenone ring. Several reports suggested that the electrophilic enone in this region was problematic from a pharmacokinetic perspective, but attenuation of reactivity through reduction or β -substitution was accompanied by a significant loss in antibacterial activity. Our strategy



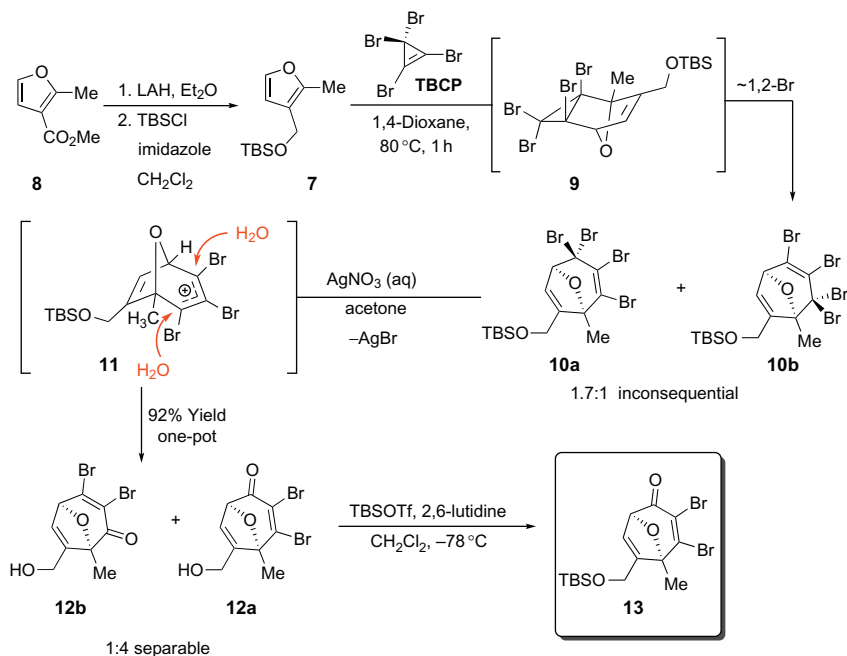
SCHEME 1 Platensimycin retrosynthetic analysis.

featuring a late stage annulation of this ring should allow the direct exploration of alternative ring sizes or compositions.

2.2 TBCP Diels–Alder with Functionalized Furan

A relatively inexpensive and appropriately substituted furan **8** emerged as an attractive bulk starting material that was directly converted to the diene cycloaddition component **7** by simple reduction and protection (Scheme 2).¹⁶ Furan **7** could be directly subjected to cycloaddition with TBCP, which proceeded smoothly on a multigram scale despite increased substitution on the furan ring, to produce a mixture of regioisomeric tetrabromides **10a/10b**, which were converted directly to the corresponding dibromoenones **12a/12b** by action of aqueous silver nitrate. The major isomer **12a** (produced in a 4:1 ratio) arises from an intermediate tribromoallyl cation **11** in which attack of water is directed to the distal terminus of the allyl cation by the bridgehead methyl group. Reprotection of the C4 alcohol was required to give **13**, as a large amount of nitric acid is produced in the reaction, cleaving the primary silyloxy group.

With **13** in hand, we saw an opportunity for the development of a resolution strategy to effect an asymmetric synthesis of the natural product. Previously, we demonstrated that Luche reduction of (\pm)-**3** proceeds with high



SCHEME 2 Diels–Alder reaction between substituted furan **7** and TBCP.

diastereoselectivity giving the *endo*-alcohol as the exclusive product.^{1b} In accord with these studies, we envisioned circumstances whereby this diastereoselectivity could be paired with a high degree of enantiodifferentiation imparted by a chiral catalyst, leading to one enantioenriched *endo*-alcohol as well as recovery of the antipode of the ketone. The original design of this project was centered around a kinetic reduction of dibromide (\pm)-**3** employing the CBS oxazaborolidine catalyst and a boron hydride source. However, preliminary results showed a more complicated process than the simple resolution initially conceived. Analysis of the product distribution from the reaction suggested that catalyst control was overriding the natural directing effects embedded in the rigid bicyclic of (\pm)-**3**, such that hydride attack from both faces of the ether bridge occurred competitively. The quasi-intramolecular hydride attack occurs from both the *endo*- and *exo*-face of the ether bridge, but only from a single face of the carbonyl (depending on catalyst preference) (Figure 5). This results in a highly selective reduction without any significant control imparted from the ether bridge.

Optimization of these initial results was met with: (a) use of excess of hydride, allowing the reaction to proceed until completion, and (b) increasing the reaction temperature to 4 °C, thus increasing catalyst coordination to both the hydride source and the carbonyl moiety and suppressing any background *exo*-hydride attack.⁸ The separation of the resulting diastereomeric *endo* and *exo* alcohols (+)-**14a** and (–)-**14b** followed by oxidation of each enantiomer, in the presence of MnO₂, gave enantioenriched dibromoenones (+)-**3** and (–)-**3** in excellent yield (not shown) allowing us to exploit a stereodivergent resolution strategy to resolve the enantiomers of (\pm)-**3**.¹⁷

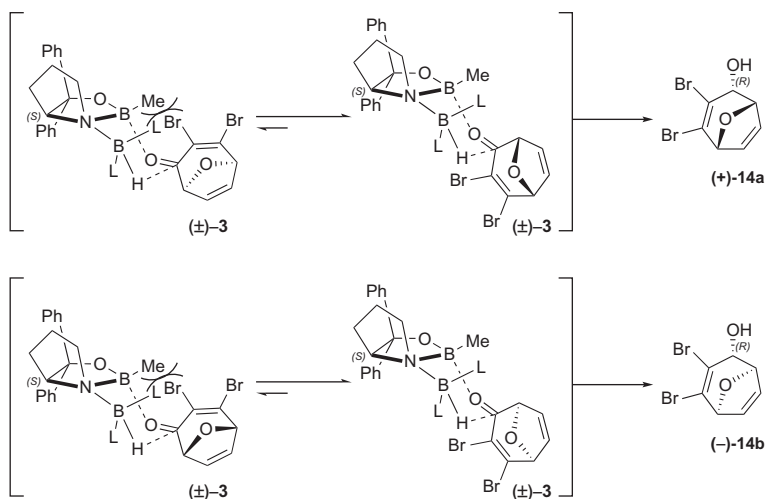
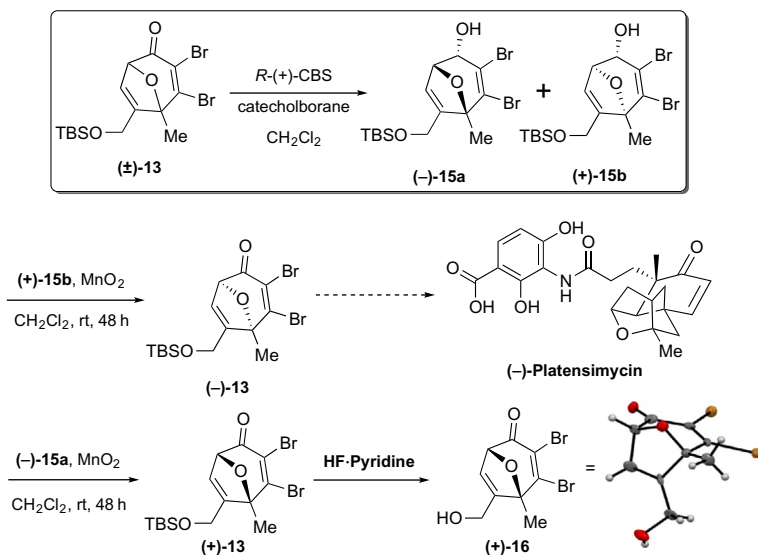


FIGURE 5 Transition state between *S*-(–)-CBS and (\pm)-**3**.

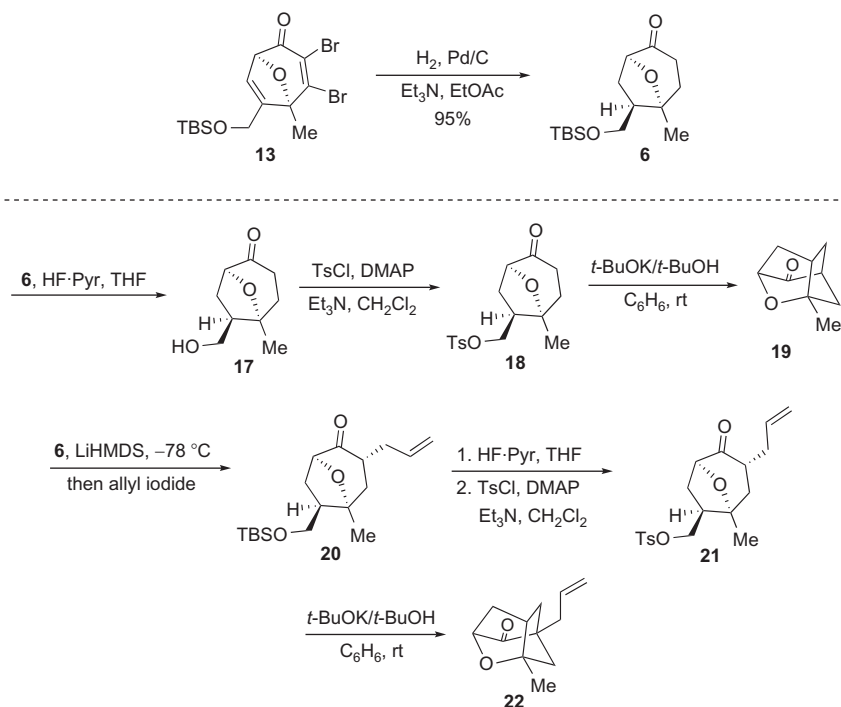


SCHEME 3 Resolution of early intermediate **(±)-13** for the synthesis of **(-)-platensimycin**: X-ray crystallographic confirmation of stereochemistry.

Subjecting **(±)-13** to our newly developed resolution conditions provided the respective *endo*-**(-)-15a** and *exo*-**(+)-15b** alcohols in high yield ($\geq 47\%$) and enantiomeric excess ($\geq 99\%$) (Scheme 3). The ability to resolve this complex material at an early stage provides entry into an asymmetric synthesis of both natural and nonnatural platensimycin. To add further confirmation to our assignment of absolute stereochemistry, material was transformed to alcohol **(+)-16**, which yielded thin plate crystals for X-ray crystallographic determination of absolute stereochemistry.

2.3 Model System to Study Intramolecular Alkylation Reaction

The dibromoenone system **13** and the isolated C11–C12 olefin could be exhaustively reduced on catalytic palladium under an atmosphere of hydrogen with an amine base added to neutralize the hydrogen bromide formed in the reaction (Scheme 4). As a result of the directing effect of the oxa-bridge, reduction occurs exclusively from the *exo*-face which correctly establishes the configuration at C12 of **6**. Two model systems were constructed to test the feasibility of the key intramolecular alkylation reaction. In the simplest case, removal of the silyl protecting group was followed by activation of the primary alcohol **17** as its tosylate **18**. Smooth intramolecular alkylation was seen when tosylate **18** was exposed to alkoxide base at room temperature giving **19**. A second model system was constructed by alkylation of **6** with allyl iodide to provide **20**. Following deprotection and tosylation, we exposed the α -allyl ketone **21** to *t*-BuOK/*t*-BuOH and again observed the desired



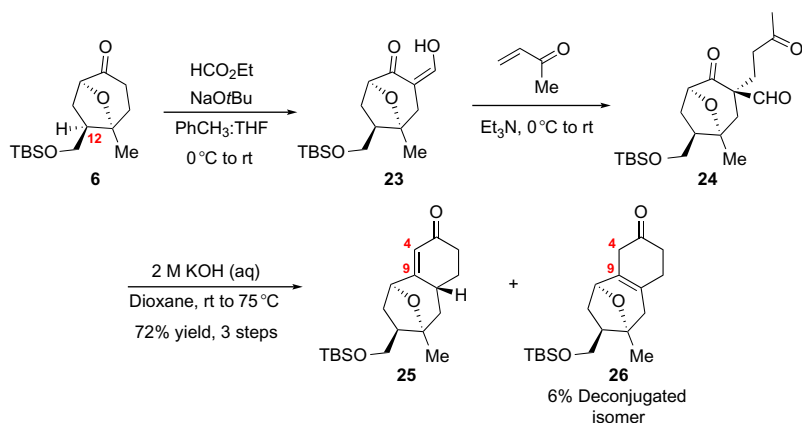
SCHEME 4 Construction of two model systems to study intramolecular alkylation reaction.

intramolecular alkylation to provide **22**. Following the discovery of this base-promoted intramolecular displacement, we then sought to apply a similar transformation to a more advanced intermediate that would provide access to the platensimycin core.

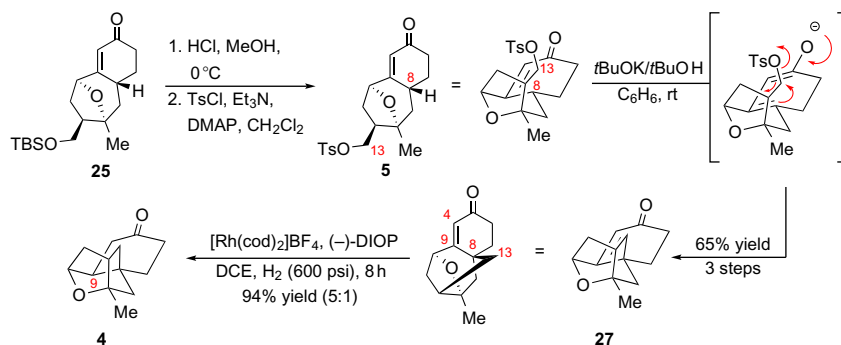
2.4 Formation of Caged Core Structure

A Robinson annulation strategy seemed to offer an attractive route for installation of the cyclohexenone, which would ultimately lead to a C4–C9 enone. Evaluation of several Robinson variants ultimately indicated the Woodward–Wilds modification as optimal for this system.¹⁸ Direct Michael addition to the ketone **6** was frustrated by low yields and required the temporary installation of a formyl group (**23**) to facilitate the addition to methyl vinyl ketone to yield **24**. Treating the resulting diketone with base promoted aldol cyclization followed by dehydration and loss of the formyl group to produce the desired enone **25** in 72% overall yield from **6** and setting the stage for the formation of the final ring in the caged system (Scheme 5).

The final ring to be formed would require the generation of a γ -enolate on the cyclohexenone ring followed by an intramolecular alkylation of a C13 electrophile. Initial removal of the silyl group was followed by routine conversion to the corresponding C13 tosylate **5** (Scheme 6). We were excited to observe that



SCHEME 5 Installation of cyclohexenone through Woodward–Witts modified Robinson annulation strategy.



Corey/Mulzer Intermediate

SCHEME 6 Intramolecular γ -alkylation of an endocyclic enone.

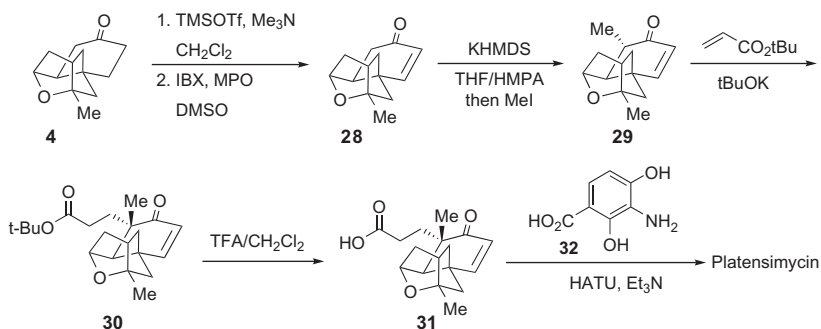
exposure of **5** to t -butoxide triggered the desired transannular cyclization to give ketone **27** in excellent overall yield. The final key transformation necessary to complete the formal synthesis was controlled reduction of the enone to correctly set the C9 stereogenic center. However, it was known that standard hydrogenation conditions produced mixtures at C9, as there was little facial bias evident in these caged systems. Similar dienone studies by Mulzer,^{14m} Corey^{14j} and Mulzer and Pfaltz,¹⁴ⁱ had shown that chiral hydrogenation catalysts were effective at mediating these reductions and could impart high levels of control at the C9 stereocenter. Employing the same chiral rhodium catalyst for **27** gave **4** in a 5:1 diastereomeric ratio. Spectral data for **4** matched the reported spectral information from Corey.

Conversion of ketone **4** to platensimycin could be achieved by utilizing procedures previously reported. It had been shown that **4** could be readily converted to enone **28** by IBX-promoted dehydrogenation of the corresponding

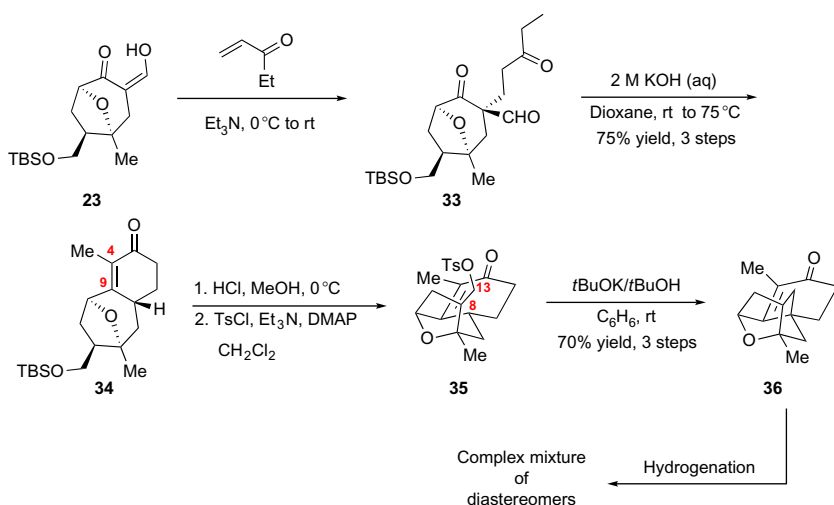
silyl enol ether (Scheme 7).^{14j} Methylation of this intermediate yielded **29**, and subsequent Michael addition to *t*-butyl acrylate generated ester **30**. Hydrolysis of the ester provided the requisite acid **31**, which could be coupled to aniline **32**, thus installing the polar head group and completing the natural product.^{14o}

2.5 Medicinal Chemistry Efforts

With the success of the direct and high-yielding conversion of **6** to **27**, a more difficult case was targeted that would deliver the C-4 methyl group earlier in the synthesis (Scheme 8). Simple modification of the Robinson annulation allowed for introduction of this methyl group. Hydroxymethylene ketone **23**, was allowed to react with ethyl vinyl ketone in the presence of Et₃N to provide **33**, which was then exposed to hydroxide base, triggering the final



SCHEME 7 Completion of formal total synthesis of (–)-platensimycin.

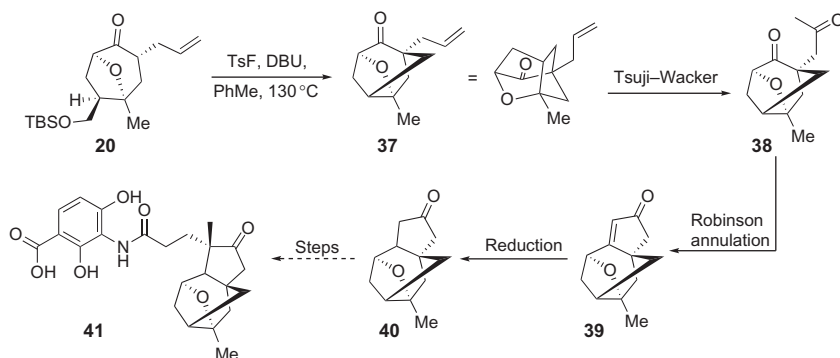


SCHEME 8 Attempts at an early installation of the C4 α -keto methyl moiety.

aldol/dehydration/deformylation sequence yielding **34**. Following deprotection and tosylation, **35** was converted to methyl enone **36** upon treatment with *t*-BuOK/*t*-BuOH. The success of this route was soon frustrated by attempts to hydrogenate the tetrasubstituted olefin. Enone **36** was resistant to hydrogenation in the presence of the same chiral rhodium complex at elevated pressure. Effective hydrogenation was achieved with Pd/C in ethanol; however, the reaction produced an inseparable mixture of compounds that appeared to be both C-4 and C-9 diastereomers. This mixture was further complicated by the ease with which the C-4 methyl group epimerized.

Only a few synthetic efforts have been made toward singly altering the cyclohexenone ring of platensimycin, mainly based on prohibitive synthetic methods. However, the chemistry developed for our platensimycin synthesis is quite amenable to alteration of this region of the natural product. Interestingly, it is clear that the carbonyl oxygen has significant interactions with A309 of the enzyme pocket crucial to the drug's efficacy (Figure 4); yet a majority of the poor pharmacokinetics is derived from this enone's disposition as a strong Michael acceptor. With this in mind, current work is focused on the utilization of this furan-based route for the preparation of novel platensimycin analogs. As this route is unique in allowing a late stage annulation of the cyclohexanone ring onto a preformed oxabicyclic core, it should be easily adapted to allow the investigation of alternative sizes and compositions of the ring systems in this region of the natural product. This area appears to be an attractive domain for analog generation, as alterations to this region have been shown to have demonstrable effects on biological activity.

One such example is shown in Scheme 9, where intermediate **20** was swiftly taken to **37** in a one-pot deprotection-tosylation-intramolecular γ -alkylation mechanism utilizing tosyl fluoride. The resulting terminal olefin, when subject to Tsuji–Wacker oxidation conditions, furnished methyl ketone **38**, which when exposed to strongly basic conditions triggered the Robinson annulation sequence, providing us with a cyclopentenone annulated analog **39**.



SCHEME 9 Synthesis of a ring contracted platensimycin analog.

Through the same high pressure hydrogenation steps as seen in the conversion of **27** to **4**, we successfully saturated the C3–C4 olefin producing **40** and efforts are ongoing to provide a compound with an attached polar head group for biological evaluation of **41**.

Thus, a concise and direct formal asymmetric total synthesis of platensimycin based on the key use of a furan–TBCP cycloaddition reaction has been described. Two sequential annulations on the oxabicyclo[3.2.1]octane core established the hydrophobic cage domain found in the natural product.

The application of the TBCP:furan cycloaddition chemistry to the platensimycin system highlights the ability to directly access the oxa-bridged core found in these natural products. In a second application, we describe how opening of the oxa-bridge can lead to the highly substituted cycloheptane ring found in the marine natural product frondosin A.

3 ASYMMETRIC TOTAL SYNTHESIS OF (+)-FRONDOSIN A

In 1997, researchers discovered that an extract of the Micronesian sponge *Dysidea frondosa* exhibited significant inhibitory activity for the binding of the cytokine interleukin-8 (IL-8) to its receptor, CX-CLR1/2.¹⁹ Isolation of the natural product from the extracts eventually attributed the biological activity to five structurally related novel sesquiterpenes, frondosins A–E (Figure 6). These natural products all shared the same unique bicyclo[5.4.0]undecane core and featured either an annulated (frondosins B–E) or tethered (frondosin A) hydroquinone derivative.²⁰ Much effort has been invested in the total synthesis of these compounds as recent studies have suggested that IL-8 plays an important role in tumor progression and metastasis.²¹ Furthermore, preliminary anti-HIV assays have revealed that frondosins A and D exhibit HIV-inhibitory activity at the low micromolar level.²²

3.1 Retrosynthetic Scheme

Our retrosynthetic strategy targeted late stage intermediate **42**, containing the intact carbocyclic framework of the natural product and corresponding to the structure of a previously synthesized racemic intermediate of the Ovaska group (Scheme 10).^{20b} Intermediate **42** was thought to arise from

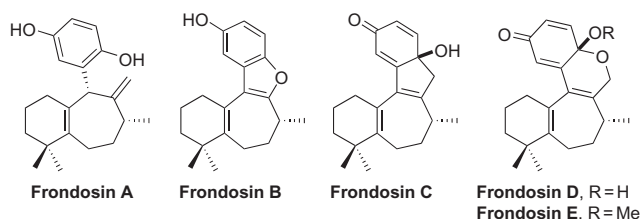
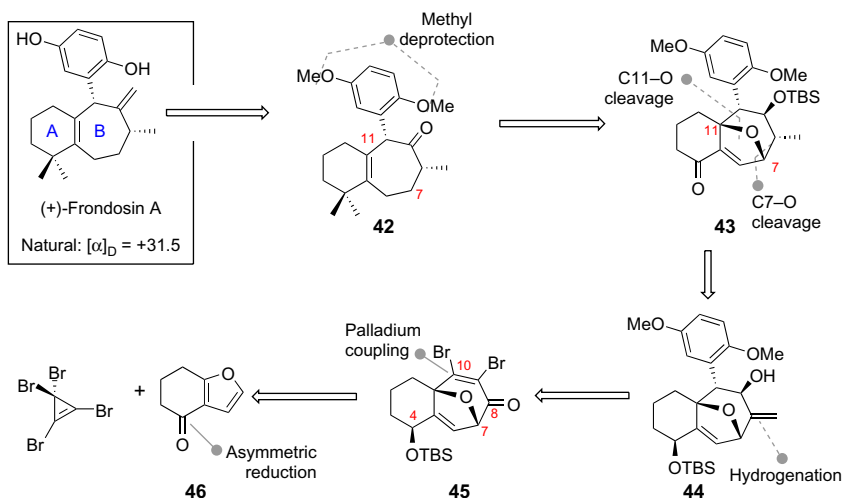


FIGURE 6 Novel frondosin natural products.



SCHEME 10 (+)-Fronodosin A retrosynthetic analysis.

manipulations of the tricyclic framework embodied in **43**, focusing on (1) a previously developed phosphine-mediated cleavage of the bridging ether spanning C7–C11 of the B-ring and (2) transformation of C4 carbonyl to a geminal dimethyl moiety. It was envisioned that the absolute stereochemistry at C8 could be established via directed hydrogenation of allylic alcohol **44** and that the C4-protected alcohol would serve as a suitable placeholder for the ensuing carbonyl. Complex intermediate **44** requires a highly functionalizable starting material that was thought to come about through exploitations of dibromoeneone **45**. The soft electrophilic β -vinylic bromide of the α,β -unsaturated enone of **45** provides a favorable target for palladium-catalyzed reactions to incorporate the necessary aryl functionality. Moreover, the embedded oxabicyclo[3.2.1]octadiene core of **45** imparts significant concavity to the molecule, allowing our synthetic route to exploit considerable facial selectivity and controlling diastereoselective addition of incoming functionality. The commercially available ketone **46** seemed an ideal starting point and in fact, asymmetric reduction of **46** to the *R*-alcohol had been previously reported by Noyori.²³

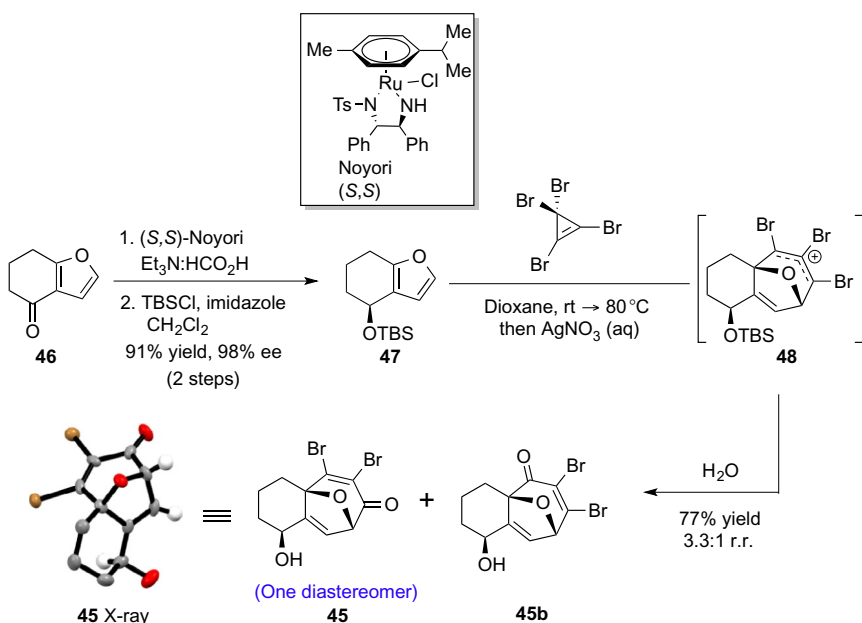
3.2 First Synthetic Plan and Initial Studies

Completion of the formal total synthesis of platensimycin enhanced our scope of furan Diels–Alder reactions with TBCP and simple substituted furans. Extension of this formal [4+3]-cycloaddition to annulated furans such as **46** would be necessary for access to the [5.4.0]undecane carbocyclic core of frondosin A. Although the analogous reaction between annulated furans and oxyallyl cations are known to be difficult, with simple electrophilic substitution

products arising, it was hoped that the high reactivity of TBCP toward Diels–Alder reaction with furan would have the ability to overcome the increased steric demands.²⁴ Moreover, we were attracted to the notion that an asymmetric center at C4 of the A-ring could control the diastereoselectivity of the cycloaddition and that the information could be relayed throughout the synthesis to manipulate functionality in a diastereoselective manner.

In this approach to key building block **45**, we employed a single asymmetric step to effect the diastereoselective total synthesis. The commercially available ketone **46** seemed an ideal starting point and we initially prepared the requisite alcohol with reasonable selectivity (88% ee) through reduction of ketone **46** with the (*R*)-(+)-2-methyl-CBS-oxazaborolidine catalyst. This reduction was not amenable to a large-scale production due to the cost of the catalyst and difficult purification. Further investigation into this reduction showed that the alcohol could be produced in 98% ee with the utilization of the (*S,S*)-Noyori transfer hydrogenation catalyst (Scheme 11).²⁰ The reduction was much more cost-effective with only a 1% catalyst load and with a significant increase in enantiomeric excess.

The alcohol was converted to the silyl ether **47** and condensed with TBCP to give a mixture of regioisomeric tetrabromides in excellent overall yield. Pleasingly, the facial selectivity was high with the C4-silyloxy group exerting

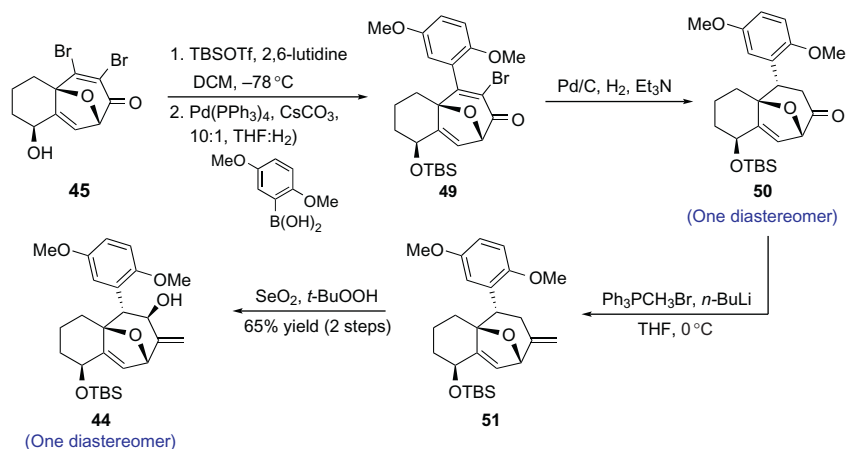


SCHEME 11 Diels–Alder reaction between annulated furan **47** and TBCP: X-ray crystallographic confirmation of stereochemistry.

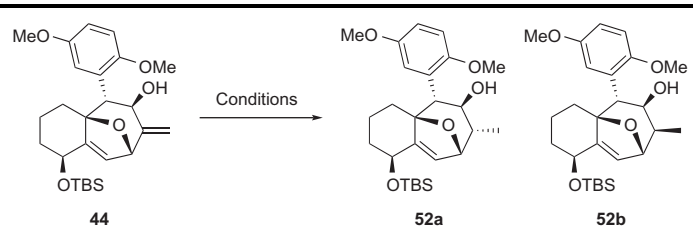
a strong directing effect on the initial Diels–Alder reaction leading to a *syn*-relationship between the protected alcohol and the oxo-bridge. The bridgehead substitution at C11 provided a reasonable directing effect that favored the formation of **45** as the major regioisomer (r.r., 3.3:1), with the standard silver-promoted hydrolysis of the tetrabromides.

Previous studies on this key intermediate demonstrated that the two vinylic bromides of **45** displayed substantially different levels of activity, allowing Suzuki–Miyaura cross-coupling of **45** with dimethoxyphenyl boronic acid to occur exclusively at the more electron deficient β -bromide to deliver the *dimethoxy*-hydroquinone **49** in an efficient manner (Scheme 12). We anticipated that it should be possible to exploit the curvature embedded in the oxabicyclo[3.2.1]octadiene core of **49** to control the facial selectivity of incoming functionality and to set the absolute stereochemistry of the natural product. With this in mind, hydrogenation of **49** in the presence of triethylamine effected reduction with complete facial selectivity, with palladium coordinating from the less encumbered *exo*-face to correctly set the C10 center of **50**. Further exploiting the facial bias that the temporary ether bridge provided, Wittig condensation gave exocyclic methylene derivative **51**, which when subjected to allylic oxidation conditions with SeO_2 provided alcohol **44** with high diastereoselectivity (*exo:endo*, 97:3).²⁵ We thought that an *exo*-alcohol at C9 could serve not only as a suitable surrogate for the exocyclic olefin present in the natural product, but also as a directing group for the stereoselective introduction of the C8 methyl group of frondosin A (Scheme 12).

We assumed that the *exo*-alcohol in **44** would participate in a directed hydrogenation adding hydrogen in an *exo*-mode to produce the *endo*-methyl group at C8. We initiated studies to probe the natural preference for hydrogenation, subjecting alcohol **44** to hydrogenation in the presence of Pd/C and



SCHEME 12 Diastereoselective introduction of exocyclic functionality.

TABLE 1 Diastereoselective Reduction of **44** with Various Hydrogenation Conditions


Entry	Conditions	52a:52b ^a	Yield (%) ^b
1	Pd/C (10 mol%), EtOAc (0.1 M) ^c	4:1	98
2	PtO ₂ (20 mol%), C ₆ H ₆ (0.1 M) ^c	4:1	96
3	Crabtree's catalyst (20 mol%), CH ₂ Cl ₂ (0.05 M) ^c	5:1	94
4	[Rh(nbd)(diphos-4)]BF ₄ (20 mol%), THF (0.1 M) ^d	10:1	98
5	[Rh(nbd)(diphos-4)]BF ₄ (2.5 mol%), THF (0.1 M) ^d	3:1	98
6	[Rh(nbd)(diphos-4)]BF ₄ (20 mol%), THF (0.05 M) ^d	20:1	98
7	[Rh(nbd)(diphos-4)]BF ₄ (20 mol%), THF (0.025 M) ^d	>99:1	98

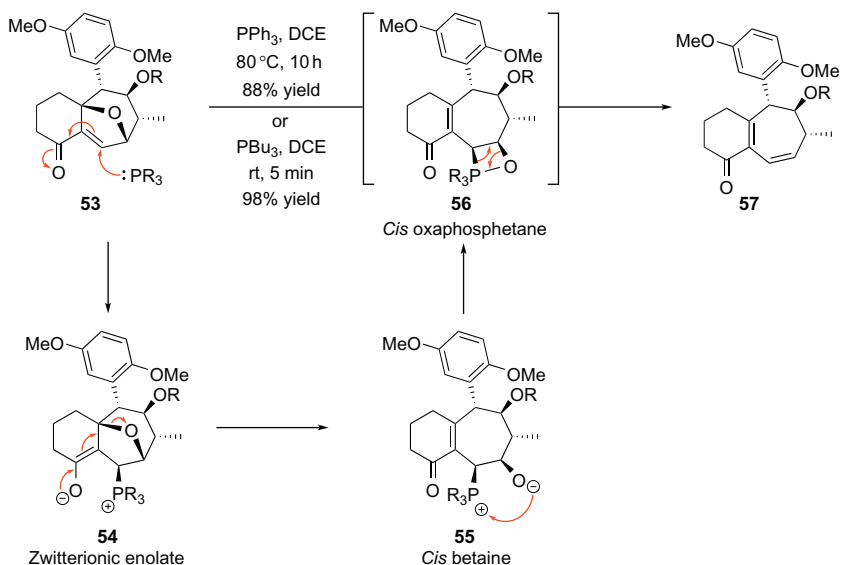
^aRatio based on NMR analysis.^bIsolated yield.^cPerformed at 1 atm of H₂ gas.^dPerformed at 600 psi of H₂ gas.

PtO₂ at 1 atm of H₂ pressure (Table 1). In both cases, a high yielding reduction occurred to give a 4:1 mixture of diastereomers **52a:52b**, expressing the directing effect that the oxy-bridge was still imparting on the system. However, not satisfied with this diastereomeric ratio; we explored a stronger hydroxyl-directed hydrogenation, exposing **44** to Crabtree's catalyst²⁶ (20 mol%) at 1 atm of H₂ pressure. Surprisingly, this catalyst had little effect on the product ratio, giving only a slightly improved 5:1 mixture of diastereomers in good yield. With the ability to conduct hydrogenations at elevated pressure, [Rh(nbd)(diphos-4)]BF₄ was employed as catalyst at 600 psi of H₂ pressure.²⁷ Interestingly, it was found that a higher catalyst load (20 mol%) was needed to achieve at 10:1 mixture, as the initial 2.5 mol% of catalyst gave only a 3:1 mixture of diastereomers. Furthermore, it was found that the concentration of the reaction had a dramatic effect on the diastereomeric ratio. Performing the reaction at 0.05 M in THF produced a 20:1 mixture, while further dilution (0.025 M in THF) led to a completely diastereoselective hydrogenation producing **52a** exclusively in high yield.

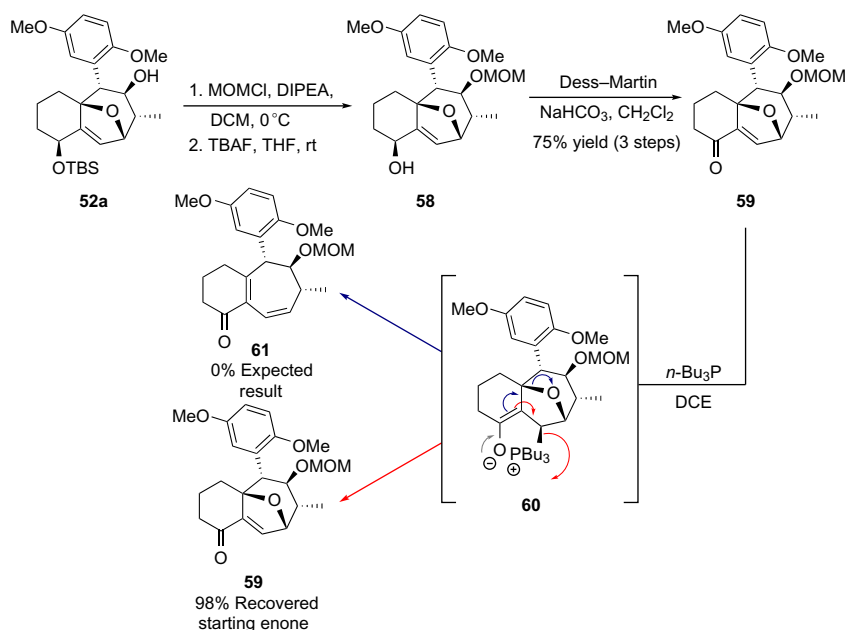
3.3 Lewis Acid Assisted Trialkylphosphine Ring Opening

With the appropriate stereocenters of frondosin A installed, the stage was set for the cleavage of the temporary bridging ether. We extrapolated from our earlier studies on the ether bridge-opening that **53** would be an ideal substrate on which to affect an addition/elimination sequence with a trialkylphosphine nucleophile. A probable mechanism for this deoxygenation, akin to the phosphine-induced reduction of epoxides to olefins, involves an initial conjugate addition of the phosphine to the more accessible *exo*-face of **53** to produce an enolate **54** followed by ejection of the β -disposed ether. The elimination yields a transient betaine intermediate **55** that collapses through the intermediacy of the oxaphosphetane **56** to deliver the desired olefin **57** (Scheme 13).

Initially, we were attracted to a chemoselective allylic oxidation at C4 in the presence of MnO_2 to selectively construct intermediate **53**. Unfortunately, after a multitude of attempts the desired enone product was never formed, returning only starting alcohol. Refocusing our efforts to generate intermediate **53**, we produced two chemically different protected alcohols for selective deprotection at the C4 alcohol. Protection of the C9 alcohol of **52a** as its MOM ether derivative was followed by deprotection of the silyl ether and Dess–Martin periodinane (DMP) oxidation of the resulting C4 allylic alcohol **58** to give enone **59** (Scheme 14). Enone **59** represented the first appropriate intermediate to probe the effectiveness of the phosphine-mediated ring-opening/elimination procedure to deliver diene **61**. However, it was found that the system was not predisposed toward the addition of phosphine reagents.



SCHEME 13 Proposed phosphine-mediated ring-opening mechanism.

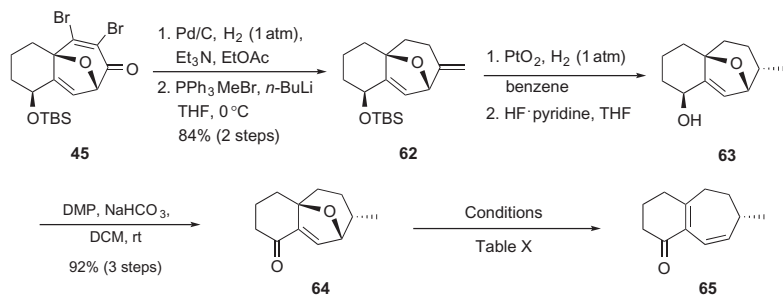


SCHEME 14 Initial attempts at ring-cleavage with MOM protected enone **59**.

Addition of triphenyl- or tributylphosphine at either room temperature or elevated temperature did not produce the desired ring-opened product and the starting enone was recovered unchanged. Prolonged reaction times at elevated temperatures delivered an unidentifiable compound that appeared to contain a new phosphine–carbon bond with the ether bridge still intact. We assumed that 1,4-addition of phosphine to the enone occurred rapidly, producing zwitterionic enolate **60**; however, the resulting enolate simply released the phosphine to produce starting material (bottom arrow) rather than ejecting the β -disposed ether (top arrow).

We employed a simplified model system to probe the effectiveness of the phosphine-mediated ring-opening and to determine conditions necessary to effect cleavage (Table 2). Intermediate **45** was advanced to **64** by the series of: (1) hydrogenation of the C6–C7 olefin, (2) Wittig condensation of the C8 carbonyl producing exocyclic olefin **62**, (3) hydrogenation of the newly produced methine moiety with Adam's catalyst, (4) deprotection of the C4 silyl group in the presence of HF·pyridine to produce allylic alcohol **63**, and (5) oxidation of the resulting allylic alcohol with DMP to give **64** with complete diastereoselectivity through this series of steps.

With enone **64** in hand, we initially observed that trialkylphosphines alone could not affect ring-opening in these less strained systems. As seen in Table 2, a series of trialkylphosphine reagents were explored, all returning starting material (entries 1 and 5). As seen earlier, prolonged reaction times

TABLE 2 Model System: Trends in Phosphine-Mediated Ring Opening of **64**

Entry	Phosphine ^a	Lewis acid ^b	Solvent/temp	Yield 64 (%) ^c	Yield 65 (%) ^c
1	<i>n</i> -Bu ₃ P	—	DCM/23 °C	98	—
2	<i>n</i> -Bu ₃ P	—	DCE/90 °C	70	—
3	<i>n</i> -Bu ₃ P	InCl ₃	DCM/23 °C	80	—
4	<i>n</i> -Bu ₃ P	InCl ₃	DCE/90 °C	—	—
5	<i>t</i> -Bu ₃ P	—	DCM/23 °C	98	—
6	<i>t</i> -Bu ₃ P	—	THF/140 °C ^d	66	—
7	<i>t</i> -Bu ₃ P	InCl ₃	THF/70 °C	10	—
8	Me ₃ P	InCl ₃	DCM/23 °C	—	25
9	Me ₃ P	InCl ₃	DCE/90 °C	—	55
10	Me ₃ P	BF ₃ ·Et ₂ O	DCE/90 °C	—	88
11	Me ₃ P	Ti(O <i>i</i> Pr) ₄	DCE/90 °C	—	85

^aThree equivalents of trialkylphosphines used in all reactions.^bSix equivalents of Lewis acid used in all reactions.^cIsolated yield.^dPerformed in microwave reactor.

at elevated temperatures delivered an unidentifiable compound that appeared to contain a phosphine–carbon bond with starting material being recovered in lower yields (entries 2 and 6).

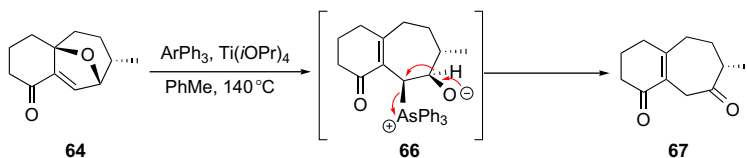
Traditionally, Lewis acids have been employed to facilitate the opening of similar oxabicyclic intermediates and we thought that this case might react similarly.²⁸ With this in mind, we began to methodically pair Lewis acids with a series of trialkylphosphine reagents. Initial results were poor, with a variety of Lewis acid/phosphine combinations still falling short with no

reactivity (entry 3), or at higher temperature's decomposition of material (entries 4 and 7). It was not until we paired the highly reactive, trimethylphosphine (Me_3P) with In(III)Cl that a productive ring-opening/elimination occurred (entry 8). Optimization of this ring-opening revealed that increased temperatures were required (entry 9) and that combination with more reactive Lewis acids (entries 10 and 11) provided a ring-opened product **65** in acceptable yield.

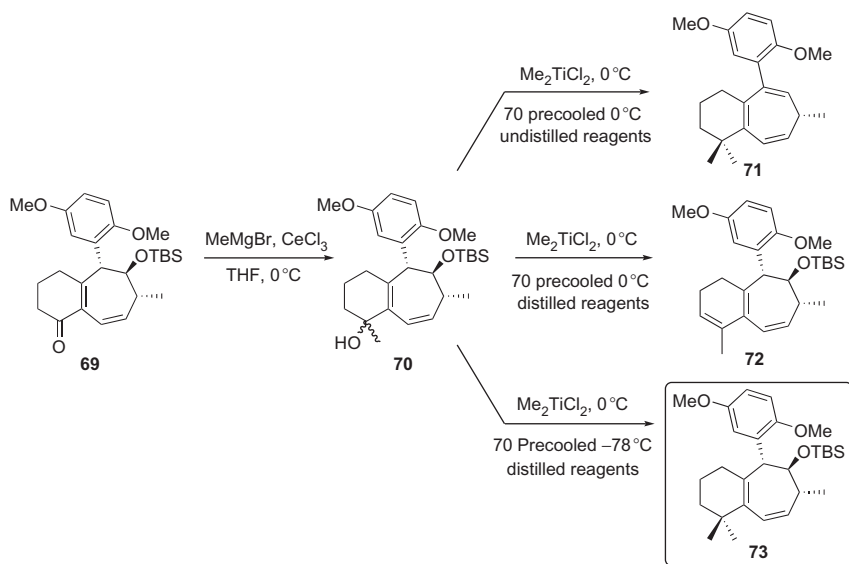
Interestingly, while working with our model system **64** we stumbled upon an interesting variation. While screening Ph_3As with a panel of Lewis acids, the addition of Ph_3As produced a ring-opened diketone product **67** in reasonable yield (Scheme 15). It appeared that Ph_3As , added in the usual *exo*-mode to produce an enolate, upon collapse generated oxide **66**. Given the *syn*-relationship of the oxide to the arsenic, the proposed mechanism involves a 1,2-hydride shift leading to the formation of the carbonyl with departure of the arsenic group. This result was interesting to us as it not only served as a productive method for cleavage of the bridging ether but it would also allow for a viable “chemical handle” for further analog generation.

Returning to our intended system, when enone **59** was exposed to a mixture of $\text{BF}_3 \cdot \text{Et}_2\text{O}$ and Me_3P , a productive ring-opening/elimination reaction occurred; however, the isolated yield was only 15%, with about 10% of the unidentified phosphine product seen before. More undesirably, we were unable to account for the mass balance of the reaction mixture, as only ~25% of the material was recovered. A screen of Lewis acids determined that more reactive Lewis acids (Ti(OiPr)_4 , $\text{BF}_3 \cdot \text{Et}_2\text{O}$, AlCl_3) led to decomposition of bridged material, most likely through deprotection and elimination of the MOM ether. Unsatisfied with these yields, we suspected that the MOM protecting group was not durable enough to withstand the Lewis acid conditions necessary for the desired transformation.

Returning to intermediate **52a**, we quickly learned that the C9 alcohol was well shielded by the proximal arene at C10 and that the bulky silyl ethers (TBDPS, TIPS) or esters (PIV) needed to withstand the Lewis acid conditions could not be produced in acceptable yield. However, silylation with TBSOTf provided a disilyl product in excellent yield and to our delight the C4 allylic silyl ether could be selectively deprotected in the presence of tetra-*N*-butylammonium fluoride (TBAF). Oxidation of **68** utilizing DMP conditions provided intermediate **43** (Scheme 16).



SCHEME 15 Diketone **67** as a result of ring-opening attempt with Ph_3As nucleophile.



SCHEME 16 Transformation of enone **69** to geminal dimethyl moiety.

The robust TBS protecting group allowed for a screen of several Lewis acid/trialkylphosphine combinations. Table 3 demonstrates a trend in the trialkylphosphines whereby increasing nucleophilicity of the phosphine greatly impacts the isolated yield of ring-opened diene **69**. Treatment with Me_3P in the presence of In(III)Cl showed improved results (55% yield) but seemed to form a complex with the indium salts that could not be broken up to give desired product. However, it was apparent that the combination of Me_3P and Ti(OiPr)_4 was superior to others in effecting the desired reaction. With a short string of reactions to optimize the reaction conditions, we were able to produce ring-opened/elimination diene **69** in a satisfying 86% yield.

3.4 Carbonyl Transformation to Geminal Dimethyl Moiety

Following conversion to diene **69**, our initial inclination was to saturate the C6–C7 olefin of this compound, reducing the likelihood of olefin isomerization destroying the C8 chiral center. Attempts to hydrogenate were unsuccessful, most likely because of the cross-conjugation imparted on the diene by the C4 carbonyl. Traditional hydrogenation catalysts (Pd/C and PtO_2) resulted in a nonselective reduction of both alkenes, whereas homogenous catalysts (Wilkinson's and Crabtree's) returned only starting material.

Transformation of the C4 carbonyl to the necessary geminal dimethyl group would eliminate the cross-conjugation and allow for a selective saturation of the less substituted C6–C7 alkene. It was intended that compound **69**

TABLE 3 Trends in Phosphine Mediated Ring-Opening of **43**

Entry	Lewis acid ^a	Phosphine ^b	Solvent/temp	Yield 43 (%) ^c	Yield 69 (%) ^c
1	–	<i>n</i> -Bu ₃ P	DCE/80 °C	56	–
2	InCl ₃	<i>n</i> -Bu ₃ P	THF/70 °C	–	25
3	InCl ₃	Me ₃ P	THF/70 °C	–	55
4	Ti(O <i>i</i> Pr) ₄	<i>n</i> -Bu ₃ P	THF/70 °C	–	62
5	Ti(O <i>i</i> Pr) ₄	<i>t</i> -Bu ₃ P	THF/70 °C	–	70
6	Ti(O <i>i</i> Pr) ₄	Me ₃ P	THF/70 °C	–	77
7	Ti(O <i>i</i> Pr) ₄ ^d	Me ₃ P	THF/70 °C	–	86

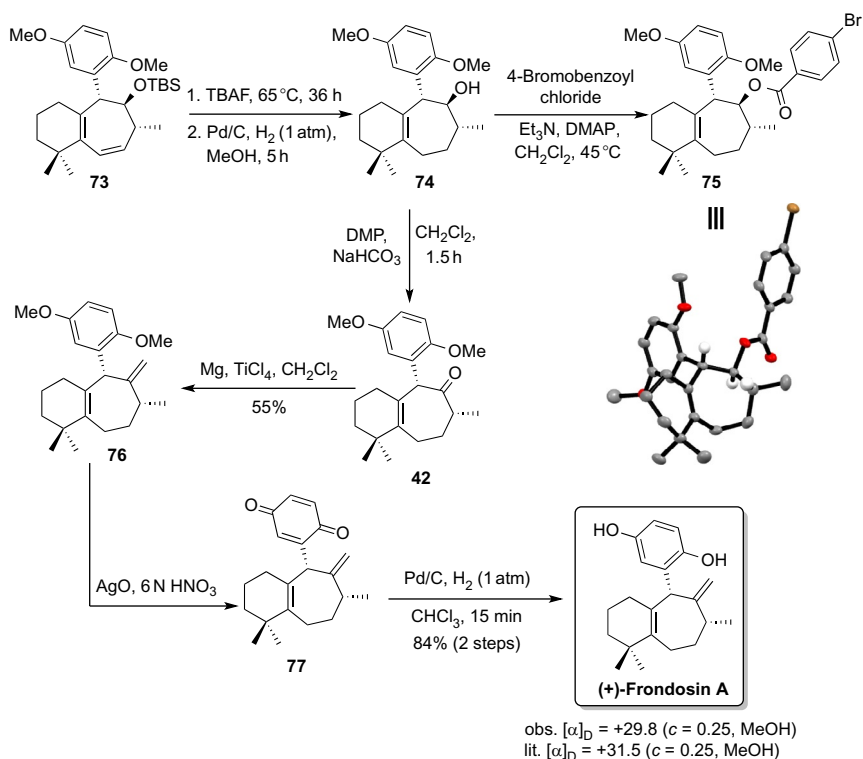
^aSix equivalents of Lewis acid used unless otherwise stated.^bThree equivalents of trialkylphosphines used in all reactions.^cIsolated yield.^dPerformed with three equivalents of Lewis acid.

would be advanced with a modified two-step procedure employed by the Trauner group in their frondosin B synthesis (Scheme 16).²⁹ However, installation of the geminal dimethyl group proved to be more sensitive than described in this system. The C9 silyloxy was quite susceptible to elimination producing **71** and required the use of freshly distilled reagents at the highest purity to effect the transformation and obtain optimal yields of **73**. Along the same lines, the C4 dehydration product **72** was a major impurity and optimization of this procedure showed that precooling to $-78\text{ }^{\circ}\text{C}$ and adding it to a $0\text{ }^{\circ}\text{C}$ solution of Me_2TiCl_2 completely suppressed elimination product **72** that was seen at higher temperatures, producing **73** in optimal yields.

3.5 Completion of Total Synthesis

Deprotection of **73** in the presence of TBAF at elevated temperature followed by traditional hydrogenation conditions (Pd/C, MeOH, 1 atm H₂) proceeded without complications to produce intermediate **74** in a 61% yield through this string of steps (Scheme 17). The three contiguous chiral centers of alcohol **74** provided us with an ideal intermediate to validate the absolute stereochemistry. Alcohol **74** was condensed with 4-bromobenzoyl chloride to generate highly crystalline benzoate **75** that produced thin plate crystals in a simple diffusion method. X-ray crystallographic analysis of **75** allowed for the unambiguous assignment of the absolute stereochemistry, confirming our diastereoselective synthesis. Alcohol **74** was oxidized with DMP to late stage intermediate **42** matching the spectral data reported by the Ovaska group.^{20b}

Having prepared the Ovaska intermediate, it was still necessary to produce exocyclic alkene **76** to match the optical rotation of this common asymmetric intermediate with that reported by Trost.^{20a} A variety of olefination procedures (Wittig, Petasis, and Tebbe) were employed to effect the transformation



SCHEME 17 Completion of the total synthesis of (+)-frondosin A: X-ray crystallographic confirmation of absolute stereochemistry.

to exocyclic alkene **76**, but only returned unreacted starting material. The desired olefination of the hindered B ring carbonyl carbon was then generated by applying the bimetallic $\text{TiCl}_4\text{--Mg}$ promoted methylene transfer reaction to fabricate *di-methoxy-frondosin A* in a 55% yield.³⁰ Reports of deprotection of **77** with BBr_3 are known to result in decomposition, while reports of deprotection with sodium ethanethiolate only yielded monodeprotected products. Initial attempts at final deprotection of the dimethoxyarene **77** with $\text{CAN}/\text{Na}_2\text{S}_2\text{O}_4$, as disclosed in previous total syntheses of frondosin A, resulted in a less than effective deprotection with only around 35% recovered product. A significant improvement was made through a two-step oxidative (AgO , HNO_3)/reductive (Pd/C , H_2) procedure to provide the enantiomerically pure frondosin A in a 84% yield over the two steps and possessing optical rotation reflective of the natural product $[\alpha]_{\text{D}}^{22} = +29.8$ ($c = 0.25$, MeOH); lit. $[\alpha]_{\text{D}} = +31.5$ ($c = 0.25$, MeOH).³¹

4 CONCLUSION

The direct cycloaddition of tetrahalocyclopropenes with both substituted and annulated furans provides for a high-complexity-building operation to produce restricted cycloheptanoid systems from readily available starting materials. These intermediates provide much freedom to operate around the carbocyclic system owing to the presence of multiple functionality that can be elaborated in a direct and predictable fashion. In this chapter, we describe the recent completion of two terpenoid natural products, platensimycin and frondosin A, based on the central application of this cycloaddition methodology. In both syntheses, the facial differentiation imparted by the oxa-bridge was integral to controlling the placement of key stereogenic centers in the molecule. We are currently pursuing additional natural products from these bicyclic synthons containing heterocyclic as well as other carbocyclic substructures.

REFERENCES

1. Fringuelli, F.; Tatchi, A. In: *The Diels Alder Reaction: Selected Practical Methods*; John Wiley & Sons Ltd.: West Sussex, England, 2002.
2. (a) Carruthers, W. *Cycloaddition Reactions in Organic Synthesis*. Pergamon: Oxford, 1990; (b) Fringuelli, F.; Tatchi, A. *Dienes in the Diels-Alder Reaction*; Wiley: New York, 1990; (c) Oppolzer, W. Paquette, L. A., Ed.; *Comprehensive Organic Synthesis*; Vol. 5; Pergamon: Oxford, 1991; p 315; (d) Roush, W. R. Paquette, L. A., Ed.; *Comprehensive Organic Synthesis*; Vol. 5; Pergamon: Oxford, 1991; p 513; (e) Coxon, J. M.; McDonald, D. Q.; Steel, P. J. In: *Advances in Detailed Reaction Mechanisms*; Coxon, J. M., Ed.; JAI Press: Greenwich, 1994.
3. (a) Helmchen, G.; Karge, R.; Weetman, J. Scheffold, R., Ed.; *Modern Synthetic Methods*; Vol. 4; Springer: Berlin, 1986; p 216; (b) Waldmann, H. *Synthesis* **1994**, 535–551.

4. (a) Hoffmann, H. M. R.; Joy, D. R. *J. Chem. Soc. B* **1968**, 1182–1186; Ashcroft, M. R.; Hoffmann, H. M. R. *Org. Synth.* **1978**, 58, 17–22.
5. (a) Takaya, H.; Makimo, S.; Hayakawa, Y.; Noyori, R. *J. Am. Chem. Soc.* **1978**, 100, 1759–1765; (b) Noyori, R.; Hayakawa, Y. *Tetrahedron* **1985**, 41, 5879–5886.
6. (a) For reviews, see: Harmata, M.; Rashatasakhon, P. *Tetrahedron* **2003**, 59, 2371–2395; (b) Harmata, M. *Acc. Chem. Res.* **2001**, 34, 595–605; (c) For recent reagents used to obtain oxo-allyl cations, please see: Handy, S. T.; Okello, M. *Synlett* **2002**, 489–491; (d) Montana, A. M.; Grima, P. M. *Tetrahedron Lett.* **2001**, 42, 7809–7813; (e) Cho, S. Y.; Lee, H. I.; Cha, J. K. *Org. Lett.* **2001**, 3, 2891–2893; (f) Sarhan, A. *Curr. Org. Chem.* **2001**, 5, 827–844; (g) Föhlisch, B.; Korfant, H.; Meining, H.; Frey, W. *Eur. J. Org. Chem.* **2000**, 1335–1344.
7. (a) For applications, please see: Harmata, M.; Ghosh, S. K.; Hong, X. C.; Wacharasindhu, S.; Kirchhoefer, P. *J. Am. Chem. Soc.* **2003**, 125, 2058–2059; (b) Vakalopoulos, A.; Lampe, T. F. J.; Hoffmann, H. M. R. *Org. Lett.* **2001**, 3, 929–932; (c) Kim, H.; Hoffmann, H. M. R. *Eur. J. Org. Chem.* **2000**, 2195–2201; (d) Harmata, M.; Bohnert, G. J. *Org. Lett.* **2003**, 5, 59; (e) Lee, J. C.; Cha, J. K. *Tetrahedron* **2000**, 56, 10175–10184.
8. (a) Law, D. C. F.; Tobey, S. W. *J. Am. Chem. Soc.* **1968**, 90, 2376–2386; (b) Tobey, S. W.; Law, D. C. F. *Angew. Chem. Int. Ed. Engl.* **1968**, 7, 649; (c) Tobey, S. W.; Law, D. C. F. U.S. Patent 3,538,117, November 3, 1970.
9. (a) Pelphrey, P. M.; Bolstad, D. B.; Wright, D. L. *Synlett* **2007**, 2647–2650; (b) Pelphrey, P. M.; Orugunty, R. S.; Helmich, R. J.; Battiste, M. A.; Wright, D. L. *Eur. J. Org. Chem.* **2005**, 4296–4303; (c) Pelphrey, P. M.; Abboud, K. A.; Wright, D. L. *J. Org. Chem.* **2004**, 69, 6931–6933; (d) Batson, W. A.; Abboud, K. A.; Battiste, M. A.; Wright, D. L. *Tetrahedron Lett.* **2004**, 45, 2093–2096; (e) Orugunty, R. S.; Wright, D. L.; Battiste, M. A.; Helmich, R. J.; Abboud, K. J. *Org. Chem.* **2004**, 69, 406–416.
10. Oblak, E. Z.; Bolstad, E. S. D.; Ononye, S. N.; Priestley, N. D.; Hadden, M. K.; Wright, D. L. *Org. Biomol. Chem.* **2012**, 10, 8597–8604.
11. Oblak, E. Z.; Wright, D. L. *Org. Lett.* **2011**, 13, 2263–2265.
12. Oblak, E. Z.; VanHeyst, M. D.; Wright, D. L. *J. Am. Chem. Soc.* **2014**. <http://dx.doi.org/10.1021/ja413106t>, Accepted.
13. (a) Singh, S. B.; et al. *J. Am. Chem. Soc.* **2006**, 128, 11916–11920; (b) Wang, J.; et al. *Nature* **2006**, 441, 358–361.
14. (a) Nicolaou, K. C.; Li, A.; Edmonds, D. J. *Angew. Chem. Int. Ed.* **2006**, 45, 7086–7090; (b) Nicolaou, K. C.; Edmonds, D. J.; Li, A.; Tria, G. S. *Angew. Chem. Int. Ed.* **2007**, 46, 3942–3945; (c) Nicolaou, K. C.; Lister, T.; Denton, R. M.; Montero, A.; Edmonds, D. J. *Angew. Chem. Int. Ed.* **2007**, 46, 4712–4714; (d) Nicolaou, K. C.; Tang, Y.; Wang, J. *Chem. Commun.* **2007**, 19, 1922–1923; (e) Zou, Y.; Chen, C.-H.; Taylor, C. D.; Foxman, B. M.; Snider, B. B. *Org. Lett.* **2007**, 9, 1825–1828; (f) Li, P.; Payette, J. N.; Yamamoto, H. *J. Am. Chem. Soc.* **2007**, 129, 9534–9535; (g) Kaliappan, K. P.; Ravikumar, V. *Org. Lett.* **2007**, 9, 2417–2419; (h) Ghosh, A. K.; Kai, X. *Org. Lett.* **2007**, 9, 4013–4016; (i) Tiefenbacher, K.; Mulzer, J. *Angew. Chem. Int. Ed.* **2007**, 46, 8074–8075; (j) Lalic, G.; Corey, E. J. *Org. Lett.* **2007**, 9, 4921–4923; (k) Matsuo, J.; Takeuchi, K.; Ishibashi, H. *Org. Lett.* **2008**, 10, 4049–4052; (l) Kim, C. H.; Jang, K. P.; Choi, S. Y.; Chung, Y. K.; Lee, E. *Angew. Chem. Int. Ed.* **2008**, 47, 4009–4011; (m) Tiefenbacher, K.; Mulzer, J. *Angew. Chem. Int. Ed.* **2008**, 47, 2548–2555; (n) Nicolaou, K. C.; Pappo, D.; Tsang, K. Y.; Gibe, R.; Chen, D. Y.-K. *Angew. Chem. Int. Ed.* **2008**, 47, 944–946; (o) Nicolaou, K. C.; Li, A.; Edmonds, D. J.; Tria, G. S.; Ellery, S. P. *J. Am. Chem. Soc.* **2009**, 131, 16905–16918; (p) McGrath, N. A.; Bartlett, E. S.; Sittihan, S.; Njardarson, J. T. *Angew. Chem. Int. Ed.* **2009**, 48, 8543–8546; (q) Nicolaou, K. C.; Li, A.; Ellery, S. P.; Edmonds, D. J. *Angew. Chem.*

- Int. Ed.* **2009**, *48*, 6293–6295; (r) Yun, S. Y.; Zheng, J.-C.; Lee, D. *J. Am. Chem. Soc.* **2009**, *131*, 8413–8415; (s) Ghosh, A. K.; Xi, K. *J. Org. Chem.* **2009**, *74*, 1163–1170; (t) Tiefenbacher, K.; Trondlin, L.; Mulzer, J.; Pfaltz, A. *Tetrahedron* **2010**, *66*, 6508–6513; (u) Eey, S. T.-C.; Lear, M. *J. Org. Lett.* **2010**, *12*, 5510–5513.
15. (a) Herath, K. B.; Zhang, C.; Jayasuriya, H.; Ondeyka, J. G.; Zink, D. L.; Burgess, B.; Wang, J.; Singh, S. B. *Org. Lett.* **2008**, *10*, 1699–1702; (b) Jayasuriya, H.; Herath, K. B.; Ondeyka, J. G.; Zink, D. L.; Burgess, B.; Wang, J.; Singh, S. B. *Tetrahedron Lett.* **2008**, *49*, 3648–3651; (c) Singh, S. B.; Herath, K. B.; Wang, J.; Tsou, N.; Ball, R. G. *Tetrahedron Lett.* **2007**, *48*, 5429–5433; (d) Nicolaou, K. C.; Stepan, A. F.; Lister, T.; Li, A.; Montero, A.; Tria, G. S.; Turner, C. I.; Tang, Y.; Wang, J.; Denton, R. M.; Edmonds, D. J. *J. Am. Chem. Soc.* **2008**, *130*, 13110–13119.
16. Paterson, I.; Mark, G.; Banks, B. *J. Tetrahedron* **1989**, *45*, 5283–5292.
17. (a) Miller, L. C.; Sarpong, R. *Chem. Soc. Rev.* **2011**, *40*, 4550–4562; (b) Kurosu, M.; Kishi, Y. *J. Org. Chem.* **1998**, *63*, 6100–6101; (c) Turgut, Y.; Azizoglu, M.; Erdogan, A.; Arslan, N.; Hosgoren, H. *Tetrahedron Asymmetry* **2013**, *24*, 853–859; (d) Sridhar, Y.; Srihari, P. *Eur. J. Org. Chem.* **2013**, *2013*, 578–587.
18. (a) Shunk, H.; Wilds, A. L. *J. Am. Chem. Soc.* **1949**, *71*, 3946–3950; (b) Woodward, R. B.; Sondheimer, F.; Taub, D.; Heusler, K.; McLamore, W. M. *J. Am. Chem. Soc.* **1952**, *74*, 4223–4251.
19. (a) Patil, A. D.; Freyer, A. J.; Killmer, L.; Offen, P.; Carte, B.; Jurewicz, A. J.; Johnson, R. K. *Tetrahedron* **1997**, *53*, 5047–5060; (b) Hallock, Y. F.; Cardellina, J. H., II; Boyd, M. R. *Nat. Prod. Lett.* **1998**, *11*, 153–160.
20. (a) For syntheses of frondosin A, see: Trost, B. M.; Hu, Y.; Horne, D. B. *J. Am. Chem. Soc.* **2007**, *129*, 11781–11790; (b) Li, X.; Keon, A. E.; Sullivan, J. A.; Ovaska, T. V. *Org. Lett.* **2008**, *10*, 3287–3290; (c) Mehta, G.; Likhite, N. S. *Tetrahedron Lett.* **2008**, *49*, 7113–7116.
21. (a) Brat, D. J.; Bellail, A. C.; Van Meir, E. G. *Neuro-Oncology* **2005**, *7*, 122–133; (b) Zhu, Y. M.; Webster, S. J.; Flower, D.; Woll, P. J. *Br. J. Cancer* **2004**, *91*, 1970–1976.
22. Lane, B. R.; Liu, J.; Bock, P. J.; Schols, D.; Coffey, M. J.; Strieter, R. M.; Polverini, P. J.; Markovitz, D. M. *J. Virol.* **2002**, *76*, 11570–11583.
23. (a) Ohkuma, T.; Hattori, T.; Ooka, H.; Inoue, T.; Noyori, R. *Org. Lett.* **2004**, *6*, 2681–2683; (b) For Noyori transfer hydrogenation catalyst see: Fujii, A.; Hashiguchi, S.; Uematsu, N.; Ikariya, T.; Noyori, R. *J. Am. Chem. Soc.* **1996**, *118*, 2521–2522.
24. Rigby, J. H.; Pigge, F. C. *Org. React.* **1997**, *51*, 351–478.
25. Umbreit, M. A.; Sharpless, K. B. *J. Am. Chem. Soc.* **1977**, *99*, 5526–5528.
26. Crabtree, R. H.; Davis, M. W. *J. Org. Chem.* **1986**, *51*, 2655–2661.
27. Hoveyda, A. H.; Evans, D. A.; Fu, G. C. *Chem. Rev.* **1993**, *93*, 1307–1370.
28. Chiu, P.; Lautens, M. *Top. Curr. Chem.* **1997**, *190*, 1–85.
29. (a) Hughes, C. C.; Trauner, D. *Angew. Chem. Int. Ed.* **2002**, *41*, 2227; (b) Seebach, D. *Angew. Chem. Int. Ed.* **2011**, *50*, 96–101.
30. Yan, T.; Tsai, C.; Chien, C.; Cho, C.; Huang, P. *Org. Lett.* **2004**, *6*, 4961–4963.
31. Snyder, C. D.; Rapoport, H. *J. Am. Chem. Soc.* **1972**, *94*, 227–231.

Structure Inspires a New Method That Delivers the Synthesis of Natural Products and Analogs in the Pederin Family

Paul E. Floreancig¹

Department of Chemistry, University of Pittsburgh, Pittsburgh, Pennsylvania, USA

¹Corresponding author: florean@pitt.edu

Chapter Outline

1. Introduction	184	4.2. Demonstration of Concept	191
2. Total Synthesis of Theopederin D	184	5. Total Synthesis of Pederin	192
2.1. Acyliminium Ions Through Oxidative Carbon–Carbon Bond Cleavage	184	5.1. Subunit Synthesis	192
2.2. Mycalamides and Theopederins	184	5.2. Fragment Coupling Through <i>N</i> -Acylaminal Formation and Completion of the Synthesis	194
2.3. Amido Trioxadecalin Synthesis	185	6. Total Synthesis of Psymberin	195
2.4. Total Synthesis	185	7. Analog Synthesis	196
3. Psymberin	186	7.1. Pederin Analogs	196
3.1. Structural Connection with Theopederin D	186	7.2. Hybrid Analogs	198
3.2. Initial Studies	188	7.3. Non- <i>N</i> -Acylaminal-Containing Analogs	199
3.3. A Fortuitous Scooping	190	8. Biological Studies	200
4. <i>N</i>-Acylaminals from Nitrile Hydrozirconation	190	9. Conclusions	202
4.1. Inspiration from Natural Product Synthesis	190	Acknowledgments	203
		References	203

1 INTRODUCTION

Natural product total synthesis has long served as a motivation for developing new chemical reactions. The converse, in which new reactions inspire efforts in natural product synthesis, is also widely observed. The work that is described in this chapter shows that these efforts can be symbiotic, and that this relationship can be useful for studying the biological activity of complex molecules.

2 TOTAL SYNTHESIS OF THEOPEDERIN D

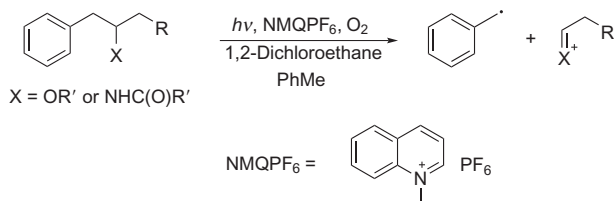
2.1 Acyliminium Ions Through Oxidative Carbon–Carbon Bond Cleavage

This project arose from a desire to find a unique application for some methodological work that my group had developed on oxidative carbocation formation.¹ This process (Scheme 1) showed that oxocarbenium and acyliminium ions could be formed from oxidative cleavage reactions of homobenzylic ethers² and amides,³ respectively. Cyclization reactions ensued when a nucleophilic group was incorporated into the cationic fragment.

The transformation proceeds through a single-electron oxidation of the arene to form a radical cation intermediate. Radical cations cleave to yield cationic and radical fragments if the resulting products are sufficiently stable.⁴ Our studies showed that the stabilities of the benzyl radical and the oxocarbenium or acyliminium ions were sufficient to promote fragmentation, thereby allowing for these useful reactive intermediates to be formed under nonacidic conditions. These photoinitiated reactions can be conducted with *N*-methylquinolinium hexafluorophosphate (NMQPF₆)⁵ as a catalytic oxidant and O₂ as the terminal oxidant (a stream of air is sufficient),⁶ making this process attractive with respect to reagent accessibility. These transformations were very satisfying from a fundamental science perspective, but we needed to identify applications that would benefit uniquely from this approach to justify further methodological development.

2.2 Mycalamides and Theopederins

One clear benefit of this method is that electrophilic intermediates can be generated under neutral conditions rather than the acidic protocols that are



SCHEME 1 Carbocation formation via oxidative carbon–carbon bond cleavage.

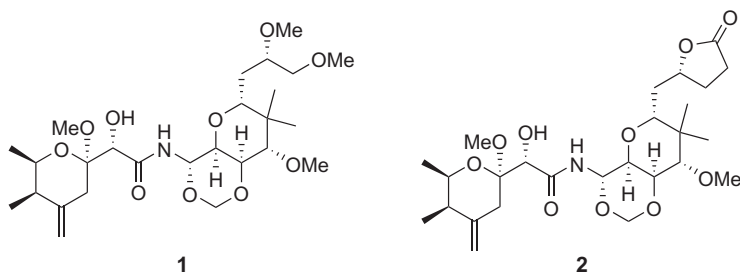


FIGURE 1 Representatives of the mycalamide/theopederin class of natural products.

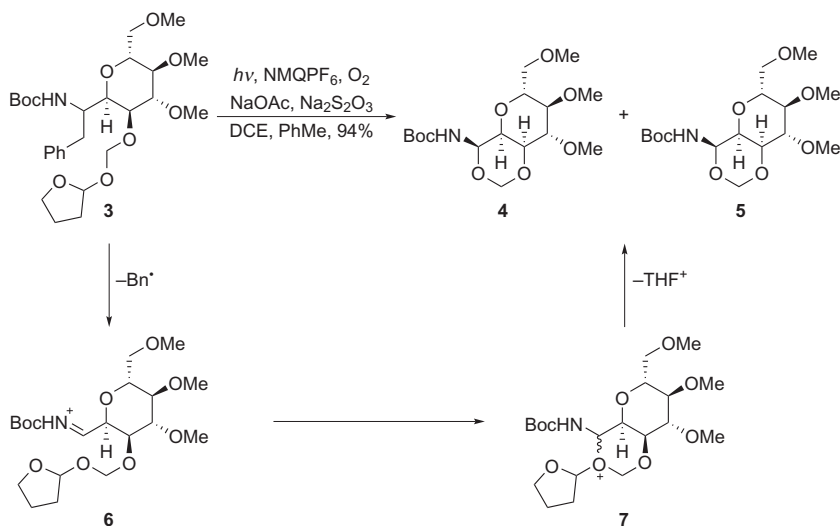
generally utilized to access such species. Thus, acid-sensitive functional groups can be incorporated into reaction substrates, and acid-sensitive products can be prepared without worries of decomposition. Oxidatively initiated epoxide cascade reactions to generate polycyclic ether products proved to be a fruitful area of investigation for these processes.⁷ Another intriguing research direction was provided by the mycalamide/theopederin class of molecules.⁸ These structures are represented in Figure 1 with mycalamide B (**1**) and theopederin D (**2**). These compounds are ideal targets for synthesis. They combine intriguing structures with high potency as cytotoxic and immunosuppressive agents. Several syntheses of these structures had been reported in the literature,⁹ but the challenges associated with constructing these densely functionalized structures led to lengthy routes. We thus felt that we could still make significant contributions in this area.

2.3 Amido Trioxadecalin Synthesis

Our initial research objective was to utilize our oxidative cleavage chemistry to synthesize the amido trioxadecalin subunit. We envisioned that this group could be accessed through the addition of a formaldehyde hemiacetal or a functional surrogate into an oxidatively generated acyliminium ion. Jason Rech successfully achieved this objective (Scheme 2) by oxidizing glucose-derived homobenzylic carbamate **3** under aerobic photochemical oxidation conditions to yield a 10:1 mixture of diastereomeric trioxadecalins **4** and **5** in excellent yield.¹⁰ This reaction proceeds through carbon–carbon bond cleavage to form acyliminium ion **6** followed by the addition of an acetal oxygen to provide oxonium ion **7**. Tetrahydrofuryl cation loss produces the desired product.

2.4 Total Synthesis

This successful trioxadecalin formation justified further efforts to employ the protocol in the synthesis of a natural product. We selected theopederin D (**2**) as the target for this study.¹¹ This required us to devise an efficient sequence for the synthesis of the tetrahydropyran unit of the cyclization precursor.



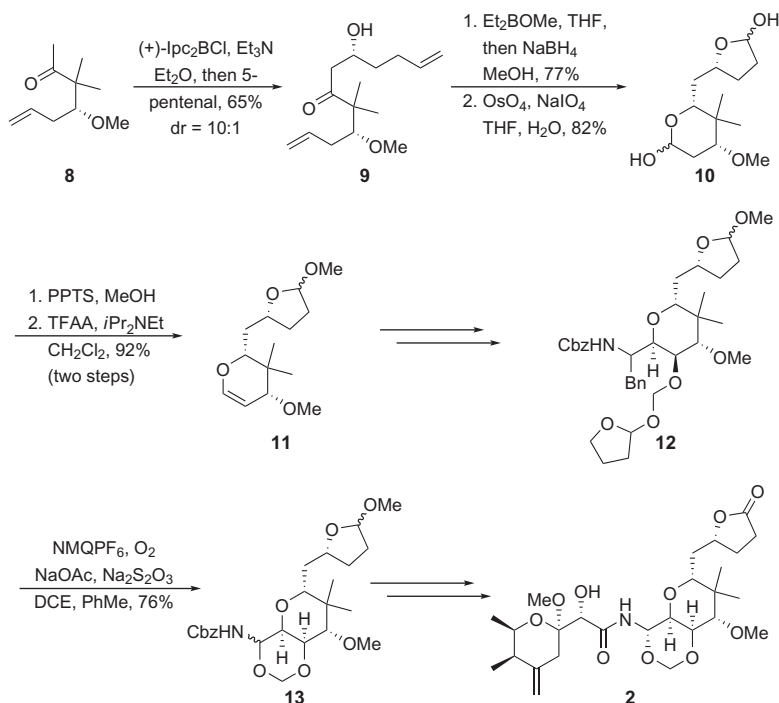
SCHEME 2 Oxidative route to the amido trioxadecalin ring system.

Michael Green and Jason Rech designed a route¹² that utilized a stereoselective aldol reaction followed by a directed ketone reduction and oxidative alkene cleavage to achieve this objective (Scheme 3). Ketone **8** was converted to a boron enolate with (+)-Ipc₂BCl¹³ followed by coupling with 5-pentenal to yield **9**. Reduction by NaBH₄ and Et₂BOMe¹⁴ and alkene cleavage by modified Johnson–Lemieux conditions¹⁵ yielded bis-lactol **10**. Exposing **10** to MeOH and PPTS selectively formed the tetrahydrofuryl ether, leaving the tetrahydropyranyl ether for dehydration with TFAA to form **11**. Green used this route to access homobenzyl carbamate **12**, which successfully underwent oxidative cyclization to form trioxadecalin **13**. The total synthesis of theopederin D was achieved from **13** in three steps.

3 PSYMBERIN

3.1 Structural Connection with Theopederin D

The role of organic synthesis in providing material for biological studies is becoming increasingly important. Unfortunately, the difficulty of synthesizing the amido trioxadecalin core of the mycalamide/theopederin class of natural products hinders efforts to prepare sufficient quantities of the natural product and analogs for biological studies. During the course of our studies on theopederin D, however, Pettit and Crews independently reported¹⁶ the isolation and structure determination of irciniastatin A (**14**), which is also known as psymberin. This structure contains the acyclic *N*-acyl aminal motif that is found in the cytotoxic natural product pederin (**15**).¹⁷ These



SCHEME 3 Total synthesis of theopederin D.

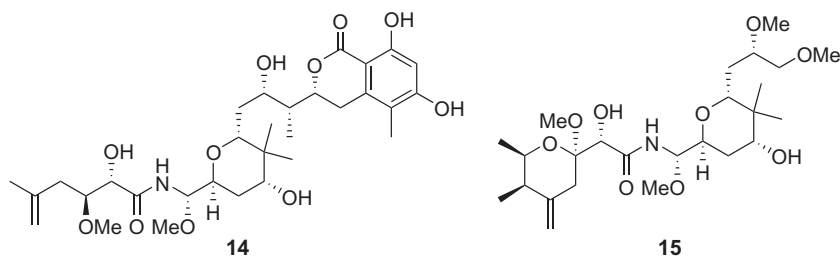


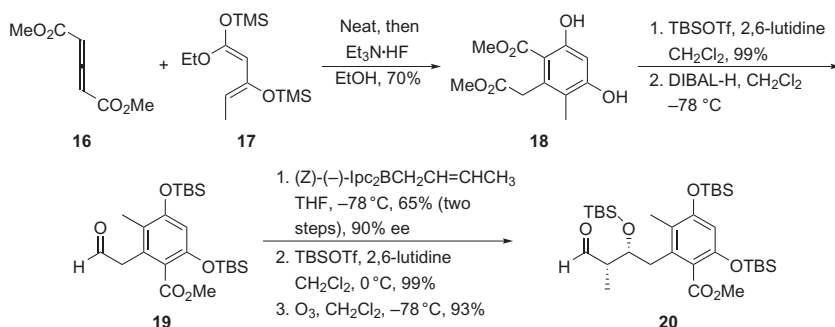
FIGURE 2 Psymberin (irciniastatin A) and pederin.

compounds (Figure 2) contain many structural features that are identical to those found in the mycalamides and theopederins. Psymberin contains a similar central tetrahydropyran unit, but has a simpler acyl fragment and a complex dihydroisocoumarin unit. Psymberin's potent, and reportedly cell line selective, toxicity and our experience in the synthesis of the tetrahydropyran group in theopederin D led us to initiate efforts toward its synthesis. Several other elegant total syntheses of psymberin have been reported.¹⁸

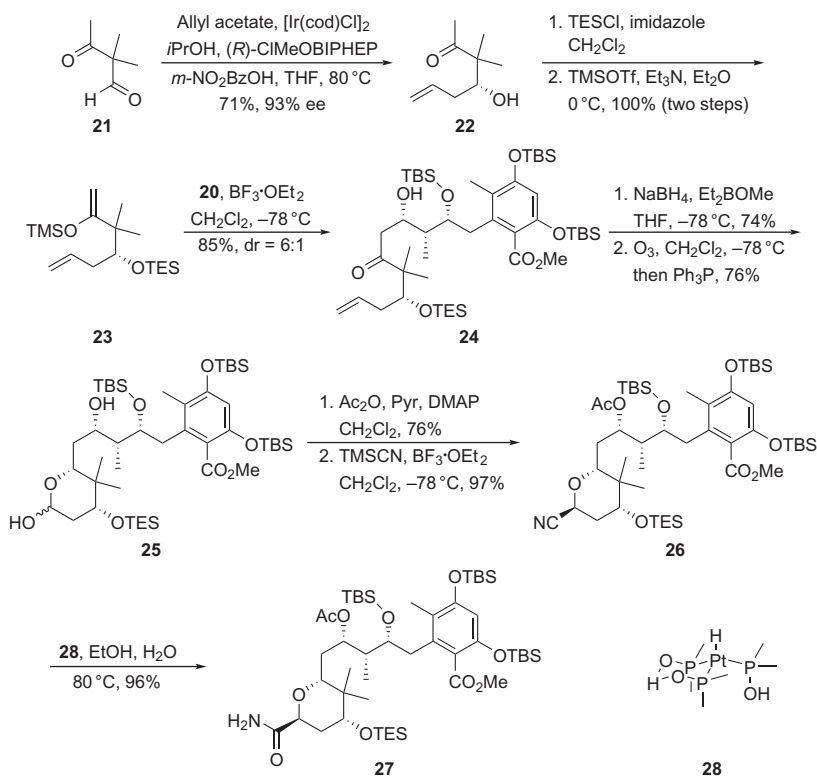
3.2 Initial Studies

Our strategy¹⁹ involved the use of the aldol coupling, directed reduction, and oxidative alkene cleavage sequence that was developed in the theopederin route. The complexity of the dihydroisocoumarin unit, however, presented the unique challenge of constructing a penta-substituted arene. We decided to approach this challenge through a *de novo* arene construction rather than through manipulations of an existing aromatic structure. This was achieved (Scheme 4) through a process from the Langer group²⁰ in which allene **16**²¹ and diene **17**,²² both easily accessed in multigram scale in one step from commercially available materials, undergo a cycloaddition reaction in the absence of solvent. The resulting intermediate was then treated with ethanolic Et₃N·HF to yield arene **18**. Silylation of the phenolic hydroxyl groups and selective reduction of the less hindered ester with DIBAL-H afforded **19**. Selectivity in this reaction presumably arises from the steric shielding that the two *ortho*-substituents confer upon the aromatic ester group. The aldehyde unit was constructed through the three-step sequence of Brown crotylation,²³ hydroxyl group protection, and ozonolytic alkene cleavage. Aldehyde **20** could be prepared in multigram scale through this facile and brief pathway.

The remainder of the right-hand fragment was prepared (Scheme 5) in accord with our efforts in the theopederin D synthesis. Keto-aldehyde **21**, available through the condensation of the enamine of isobutyraldehyde with acetyl chloride,²⁴ was subjected to a Krische allylation²⁵ to provide secondary alcohol **22** in 93% ee. Protection as a triethylsilyl ether and exposure to TMSOTf yielded enolsilane **23**. The enolsilane was selected as the nucleophile for the fragment-coupling aldol reaction based on Evans' studies²⁶ on the influence of various substituents on complex aldol reactions. While the silyloxy group in aldehyde **20** was expected to direct nucleophiles toward the undesired face of the aldehyde, consistent with the extended Felkin model,²⁷ the methyl group adjacent to the aldehyde was expected to direct the nucleophile to the desired face of the aldehyde, in accord with the

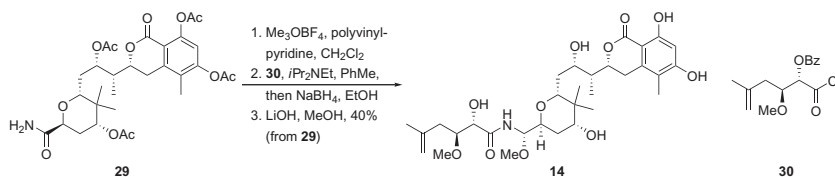


SCHEME 4 Synthesis of the penta-substituted arene subunit of psymberin.



SCHEME 5 Synthesis of the psymberin tetrahydropyran.

Felkin–Anh model.²⁸ The Felkin–Anh model generally dominates the extended Felkin model for bulky enolsilanes under Lewis acidic conditions.²⁶ Consistent with this analysis, combining **20** with **23** in the presence of $\text{BF}_3\cdot\text{OEt}_2$ at low temperature provided aldol product **24** in excellent chemical yield and with an acceptable degree of stereocontrol. Attempts to improve the stereocontrol through Paterson’s protocol¹³ were unsuccessful, leading to extensive decomposition. Directed reduction of the ketone group¹⁴ proceeded with excellent diastereocontrol. Ozonolytic cleavage of the terminal alkene resulted in the formation of lactol **25**. Acylation of the two hydroxyl groups under standard conditions followed by ionization of the anomeric acetoxy group in the presence of TMSCN²⁹ provided nitrile **26** as a single stereoisomer. Our initial plan for the construction of the *N*-acyl aminal unit required the hydration of the cyano group in **26** to form primary amide **27**. Although conditions for this transformation are quite harsh using standard protocols, we were encouraged by a report from Myers³⁰ on the use of the Ghaffar–Parkins catalyst (**28**)³¹ to hydrate a similarly functionalized nitrile. Heating **26** in wet ethanol in the presence of **28** indeed yielded amide **27** in nearly quantitative yield.



SCHEME 6 De Brabander's completion of the psymberin synthesis.

3.3 A Fortuitous Scooping

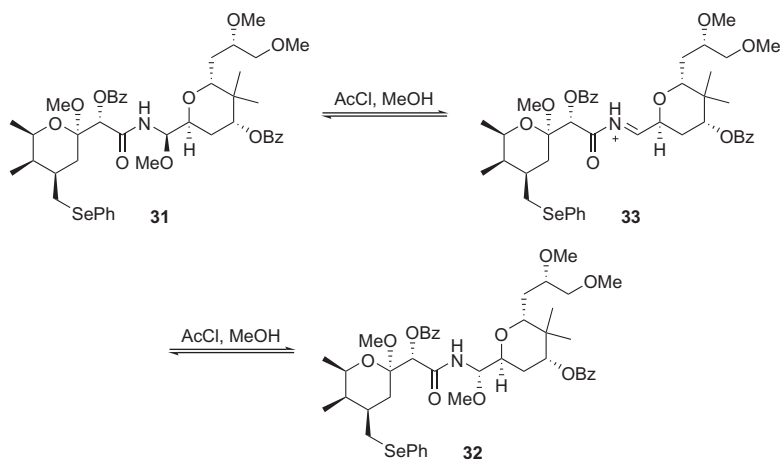
Our initial plan for constructing the *N*-acyl aminal subunit involved using the protocol that Matsuda and co-workers developed for their synthesis of pederin.³² This route proceeds through the conversion of the amide to an imidate with MeOTf followed by acylation with the left-hand acid chloride and reduction. As we commenced this plan, the De Brabander group reported^{18a} the completion of their psymberin synthesis through the identical protocol (**Scheme 6**) in which amide **29** and acid chloride **30** were successfully coupled. While this was a disappointment with respect to completing the synthesis rapidly and uniquely, this report led us to consider alternative approaches to *N*-acyl aminal structures that could prove to be more versatile for analog synthesis.

4 N-ACYLAMINALS FROM NITRILE HYDROZIRCONATION

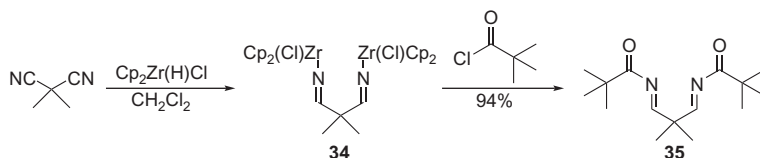
4.1 Inspiration from Natural Product Synthesis

Our inspiration for a revised end game arose from examining the pederin synthesis by the Matsuda group.³² Their application of the imidate acylation and reduction sequence provided a major product (**31**) with the undesired stereochemical orientation at the *N*-acyl aminal site. However, they were able to access the natural stereoisomer (**32**) by treating the major product with acetyl chloride in MeOH (**Scheme 7**). The mechanism of this interconversion was not discussed, but a logical pathway proceeds through methoxy group protonation, ionization to form an acyliminium ion (**33**), readdition of MeOH , and proton loss. Changing the alcoholic solvent allowed other alkoxy groups to be incorporated into the structure, consistent with the proposed mechanism. Thus, we hypothesized that accessing an acylimine linkage between the subunits of psymberin followed by MeOH addition would provide an advanced intermediate in the natural product synthesis. Moreover, this route would provide access to a number of analogs.

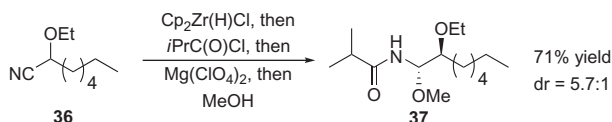
The major obstacle to this pathway was the lack of viable methods to form acylimines from sensitive structures. We postulated that the logical direct coupling between an aldehyde and a primary amide would not be viable in a complex structure. A literature search led us to an intriguing alternative protocol for acylimine formation that was developed by Majoral and co-workers



SCHEME 7 Matsuda's acid-mediated *N*-acyl amination epimerization reaction.



SCHEME 8 Majoral's acylimine formation from nitriles.



SCHEME 9 Acylaminal formation through nitrile hydrozirconation, acylation, and alcohol addition.

(Scheme 8).³³ This report described the hydrozirconation of dimethylmalononitrile³⁴ to form bis-metalloimine **34**. A number of electrophiles can react with **34**, though from our perspective the most compelling reaction was the coupling with pivaloyl chloride to form bis-acylimine **35** in 94% yield. Thus, we envisioned a multicomponent reaction in which a nitrile, an acid chloride, a metal hydride, and an alcohol could combine in a single reaction flask to form an *N*-acyl amination.

4.2 Demonstration of Concept

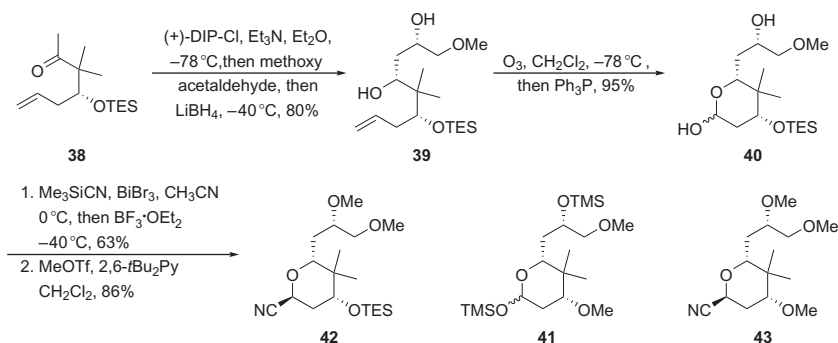
This potentially very useful route to acylaminals was initially tested on simpler substrates, and did prove to be a viable procedure, as shown in Scheme 9.³⁵ Nitrile **36** was selected as the initial substrate because of our ultimate objective of conducting the procedure on a complex α -alkoxy nitrile psymberin

precursor. Hydrozirconation proceeds rapidly at room temperature. Acylation also proceeds rapidly to form the acylimine intermediate. $\text{Mg}(\text{ClO}_4)_2$ was added to promote chelation between the acylimine nitrogen and the ethoxy group. Methanol addition proceeded predominantly through the chelated intermediate to yield acylaminal **37** in 71% yield as a 5.7:1 mixture of diastereomers. An effort led by Shuangyi Wan and Michael Green showed that the nucleophile could be changed to water, sterically bulky alcohols, phenols, and thiols. Various acid chlorides and chloroformates could be utilized, and sulfonamides could be prepared by using sulfonyl chlorides as the electrophile, albeit in somewhat poor yield. Further efforts by Mikkel Debenedetto, Qing Xiao, Chunliang Lu, and Adam Mosey expanded the scope of the method by showing that π -nucleophiles can also add to the acylimine intermediates to form α -branched amides,³⁶ that cyclization reactions could be conducted by appending a nucleophile to the nitrile,³⁷ and that stimulus-responsive drug release conjugates can be readily accessed through this route.³⁸

5 TOTAL SYNTHESIS OF PEDERIN

5.1 Subunit Synthesis

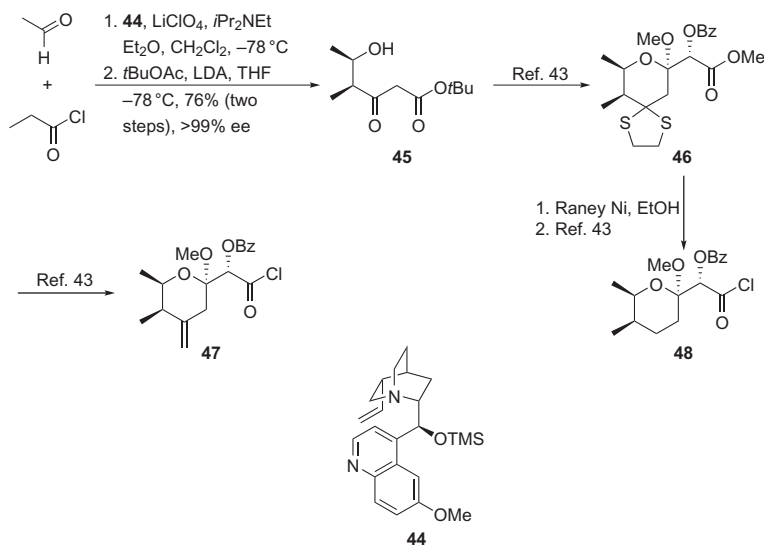
These successful results boosted our confidence in applying the method at a late stage in natural product syntheses. We selected the potent cytotoxin pederin as the initial target because, though it has been synthesized on a number of occasions,^{32,39} only one synthesis required less than 20 steps.^{39c} Fanghui Wu skillfully applied the lessons from our theopederin D synthesis for the construction of the tetrahydropyranyl nitrile substrate for the multicomponent reaction (Scheme 10). A one-pot Paterson aldol reaction between silyloxy ketone **38** and methoxyacetaldehyde was followed by the addition of LiBH_4 ⁴⁰ to provide diol **39** in excellent yield with high stereocontrol. Ozonolytic cleavage of the terminal alkene provided lactol **40**. We chose to exploit the greater propensity for ionization of the anomeric hydroxyl group in



SCHEME 10 Synthesis of the nitrile component for the pederin synthesis.

comparison with the nonanomeric secondary alcohol for the introduction of the cyano group. Drawing upon our observation in the synthesis of leucascandrolide **A**⁴¹ that BiBr_3 is a superb Lewis acid for lactol ionization, Fanghui exposed **40** to TMSCN and BiBr_3 .⁴² While this reaction provided an isolable amount of the desired nitrile, a significant amount of bis-silyl ether **41** was also formed. This compound could be isolated and resubjected to the reaction conditions, but was inert toward BiBr_3 . We reasoned that BiBr_3 , or the HBr that forms when it reacts with water or alcohols, was not sufficiently potent to promote the ionization of the silylated lactol group. Thus, we monitored the reaction until progress appeared to be stalled. At that point $\text{BF}_3 \cdot \text{OEt}_2$ was added to complete the ionization and cyanation. Interestingly, $\text{BF}_3 \cdot \text{OEt}_2$ was not a suitable Lewis acid for the cyanation from **40** as it led to significant decomposition. The resulting nitrile was converted to methyl ether **42** with MeOTf and 2,6-di-*tert*-butylpyridine. Thus, the nitrile precursor for the synthesis of pederin was prepared in eight steps from commercially available precursors. Fanghui also prepared nitrile **43** by using methyl ether **8** as the starting material for the sequence in the interest of preparing analogs for biological evaluation.

The acid chloride precursor for the multicomponent reaction was accessed (Scheme 11) through the method that was developed in the theopederin D synthesis. The sequence largely followed the excellent route that was reported by Nakata.⁴³ Our variation on this route was the incorporation of a catalytic asymmetric β -lactone formation⁴⁴ from acetaldehyde and propionyl chloride in the presence of **44** to yield, after opening with the lithium enolate of *t*-butyl

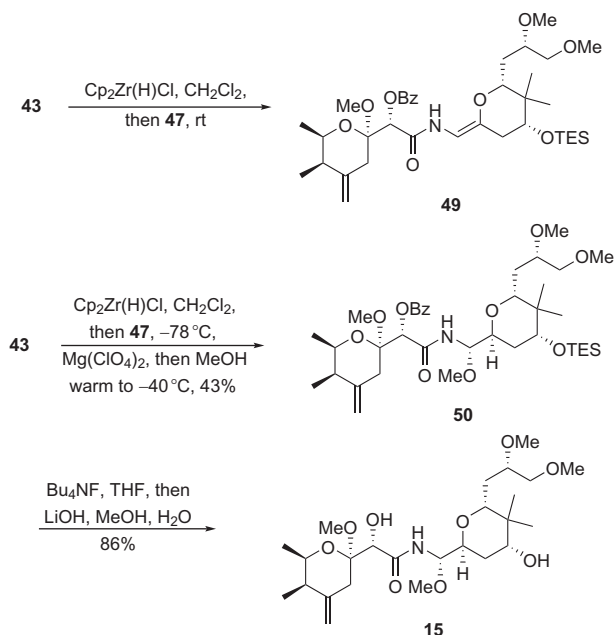


SCHEME 11 Synthesis of the acid chloride subunit of pederin.

acetate, ketoester **45**. This resulted in the first synthesis of this fragment in which the absolute and relative stereochemistry was set through catalytic, rather than stoichiometric, chiral agents. The route proceeded through thioacetal **46**. This allowed for the formation of **47**, the acid chloride for natural product synthesis, through deprotection and methylenation. Additionally, des-methylene analog **48** was prepared through thioacetal desulfurization with Raney nickel.

5.2 Fragment Coupling Through *N*-Acylaminal Formation and Completion of the Synthesis

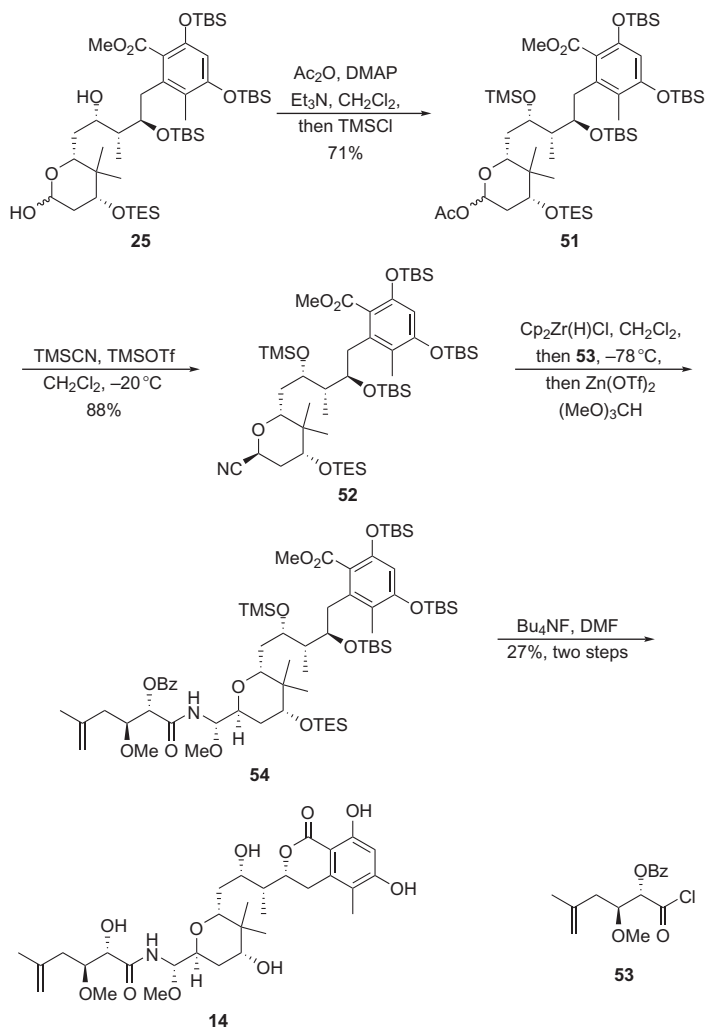
The total synthesis was completed as shown in Scheme 12. Hydrozirconation of **43** followed by acylation with **47**, however, resulted in the formation of enamide **49** via tautomerization of the intermediate acylimine. This problem was not encountered with simpler systems, and it could be prevented by cooling the intermediate metalloimine to $-78\text{ }^{\circ}\text{C}$ prior to acylation. Adding $\text{Mg}(\text{ClO}_4)_2$ then MeOH completed the acylaminal formation, yielding **50** in 43% yield. Pederin was prepared through a one-pot deprotection of the ester and silyl ether groups under conditions that were developed by the Rawal group.^{39c} Thus, pederin (**15**) could be prepared in 10 steps through its longest linear sequence.



SCHEME 12 Total synthesis of pederin.

6 TOTAL SYNTHESIS OF PSYMBERIN

The successful completion of the pederin synthesis gave us the appropriate level of confidence to apply the method to the synthesis of psymberin (Scheme 13).⁴⁵ We were unable to effect a cyanation reaction of diol **25** under the conditions that were effective in the pederin synthesis, forcing us to activate the hydroxyl group prior to ionization. Concerns about the compatibility of an acetate group in the nitrile fragment from our original approach led us to



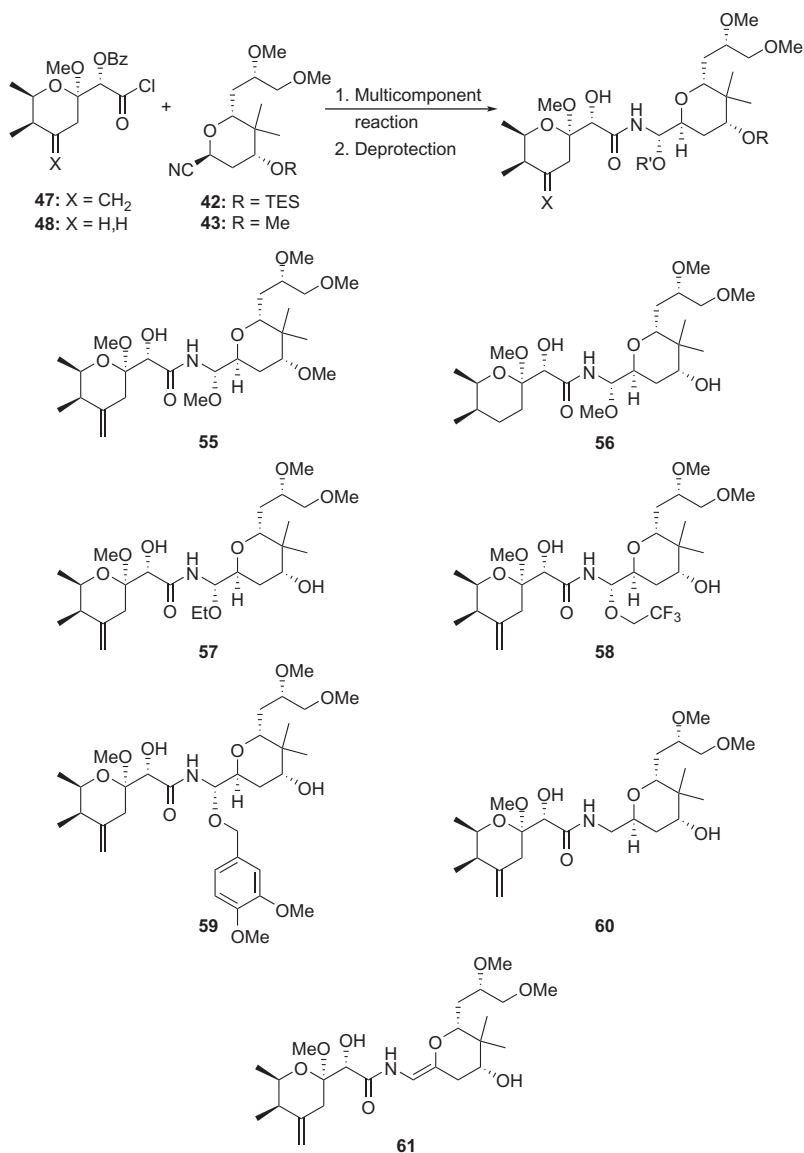
SCHEME 13 Synthesis of psymberin.

modify the protecting group scheme. The hydroxy group in the lactol subunit of **25** proved to be the more reactive group toward acylating agents. Therefore, exposing **25** to standard acylation conditions provided predominantly the monoacetate. Adding the more reactive electrophile TMSCl to the acylation reaction mixture resulted in the formation of **51** in 71% yield for the one-pot procedure. Cyanation was best achieved by using TMSOTf as the Lewis acid in the presence of TMSCN to provide **52**, the nitrile fragment for the multicomponent reaction, in 88% yield. While other approaches have been reported,^{18,46} we chose to prepare the acid chloride fragment for the multicomponent reaction (**53**) according to Pietruszka's protocol,⁴⁷ since that pathway offered the proper protecting group pattern in a minimal number of steps. The multicomponent reaction was less stereoselective than the reaction to form pederin. This result is consistent with the discrepancy in the stereochemical outcomes between Matsuda's acyl amination formation in the pederin synthesis and De Brabander's acyl amination formation in the psymberin synthesis. These reactions show that functional groups that are remote from the acyl amination center can exert a strong influence over its reactivity. A screen of reaction conditions revealed that acceptable product yields could be attained by using (MeO)₃CH as the source of the methoxy nucleophile and Zn(OTf)₂ as the Lewis acid. Zn(OTf)₂ was not the optimal Lewis acid for selectivity, providing only a 1.5:1 ratio of the desired stereoisomer to the undesired stereoisomer, but it led to the cleanest conversion to **54**. The process formed a mixture of products that contained stereoisomers and partially deprotected compounds. Therefore, the material was not purified at this stage. Exposing the reaction mixture to Bu₄NF in DMF led to the cleavage of all silyl ethers, cleavage of the benzoate group, and closure of the dihydroisocoumarin to provide psymberin in 27% yield for the two-step sequence along with 12% of its acyl amination stereoisomer. The longest linear sequence for this route was 14 steps, and this is the shortest reported route to this structure that has yet been reported.

7 ANALOG SYNTHESIS

7.1 Pederin Analogs

Incorporating the multicomponent reaction toward the end of the sequence allows for facile access to analogs with minimal additional effort through changes of the building blocks or the alcohol nucleophile (Scheme 14). Methyl ether analog **55** could be prepared by utilizing nitrile **43** rather than **42**, while des-methylene analog **56** was accessed by employing acid chloride **48** rather than **47**. The alkoxy group was readily varied through the addition of different alcohols to the intermediate acylimine, as seen through the preparation of analogs **57–59**. Amide **60** was formed from the combined minor amounts



SCHEME 14 Synthesis of pederin analogs.

of over-reduced material in the coupling reactions that resulted from excess Cp₂Zr(H)Cl reacting with the acylimine intermediate. Enamide analog **61** was formed during the deprotection reaction that led to trifluoroethoxy analog **58**, with the trifluoromethyl group destabilizing the *N*-acylaminal toward basic conditions.

7.2 Hybrid Analogs

Access to pederin and psymberin fragments allowed us to contemplate the synthesis of pederin–psymberin hybrid structures. The De Brabander group had prepared a hybrid in which the acyl group from psymberin was coupled with the pederin tetrahydropyran.⁴⁸ This structure (**62**), named psympederin, showed dramatically decreased potency in cytotoxicity assays in comparison with pederin or psymberin. This result could suggest that pederin and psymberin have different biological targets, or could indicate that pederin's potency lies in its acyl group and psymberin's potency lies in the dihydroisocoumarin group. Thus, we identified hybrid **63** as our target structure to test the latter hypothesis (Figure 3).

The synthesis of **63** (Scheme 15) followed the pathways that were previously developed, as shown in Scheme 14. Hydrozirconation of **52** followed by acylation with **47**, MeOH addition, and deprotection provided the desired hybrid. A two-step protocol was employed for the deprotection since the benzoate ester of the hybrid was only partially cleaved under the Bu₄NF-mediated conditions. Purification was delayed until the final deprotection step because of the mixtures that resulted from partial deprotection in the earlier steps. Although the yield of this sequence was a modest 22%, a sufficient quantity of material was isolated for cytotoxicity studies. We named **63** “pedestatin” as an homage to Robert Petit, who first reported the isolation of irciniastatin A, because of his frequent use of the “statin” suffix in the cytostatic natural products that his group has isolated and studied.

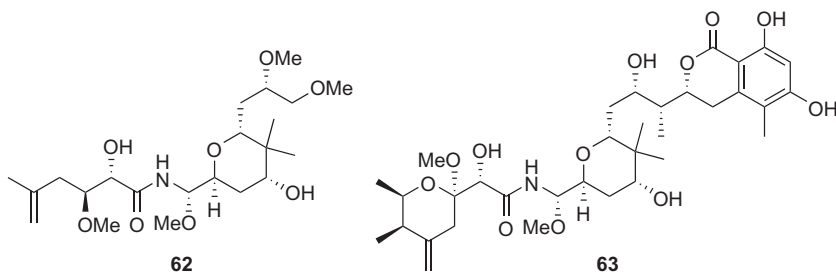
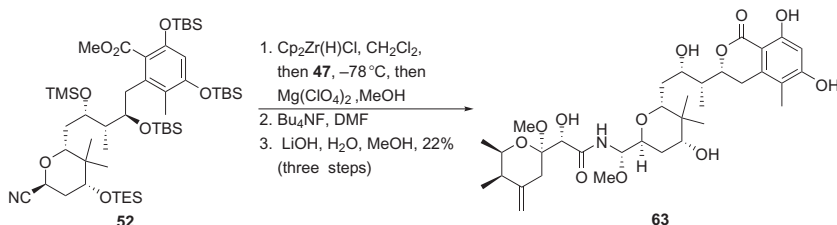


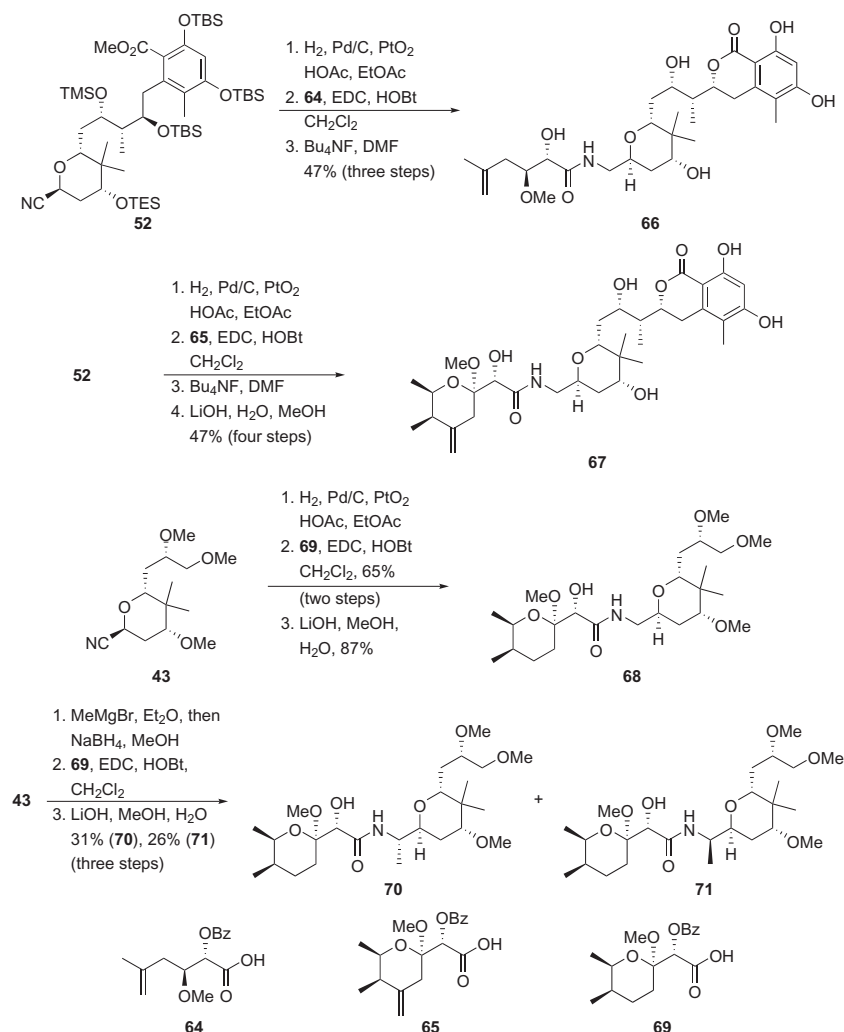
FIGURE 3 Pederin/psymberin hybrid structures.



SCHEME 15 Synthesis of pedestatin.

7.3 Non-*N*-Acylaminal-Containing Analogs

The subunits also allowed us to prepare analogs that provide insight into the role of the *N*-acylaminal in the biological activity of these compounds (Scheme 16). Pederin analog **60** was isolated as a result of over-reduction in the multicomponent coupling, but we sought a method for preparing desmethoxy analogs directly, since the *N*-acylaminal group is likely to be a metabolic liability. Therefore, we employed catalytic hydrogenation conditions to convert nitrile **52** to an amine. Coupling the crude amine with acids **64** and



SCHEME 16 Synthesis of amide variants.

65 in the presence of EDC, followed by deprotection, provided analogs **66** and **67**. Simplified pederin analog **68** was also prepared through this route by reducing **43**, coupling with acid **69**, and deprotecting. We additionally wanted to prepare an analog that contained a branched amide group to mimic the shape, but not the polarity and lability of the *N*-acylaminal group. Thus, we exposed **43** to MeMgBr, reduced the intermediate imine with NaBH₄ and MeOH, and coupled with **69**. Deprotection provided a mixture of branched amides **70** and **71**.

8 BIOLOGICAL STUDIES

The purpose of preparing these analogs was to study their cytotoxicity and develop structure–activity relationships for this family of molecules. This was made possible through a collaboration with Billy Day, a professor in the Department of Pharmaceutical Sciences at the University of Pittsburgh, and his postdoctoral associate Raghavan Balachandran (Balu). The compounds were screened for their capacity to inhibit HCT116 (human colon cancer) cell growth. The results of this study are summarized in Table 1.

TABLE 1 GI₅₀ Values for the Natural Products and Their Analogs^a

Entry	Compound	Description	GI ₅₀ (nM)
1	15	Pederin	0.6 ± 0.1
2	55	13- <i>O</i> -Methyl pederin	0.081 ± 0.01
3	56	4-Desmethylene pederin	6.5 ± 0.8
4	57	10-Ethoxy pederin	0.34 ± 0.1
5	58	10-Trifluoroethoxy pederin	0.55
6	59	10-Dimethoxybenzyloxy pederin	0.32 ± 0.09
7	60	10-Desmethoxy pederin	7.7 ± 0.2
8	61	Pederin enamide	27 ± 0.9
9	14	Psymberin	0.052 ± 0.02
10	63	Pedestatin	0.004 ± 0.003
11	66	8-Desmethoxy psymberin	0.83 ± 0.1
12	67	10-Desmethoxy pedestatin	0.068 ± 0.02
13	68	Simplified pederin analog	79 ± 8
14	70	(<i>S</i>)-Branched amide	42 ± 5
15	71	(<i>R</i>)-Branched amide	>9000

^aCell viability studies were conducted by the MTS dye reduction assay with PMS as an electron acceptor. Quantitation was conducted after a 72-h incubation at 37 °C.

These studies led to several useful conclusions, though these must be viewed with caution since only cytotoxicity and not ribosome-binding assays were conducted. Thus, differences in cellular transport or metabolism could account for potency differences, as has been recently suggested.⁴⁹ The dihydroisocoumarin subunit in psymberin is essential for its biological activity, as is the pederic acid unit in pederin. These structural units can cause an additive effect when placed in the same structure, making pedestatin an impressively potent cytotoxin.

The *N*-acylaminal unit is tolerant of structural change, with basically no change in potency being observed for the significant mutation of a methoxy group to a dimethoxybenzyl group. The presence of an alkoxy group is not essential for activity but does enhance potency, however, as shown by the comparison of the *N*-acylaminals with the des-alkoxy amides. The origin of this effect can at least partially be attributed to conformational rigidification. Minimizing steric interactions between the *N*-acylaminal group and the tetrahydropyran ring leads to a conformation that is essentially identical to the conformation of the bicyclic theopederins and mycalamides. This hypothesis would dictate that the stereochemical orientation at that site would be critically important for potency, and this is demonstrated by the dramatic difference in potency exhibited by diastereomers **70** and **71**. Modeling of the structure of pederin to the ribosome by my colleague Horne based on a crystal structure from the Steitz and Moore groups⁵⁰ showed the potential for a hydrogen bond between the alkoxy group of the *N*-acylaminal and a nucleobase. The relatively modest potency of branched amide **70** in comparison to *N*-acylaminal analogs suggests that hydrogen bonding to the alkoxy group can enhance ribosome binding.

Methyl ether analog **55** showed an increase in potency relative to pederin. Modeling showed no interactions between the tetrahydropyranyl hydroxy (pederin) or methoxy (**55**) groups and the ribosome, suggesting that added potency could arise from increased hydrophobicity. Other analogs in this family appear to support the hypothesis that potency increases as a function of hydrophobicity.⁵¹

The exocyclic alkene in pederin also plays a role in potency. Analog **56**, which lacks this group, is approximately one order of magnitude less potent than the natural product. Modeling studies indicate that this unit intercalates between two nucleobases in the ribosome and orients the acyl fragment for proper binding. Significantly, mouse ear swelling tests showed⁴⁹ that **56** does not cause the inflammatory response that plagues pederin, and the mycalamides, theopederins, and onnamides.⁵² The inflammatory response is also not observed for psymberin. These results suggest that the β,γ -unsaturated acetal group is the source of the undesired blistering properties.

Figure 4 summarizes the structure–activity relationships that have been established in this study.

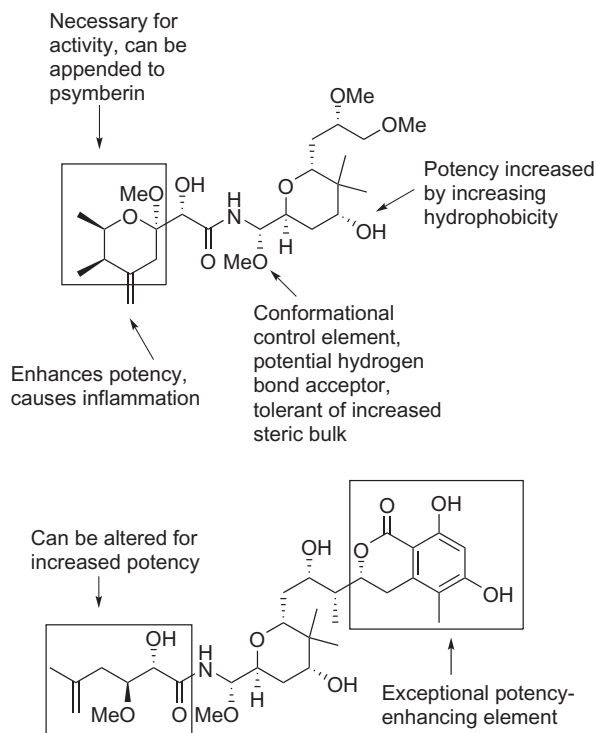


FIGURE 4 Structure–activity relationships for pederin and psymberin.

9 CONCLUSIONS

Natural products remain an unparalleled source of inspiration for organic synthesis because of their structural challenges and capacity to effect biological responses. This work highlights the role that the cytotoxic marine natural product theopederin D played in directing an aspect of my research group's oxidative carbocation formation method to enable amido trioxadecalin ring systems to be accessed under mild conditions. The total synthesis of theopederin D demonstrated that the oxidative carbocation method is compatible with complex molecule synthesis while inspiring the design of an efficient route to prepare the key cyclization substrate. The challenges that were solved during this substrate synthesis led us to adapt the sequence to the synthesis of psymberin. The need for a new approach to *N*-acylaminal formation that leads to facile structural diversification at a late stage in a synthetic sequence inspired us to develop a new amide synthesis that proceeded through nitrile hydrozirconation, acylation, and nucleophilic addition. This protocol proved to be useful for diversity-oriented synthesis, and success in this endeavor provided us with the confidence to apply the method to natural product

synthesis. The ease by which cyano groups can be introduced in complex molecules and the significant complexity increases that arise through the nitrile-based *N*-acylaminal synthesis allowed for the shortest reported syntheses of pederin and psymberin. Moreover, the route led to the synthesis of several analogs that provided a great deal of insight into the structure–activity relationships of this family of molecules and yielded extremely potent nonnatural analogs. The design of new chemical reactions that allow for structural diversification at late stages in chemical syntheses has great potential for minimizing the effort required for establishing structure–activity relationships in complex, biologically active molecules.

ACKNOWLEDGMENTS

This study was the result of the hard work and insightful analysis of several talented scientists with whom I have had the pleasure to interact. The experiments were conducted by Jason Rech, Michael Green, Shuangyi Wan, Mikkel DeBenedetto, Qing Xiao, Fanghui Wu, Chunliang Lu, and Adam Mosey. I am indebted to them for executing and inspiring this most enjoyable project, and to the rest of my research group for their input and support. This project was funded by generous grants from the National Institutes of Health and the National Science Foundation.

REFERENCES

1. (a) Kumar, V. S.; Floreancig, P. E. *J. Am. Chem. Soc.* **2001**, *123*, 3842–3843; (b) Seiders, J. R., II; Wang, L.; Floreancig, P. E. *J. Am. Chem. Soc.* **2003**, *125*, 2406–2407; (c) Wang, L.; Seiders, J. R., II; Floreancig, P. E. *J. Am. Chem. Soc.* **2004**, *126*, 12596–12603; (d) Floreancig, P. E. *Synlett* **2007**, *17*, 191–203.
2. (a) Popielarz, R.; Arnold, D. R. *J. Am. Chem. Soc.* **1990**, *112*, 3068–3082; (b) Freccero, M.; Pratt, A.; Albin, A.; Long, C. *J. Am. Chem. Soc.* **1998**, *120*, 284–297.
3. (a) Aubele, D. L.; Floreancig, P. E. *Org. Lett.* **2002**, *20*, 3443–3446; (b) Aubele, D. L.; Rech, J. C.; Floreancig, P. E. *Adv. Synth. Catal.* **2004**, *346*, 359–366.
4. (a) Schmittel, M.; Burghart, A. *Angew. Chem. Int. Ed. Engl.* **1997**, *36*, 2550–2589; (b) Baciocchi, E.; Bietti, M.; Lanzalunga, O. *Acc. Chem. Res.* **2000**, *33*, 243–251.
5. Dockery, K. P.; Dinnocenzo, J. P.; Farid, S.; Goodman, J. L.; Gould, I. R.; Todd, W. P. *J. Am. Chem. Soc.* **1997**, *119*, 1876–1883.
6. Kumar, V. S.; Aubele, D. L.; Floreancig, P. E. *Org. Lett.* **2001**, *3*, 4123–4125.
7. (a) Kumar, V. S.; Aubele, D. L.; Floreancig, P. E. *Org. Lett.* **2002**, *4*, 2489–2492; (b) Wan, S.; Gunaydan, H.; Houk, K. N.; Floreancig, P. E. *J. Am. Chem. Soc.* **2007**, *129*, 7915–7923; (c) Clausen, D. J.; Wan, S.; Floreancig, P. E. *Angew. Chem. Int. Ed. Engl.* **2011**, *50*, 5178–5181.
8. (a) Bielitz, M.; Pietruszka, J. *Angew. Chem. Int. Ed. Engl.* **2013**, *52*, 10960–10985; (b) Mosey, R. A.; Floreancig, P. E. *Nat. Prod. Rep.* **2012**, *29*, 980–995; (c) Narquizian, R.; Kocienski, P. *The Role of Natural Products in Drug Discovery*. Mulzer, J.; Bohlman, R., Eds.; Ernst Schering Research Foundation Workshop; Vol. 32; Springer: New York, 2000; pp 25–56.

9. (a) Hong, C.; Kishi, Y. *J. Org. Chem.* **1990**, *55*, 4242–4245; (b) Hong, C.; Kishi, Y. *J. Am. Chem. Soc.* **1991**, *111*, 9693–9694; (c) Nakata, T.; Matsukura, H.; Jian, D. L.; Nagashima, H. *Tetrahedron Lett.* **1994**, *35*, 8229–8232; (d) Kocienski, P. J.; Narquizian, R.; Raubo, P.; Smith, C.; Boyle, F. T. *Synlett* **1998**, *9*, 869–871; (e) Kocienski, P. J.; Narquizian, R.; Raubo, P.; Smith, C.; Boyle, F. T. *Synlett* **1998**, *9*, 1432–1434; (f) Roush, W. R.; Pfeifer, L. A. *Org. Lett.* **2000**, *2*, 859–862; (g) Trost, B. M.; Yang, H.; Probst, G. D. *J. Am. Chem. Soc.* **2004**, *126*, 48–49; (h) Sohn, J. H.; Waizumi, N.; Zhong, H. M.; Rawal, V. H. *J. Am. Chem. Soc.* **2005**, *127*, 7290–7291; (i) Kigawa, N.; Ihara, M.; Toyota, M. *Org. Lett.* **2006**, *8*, 875–878; (j) Nishii, Y.; Higa, T.; Takahashi, S.; Nakata, T. *Tetrahedron Lett.* **2009**, *50*, 3597–3601; (k) Jewett, J. C.; Rawal, V. H. *Angew. Chem. Int. Ed. Engl.* **2010**, *49*, 8682–8685.
10. Rech, J. C.; Floreancig, P. E. *Org. Lett.* **2003**, *5*, 1495–1498.
11. Fusetani, N.; Sugawara, T.; Matsunaga, S. *J. Org. Chem.* **1992**, *57*, 3828–3832.
12. Green, M. E.; Rech, J. C.; Floreancig, P. E. *Angew. Chem. Int. Ed. Engl.* **2008**, *47*, 7317–7320.
13. Paterson, I.; Goodman, J. M.; Lister, M. A.; Schumann, R. C.; McClure, C. K.; Norcross, R. D. *Tetrahedron* **1990**, *46*, 4663–4684.
14. Chen, K.-M.; Hardtmann, G. E.; Prasad, K.; Repic, O.; Shapiro, M. J. *Tetrahedron Lett.* **1987**, *28*, 155–158.
15. Yu, W.; Mei, Y.; Kang, Y.; Hua, Z.; Jin, Z. *Org. Lett.* **2004**, *6*, 3217–3219.
16. Pettit, G. R.; Xu, J.-P.; Chapuis, J.-C.; Pettit, R. K.; Tackett, L. P.; Doubek, D. L.; Hooper, J. N. A.; Schmidt, J. M. *J. Med. Chem.* **2004**, *47*, 1149–1152; (b) Cichewicz, R. H.; Valeriote, F. A.; Crews, P. *Org. Lett.* **2004**, *6*, 1951–1954.
17. (a) Cardani, C.; Ghiringelli, D.; Mondelli, R.; Quillico, A. *Tetrahedron Lett.* **1965**, *6*, 2537–2545; (b) Furusaki, A.; Watanabe, T.; Matsumoto, T.; Yanagiya, M. *Tetrahedron Lett.* **1968**, *9*, 6301–6304.
18. (a) Jiang, X.; Garcia-Fortanet, J.; De Brabander, J. K. *J. Am. Chem. Soc.* **2005**, *127*, 11254–11255; (b) Shangguan, N.; Kiren, S.; Williams, L. J. *Org. Lett.* **2007**, *9*, 1093–1096; (c) Huang, X.; Shao, N.; Palani, A.; Aslanian, R.; Buevich, A. *Org. Lett.* **2007**, *9*, 2597; (d) Smith, A. B., III; Jurica, J. A.; Walsh, S. P. *Org. Lett.* **2008**, *10*, 5625–5628; (e) Crimmins, M. T.; Stevens, J. M.; Schaaf, G. M. *Org. Lett.* **2009**, *11*, 3990–3993; (f) Watanabe, T.; Imaizumi, T.; Chinen, T.; Nagumo, Y.; Shibuya, M.; Usui, T.; Kanoh, N.; Iwabuchi, Y. *Org. Lett.* **2010**, *12*, 1040–1043; (g) Byeon, S. R.; Park, H.; Kim, H.; Hong, J. *Org. Lett.* **2011**, *13*, 5816–5819; (h) An, C.; Hoye, A. T.; Smith, A. B., III *Org. Lett.* **2012**, *14*, 4350–4353; (i) Feng, Y.; Jiang, X.; De Brabander, J. K. *J. Am. Chem. Soc.* **2012**, *134*, 17083–17093; (j) Bielitz, M.; Pietruszka, J. *Chem. Eur. J.* **2013**, *19*, 8300–8308.
19. Rech, J. C.; Floreancig, P. E. *Org. Lett.* **2005**, *7*, 5175–5178.
20. Langer, P.; Kracke, B. *Tetrahedron Lett.* **2000**, *41*, 4545–4547.
21. Noda, M.; Fujiwara, T.; Ichihashi, S.; Nishide, K. *Tetrahedron Lett.* **1998**, *39*, 6331–6334.
22. Barker, D.; Brimble, M. A.; Do, P.; Turner, P. *Tetrahedron* **2003**, *59*, 2441–2449.
23. Brown, H. C.; Bhat, K. S. *J. Am. Chem. Soc.* **1986**, *108*, 5919–5923.
24. Inukai, T.; Yoshizawa, R. *J. Org. Chem.* **1967**, *32*, 404–407.
25. Kim, I. S.; Ngai, M.-Y.; Krusche, M. J. *J. Am. Chem. Soc.* **2008**, *130*, 14891–14899.
26. Evans, D. A.; Dart, M. J.; Duffy, J. L.; Yang, M. G. *J. Am. Chem. Soc.* **1996**, *118*, 4322–4343.
27. Evans, D. A.; Duffy, J. L.; Dart, M. J. *Tetrahedron Lett.* **1994**, *35*, 8537–8540.
28. (a) Anh, N. T.; Eisenstein, O. N. *New J. Chem.* **1977**, *1*, 61–70; (b) Lodge, E. P.; Heathcock, C. H. *J. Am. Chem. Soc.* **1987**, *109*, 3353–3361.
29. Hoffmann, R. W.; Schlappbach, A. *Tetrahedron* **1992**, *48*, 1959–1968.

30. Herzon, S. B.; Myers, A. G. *J. Am. Chem. Soc.* **2005**, *127*, 5342–5344.
31. Ghaffar, T.; Parkins, A. W. *J. Mol. Catal. A* **2000**, *160*, 249–261.
32. Matsuda, F.; Tomiyoshi, N.; Yanagiya, M.; Matsumoto, T. *Tetrahedron* **1988**, *44*, 7063–7080.
33. Maraval, A.; Igau, A.; Donnadieu, B.; Majoral, J. P. *Eur. J. Org. Chem.* **2003**, 385–394.
34. (a) Erker, G.; Fromberg, W.; Atwood, J. L.; Hunter, W. E. *Angew. Chem. Int. Ed. Engl.* **1984**, *23*, 68–69; (b) Fromberg, W.; Erker, G. *J. Organomet. Chem.* **1985**, *280*, 343–354; (c) Anbhaikar, N. B.; Herold, M.; Liotta, D. C. *Heterocycles* **2004**, *62*, 217–222.
35. Wan, S.; Green, M. E.; Park, J.-H.; Floreancig, P. E. *Org. Lett.* **2007**, *9*, 5385–5388.
36. DeBenedetto, M. V.; Green, M. E.; Wan, S.; Park, J.-H.; Floreancig, P. E. *Org. Lett.* **2009**, *11*, 835–838.
37. (a) Xiao, Q.; Floreancig, P. E. *Org. Lett.* **2008**, *47*, 1139–1142; (b) Zhang, L.; Xiao, Q.; Ma, C.; Xie, X.-Q.; Floreancig, P. E. *J. Comb. Chem.* **2009**, *11*, 640–644; (c) Lu, C.; Xiao, Q.; Floreancig, P. E. *Org. Lett.* **2010**, *12*, 5112–5115; (d) LaPorte, M. G.; Tsegay, S.; Hong, K. B.; Lu, C.; Fang, C.; Wang, L.; Xie, X.-Q.; Floreancig, P. E. *ACS Comb. Sci.* **2013**, *15*, 344–349.
38. Mosey, R. A.; Floreancig, P. E. *Org. Biomol. Chem.* **2012**, *10*, 7980–7985.
39. (a) Kocienski, P.; Narquizian, R.; Raubo, P.; Smith, C.; Farrugia, L. J.; Muir, K.; Boyle, F. T. *J. Chem. Soc., Perkin Trans. 1* **2000**, 2357–2384; (b) Takemura, T.; Nishii, Y.; Takahashi, S.; Kobayashi, J.; Nakata, T. *Tetrahedron* **2002**, *58*, 6359–6365; (c) Jewett, J. C.; Rawal, V. H. *Angew. Chem. Int. Ed. Engl.* **2007**, *46*, 6502–6504.
40. Paterson, I.; Perkins, M. V. *Tetrahedron Lett.* **1992**, *33*, 801–804.
41. Jung, H. H.; Seiders, J. R., II; Floreancig, P. E. *Angew. Chem. Int. Ed. Engl.* **2007**, *46*, 8464–8467.
42. (a) Komatsu, N.; Uda, M.; Suzuki, H.; Takahashi, T.; Domae, T.; Wada, M. *Tetrahedron Lett.* **1997**, *38*, 7215–7218; (b) Evans, P. A.; Cui, J.; Gharpure, S.; Hinkle, R. J. *J. Am. Chem. Soc.* **2003**, *125*, 11456–11457.
43. Trotter, N. S.; Takahashi, S.; Nakata, T. *Org. Lett.* **1999**, *1*, 957–959.
44. Zhu, C.; Shen, X.; Nelson, S. G. *J. Am. Chem. Soc.* **2004**, *126*, 5352–5353.
45. Wan, S.; Wu, F.; Rech, J. C.; Green, M. E.; Balachandran, R.; Horne, W. S.; Day, B. W.; Floreancig, P. E. *J. Am. Chem. Soc.* **2011**, *133*, 16668–16679.
46. Kiren, S.; Williams, L. J. *Org. Lett.* **2005**, *7*, 2905–2908; (b) Green, M. E.; Rech, J. C.; Floreancig, P. E. *Org. Lett.* **2005**, *7*, 4117–4120; (c) Lachance, H.; Marion, O.; Hall, D. G. *Tetrahedron Lett.* **2008**, *49*, 6061–6064; (d) Brown, L. E.; Landaverry, Y. R.; Davies, J. R.; Milinkevich, K. A.; Ast, S.; Carlson, J. S.; Oliver, A. G.; Konopelski, J. P. *J. Org. Chem.* **2009**, *74*, 5405–5410.
47. Pietruszka, J.; Simon, R. C. *Eur. J. Org. Chem.* **2009**, 3628–3634.
48. Jiang, X.; Williams, N.; De Brabander, J. K. *Org. Lett.* **2007**, *9*, 227–230.
49. Wu, C.-Y.; Feng, Y.; Cardenas, E. R.; Williams, N.; Floreancig, P. E.; De Brabander, J. K.; Roth, M. G. *J. Am. Chem. Soc.* **2012**, *134*, 18998–19003.
50. Gürel, G.; Blaha, G.; Steitz, T. A.; Moore, P. B. *Antimicrob. Agents Chemother.* **2009**, *53*, 5010–5014.
51. (a) Richter, A.; Kocienski, P.; Raubo, P.; Davies, D. E. *Anticancer Drug Des.* **1997**, *12*, 217–227; (b) Huang, X.; Shao, N.; Huryk, R.; Palani, A.; Aslanian, R.; Seidel-Dugan, C. *Org. Lett.* **2009**, *11*, 867–870.
52. Frank, J. H.; Kanamitsu, K. *J. Med. Entomol.* **1987**, *24*, 155–191.

Gliocladin C: The Development and Application of a Pyrroloindoline–Indole Radical Coupling Reaction

Laura Furst¹ and Corey R.J. Stephenson²

Department of Chemistry, University of Michigan, Ann Arbor, Michigan, USA

²Corresponding author: crjsteph@umich.edu

Chapter Outline

1. Introduction	208	Decarbonylation Challenge	213
2. Retrosynthetic Strategies and Model System Studies	210	3.2. Sequence Reorder and Key Step Optimization	215
2.1. Initial Gliocladin C Retrosynthesis	210	3.3. Catalytic Decarbonylation	216
2.2. Photoredox Radical Coupling of Pyrroloindolines and Indoles	211	4. Backbone Oxidation and TKP Formation Studies	218
2.3. Optimization of Model System and Indole Directing-Group Removal Strategies	213	4.1. Acylation/Annulation and Dehydrogenation Attempts	218
3. Synthesis of the C3–C3' Bisindole Skeleton	213	4.2. A Woodward-Inspired Annulation Strategy and Completion of the Synthesis	220
3.1. Forward Synthesis and Unexpected		5. Conclusion	222
		Acknowledgments	223
		References	223

¹Current affiliation: Yale University, New Haven, Connecticut, USA.

1 INTRODUCTION

My career (C. R. J. S.) began in 2007 at Boston University and was focused toward the synthesis of complex natural products with promising biological activities. I recruited postdoctoral fellow Jagan Narayanam as well as first-year graduate student Laura Furst to be part of a team to tackle the synthesis of indole alkaloid natural products such as actinophyllic acid,¹ among others (Figure 1). Our team was particularly intrigued by the indole substitution pattern and we began to investigate methods for regioselective indole functionalizations. This would enable a common synthetic strategy to be implemented for related alkaloids based on direct C—H bond functionalizations rather than multistep preparations of substituted heteroarenes. Radical-based methods provided the highest C2-regioselectivity, but conditions available at the time were not generally applicable or practically favorable. Issues ranged from use of toxic² or pyrophoric reagents,³ superstoichiometric amounts of metals,⁴ or expensive UV reactors.⁵ Chemoselectivity was another concern, since complex natural product synthesis involves the generation of intermediates with a range of sensitive moieties.

Visible light photocatalysis has been a boon to the field of radical chemistry by enabling chemoselective and efficient transformations under mild reaction conditions.⁶ In 2008, the research groups of MacMillan and Yoon demonstrated the use of photoredox catalysis to promote enantioselective alkylation of aldehydes⁷ and [2+2] cycloadditions,⁸ respectively, via generation of alkyl radicals using visible light. These reactions employed low amounts of light-active metal catalyst along with a trialkylamine as a stoichiometric reducing agent. Additionally, they were functional group-tolerant, high-yielding, and chemoselective. Inspired by these reports, we developed a method for C2-selective indole alkylations with diethyl bromomalonate using photoredox catalysis.⁹ The chemoselectivity, regioselectivity, and yields were all excellent; although problems arose with more complex alkyl bromides. Our long-term goals were

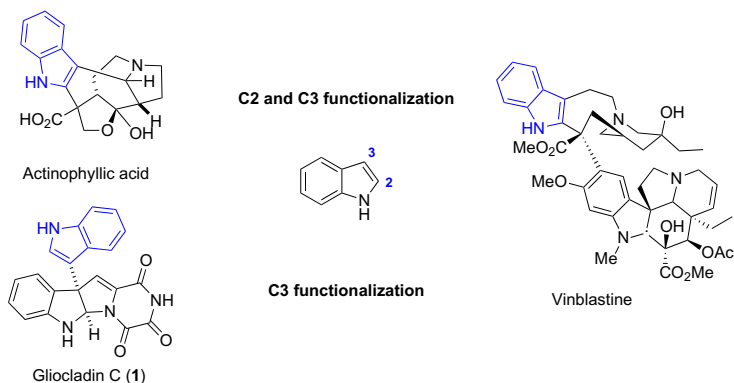
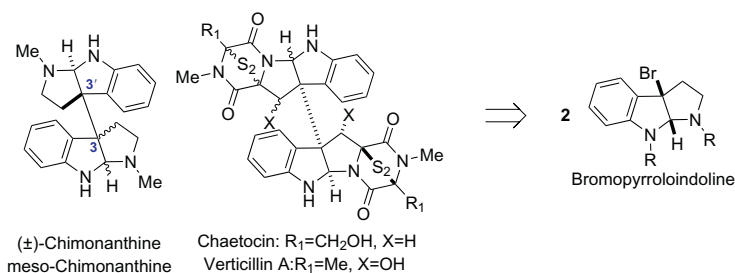


FIGURE 1 Indole alkaloid natural products.

C3—C3' Dimers



C3—C3' Heterodimers

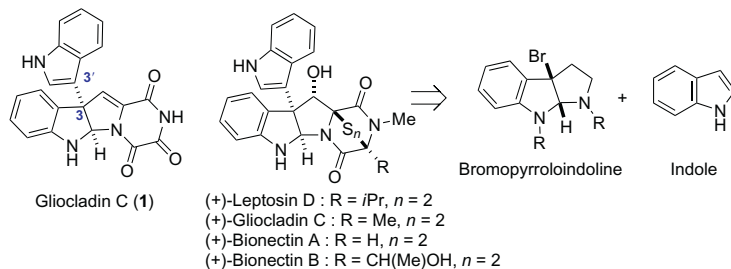


FIGURE 2 C3—C3' bisindole alkaloids from bromopyrroloindolines.

then to develop conditions to improve upon the current state of the art in radical alkylations and to apply them to complex molecule synthesis.

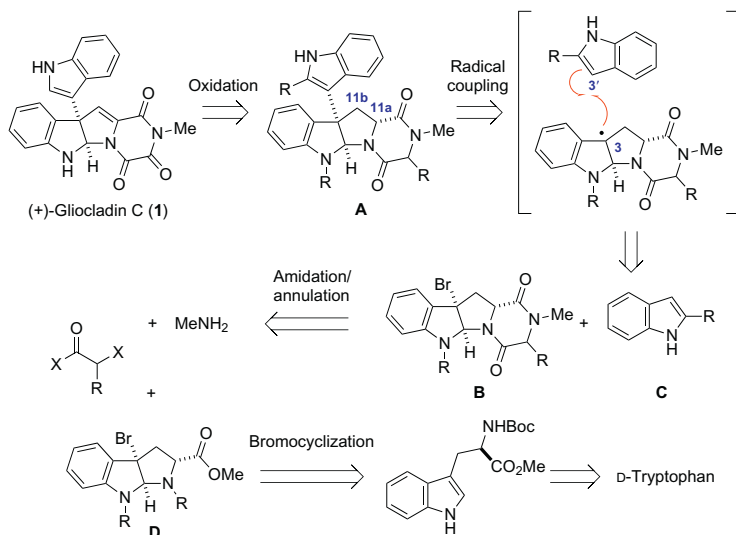
Radical C—C bond formations have long been utilized in total synthesis, including for the preparation of bisindole alkaloids (Figure 2). Bispyrrolo [2,3-b]indolines, or bisindoles, encompass several structural isomers and have a variety of biological activities.¹⁰ A number of C3—C3' dimeric bisindole alkaloids, including (+)-chimonanthine¹¹ and (+)-11,11'-dideoxyverticillin A,¹² were synthesized by Movassaghi and co-workers via a radical dimerization of bromopyrroloindolines **2** using $\text{CoCl}(\text{PPh}_3)_3$. Alternatively, we began to investigate the use of photoredox catalysts for radical dehalogenation of similar bromopyrroloindolines. Dimerization was not observed under those conditions, presumably due to low local concentrations of radicals; however, bromopyrroloindolines and other activated alkyl halides were effectively hydrodehalogenated.¹³ Looking at related natural products, Jagan proposed that C3—C3' heterodimeric bisindole alkaloids (Figure 2) may instead be accessed with this methodology using more suitable radical acceptors such as indoles. Bisindole alkaloids such as the bionectins,¹⁴ leptocin D,¹⁵ and (+)-gliocladin C¹⁶ exhibit a range of antibacterial and cytotoxic activities. Gliocladin C (**1**, Figures 1 and 2), for example, has activity against P388 lymphocytic leukemia cell lines (ED_{50} of $2.4 \mu\text{g mL}^{-1}$).¹⁷ A key synthetic challenge posed by such molecules is the creation of a chiral quaternary center adjacent to the indole. Indeed, at the time of our initial investigations in

2009, there were only a few reports describing the synthesis of these molecules, including a 22-step synthesis of gliocladin C by Overman and co-workers.^{18,19} As an alternative strategy, Jagan focused on using photoredox catalysis to generate pyrroloindoline radicals and trap them with indoles in order to provide direct access to these biologically relevant molecules.

2 RETROSYNTHETIC STRATEGIES AND MODEL SYSTEM STUDIES

2.1 Initial Gliocladin C Retrosynthesis

To investigate the utility of the photoredox-based approach toward the construction of the bisindole C3—C3' linkage, gliocladin C (**1**) was chosen as the initial synthetic target. Unlike related members of its class, **1** contains an unusual triketopiperazine (TKP) unit instead of the more common epidithiodiketopiperazine (see Figure 2). Thus, in our initial retrosynthesis, we identified intermediate **A** as the key structure *en route* to the natural product (Scheme 1). We envisioned a late-stage oxidation at C11a—C11b to subsequently introduce the olefin into the backbone of the molecule. The main bond-forming event, however, was a fragment coupling between a substituted bromopyrroloindoline (**B**) and a substituted indole (**C**) via generation of a pyrroloindoline radical using photoredox catalysis. This step would establish the C3—C3' bisindole skeleton as well as generate a chiral quaternary center. The TKP unit of radical coupling precursor **B** would come from acylation/annulation of bromopyrroloindoline **D** with methylamine and α -acyl electrophile.



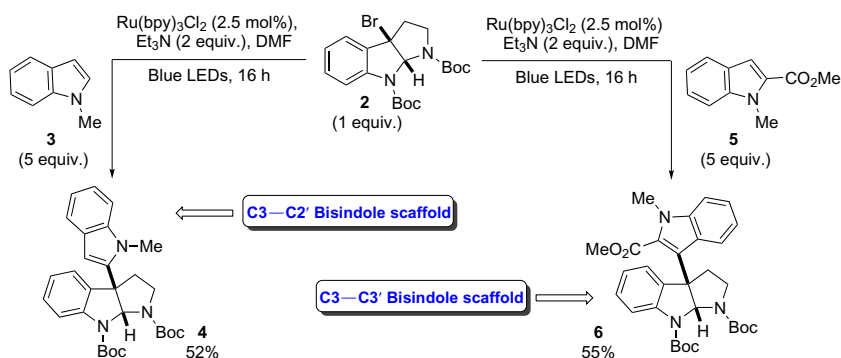
SCHEME 1 First-generation retrosynthesis.

Intermediate **D** would be furnished via bromocyclization of a D-tryptophan derivative that would also set the desired configuration of the 5,5-fused ring system.

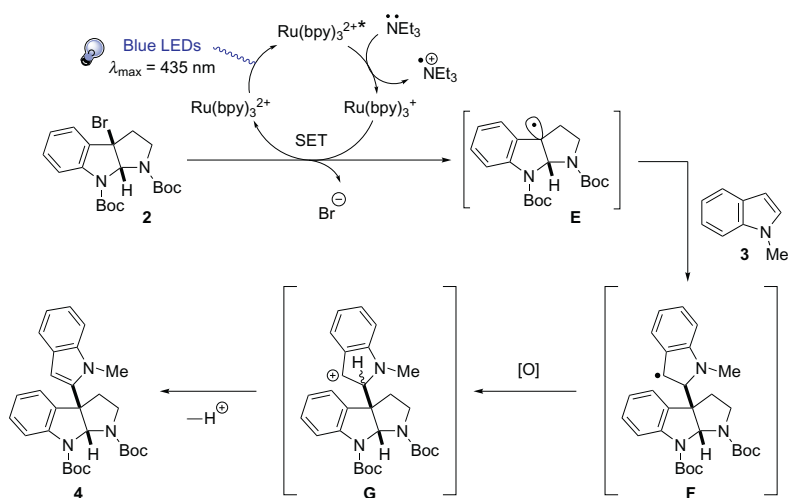
2.2 Photoredox Radical Coupling of Pyrroloindolines and Indoles

Jagan was initially engaged in the development of a photoredox-based methodology for the radical coupling of pyrroloindolines with indoles. To test the feasibility of the proposed coupling strategy, he conducted investigations on model systems based on simple tryptamine-derived bromopyrroloindolines such as **2** using commercially available photocatalyst $\text{Ru}(\text{bpy})_3\text{Cl}_2$.²⁰ He found that reacting bromopyrroloindoline **2** with *N*-methylindole (**3**) in the presence of $\text{Ru}(\text{bpy})_3\text{Cl}_2$ (2.5 mol%), Et_3N (2 equiv.), and blue LEDs in DMF resulted in the formation of C3—C2' bisindole **4** in 52% yield. The observed regioselectivity for this reaction was not surprising, as radical additions onto indoles are known to prefer attack at the C2' position.^{2–5,9} However, the reactivity could be directed at the C3' position by using an indole coupling partner with a blocked C2' position. Jagan discovered that the reaction of **2** with methyl indole-2-carboxylate (**5**) under the same conditions produced the desired C3—C3' bisindole **6** in 55% yield. We were unaware of any reports in the literature of naturally occurring bisindoles that contained the C3—C2' connectivity, but these results demonstrated a rapid and divergent preparation of two distinct bisindole scaffolds using photoredox catalysis (Scheme 2).

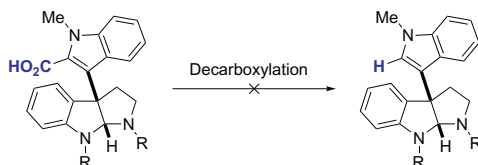
Based on our previous investigations, we believed the reaction was occurring via the reductive quenching cycle of the photocatalyst. A proposed mechanism for radical coupling of **2** with **3** is outlined in Scheme 3. First, excited-state $\text{Ru}(\text{bpy})_3^{2+*}$ is generated upon visible light irradiation of $\text{Ru}(\text{bpy})_3^{2+}$. The excited species oxidizes triethylamine, producing $\text{Ru}(\text{bpy})_3^+$, a powerful



SCHEME 2 Accessing bisindole scaffolds with photoredox catalysis.



SCHEME 3 Proposed mechanism of radical coupling reaction.



SCHEME 4 Attempted decarboxylation of bisindoles.

reducing agent, and the corresponding amine radical cation ($\text{Et}_3\text{N}^{\bullet+}$). The $\text{Ru}(\text{bpy})_3^+$ can reduce **2** via single electron transfer into the activated C—Br bond to generate pyrroloindoline radical **E** and $\text{Ru}(\text{bpy})_3^{2+}$. The carbon-centered radical then attacks the indole π -system (preferentially at C2', followed by C3') to form adduct radical **F**. Oxidation of **F** by $\text{Ru}(\text{bpy})_3^{2+*}$ or $\text{Et}_3\text{N}^{\bullet+}$ forms a stabilized cation **G**, which then undergoes deprotonation to form **4**. Other possible pathways we considered for the oxidation of **F** include radical-chain transfer or atom transfer to form the bromoindoline, followed by elimination.

With the preliminary results in hand, it was crucial that the C2' group on the indole could be readily removed. The C2' carboxylic acid derivatives of coupling products were initially employed toward this endeavor (Scheme 4). There are relatively few decarboxylation methods on indole acids reported in the literature, most of which utilize harsh reaction conditions. Nevertheless, Jagan tested several of the reported methods, including the use of copper chromite in quinoline at 215 °C,²¹ copper(I)oxide in DMA at 200 °C,²² and substoichiometric amounts of indole acid copper salts at 200 °C.²³ Much to his dismay, most of these reactions led to decomposition. Moreover, adjusting temperature or switching to microwave heating failed to provide the desired decarboxylation.

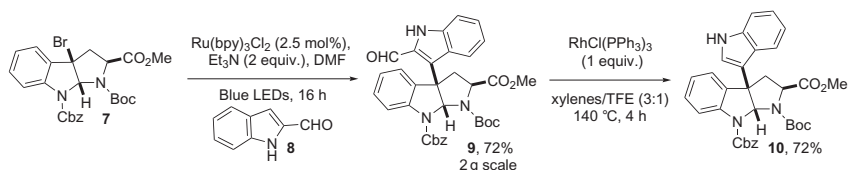
2.3 Optimization of Model System and Indole Directing-Group Removal Strategies

Undeterred, we decided to explore the use of alternative coupling partners. One strategy was to use bulky *N*-protecting groups to sterically block the C2' position and promote addition at C3'. However, under the photoredox conditions, the use of either *N*-trimethylsilyl indole or *N*-triisopropylsilyl indole²⁴ as a coupling partner for **2** resulted in desilylation and a complex mixture of products. It was soon discovered that indole-2-carboxaldehyde (**8**) was an excellent radical acceptor and the reaction of **8** with a variety of bromopyrroloindolines provided consistently higher coupling yields compared with indole carboxylates. Laura joined Jagan and prepared a bromopyrroloindoline model system from L-tryptophan (**7**). To her delight, reaction of **7** with **8** under the photoredox conditions using only 2.5 mol% photocatalyst, the desired C3—C3' bisindole product (**9**) was produced in 72% yield on up to a 2 g scale (Scheme 5). Although these results were encouraging, the removal of indole carboxaldehydes was not well known, especially on highly functionalized molecules. Several reports have utilized Wilkinson's catalyst, RhCl(PPh₃)₃, in stoichiometric amounts to effect the decarbonylation of various aldehydes under mild conditions.²⁵ Adapting these conditions, we subjected model system **9** to 1 equiv. RhCl(PPh₃)₃ in 3:1 xylenes/TFE at 140 °C for 4 h. This strategy was successful and the requisite C2'—H bisindole product (**10**) was obtained in 72% yield.

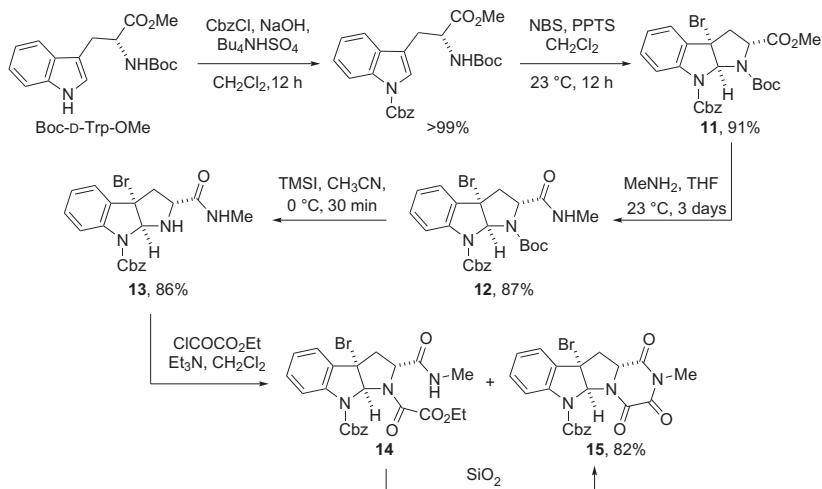
3 SYNTHESIS OF THE C3—C3' BISINDOLE SKELETON

3.1 Forward Synthesis and Unexpected Decarbonylation Challenge

The success of our model system studies demonstrated the utility of the radical coupling reaction for the preparation of C3—C3' heterodimeric bisindole scaffolds. Reasoning that bisindole **10** contained the fundamental structure common to several natural products, we were encouraged to move forward with our original proposal for the synthesis of **1**, with Laura focusing on the forward route. The sequence began with the protection of commercially available Boc-D-tryptophan methyl ester with a Cbz group, followed by bromocyclization²⁶ using NBS and PPTS (Scheme 6). Bromopyrroloindoline **11** was



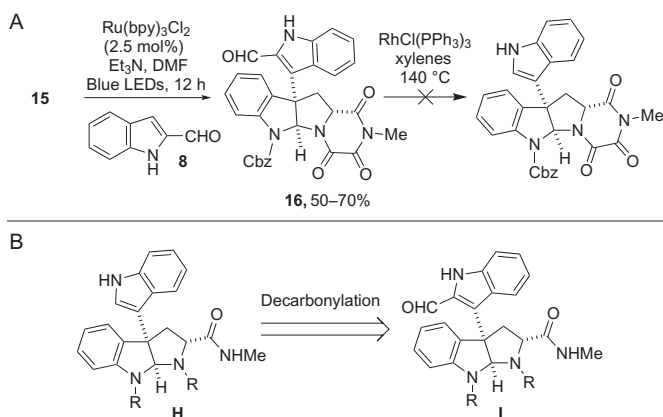
SCHEME 5 Key step optimization on model system **7**.



SCHEME 6 Synthesis of radical coupling precursor **15**.

obtained as a single diastereomer in 91% yield over two steps. In order to append the TKP moiety, the methyl ester was first converted to the methyl amide. The application of typical peptide-coupling reagents resulted in low yields (45%). Nevertheless, direct amidation of **11** with aqueous methylamine in THF at rt over 3 days provided methylamide **12** in 87% yield. Next, selective removal of the Boc *N*-protecting group with TMSI at 0 °C occurred in 86% yield to give 2° amine **13**. A suitable oxalyl electrophile for the generation of the TKP ring was then screened and Laura found that conditions adopted from Overman's first-generation gliocladin C synthesis¹⁸ provided the best results. Accordingly, compound **13** was reacted with ethyl chlorooxalate in the presence of Et₃N in CH₂Cl₂ at 0 °C and then warmed to room temperature, which resulted in a mixture of products that we posited to be noncyclized compound **14** as well as TKP product **15**. Surprisingly, subjection of the crude reaction mixture to flash chromatography on silica gel, converted the mixture to **15**, with an isolated yield of 82%. Also of note, neither stirring crude **14** in the presence of SiO₂ nor treatment with dilute acid (AcOH, HCl) effected the conversion as efficiently as flash chromatography.

After the serendipitous discovery of chromatography-assisted preparation of radical coupling partner **15**, the stage was set for our key bond-forming reaction. Bromopyrroloindoline **15** was then subjected to the radical fragment coupling reaction with indole-2-carboxaldehyde (**8**) using our preoptimized photoredox conditions (Scheme 7A). The supposed product of the reaction, bisindole **16**, was produced in moderate yields; however, this intermediate was unreactive toward decarbonylation conditions using RhCl(PPh₃)₃. We proposed that the presence of too many Lewis bases on the molecule, particularly on the TKP ring, was shutting down the desired reactivity by sequestering the rhodium.

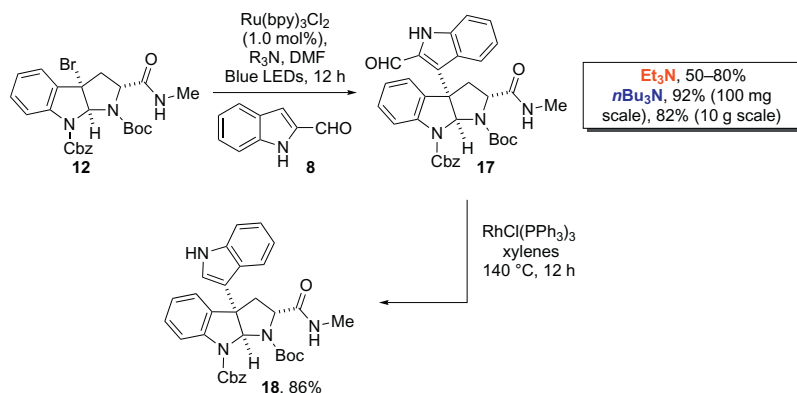


SCHEME 7 (A) Unsuccessful decarbonylation; (B) modified retrosynthesis.

Directing group removal was an obstacle we tackled during our model system studies and the recurrence of this complication seemingly set our progress back to square one. While Jagan and Laura briefly explored other deformylation strategies on compound **16**, an expedient alternative was to reorder steps such that fragment coupling preceded TKP formation (Scheme 7B). In this case, an intermediate such as **I** would be subjected to the decarbonylation conditions to form **H**, which would later undergo a similar acylation/cyclization sequence used to arrive at compound **15**.

3.2 Sequence Reorder and Key Step Optimization

We anticipated that bisindole **17**—generated from the coupling of bromopyrroloindoline **12** with indole **8**—would successfully undergo decarbonylation based on the efficacy of C2' aldehyde removal on model system **9**. When compounds **12** and **8** were subjected to the photoredox coupling reaction, the desired product **17** was produced in yields ranging from 50% to 80% (Scheme 8). Careful observations by Laura led to an interesting discovery. It appeared that if the reaction apparatus had a large volume of headspace, conversion was lower than if the reaction mixture had occupied a larger volume within the vessel. Meanwhile, this effect was minimized if argon pressure was increased. This initially confusing phenomenon was eventually attributed to equilibration of Et_3N above the reaction solution, resulting in poor catalytic turnover. By replacing Et_3N (vapor pressure = 51.8 mmHg, 20°C) with higher-boiling $n\text{-Bu}_3\text{N}$ (0.3 mmHg, 20°C) as the electron donor, inconsistencies in conversion and yield were avoided, and compound **17** was obtained in 92% yield on a 1 mmol scale. Moreover, a catalyst loading of just 1 mol% $\text{Ru}(\text{bpy})_3\text{Cl}_2$ was employed and the reaction could be effectively scaled up (3.8 mmol scale, 82% yield). Crucially, the decarbonylation of **17** with $\text{RhCl}(\text{PPh}_3)_3$ in xylenes at 140°C was successful, providing the desired bisindole **18** in 86% yield.



SCHEME 8 Improved sequence to bisindole core structure.

3.3 Catalytic Decarbonylation

Following the successful preparation of the bisindole core of gliocladin C, Laura then sought to optimize the existing sequence. In particular, the stoichiometric use of expensive $\text{RhCl}(\text{PPh}_3)_3$ for directing group removal hindered the overall efficiency and scalability up to this point. Although $\text{RhCl}(\text{PPh}_3)_3$ has commonly been employed for deformylation reactions, there had only been a few literature precedents describing catalytic variants, especially on indolyl substrates. In one such report, Tsuji and co-workers utilized 5 mol% $[\text{Ir}(\text{cod})_2\text{Cl}]\text{PPh}_3$ for their reactions and substrates were limited to aryl, vinyl, and benzylic aldehydes.²⁷ Unfortunately, under the same set of conditions, substrate **9** was unreactive (Table 1, entry 1). Other conditions were utilized based on reports by Li²⁸ (entry 2) and Dong²⁹ (entry 3), in which a decarbonylation step was achieved *en route* to a C—C bond-forming event. However, these methods similarly failed to produce desired results for substrates **17** and **9**. Efforts were then refocused toward turning over the $\text{RhCl}(\text{CO})(\text{PPh}_3)_2$ being formed as a stoichiometric byproduct from reactions with $\text{RhCl}(\text{PPh}_3)_3$.

Meyer and Kruse were able to convert $\text{Rh}(\text{CO})\text{Cl}(\text{PPh}_3)_3$ to the cationic complex $\text{Rh}(\text{dppp})_2\text{Cl}$, upon the addition of 1,3-bis-(diphenylphosphino)propane (dppp).³⁰ This species was successfully utilized in as little as 0.5 mol% for decarbonylation reactions of simple indolyl aldehydes in xylenes at 140 °C. Direct adaptation of these conditions for the deformylation of intermediate **17** was ineffective; however, slight modifications led to promising results. Upon screening various combinations of catalyst loadings (5–50 mol%), solvent systems (xylenes/TFE), and rates of substrate addition, the desired product **18** was finally attained in 65% yield via slow addition of substrate **17** into a

TABLE 1 Catalytic decarbonylation optimization

Entry	R	Catalyst	Ligand/ additives	Conditions	Result
1	OMe	[Ir(cod) ₂ Cl]PPh ₃ (5 mol%)	–	Dioxane, 100 °C	NR
2	OMe	(CO) ₂ Rh(acac) (20 mol%)	TBP (2.5 equiv.)	PhCl, 140 °C	NR
3	NHMe	[Rh(nbd) ₂]BF ₄ (20 mol%)	(<i>R</i>)- Ph-MeOBIPHEP	DCE, 120 °C	20
4	NHMe	Rh(CO)Cl(PPh ₃) ₂ (50 mol%)	dppp (1 equiv.)	Xylenes/TFE 140 °C, slow addition	65% ^a 18
5	NHMe	RhCl(PPh ₃) ₃ (20 mol%)	DPPA (2 equiv.)	Xylenes, 140 °C Slow addition	60% ^a 18
6	NHMe	Rh(CO)Cl(PPh ₃) ₂ (20 mol%)	dppp (44 mol%) DPPA (2 equiv.)	Xylenes, 140 °C Slow addition	85% ^a 18
7	NHMe	Rh(CO)Cl(PPh ₃) ₂ (10 mol%)	dppp (44 mol%) DPPA (2 equiv.)	Xylenes, 140 °C Slow addition	30% ^b 18
8	NHMe	Rh(dppp) ₂ Cl (20 mol%)	DPPA (2 equiv.)	Xylenes, 140 °C Slow addition	40% ^b 18

NR, no reaction.

^aIsolated yield upon purification on SiO₂.^bConversion.

mixture containing 50 mol% precatalyst Rh(CO)Cl(PPh₃)₃ and 1 equiv. dppp in xylenes at 140 °C (Table 1, entry 4).

O'Connor and Ma developed an alternative method for regenerating RhCl(PPh₃)₃ from Rh(CO)Cl(PPh₃)₃ using diphenylphosphoryl azide (DPPA)³¹ to promote the extrusion of CO from the rhodium center.³² The authors reported using only 5 mol% RhCl(PPh₃)₃ at room temperature in THF to effect decarbonylations of primary alkyl aldehydes upon slow addition of DPPA (1 equiv.). We adapted this procedure for the deformylation of substrate **17** by tuning reagent stoichiometry, catalyst loading, solvent, and

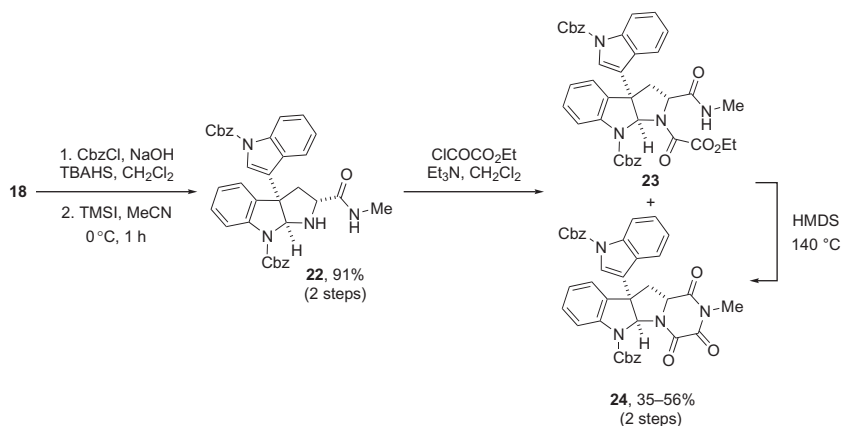
temperature. A 60% yield of **18** was obtained using 20 mol% $\text{RhCl}(\text{PPh}_3)_3$ in xylenes at 140 °C and slow addition of DPPA (Table 1, entry 5).

Laura found that a combination of Kruse's and O'Connor's methods led to an improvement in results. Accordingly, bisindole **17** was slowly added to a solution of $\text{Rh}(\text{CO})\text{Cl}(\text{PPh}_3)_3$ (20 mol%) and dppp (40 mol%) in xylenes at 140 °C, followed by slow addition of DPPA (2 equiv.). Compound **18** was generated in 85% yield (Table 1, entry 6), which is comparable to the results using 1 equiv. of $\text{RhCl}(\text{PPh}_3)_3$. Unfortunately, lowering the catalyst loading to 10 mol% or using preformed $\text{Rh}(\text{dppp})_2\text{Cl}$ (20 mol%) both led to lower conversions (entries 7 and 8, respectively). However, we were satisfied with an 80% reduction in the amount of catalyst previously required for the decarbonylation step, which enabled a more practical synthesis of intermediate **18**.

4 BACKBONE OXIDATION AND TKP FORMATION STUDIES

4.1 Acylation/Annulation and Dehydrogenation Attempts

The remaining challenges to complete the synthesis of **1** were: (1) the introduction of the TKP moiety and (2) oxidation of the pyrroloindoline backbone. We continued the sequence with protection of the indole nitrogen of compound **18** with a Cbz group, followed by selective removal of the Boc protecting group to access amine **22** (Scheme 9). Installation of the TKP unit was initially attempted using the same conditions applied for the generation of **15** (see Scheme 6). When amine **22** was treated with ethyl chlorooxalate and Et_3N in dichloromethane, a mixture of two products resulted: noncyclized oxoamino acetate **23** and the desired TKP **24** (~2.8:1). Unfortunately, flash chromatography of the mixture on silica gel did not promote intramolecular amidation as it previously had for the conversion of intermediate **14** to **15**. Instead, we adopted the protocol used in Overman's first-generation synthesis

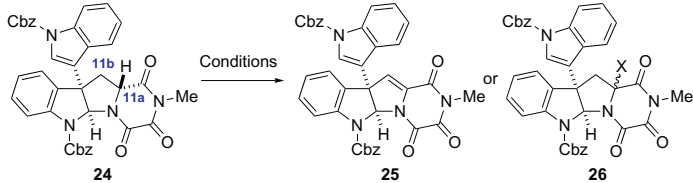


SCHEME 9 Synthesis of TKP unit.

of gliocladin C, which accomplished a similar annulation reaction, by heating the oxoamino acetate in neat HMDS at 140 °C. This method was also successful on our substrate, but provided low yields of the desired TKP **24** (35–56% over two steps).

We continued to make progress toward the completion of **1** despite the disadvantageous protocol developed for TKP formation. Our initial strategy for the oxidation of intermediate **24** involved deprotonation of the C11a methine, trapping the resulting enolate with an electrophile, followed by elimination at C11a–C11b. A complex mixture resulted when compound **24** was treated with LiHMDS at low temperature, followed by the sequential additions of NBS and DBU and no traces of desired product **25** or **26** (X=Br) were detected in the mix (Table 2, entry 1). It appeared that nucleophilic attack was a possible competing pathway, leading to decomposition. Use of less bulky LiNEt₂ as the base also did not improve results (entry 2). Further adjustments in bases, electrophiles, or temperature likewise produced a mess of compounds. We presumed that steric factors were responsible for the difficulties in the deprotonation of the C11a methine, as the molecule adopts a “bowl” shape and the targeted proton is oriented inside the concave face (Figure 3). Thus, access to the hydrogen is potentially limited by the presence of the arene or TKP ring blocking the approach of reagents. This may allow for competing decomposition pathways. Such nuisances associated with enolization methods on related diketopiperazine alkaloids were also revealed in studies by Movassaghi and co-workers.¹² In their report, they were finally

TABLE 2 C11a–C11b oxidation conditions



Entry	Conditions	Result
1	LiHMDS, THF, –78 °C, NBS, then DBU	Complex mixture
2	LiNEt ₂ , THF, –78 °C, then NBS	Complex mixture
3	Py ₂ AgMnO ₄ , CH ₂ Cl ₂	NR
4	DDQ, MeOH/CHCl ₃	NR
5	IBX, DMSO	NR
6	Pd/C, toluene, reflux, 2 days	25 , 20%

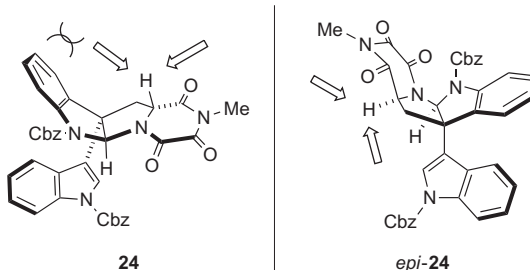


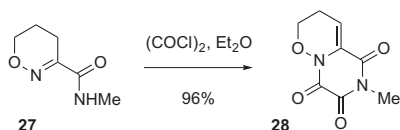
FIGURE 3 3D representation of intermediate **24**.

able to achieve radical hydroxylation using $\text{Py}_2\text{AgMnO}_4$ or Bu_4NMnO_4 via hydrogen-atom abstraction. The authors showed selective cleavage of C—H bonds situated on the *convex* face of their model systems (see *epi-24* for comparison) and observed a lack of reactivity for their epimers. Nevertheless, we attempted oxidation of **24** with $\text{Py}_2\text{AgMnO}_4$ in an effort to isolate compound **26** ($\text{X}=\text{OH}$). Unfortunately, and in accordance with Movassaghi's studies, substrate **24** remained unreactive (entry 3). Finally, a variety of dehydrogenation conditions using reagents, such as DDQ, IBX, and Pd/C, were separately screened (entries 4–6). Encouragingly, treatment of **24** with 0.5 equiv. of Pd/C in refluxing toluene furnished the desired alkene **25** in 20% yield after 2 days (entry 6). Attempts at optimizing these conditions further did not meet with success.

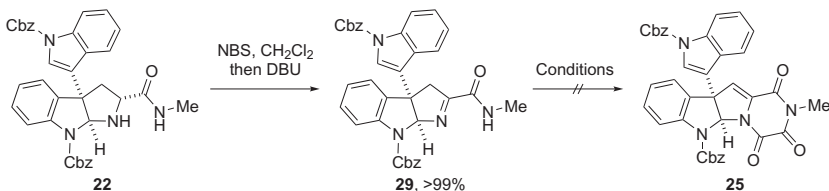
4.2 A Woodward-Inspired Annulation Strategy and Completion of the Synthesis

As we neared the completion of the synthesis, we paused to reflect on our approach to the final sequence. With an elegant solution to the C3—C3' bisindole core of gliocladin C, the preparation of the TKP and subsequent oxidation of the pyrroloindoline seemed shoddy in comparison. The conversion of amine **22** to gliocladin C precursor **25** was accomplished in low yields over three steps, two of which were required to append the TKP and the last of which relied on brute force to accomplish the oxidation. Hence, we considered reversing the steps. Jagan speculated that oxidation of the amine prior to annulation might overcome problems, particularly regarding the lability of the methine CH bond on the TKP. He then recalled a relevant transformation by Ling and Woodward³³ in which cyclic amino acid derivative **27** underwent oxime acylation with oxalyl chloride, followed by annulation to form bicyclic imide **28** (Scheme 10).

We adopted a similar annulation strategy for the synthesis of **1**. Amine **22** was converted to the corresponding imine **29** by treatment with NBS in



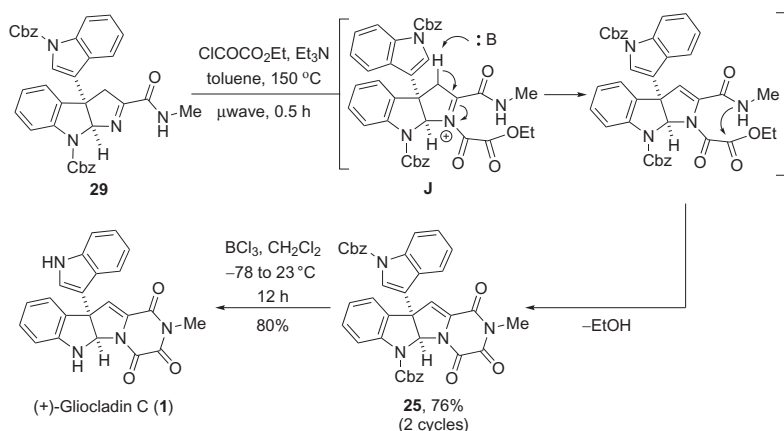
SCHEME 10 Ling and Woodward's acylation/annulation reaction of a cyclic oxime.



SCHEME 11 Oxidation of amine **22** and attempted TKP formation.

CH_2Cl_2 , followed by the addition of DBU (Scheme 11). A quantitative yield was obtained for **29** at room temperature, which is in contrast to the demanding oxidation of the TKP methine. Unfortunately, the addition of oxalyl chloride to **29** in the presence of Et_3N at room temperature did not result in any observed reactivity. The use of different oxalyl electrophiles, amine bases, and elevated temperatures likewise failed to give any desired product. We were concerned that intramolecular hydrogen bonding between the amide $\text{N}-\text{H}$ and the imine was affecting nucleophilicity, and we attempted to disrupt this potential interaction through deprotonation of the amide with strong bases such as LiHMDS . However, this approach only led to decomposition.

We next considered microwave heating as an alternative to thermal conditions to promote the desired transformation. Considerable rate improvements have been observed under microwave-promoted conditions,³⁴ and it seemed that rapid heating might help to overcome any stabilizing interactions in imine **29**. Accordingly, Laura subjected **29** to ethyl chlorooxalate and Et_3N in toluene at 150°C for 30 min and successfully produced the desired compound **25** in 76% yield after one recycle of unreacted starting material (Scheme 12). A likely mechanism involves acylation of the imine to form *N*-acyliminium ion **J**, followed by deprotonation and cyclization. This was a key accomplishment for our team, as this single transformation established both the TKP ring system as well as the C11a–C11b olefin. By opting to oxidize the pyrrolidine ring first, we were able to combine the acylation and annulation steps and shorten the overall sequence from **22** to **25** while simultaneously increasing yield. The only step that remained was deprotection of the Cbz carbamates. Treatment of **25** with excess BCl_3 in CH_2Cl_2 at -78°C led to complete consumption of starting material; however, no product was initially isolated upon aqueous work-up. It was quickly discovered that the reaction mixture required prolonged stirring between saturated aqueous NaHCO_3 and CHCl_3 in order to decomplex boron salts and extract the desired product. After optimizing the



SCHEME 12 Microwave-assisted acylation/annulation of **29** and completion of the synthesis.

procedure, gliocladin C (**1**) was obtained in 80% yield. We were able to confirm our assignment through comparison of 1D and 2D NMR, mass spectrometry, as well as $[\alpha]_D$ data to that previously reported.^{17–19}

5 CONCLUSION

This research began with the simple goal of applying a new method—a radical fragment coupling reaction—to a natural product synthesis in order to showcase its ability to work on complex substrates. In the end, the strategy we were “testing” actually expedited the sequence to gliocladin C (**1**) by laying down the structural foundation of the molecule in a concise manner (four steps). Ultimately, the complete route to the natural product required only 10 total steps from commercially available Boc-D-tryptophan methyl ester with a high overall yield of 33%. Our strategy was inspired by previous successes with photoredox catalysis and radical chemistry by our group and others. Moreover, the key reaction demonstrated a mild and selective means for the generation and subsequent transformation of alkyl radicals promoted by visible light using a readily available photocatalyst. Other highlights include the development of a substoichiometric metal-catalyzed decarbonylation reaction for directing group removal as well as the use of microwave-promoted conditions to effect a one-pot acylation/annulation reaction for the synthesis of the TKP moiety.

The most challenging C—C bond-forming event initially anticipated was the connection of the indole sp^2 carbon to a fully substituted chiral sp^3 carbon, namely the C3—C3' bisindole connection (Figure 2). This transformation was encumbered by relatively few complications, aside from the headspace equilibration of the reductive quencher (Scheme 8). Rather, the stumbling blocks that slowed progress were TKP formation and decarbonylation. The solution

to those problems could be resolved through resequencing of functional group transformations: the metal-catalyzed decarbonylation reaction had to be done in the absence of the oxamoyl moiety (Schemes 7 and 8) and the TKP ring was more conveniently introduced *after* backbone oxidation (Schemes 11 and 12), which was also more easily accomplished on amine **22** rather than on TKP **24**. It is noteworthy is that despite reordering steps, the key radical coupling reaction was successful at various stages of the synthesis using different intermediates (Schemes 2, 5, 7, and 8). This observation allowed us to conclude that not only could radical chemistry be utilized to streamline complex molecule syntheses, but also that bond formations traditionally viewed as being too demanding to accomplish in a straightforward fashion may be approached more confidently with the appropriate strategy in hand.

ACKNOWLEDGMENTS

In addition to the authors, Dr. Jagan Narayanam was instrumental to the success of the work presented herein and is gratefully acknowledged. The research described in this chapter was supported by the University of Michigan, Boston University, NIH-NIGMS (R01-GM096129), Boehringer Ingelheim, Novartis Institutes for BioMedical Research (graduate fellowship to L. F.), and the Alfred P. Sloan Foundation (fellowship to C. R. J. S.).

REFERENCES

1. Carroll, A. R.; Hyde, E.; Smith, J.; Quinn, R. J.; Guymer, G.; Forster, P. I. *J. Org. Chem.* **2005**, *70*, 1096–1099.
2. (a) Baciocchi, E.; Muraglia, E.; Sleiter, G. *J. Org. Chem.* **1992**, *57*, 6817; (b) Reyes-Gutiérrez, P. E.; Torres-Ochoa, R. O.; Martínez, R.; Miranda, L. D. *Org. Biomol. Chem.* **2009**, *7*, 1388–1396; (c) Flanagan, S. R.; Harrowven, D. C.; Bradley, M. *Tetrahedron Lett.* **2003**, *44*, 1795–1798.
3. Guerrero, M. A.; Miranda, L. D. *Tetrahedron Lett.* **2006**, *47*, 2517–2520.
4. Magolan, J.; Kerr, M. *Org. Lett.* **2006**, *8*, 4561–4564.
5. Byers, J. H.; Campbell, J. E.; Knapp, F. H.; Thissell, J. G. *Tetrahedron Lett.* **1999**, *40*, 2677–2680.
6. For a review, see: Prier, C. K.; Rankic, D. A.; MacMillan, D. W. C. *Chem. Rev.* **2013**, *113*, 5322–5363.
7. Nicewicz, D. A.; MacMillan, D. W. C. *Science* **2008**, *322*, 77–80.
8. Du, J.; Yoon, T. P. *J. Am. Chem. Soc.* **2009**, *131*, 14604–14605.
9. (a) Tucker, J. W.; Narayanam, J. M. R.; Krabbe, S. W.; Stephenson, C. R. J. *Org. Lett.* **2010**, *12*, 368–371; (b) Furst, L.; Matsuura, B. S.; Narayanam, J. M. R.; Tucker, J. W.; Stephenson, C. R. J. *Org. Lett.* **2010**, *12*, 3104–3107.
10. For an excellent review on hexahydropyrroloindolines, see: Ruiz-Sanchis, P.; Savina, S. A.; Albericio, F.; Álvarez, M. *Chem. Eur. J.* **2011**, *17*, 1388–1408.
11. Movassaghi, M.; Schmidt, M. A. *Angew. Chem. Int. Ed. Engl.* **2007**, *46*, 3725–3728.
12. Kim, J.; Ashenurst, J. A.; Movassaghi, M. *Science* **2009**, *324*, 238–241.
13. Narayanam, J. M. R.; Tucker, J. W.; Stephenson, C. R. J. *J. Am. Chem. Soc.* **2009**, *131*, 8756–8757.

14. Zheng, C. J.; Kim, C. J.; Bae, K. S.; Kim, Y. H.; Kim, W. G. *J. Nat. Prod.* **2006**, *69*, 1816–1819.
15. Takahashi, C.; Numata, A.; Ito, Y.; Matsumura, E.; Araki, H.; Iwaki, H.; Kushida, K. *J. Chem. Soc. Perkin Trans. 1* **1994**, 1859–1864.
16. Dong, J. Y.; He, H. P.; Shen, Y. M.; Zhang, K. Q. *J. Nat. Prod.* **2005**, *68*, 1510–1513.
17. Usami, Y.; Yamaguchi, J.; Numata, A. *Heterocycles* **2004**, *63*, 1123–1129.
18. Overman, L. E.; Shin, Y. *Org. Lett.* **2007**, *9*, 339–341.
19. Several total syntheses have been reported since 2009, see: (a) Delorbe, J. E.; Jabri, S. Y.; Mennen, S. M.; Overman, L. E.; Zhang, F. *J. Am. Chem. Soc.* **2011**, *133*, 6549–6552. (b) Trost, B. M.; Xie, J.; Sieber, J. D. *J. Am. Chem. Soc.* **2011**, *133*, 20611–20622. (c) Boyer, N.; Movassaghi, M. *Chem. Sci.* **2012**, *3*, 1798–1803. (d) Song, J.; Guo, C.; Adele, A.; Yin, H.; Gong, L.-Z. *Chem. Eur. J.* **2013**, *19*, 3319–3323.
20. (a) Juris, A.; Balzani, V.; Barigelli, F.; Campagna, S.; Belser, P.; Von Zelewsky, V. *Coord. Chem. Rev.* **1988**, *84*, 85–111; (b) Burstall, F. H. *J. Chem. Soc.* **1936**, 173–175.
21. Rydon, H. N.; Tweddle, J. C. *J. Chem. Soc.* **1955**, 3499–3503.
22. Sundberg, R. J.; Baxter, E. W.; Pitts, W. J.; Ahmed-Schofield, R.; Nishiguchi, T. *J. Org. Chem.* **1988**, *53*, 5097–5107.
23. Piers, E.; Brown, R. K. *Can. J. Chem.* **1962**, *40*, 559–561.
24. This strategy was successful for nucleophilic additions of indoles to bromopyrroloindolines, see Ref. 19(c).
25. Tsuji, J.; Ohno, K. *Synthesis* **1969**, 157–169.
26. Lopez, C. S.; Pérez-Balado, C.; Rodríguez-Graña, P.; de Lera, A. R. *Org. Lett.* **2008**, *10*, 77–80.
27. Iwai, T.; Fujihara, T.; Tsuji, Y. *Chem. Commun.* **2008**, 6215–6217.
28. Shuai, Q.; Yang, L.; Guo, X.; Baslé, O.; Li, C.-J. *J. Am. Chem. Soc.* **2010**, *132*, 12212–12213.
29. Shen, Z.; Khan, H.; Dong, V. M. *J. Am. Chem. Soc.* **2008**, *130*, 2916–2917.
30. Meyer, M. D.; Kruse, L. I. *J. Org. Chem.* **1984**, *49*, 3195–3199.
31. O'Connor, J. M.; Ma, J. *J. Org. Chem.* **1992**, *57*, 5075–5077.
32. Ukhin, Y. L.; Shvestsov, Y. A.; Khidekel, M. L. *Zsu. Akad. Nauk SSSR Ser. Khim.* **1967**, 957.
33. Ling, V. J.; Woodward, R. B. *J. Org. Chem.* **1979**, *44*, 2487–2491.
34. For a review, see: Rosana, M. R.; Tao, Y.; Stiegman, A. E.; Dudley, G. B. *Chem. Sci.* **2012**, *3*, 1240–1244.

Studies in the Synthesis of Biaryl Natural Products: The 6,6'-Binaphthopyranones

Michael J. Di Maso, Charles I. Grove, and Jared T. Shaw¹

Department of Chemistry, University of California, Davis, California, USA

¹*Corresponding author: jtshaw@ucdavis.edu*

Chapter Outline

1. Introduction	225	5.1. Preparation of Enantiomerically Pure α,β -Unsaturated Lactones	237
2. Axial Chirality and Biaryl Natural Products	228	5.2. Synthesis of Naphthopyranone Monomers	239
3. Strategies in the Assembly of Biaryl Natural Products: Instructive Examples that Shaped Synthetic Planning for Viriditoxin	229	5.3. Oxidative Couplings	241
4. Retrosynthetic Analysis of Viriditoxin and Related Natural Products	235	5.4. Completion of Targets	241
5. Assembly of Viriditoxin, Pigmentosin A, Talaroderxine A, Talaroderxine B	237	6. Biological Activity of the 6,6'-Binaphthopyranones	241
		7. Conclusion	245
		Acknowledgments	246
		References	246

1 INTRODUCTION

The synthesis of natural products is a pursuit that continues to fascinate organic chemists after the nearly two centuries since Wöhler first described the preparation of urea from abiotic precursors.¹ Although the techniques have evolved significantly in the ensuing decades, many of the scientific goals have remained constant. Like Wöhler, many chemists pursue natural product targets to demonstrate that their synthesis is possible. Such is the case with

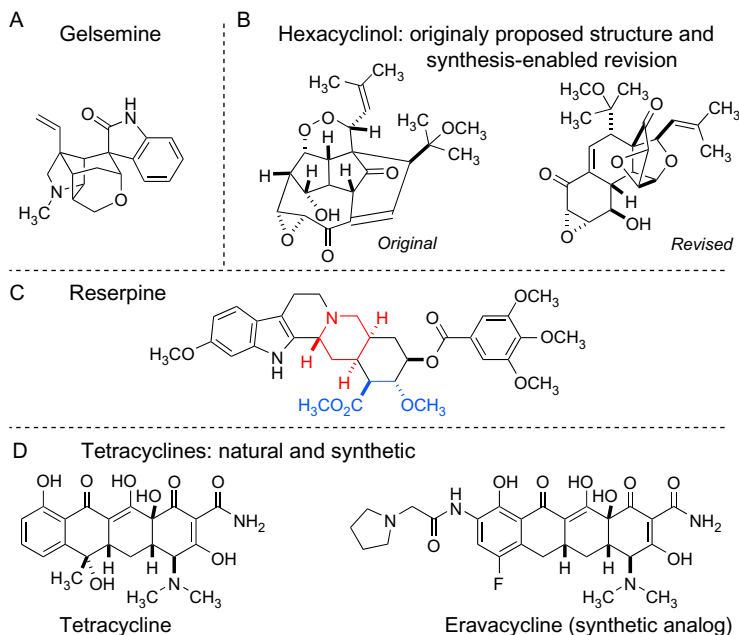


FIGURE 1 Structures of natural products highlighting the diverse goals of synthesis: (A) gelsemine, (B) proposed and revised hexacyclinol, (C) reserpine, and (D) tetracycline and its fully synthetic analog ervacycline.

gelsemine (Figure 1A). This alkaloid can be isolated from many sources, has no known commercial value, and yet has been the center of many synthetic studies.² In some cases, synthesis is the only method by which the structure of a natural product can be proven unambiguously.³ The proposed structure of hexacyclinol (Figure 1B) was significantly revised based on a biosynthetic hypothesis⁴ that was supported by a successful synthesis.⁵ In some cases, the construction of a natural product is the outgrowth of new synthetic methods that have been developed. Jacobsen's recent synthesis of reserpine highlights both organocatalytic (red) and transition metal-catalyzed (blue) asymmetric methods developed in his laboratory (Figure 1C).⁶ Finally, the synthesis of certain natural products serves as a launch-point for campaigns to fully exploit their biological activity and enable drug discovery. Although some advances come from chemical derivatives of naturally occurring materials, altered cores are sometimes required to achieve significantly enhanced activity. A recent example lies in the preparation of the core-modified tetracycline antibiotic ervacycline.⁷ The discovery of this drug candidate resulted from a total synthesis of the naturally derived parent structure (tetracycline)⁸ and would have been nearly impossible to prepare by modifying a naturally occurring member of this compound class.

Our attraction to the synthesis of binaphthopyranone natural products stems from the last of these motivations, that is, we sought a better understanding of

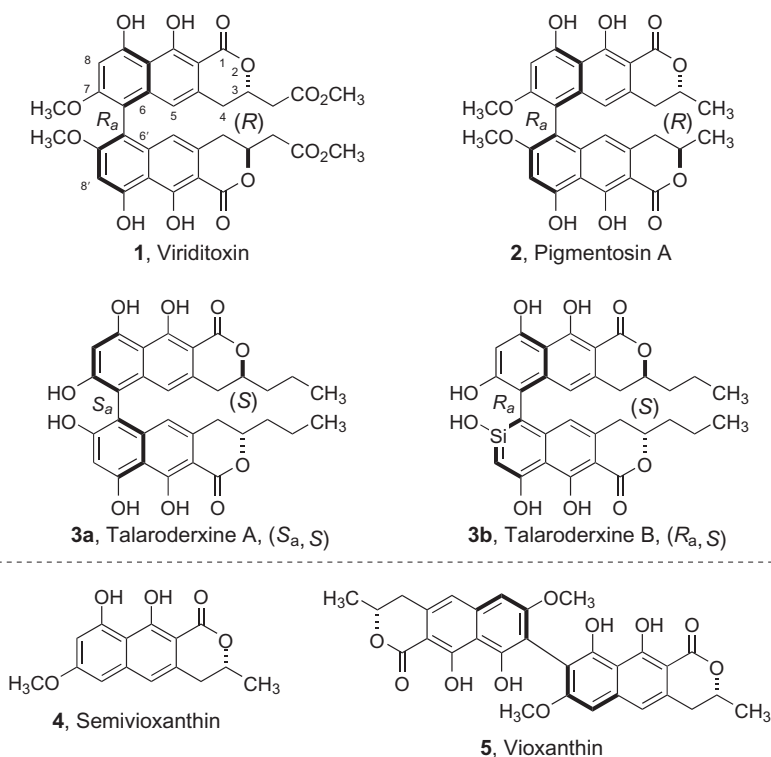


FIGURE 2 Structures of 6,6'-binaphthopyranone natural products (1–3) and related structures (4, 5).

their biology in hopes of fully realizing their potential in drug discovery. Viriditoxin (1, Figure 2) was isolated by Merck in a high-throughput screen of natural product extracts for activity against the bacterial cell division protein FtsZ.⁹ This protein is a GTPase found only in prokaryotes and has a structure that is analogous to eukaryotic tubulin. Inhibition of tubulin's function forms the basis of chemotherapies that target rapidly dividing cells, specifically those that are cancerous. By analogy, an FtsZ inhibitor could form the basis of an antibiotic by halting the growth of pathogenic bacteria.¹⁰ Although many small-molecule inhibitors of tubulin have been isolated from natural sources,¹¹ similarly selective and potent small molecules for FtsZ are lacking. At the outset of our studies, there were no inhibitors of FtsZ with activity in the nanomolar range and no drug development candidates that targeted bacterial cell division. In the interim, a single compound (PC190723) has been reported to be a nanomolar inhibitor of FtsZ,¹² though subsequent studies demonstrated that it is actually a micromolar *activator* of the GTPase activity.^{13,14} Furthermore, when we started work on viriditoxin there were no cocrystal structures of FtsZ bound to non-nucleotide small molecules! Recently, the first structure of PC190723 in a complex with *Staphylococcus aureus* FtsZ was reported.¹⁵ Even now, there is still a significant gap in the knowledge of the molecular basis of FtsZ inhibition. We felt that

a synthetic route to viriditoxin and related natural products would provide an avenue toward addressing this gap and perhaps be useful for biophysical studies, including cocrystallization.

Viriditoxin is a member of a small class of naturally occurring C_2 -symmetric dimers of naphthopyranone subunits that probably originate from the condensation of polyketide precursors (Figure 2). This molecule was originally assigned as having an 8,8' linkage,¹⁶ like that of vioxanthin (5) and reassigned as a 6,6' dimer based on CD and NMR spectroscopic studies.¹⁷ Pigmentosin A (2) is thought to be similarly derived from semivioxanthin, which is also known to form the 8,8' dimer, vioxanthin.¹⁸ Both viriditoxin and pigmentosin A are found as single isomers with respect to absolute and relative configuration, suggesting that their formation is enzymatically mediated. The atropodiastereomeric talaroderxines A and B (3a and 3b, respectively) are found to co-occur in two different organisms, seemingly arising from unselective dimerization that may not require an enzyme.¹⁹

The difficulty of a natural product synthesis project is often only realized once it has been completed, that is, many investigators would concede that assessing the relative challenge is difficult *a priori*. When we initiated our synthetic studies of viriditoxin in 2006, the high symmetry, simple appearance of the substitution pattern of the naphthopyranone rings, and apparent ease with which biaryl linkages could be prepared by cross-coupling reactions all suggested that we would complete the synthesis in a short timeframe. Ultimately, three general challenges had to be addressed. First, we had to prepare the naphthopyranone subunit. Although the preparation of semiviriditoxin was ultimately straightforward, the proper choice of oxidation state and protecting group compatibility required significant trial and error. Second, biaryl bond formation was nearly impossible using cross-coupling and oxidative homocoupling reactions of organometallic intermediates. A switch to oxidative phenol dimerization required a complete “reboot” of the subunit synthesis. Although this turned out to be an effective strategy for biaryl bond formation, stereocontrol was somewhat of an unknown at the time. On this front, we were fortunate, discovering a nice example of remote asymmetric induction and developing selective variants of bimetallic oxovanadium catalysts. In the end, our syntheses of viriditoxin and three related natural products were successful and enabled a detailed study of the biological activity of these molecules. This chapter tells the whole story, complete with anecdotes on lessons learned along the way that are instructive for this class of compounds and for the synthesis of natural products intended for subsequent biological studies.

2 AXIAL CHIRALITY AND BIARYL NATURAL PRODUCTS

Asymmetry in organic molecules can take many forms (Figure 3A), one of which is termed “axial chirality.” While organic chemists are familiar with

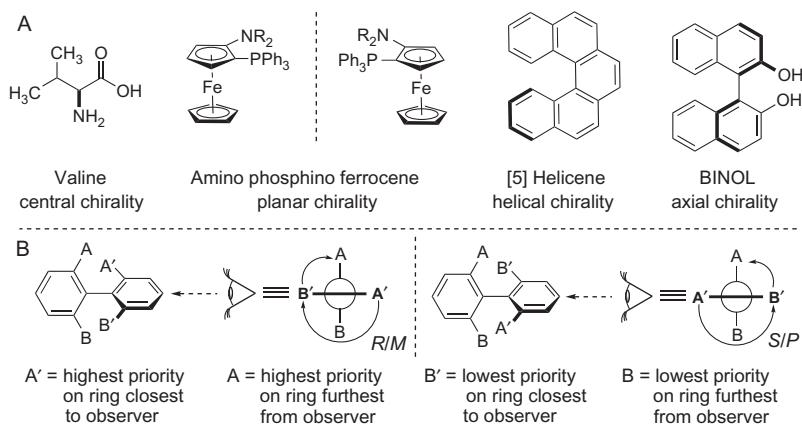


FIGURE 3 (A) elements of chirality in organic structures, (B) assignment of configuration for molecules with axial chirality.

single sp^3 atoms as stereogenic centers (central chirality, e.g., valine), asymmetry can arise from more complex structures such as differentially substituted ferrocenes (planar chirality) and helicene (helical chirality).²⁰ Axial chirality, exemplified by BINOL, is born from restricted rotation around a single bond, often between aromatic rings. Structural assignment for axial chirality follows similar conventions to that for central chirality or helical chirality. The absolute configuration is assigned as *M/P* or *R/S* as demonstrated (Figure 3B).

Axial chirality was discovered in the early twentieth century by Christie and Kenner.²¹ In 1933, Kuhn introduced the term “atropisomerism” to describe biaryl compounds with an axis with hindered rotation.²⁰ Compounds are typically described as atropisomers if the two conformations have a half-life of at least 1000 s at a given temperature. In general, tri- and tetra- *ortho*-substituted biaryl systems provide atropisomers at ambient temperature. As a result, some compounds will racemize at elevated temperatures that confer sufficient energy to overcome the barrier to rotation. For instance, BINOL (6, Figure 4A) which has a high-energy barrier for rotation, will racemize over extended periods of time at high temperatures.²² Thermally stable atropisomers can also undergo chemical and photochemical racemization as seen with BINOL,²³ michellamines A–C,²⁴ and bistriarene C²⁵ (Figure 4B).

3 STRATEGIES IN THE ASSEMBLY OF BIARYL NATURAL PRODUCTS: INSTRUCTIVE EXAMPLES THAT SHAPED SYNTHETIC PLANNING FOR VIRIDITOXIN

Biaryl motifs have presented challenges in the assembly of many natural products. The breadth of approaches has been comprehensively reviewed^{26–28} and, as such, we will not attempt to catalog all of the work that served as a

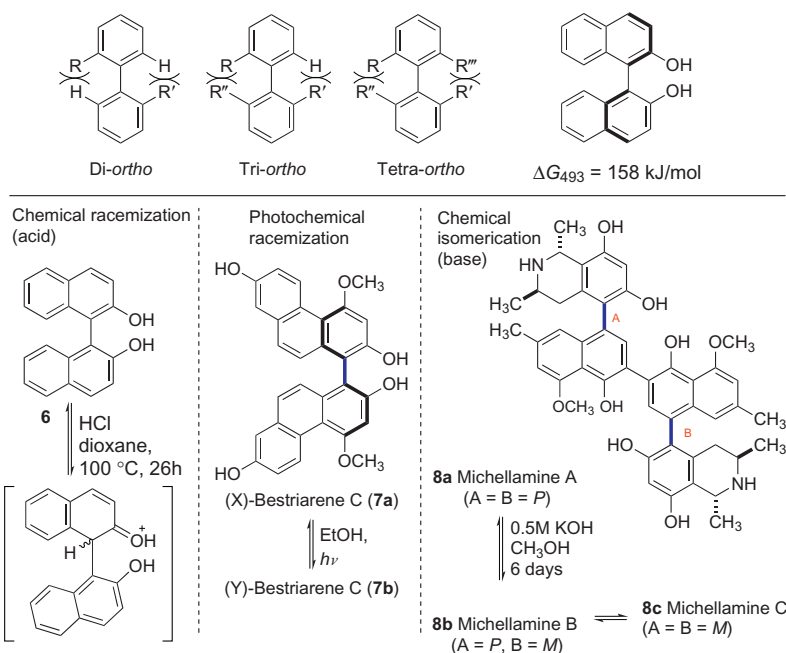
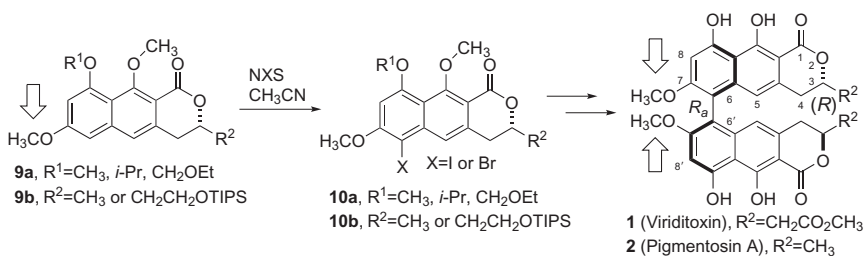


FIGURE 4 Thermal stability of atropisomers including BINOL. Chemical and photochemical isomerization of biaryl isomers.



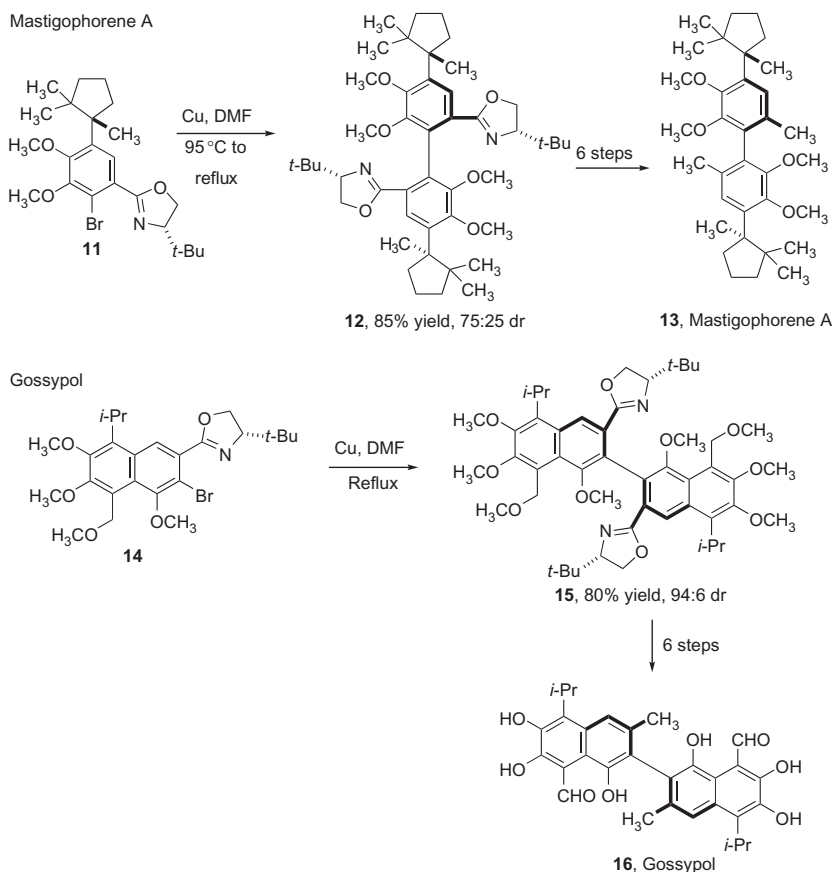
SCHEME 1 Halogenation of naphthopyranone intermediates at the 6-position.

backdrop to our efforts. Instead, we highlight some of the applications of key strategies and describe our attempts at applying these techniques to our targets, culminating in the identification of the successful route.

In the initial stages of the viriditoxin synthesis, we envisioned synthesizing the 6-halo-naphthopyranone core with the goal of executing either a homo- or cross-coupling reaction. Fortuitously, advanced intermediates underwent facile halogenation at the 6-position (Scheme 1) when there was a free phenol in the “*para*–” or 9-position. The preparation of the halogenation precursors (**9**) is described in detail later in this chapter. With this material in hand, we set out to attempt a variety of coupling reactions with the hope that the distal

stereogenic center would influence the axial chirality and with the possibility of using chiral ligands for cross-coupling reactions. Fortunately, the 7-position of viriditoxin is methylated in the final target, obviating the need for protection or deprotection of this position. That said, the lactone and ester provided an electrophilic carbon that could be a liability for certain organometallic intermediates. We elected to leave the lactone intact and bring in the ester at the hydroxyl oxidation state for later conversion to the requisite ester.

The Ullman coupling offered the simplest solution and had previously been successful in the assembly of several natural products. Although the reaction often requires elevated temperatures, the absence of acid, base, or oxidants enables the reaction to be successfully applied to relatively complex substrates. Meyers and coworkers used this approach extensively as exemplified by the successful syntheses of mastigophorene A and gossypol (Scheme 2).^{29,30} When we attempted the Ullman coupling using **10** and

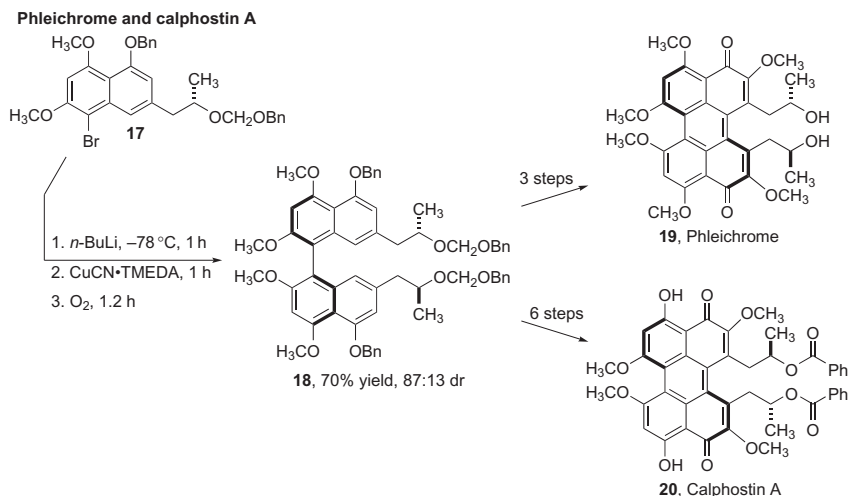


SCHEME 2 Meyers' syntheses of biaryl targets using the Ullman reaction.

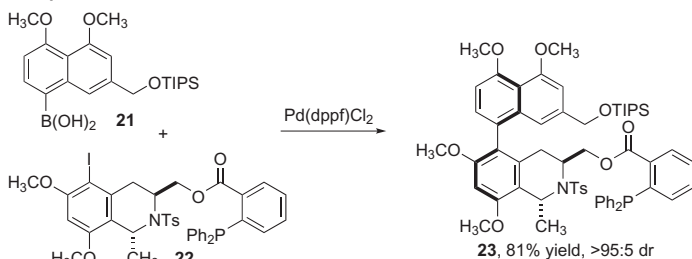
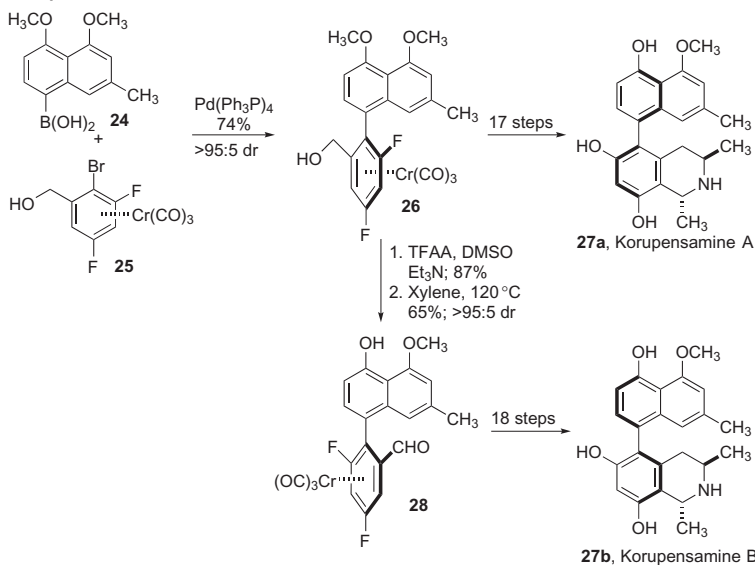
related substrates, we universally observed degradation of the starting materials before any biaryl products were formed.

Another homocoupling approach involves the formation of an organometallic intermediate, conversion to the homocuprate with a Cu(I) salt and oxidation with oxygen or a substituted quinone. This approach has been applied successfully to the preparation of the biaryl core common to phleichrome and calphostin A in work by Coleman and coworkers (Scheme 3).³¹ Importantly, significant asymmetric induction was induced by the distal stereogenic center. A closely related study was reported by Broka, albeit with lower diastereoselectivity in the coupling step.³² Mindful of the difficulties associated with metal–halogen exchange in the presence of the lactone and with the potential for any organometallic intermediate to self-destruct, we felt obligated to attempt this reaction due to the extreme efficiency it offered. Perhaps not surprisingly in retrospect, we were unable to observe significant levels of exchange or oxidative dimerization.

We next turned our attention to the use of cross-coupling reactions using our late-stage aryl halide as the source of coupling partners. This strategy, specifically in the form of the Suzuki reaction,³³ has been successfully applied to the synthesis of korupensamine and related biaryl alkaloid natural products (Scheme 4). In two different approaches, significant chemical differentiation of the coupling partners was required to achieve high diastereoselectivity. In an approach to the common core of korupensamines and michellamines, Lipschutz employed a pendant phosphine tether to induce tighter organization around the palladium catalyst. The ensuing Suzuki reaction occurred with high diastereoselectivity. In a successful synthesis



SCHEME 3 Oxidative dimerization of an aryllithium intermediate in the synthesis of perylene-quinone natural products.

Korupensamine and michellamine core**Korupensamines A and B**

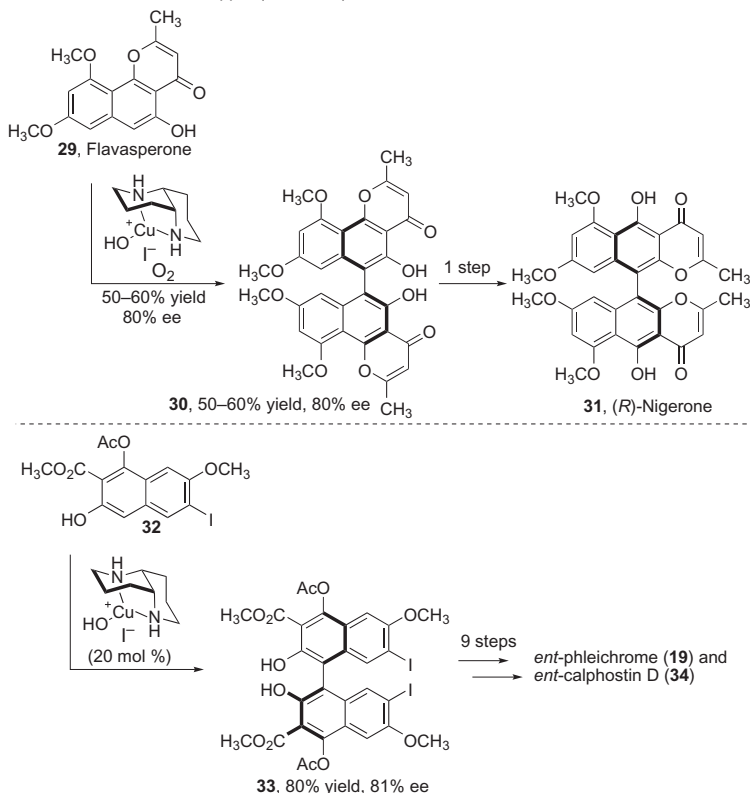
SCHEME 4 Synthesis of the korupensamine and michellamine biaryl linkages by Suzuki coupling.

of korupensamines A and B, Watanabe *et al.* used a chromium carbonyl arene complex, which breaks the planar symmetry of the aromatic ring. The coupling reaction occurred with high kinetically controlled *syn* selectivity and, after oxidation of the primary alcohol, the biaryl core could be thermally isomerized to the other diastereomer. Significant effort was required to convert the benzene ring into the requisite naphthalene unit. In both cases, the requisite boronic acid was prepared via organolithium intermediates. All of our attempts to prepare boronic acids or esters were unsuccessful, as were several attempts at Pd-catalyzed conversion of the aryl halide to a boronic ester. Other cross-couplings did not seem to offer much hope either.^{20,34} Although there has been significant effort devoted to coupling organomagnesium reagents with either palladium or nickel, these

conditions would be incompatible with our lactone substrate. Conversion to an organotin presented the same difficulties as the boronic acid and formation of an organozinc was not attempted. At the time of Bringmann's comprehensive review, there were no examples of enantioselective Stille or Negishi couplings.²⁷ All in all, the cross-coupling approach via intermediate **10** looked bleak.

At this stage, we needed to regroup and consider new options. As mentioned previously, the use of an aryl halide intermediate and either a homo- or cross-coupling reaction offered a high level of protecting group efficiency, that is, the requisite 7-*O*-methyl group could be installed early in our synthesis and left in place. As such, we had not initially considered using phenolic couplings. Although phenols were often coupled with harsh oxidants such as V(O)F₃, recent work in the area of naphthol coupling demonstrated that milder conditions, often with catalytic quantities of metal, could be extremely efficient.³⁵ The biggest contribution to the development of methods that were applied to natural product syntheses has come from the Kozlowski group. In these studies, naphthols with *ortho* carbonyl groups were effectively coupled with copper catalysts employing a novel 1,5-diaza-*cis*-decalin ligand to induce asymmetry. Catalytic efficiency is modest in some cases, but the tolerance of functional groups enables the use of this reaction in late-stage couplings. For instance, the synthesis of nigerone employed a stoichiometric quantity of the chiral copper complex in the penultimate step of the synthesis of this compound from flavasperone, another natural product (Scheme 5).³⁶ Subsequently, Kozlowski and coworkers reported efficient syntheses of phleiochrome and calphostin D³⁷ (not shown, closely related to calphostin A, Scheme 3). In these cases, a copper complex was employed as a catalyst to provide a unified strategy for several complex perylenequinones.

The use of vanadium catalysts reported by Gong offered the efficiency and functional group tolerance of the Kozlowski catalysts without the need for an *ortho* carbonyl group. Building on previous work on related catalysts,^{38,39} Gong designed bimetallic catalyst complexes that exhibited extremely high selectivities and yields, often with low catalyst loadings (Scheme 6).^{40,41} The catalysts themselves are easily made from BINOL in short, efficient sequences that culminate in the combination of a dialdehyde, amino acid, and vanadium source. This work was emerging just as we were in the middle of struggling with our cross-coupling experiments, but it did not immediately seem like a good fit, given the requirement for a naphthol substrate. Viriditoxin has two free phenolic hydroxyl groups and only the distal one, which is the most difficult to manipulate, is methylated. Fortunately, a new member of the project team (Dr. Young Sam Park) was unencumbered by the previous efforts to avoid manipulation of this methyl group and spearheaded the phenolic coupling route that was ultimately successful.

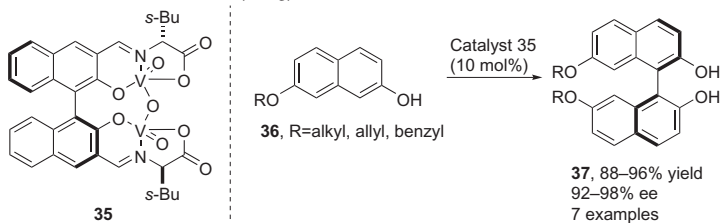
Oxidative dimerization: Copper (Kozlowski)

SCHEME 5 Asymmetric oxidative dimerization of naphthols mediated by a chiral copper complex.

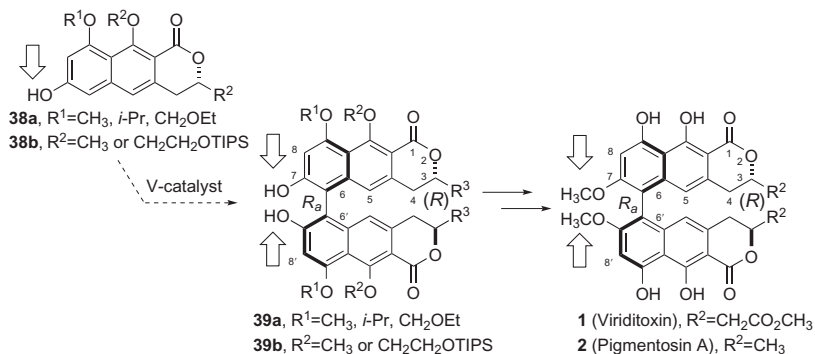
4 RETROSYNTHETIC ANALYSIS OF VIRIDITOXIN AND RELATED NATURAL PRODUCTS

The atroposelective construction of the 6,6'-biaryl linkage was recognized as the key step in the synthesis of viriditoxin. Although many atroposelective couplings of complex molecules have been completed and have been the subject of many reviews,^{27,35} most of these approaches relied on either proximal stereogenic centers or covalently linked chiral auxiliaries. Our objective was to explore the influence of distal chiral centers on the catalytic oxidative dimerization of naphthopyran-2-ones using vanadium catalysis (Scheme 7). Assembly of naphthopyran-2-ones has been well studied and recently reviewed.⁴² The Staunton–Weinreb annulation or the Michael–Dieckmann condensation is ideally suited for the rapid

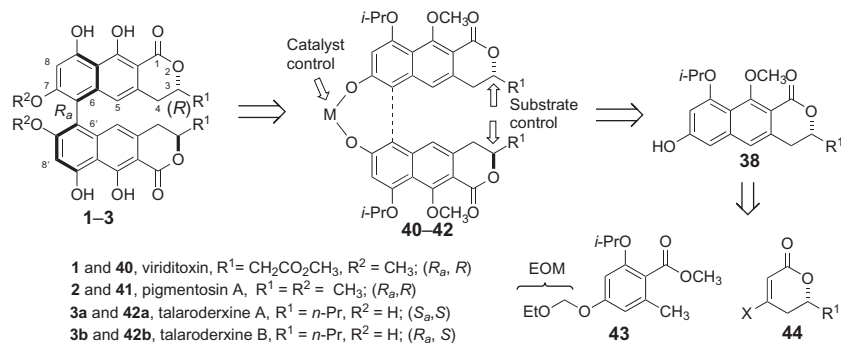
Oxidative dimerization: Vanadium (Gong)



Viriditoxin and pigmentosin synthetic plan, version 2.0



SCHEME 6 Gong's catalytic, asymmetric oxidative dimerization of naphthols using vanadium complex **35**. Reboot of viriditoxin/pigmentosin A synthetic plan.



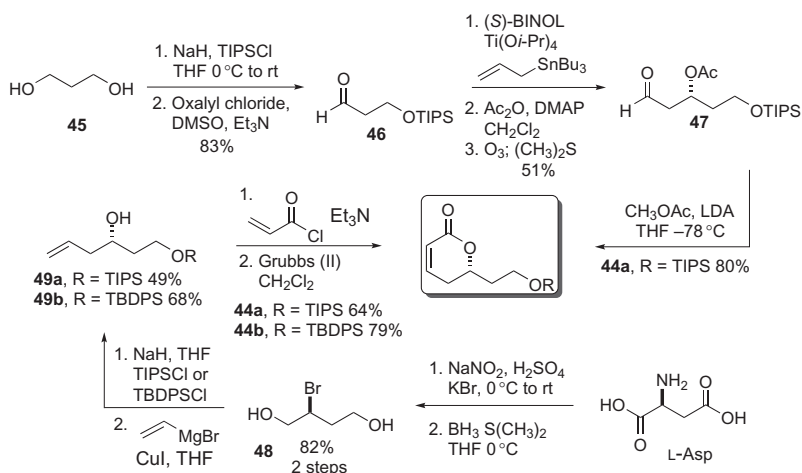
SCHEME 7 Retrosynthetic plan for viriditoxin and related natural products.

construction of naphthopyran-2-ones.^{43–45} Formation of *ortho*-toluate anions *in situ* followed by the addition of an electrophile leads to a tandem addition–condensation sequence. The Michael–Dieckmann condensation has been shown to tolerate multiple substitutions on the aromatic ring and various phenolic protecting groups. Ester **43** and α,β -unsaturated lactone **44** can be accessed from standard procedures in good yield.

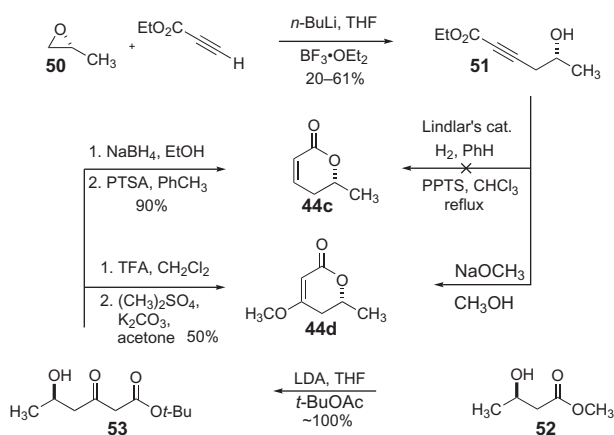
5 ASSEMBLY OF VIRIDITOXIN, PIGMENTOSIN A, TALARODERXINE A, TALARODERXINE B

5.1 Preparation of Enantiomerically Pure α,β -Unsaturated Lactones

Our synthetic efforts began with the enantioselective synthesis of the required α,β -unsaturated lactones for our natural products. While we hoped to develop a robust route to these lactones, necessity dictated that we use different routes to access each of these lactones as various pitfalls arose in our synthetic endeavors toward each lactone. Our first approach to a unified strategy began with accessing lactone **44a** via the stereoselective synthesis of homoallylic alcohols (Scheme 8). Keck allylation⁴⁶ of aldehyde **46** followed by acetylation and ozonolysis of the homoallylic alcohol provided aldehyde **47**. Our desired lactone **44a** could then be formed by a lactonization sequence also reported by Keck.⁴⁷ In the course of our studies, we discovered that the TIPS group was labile to typical conditions for ethoxymethyl ether (EOM) group removal, which is required prior to the key phenolic coupling reaction (*vide infra*). While we could circumscribe this protecting group instability by changing to a TBDPS group, we also wanted to move away from using stoichiometric amounts of toxic alkyltin reagents, so we undertook a more serious reroute to **44**. We turned to the work of Volkmann and found we were able to open an epoxide intermediate, available from L-aspartic acid, with vinylmagnesium bromide.⁴⁸ Acrylation of this alcohol allowed for the facile ring-closing metathesis to our lactone. This route, paired with switching to the TBDPS protecting group, was a significant improvement and was featured in our “second-generation” synthesis of viriditoxin.



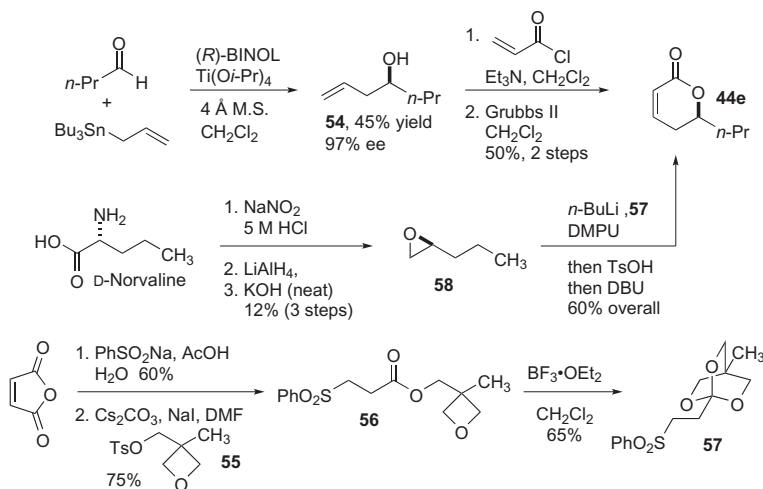
SCHEME 8 Synthesis of the viriditoxin lactone precursor.



SCHEME 9 Synthesis of chiral lactones for pigmentosin A.

The homoallylic alcohol required for pigmentosin A proved too volatile to be a viable intermediate in our synthetic route toward **44c** and another approach was pursued for the synthesis of the requisite lactone that could also allow for access to Staunton–Weinreb precursor **44d** (Scheme 9). Epoxide alkylation of (*R*)-**50** with ethyl propynoate provided homopropargyl alcohol **51** in 93% yield on gram scale. We envisioned that hydrogenation of homopropargyl alcohol with Lindlar's catalyst followed by acid-catalyzed cyclization would provide the desired lactone **44c**; however, reduction of the alkyne resulted in a mixture of inseparable alkene and alkane products. Treatment of the mixture with PPTS in CHCl3 also failed to provide the lactone. Treating **51** with sodium methoxide in methanol did provide the Staunton–Weinreb precursor, **44d**, albeit in low yield (<20%).⁴⁹ Access to the desired lactone using Müller's approach in the synthesis of semivioxanthin, the monomeric unit of pigmentosin A, was ultimately successful.^{50–52} Thus, commercially available methyl (*R*)-3-hydroxy-butanoate was converted into both of the desired products via common intermediate **53** in good yields.

The ester analogous to **52** that was required to obtain the lactone for the talaroderxines was not easily accessible by the same route as that used for the pigmentosin A lactone. As such, we turned to our original viriditoxin strategies to access the lactone (Scheme 10). We began with an enantioselective Keck allylation of butyraldehyde followed by acylation with acryloyl chloride and ring-closing metathesis to complete the lactone. While this route delivered product, we hoped to develop a new route conducive to large-scale synthesis, that is, higher yielding and avoiding stoichiometric tin reagents, while avoiding the intermediacy of the volatile homoallylic alcohol **54**. Ghosez developed an attractive lactonization reagent, trimethyl-3-phenylsulfonyl orthopropionate that could be used with enantiomerically pure epoxides to yield our desired lactone in a one-pot procedure.⁵³ Unfortunately, our attempts to synthesize



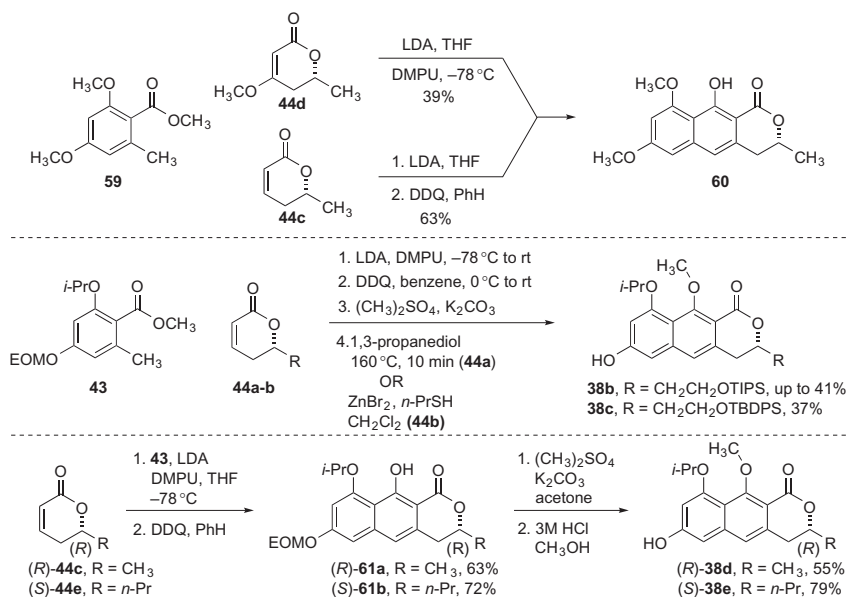
SCHEME 10 Synthesis of talaroderxine lactone precursor and development of a new sulfone annulation reagent (**57**).

the orthoester were unsuccessful as we typically isolated the methyl ester from Ghosez's reaction sequence, consistent with other attempts to synthesize this compound.⁵⁴ We thought that changing from the trimethyl orthoester to the 2,6,7-trioxabicyclo[2.2.2]octane (OBO) ester would impart a greater stability to the orthoester while retaining the desired reactivity. Conjugate addition of benzene-sulfinic acid sodium salt to maleic anhydride occurred in refluxing water to provide 3-phenylsulfonylpropionic acid after decarboxylation. Alkylation of the acid with **55** followed by BF₃·OEt₂-catalyzed rearrangement yielded multigram quantities of the desired OBO-sulfone **57** as a white solid, which can be stored on the benchtop for months with no degradation.

Enantiomerically pure epoxide **58** was available from D-norvaline via the same route to epoxides as in our viriditoxin synthesis.^{55,56} Reaction of epoxide **58** with the lithium anion of OBO-sulfone **57** produced lactone in 60% overall yield after hydrolysis, lactonization, and elimination. We were pleased to discover that this reaction allowed for use of 1.3 equivalents of **57**, whereas three equivalents of Ghosez's reagent were often used in related transformations. Although we have not examined the reactions of the viriditoxin or pigmentosin A epoxides with this reagent, we hypothesize that our modified reagent **57** would allow for a unified α,β -unsaturated lactone synthesis and thus access to a variety of derivatives of binaphthopyranones.

5.2 Synthesis of Naphthopyranone Monomers

With the necessary α,β -unsaturated lactones in hand, we were ready to construct the naphthopyranone monomers. We began with the one-step



SCHEME 11 Assembly of naphthopyranone monomers.

Staunton–Weinreb annulation toward the synthesis of pigmentosin A (Scheme 11). Unfortunately, this one-step procedure using **44d** provided poor yields of the naphthopyranone (<40%).^{43,57} After unsuccessful attempts to optimize the reaction, we turned our efforts to a two-step procedure of Michael–Dieckmann cyclization followed by oxidative aromatization. The lithium enolate of **43** reacted with all of our lactones to provide the corresponding desired naphthopyranones after oxidative aromatization with 2,3-dichloro-5,6-dicyano-1,4-benzoquinone (DDQ). During the course of our synthesis of this important subunit, closely related work was published by another group, confirming our observations regarding the relative efficiency of these two annulation routes.⁴⁹

Manipulation of our phenol protecting groups accessed our desired coupling precursors. Methylation of the free phenol followed by EOM (ethoxymethyl) deprotection allowed access to our coupling precursors **38**. While acid deprotection worked well with the pigmentosin A and talaroderxines monomers, the TIPS and TBDPS groups would not survive the harsh acidic conditions. Heating the TIPS-protected naphthopyranone in neat 1,3-propanediol at 150 °C provided the deprotected product in good yield on small scale (<20 mg) but was not reproducible on larger scales. Changing to the more stable TBDPS group now proved essential to a scalable synthesis of viriditoxin. Treatment of the naphthopyranone with ZnBr₂ followed by addition of propyl mercaptan provided the deprotected product **38c** in excellent yield.⁵⁸

5.3 Oxidative Couplings

After completing the synthesis of our required naphthopyranone monomers, we began screening catalysts for our phenolic couplings (Table 1). Fortunately, catalysis with $\text{VO}(\text{acac})_2$, provided 6,6'-coupled product with modest substrate control from our distal stereogenic center.^{38,39} The chiral center (C-3) of **38** provided enough of a steric interaction to favor one isomer in our synthesis of viriditoxin (entry 1), but with the smaller methyl and propyl groups the selectivity diminished (entries 7 and 13). These results prompted us to pursue chiral vanadium catalysts in hopes of reinforcing our selectivity. Using Gong's scaffold, we made several catalysts (**35a–i**) to influence the oxidative coupling reaction. Treatment of either enantiomer of dialdehyde **62** with a natural or unnatural amino acid formed the Schiff base and subsequent addition of vanadium sulfate provided the corresponding catalysts.

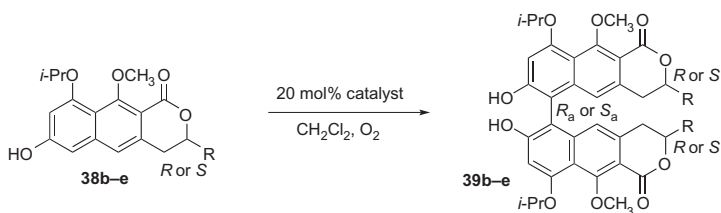
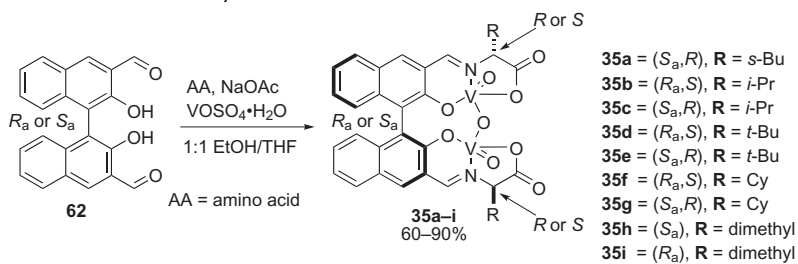
Reexamination of the oxidative coupling reaction with the chiral catalysts provided our desired products with excellent selectivity. In our synthetic efforts toward viriditoxin, we found that the TIPS substrate **38b** reacted with good selectivity with the catalysts; however, the TBDPS substrate **38c** provided the best selectivities (entries 4–6). In our efforts to synthesize pigmentosin A and the talaroderxines, we still observed good diastereoselectivities and could favor the formation of either atropisomer precursor **39d–e** for the talaroderxines (entries 14–17) through catalyst control. These results provide a robust synthetic method toward these natural products and potentially other binaphthol natural products.

5.4 Completion of Targets

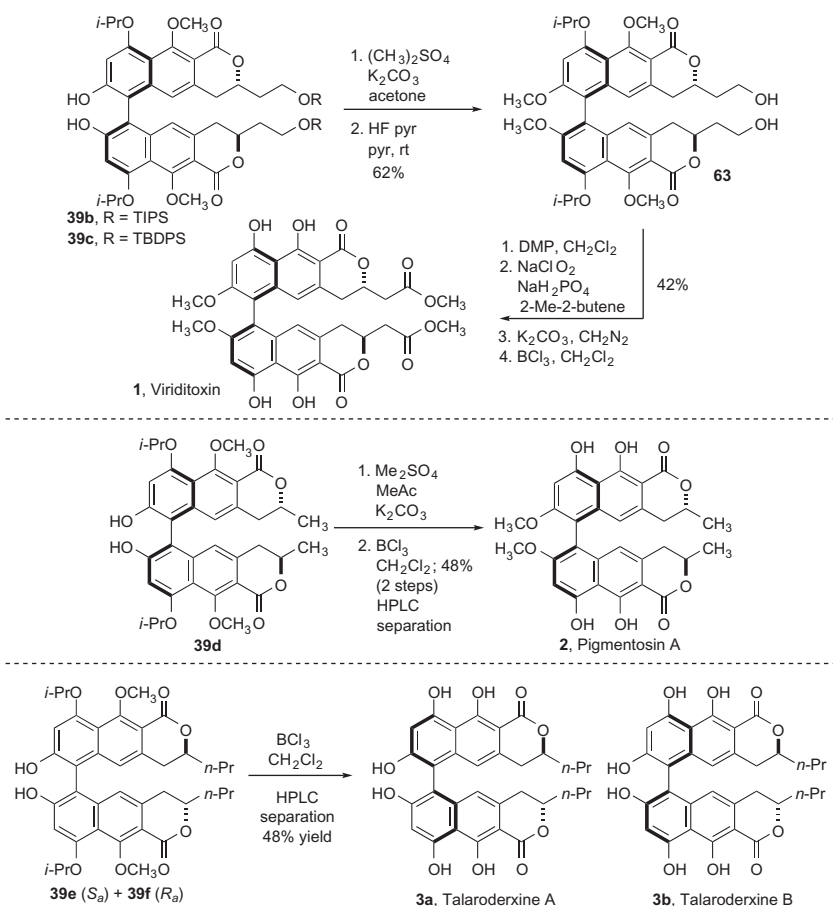
With the key biaryl bond installed, we were a few protecting group and oxidation manipulations away from the completion of the natural products viriditoxin, pigmentosin A, and talaroderxines A and B (Scheme 12). In order to complete the synthesis of viriditoxin, we first installed the methyl aryl ethers and followed with silyl deprotection to yield **63**. Oxidation, methylation, and phenol deprotection provided viriditoxin.^{59,60} The completion of pigmentosin A required the formation of a methyl ether followed by phenol deprotection with BCl_3 . HPLC separation of the minor diastereomer from our biaryl bond formation yielded pigmentosin A (**2**). As for the talaroderxines, a global deprotection provided access to an atropisomerically enriched mixture of the (R_a) and (S_a) isomers that were separated by HPLC to afford the two natural products.⁶¹

6 BIOLOGICAL ACTIVITY OF THE 6,6'-BINAPHTHOPYRANONES

Having assembled viriditoxin and the related natural products, we could test our central hypothesis regarding the common mechanism by which these

TABLE 1 Exploration of Biaryl Bond Formation with Bimetallic Oxovanadium Catalysts

Entry	Naphthopyranone	Catalyst	Product	dr (<i>R</i> _a : <i>S</i> _a)	Yield (%)
1	38b	VO(acac) ²	39b	76:24	67
2	38b	35b	39b	19:81	–
3	38b	35c	39b	89:11	87
4	38c	35c	39b	>95:5	65
5	38c	35e	39b	>95:5	85
6	38c	35a	39b	>95:5	80
7	38d	VO(acac) ²	39c	53:47	80
8	38d	35a	39c	92:08	90
9	38d	35e	39c	90:10	90
10	38d	35g	39c	94:06	99
11	38d	35h	39c	91:09	80
12	38d	35i	39c	54:46	75
13	38e	VO(acac) ²	39d	34:66	75
14	38e	35e	39e	86:14	70
15	38e	35g	39e	76:24	65
16	38e	35d	39d	14:86	60
17	38e	35f	39d	18:82	99



SCHEME 12 Final steps to complete binaphthopyranone targets.

compounds exhibit antimicrobial activity. Assessing the function of FtsZ, and many skeletal proteins for that matter, is challenging, given the multiple functions performed by these proteins. The enzymatic activity of FtsZ can be tested by several GTPase assays that monitor the consumption of GTP, while the polymerization of FtsZ can be directly measured by light scattering. In addition, the formation of Z-rings, which are the structures formed *in vivo* by polymerizing FtsZ, can be monitored with proteins labeled with GFP. Finally, the inability to form a Z-ring at the middle of the cell will cause bacteria such as *Escherichia coli* and *Bacillus subtilis* to form long, filamented cells. This last assay is complicated by the fact that many other proteins are involved in bacterial cell division and inhibition of any of these, either directly or indirectly, might also lead to the filamented cell shape. All in all, the GTPase assay is the most straightforward experiment and enables an

“apples-to-apples” comparison across inhibitors. The Merck group had documented that viriditoxin inhibited the consumption of GTP by FtsZ and caused polymerized protein to depolymerize using a filtration assay. Although they observed slight elongation of *E. coli* cells, the caveats mentioned above limited the extent to which these results supported the notion that FtsZ was the main target of viriditoxin. Pigmentosin A and the talaroderxines also exhibited antimicrobial activity and the structural similarity of these compounds to viriditoxin suggested that they all shared a common mechanism of action.

We examined the activity of these compounds using several different assays. First, we established that they all had antimicrobial activity comparable to what was initially reported. Assessing the minimum inhibitory concentration of a small molecule is a straightforward experiment requiring little specialized equipment. In fact, growth of bacteria is often judged “by eye”; a test tube with bacterial growth will be cloudy and one with no growth will be clear. Testing GTPase inhibition is a little more complicated. A postdoctoral fellow (Dr. David Anderson) from Prof. Harold Erickson’s group at Duke University came to work in our lab under the joint supervision of Prof. Jim Ames, a skilled biophysical chemist with a lab equipped with all the necessary accouterments for protein biochemistry. FtsZ was expressed and purified, assessed for baseline enzymatic activity, inhibited with a positive control (zantrin Z3),⁶² and then used in assays for the natural products. It should be noted that this is where protein biochemistry can be complicated. First, the conditions under which the protein is examined can cause the baseline activity to vary by one or two orders of magnitude. As a result, data are often reported as a “percent of control” to account for the fact that the activity might be very different between different batches of protein. Second, assaying the consumption of GTP can be done by several different methods. Older reports use radioisotopes of phosphorous that are often avoided now. Malachite green can be used to detect free phosphate by forming a complex whose degree of light absorbance varies linearly with the concentration of phosphate, albeit by a slightly ill-defined mechanism. This assay, like the radioisotope experiment, involves pulling aliquots at different time points, halting the enzyme’s function, and measuring the amount of inorganic phosphate that has formed. Descriptions of this assay vary widely and are difficult to compare with each other, given that each investigator has often introduced slight modifications to the procedure. We used an enzyme-coupled assay in which the GDP product is converted back to GTP by a process that ultimately consumes NADH and the reduction in absorbance by this chromophore gives a “live” readout of GTP consumption.^{62,63} One caveat with this assay is that the small molecule that is being assessed may perturb the function of the coupling enzymes and produce a falsely positive result.

Why take the time to describe the assays in such detail? Many organic chemists have little appreciation for the subtlety and complexity of biochemical and cell-based assays. In fact, many presentations of natural product synthesis

will give short shrift to the biological activity of the compounds that are being synthesized. Compounds are often described as having “interesting bioactivity” without noting the experiments employed, the concentrations used, and the potential alternative interpretations of the results. *Almost any chemical compound at sufficient concentration will perturb the function of at least one biological system and often by completely unselective mechanisms!* As such, claims of cytotoxicity, “anti-inflammatory activity,” and other broad descriptions of effects on living systems or their *ex vivo* components should be viewed in the context of the experiments that revealed the reported activity.

In the end, viriditoxin’s activity is still a bit of a mystery. We were able to reproduce the cytotoxicity to Gram-positive bacteria (*B. subtilis*). We did not observe any inhibition of the GTPase activity of FtsZ when we employed the enzyme-coupled assay. Upon careful examination of the Merck paper, we noticed two things. We initially suspected that the difference lay in either (a) the fact that they used an end-point (radioisotope) assay or (b) the concentration of the protein and the exact nature of the buffer. We elected to switch to Malachite green which, like the radioisotope assay, examines concentrations of phosphorous at different time points. We also switched our conditions to closely monitor those reported by the Merck group, which produced a 100-fold drop in enzymatic activity, consistent with their results. Unfortunately, we still observed no inhibition of GTP hydrolysis. Although we could never explain this disparity, we elected to abandon viriditoxin and the related natural products as tools that would help illuminate the origin of inhibition of FtsZ by small molecules.

In spite of this setback to our broader aims, it was extremely satisfying to set our sights on targets, achieve their syntheses, and study their function in great detail. A similar story played out with two other natural products that we synthesized: (1) the benzylated flavanone dichamanetin⁶⁴ and (2) the diterpenoid totarol,⁶⁵ both of which had also been identified FtsZ inhibitors. The story of these compounds is nearly as long as the preceding description of our adventures with viriditoxin and has been documented in several publications.^{13,66,67} Collectively these investigations highlight a key difference between FtsZ and tubulin. Nature has provided many useful small molecules that perturb the function of tubulin, and some of these have become drugs and tools for cell biology. In spite of the structural and functional similarity between tubulin and FtsZ, no natural product has proven to be as useful for perturbing the function of the latter protein. Is it because the FtsZ is less susceptible to inhibition by small molecules or is it because we have not yet found the right source? Only time, and a lot more hard work in the lab, will tell.

7 CONCLUSION

The synthetic endeavors surrounding viriditoxin and related natural compounds have been extremely enlightening. Several important lessons emerged.

First, one should make sure that the goal of the synthesis is clear and that synthesis is the best way to answer the bigger question. We could have probably acquired the producing organism, isolated natural viriditoxin, and studied the biochemistry in less time than the synthesis required, but this only became clear once we were in the thick of it. Second, it is important to carefully balance “staying the course” with “going back to square one.” Time and effort are required to fully evaluate a particular route and it can be unwise to give up on it prematurely. That said, it is easy to get in the mindset that a technique or route can be made to work with enough dedication. Finally, the synthesis of natural products is extremely important, informative, and fun, even when it is nauseatingly frustrating at times.

ACKNOWLEDGMENTS

This account describes work that was done by the authors and by many other teammates who contributed along the way. They include Young Sam Park, Marcos González-López, Sameer Urgaonkar, and Firoz Jaipuri.

REFERENCES

1. Cohen, P. S.; Cohen, S. M. *J. Chem. Educ.* **1996**, *73*, 883–886.
2. Lin, H.; Danishefsky, S. J. *Angew. Chem. Int. Ed.* **2003**, *42*, 36–51.
3. Nicolaou, K. C.; Snyder, S. A. *Angew. Chem. Int. Ed.* **2005**, *44*, 1012–1044.
4. Rychnovsky, S. D. *Org. Lett.* **2006**, *8*, 2895–2898.
5. Porco, J. A., Jr.; Su, S.; Lei, X.; Bardhan, S.; Rychnovsky, S. D. *Angew. Chem. Int. Ed.* **2006**, *45*, 5790–5792.
6. Rajapaksa, N. S.; McGowan, M. A.; Rienzo, M.; Jacobsen, E. N. *Org. Lett.* **2013**, *15*, 706–709.
7. Ronn, M.; Zhu, Z.; Hogan, P. C.; Zhang, W.-Y.; Niu, J.; Katz, C. E.; Dunwoody, N.; Gilicky, O.; Deng, Y.; Hunt, D. K.; He, M.; Chen, C.-L.; Sun, C.; Clark, R. B.; Xiao, X.-Y. *Org. Process Res. Dev.* **2013**, *17*, 838–845.
8. Charest, M. G.; Siegel, D. R.; Myers, A. G. *J. Am. Chem. Soc.* **2005**, *127*, 8292–8293.
9. Wang, J.; Galgoci, A.; Kodali, S.; Herath, K. B.; Jayasuriya, H.; Dorso, K.; Vicente, F.; Gonzalez, A.; Cully, D.; Bramhill, D.; Singh, S. J. *Biol. Chem.* **2003**, *278*, 44424–44428.
10. Ma, S.; Ma, S. *ChemMedChem* **2012**, *7*, 1161–1172.
11. Kingston, D. G. I. *J. Nat. Prod.* **2009**, *72*, 507–515.
12. Haydon, D. J.; Stokes, N. R.; Ure, R.; Galbraith, G.; Bennett, J. M.; Brown, D. R.; Baker, P. J.; Barynin, V. V.; Rice, D. W.; Sedelnikova, S. E.; Heal, J. R.; Sheridan, J. M.; Aiwale, S. T.; Chauhan, P. K.; Srivastava, A.; Taneja, A.; Collins, I.; Errington, J.; Czaplowski, L. G. *Science* **2008**, *321*, 1673–1675.
13. Anderson, D. E.; Kim, M. B.; Moore, J. T.; O'Brien, T. E.; Sorto, N. A.; Grove, C. I.; Lackner, L. L.; Ames, J. B.; Shaw, J. T. *ACS Chem. Biol.* **2012**, *7*, 1918–1928.
14. Elsen, N. L.; Lu, J.; Parthasarathy, G.; Reid, J. C.; Sharma, S.; Soisson, S. M.; Lumb, K. J. *J. Am. Chem. Soc.* **2012**, *134*, 12342–12345.
15. Tan Christopher, M.; Therien Alex, G.; Lu, J.; Lee Sang, H.; Caron, A.; Gill Charles, J.; Lebeau-Jacob, C.; Benton-Perdomo, L.; Monteiro Joao, M.; Pereira Pedro, M.; Elsen

- Nathaniel, L.; Wu, J.; Deschamps, K.; Petcu, M.; Wong, S.; Daigneault, E.; Kramer, S.; Liang, L.; Maxwell, E.; Claveau, D.; Vaillancourt, J.; Skorey, K.; Tam, J.; Wang, H.; Meredith Timothy, C.; Sillaots, S.; Wang-Jarantow, L.; Ramtohul, Y.; Langlois, E.; Landry, F.; Reid John, C.; Parthasarathy, G.; Sharma, S.; Baryshnikova, A.; Lumb Kevin, J.; Pinho Mariana, G.; Soisson Stephen, M.; Roemer, T. *Sci. Transl. Med.* **2012**, *4*, 126ra35.
16. Weisleder, D.; Lillehoj, E. B. *Tetrahedron Lett.* **1971**, *12*, 4705–4706.
17. Suzuki, K.; Nozawa, K.; Nakajima, S.; Kawai, K. *Chem. Pharm. Bull.* **1990**, *38*, 3180–3181.
18. Elix, J. A.; Wardlaw, J. H. *Aust. J. Chem.* **2004**, *57*, 681–683.
19. Suzuki, K.; Nozawa, K.; Nakajima, S.; Udagawa, S.; Kawai, K. *Chem. Pharm. Bull.* **1992**, *40*, 1116–1119.
20. Grimme, S.; Harren, J.; Sobanski, A.; Vögtle, F. *Eur. J. Org. Chem.* **1998**, 1491–1509.
21. Christie, G. H.; Kenner, J. *J. Chem. Soc. Trans.* **1922**, *121*, 614–620.
22. Meca, L.; Řeha, D.; Havlas, Z. *J. Org. Chem.* **2003**, *68*, 5677–5680.
23. Kyba, E. P.; Gokel, G. W.; De Jong, F.; Koga, K.; Sousa, L. R.; Siegel, M. G.; Kaplan, L.; Sogah, G. D. Y.; Cram, D. J. *J. Org. Chem.* **1977**, *42*, 4173–4184.
24. Boyd, M. R.; Hallock, Y. F.; Cardellina, J. H.; Manfredi, K. P.; Blunt, J. W.; McMahon, J. B.; Buckheit, R. W.; Bringmann, G.; Schaeffer, M. *J. Med. Chem.* **1994**, *37*, 1740–1745.
25. Hattori, T.; Shimazumi, Y.; Goto, H.; Yamabe, O.; Morohashi, N.; Kawai, W.; Miyano, S. *J. Org. Chem.* **2003**, *68*, 2099–2108.
26. Adams, R.; Yuan, H. C. *Chem. Rev.* **1933**, *12*, 261–338.
27. Bringmann, G.; Price Mortimer, A. J.; Keller, P. A.; Gresser, M. J.; Garner, J.; Breuning, M. *Angew. Chem. Int. Ed.* **2005**, *44*, 5384–5427.
28. Bringmann, G.; Gulder, T.; Gulder, T. A. M.; Breuning, M. *Chem. Rev.* **2011**, *111*, 563–639.
29. Degnan, A. P.; Meyers, A. I. *J. Am. Chem. Soc.* **1999**, *121*, 2762–2769.
30. Meyers, A. I.; Willemsen, J. J. *Tetrahedron* **1998**, *54*, 10493–10511.
31. Coleman, R. S.; Grant, E. B. *J. Am. Chem. Soc.* **1995**, *117*, 10889–10904.
32. Broka, C. A. *Tetrahedron Lett.* **1991**, *32*, 859–862.
33. Baudoin, O. *Eur. J. Org. Chem.* **2005**, *2005*, 4223–4229.
34. Bolm, C.; Hildebrand, J. P.; Muñoz, K.; Hermanns, N. *Angew. Chem. Int. Ed.* **2001**, *40*, 3284–3308.
35. Kozłowski, M. C.; Morgan, B. J.; Linton, E. C. *Chem. Soc. Rev.* **2009**, *38*, 3193–3207.
36. DiVirgilio, E. S.; Dugan, E. C.; Mulrooney, C. A.; Kozłowski, M. C. *Org. Lett.* **2007**, *9*, 385–388.
37. Morgan, B. J.; Dey, S.; Johnson, S. W.; Kozłowski, M. C. *J. Am. Chem. Soc.* **2009**, *131*, 9413–9425.
38. Chu, C.-Y.; Hwang, D.-R.; Wang, S.-K.; Uang, B. J. *Chem. Commun.* **2001**, 980–981.
39. Hwang, D.-R.; Chen, C.-P.; Uang, B. J. *Chem. Commun.* **1999**, 1207–1208.
40. Guo, Q.-X.; Wu, Z.-J.; Luo, Z.-B.; Liu, Q.-Z.; Ye, J.-L.; Luo, S.-W.; Cun, L.-F.; Gong, L.-Z. *J. Am. Chem. Soc.* **2007**, *129*, 13927–13938.
41. Takizawa, S.; Katayama, T.; Sasai, H. *Chem. Commun.* **2008**, 4113–4122.
42. Donner, C. D. *Tetrahedron* **2013**, *69*, 3747–3773.
43. Evans, G. E.; Leeper, F. J.; Murphy, J. A.; Staunton, J. *Chem. Commun.* **1979**, 205–206.
44. Tatsuta, K.; Yamazaki, T.; Yoshimoto, T. *J. Antibiot.* **1998**, *51*, 383–386.
45. White, J. D.; Demnitz, F. W. J.; Xu, Q.; Martin, W. H. C. *Org. Lett.* **2008**, *10*, 2833–2836.
46. Keck, G. E.; Welch, D. S.; Vivian, P. K. *Org. Lett.* **2006**, *8*, 3667–3670.
47. Keck, G. E.; Li, X.-Y.; Knutson, C. E. *Org. Lett.* **1999**, *1*, 411–414.
48. Volkmann, R. A.; Kelbaugh, P. R.; Nason, D. M.; Jasys, V. J. *J. Org. Chem.* **1992**, *57*, 4352–4361.

49. Tan, N. P. H.; Donner, C. D. *Tetrahedron* **2009**, *65*, 4007–4012.
50. Drochner, D.; Muller, M. *Eur. J. Org. Chem.* **2001**, 211–215.
51. Wolberg, M.; Hummel, W.; Muller, M. *Chem. Eur. J.* **2001**, *7*, 4562–4571.
52. Bode, S. E.; Drochner, D.; Mueller, M. *Angew. Chem. Int. Ed.* **2007**, *46*, 5916–5920.
53. De Lombaert, S.; Nemery, I.; Roekens, B.; Carretero, J. C.; Kimmel, T.; Ghosez, L. *Tetrahedron Lett.* **1986**, *27*, 5099–5102.
54. Craig, D.; Lu, P.; Mathie, T.; Tholen, N. T. H. *Tetrahedron* **2010**, *66*, 6376–6382.
55. Koppenhoefer, B.; Schurig, V. *Org. Synth.* **1988**, *66*, 151–159.
56. Koppenhoefer, B.; Schurig, V. *Org. Synth.* **1988**, *66*, 160–172.
57. Dodd, J. H.; Weinreb, S. M. *Tetrahedron Lett.* **1979**, *20*, 3593–3596.
58. Han, J. H.; Kwon, Y. E.; Sohn, J.-H.; Ryu, D. H. *Tetrahedron* **2010**, *66*, 1673–1677.
59. Park, Y. S.; Grove, C. I.; González-López, M.; Urgaonkar, S.; Fettingner, J. C.; Shaw, J. T. *Angew. Chem. Int. Ed.* **2011**, *50*, 3730–3733.
60. Grove, C. I.; Fettingner, J. C.; Shaw, J. T. *Synthesis* **2012**, *44*, 362–371.
61. Grove, C. I.; Di Maso, M. J.; Jaipuri, F. A.; Kim, M. B.; Shaw, J. T. *Org. Lett.* **2012**, *14*, 4338–4341.
62. Margalit, D. N.; Romberg, L.; Mets, R. B.; Hebert, A. M.; Mitchison, T. J.; Kirschner, M. W.; RayChaudhuri, D. *Proc. Natl. Acad. Sci. U.S.A.* **2004**, *101*, 11821–11826.
63. Ingberman, E.; Nunnari, J. *Methods Enzymol.* **2005**, *404*, 611–619.
64. Urgaonkar, S.; La Pierre, H. S.; Meir, I.; Lund, H.; RayChaudhuri, D.; Shaw, J. T. *Org. Lett.* **2005**, *7*, 5609–5612.
65. Jaiswal, R.; Beuria, T. K.; Mohan, R.; Mahajan, S. K.; Panda, D. *Biochemistry* **2007**, *46*, 4211–4220.
66. Kim, M. B.; Shaw, J. T. *Org. Lett.* **2010**, 3324–3327.
67. Kim, M. B.; O'Brien, T. E.; Moore, J. T.; Anderson, D. E.; Foss, M. H.; Weibel, D. B.; Ames, J. B.; Shaw, J. T. *ACS Med. Chem. Lett.* **2012**, *3*, 818–822.

Sleepless Nights: The Total Synthesis of the Anticancer Australian Rainforest Polyketide EBC-23

Craig M. Williams¹

School of Chemistry and Molecular Biosciences, University of Queensland, Brisbane, Queensland, Australia

¹Corresponding author: c.williams3@uq.edu.au

Chapter Outline

1. Introduction	249	7. Refining the Synthetic Campaign	260
2. Structure Elucidation	250	8. Completing the Total Synthesis	264
3. Retrosynthetic Plan	253	9. Biomimetic Attempts	267
4. Starting the Total Synthesis	253	10. Yamamoto Synthesis	268
5. Understanding Acyl Anion Equivalents	257	11. Conclusion	268
6. Tietze–Smith Linchpin Reaction	259	Acknowledgments	269
		References	269

1 INTRODUCTION

In 2006, EcoBiotics Limited, an Australian company that specializes in the discovery and preclinical development of small-molecule drug leads from the tropical rainforests of Australia and Melanesia, approached me to undertake a total synthesis of EBC-23 (**1**) (Figure 1). EBC-23 (**1**) had been isolated from *Cinnamomum laubatii* (family Lauraceae) in the rainforest in northern Queensland, Australia,¹ after the latter was identified by Dr. Paul Reddell (CSO, EcoBiotics) as a plant of interest. The reason for the synthesis request was that a screening program had identified **1** as a growth inhibitor of the androgen-independent prostate tumor cell line DU145, which was reinforced

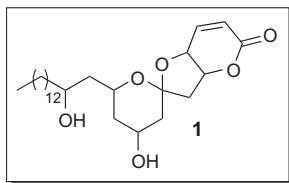


FIGURE 1 Flat structure of EBC-23.

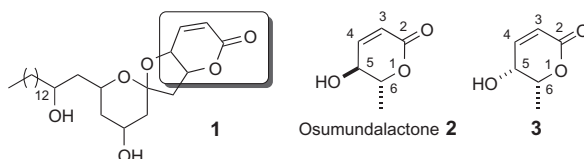


FIGURE 2 Deducing the relative stereochemistry of EBC-23 by structural comparison to the natural product osumundalactone.

in a mouse xenograph model using the same cell line (Prof. Peter Parsons, Queensland Institute of Medical Research), thus indicating potential for the treatment of refractory solid tumors in humans. However, only a flat structure had been deduced from NMR² using ACDLabs Structure Elucidator software.³ Thus, total synthesis was required to confirm relative and absolute stereochemistry, and perhaps more importantly determine process chemistry viability.

2 STRUCTURE ELUCIDATION

Before total synthesis could begin a relative stereochemical assignment was required as EBC-23 (**1**) has six stereocenters, which gives rise to 64 possible stereoisomers (2^n , n =stereocenters) or 32 relative stereochemical possibilities, and it was not going to be feasible to make them all. Therefore, in attempting to determine the relative stereochemistry of **1**, I focused on searching the literature for similar fragments; the first being the lactone moiety highlighted (Figure 2). The literature revealed the natural product osumundalactone (**2**)⁴ and the corresponding *syn*-isomer (**3**).⁵

Comparison of ¹H NMR chemical shifts (ppm) was not definitive; however, peak splitting patterns were very informative. For example, osumundalactone (**2**) displayed two sets of doublets of doublets for positions 3 and 4, whereas the *syn*-isomer (**3**) showed only one set of doublet of doublets for position 4 together with a single doublet for position 3. In comparison to the ¹H NMR spectra of **1** this suggested a match with the *syn*-isomer **3**, indicating a stereochemical relationship as demonstrated in structure **4** (see Figure 3). Unfortunately, I was unable to compare ¹³C NMR data for the

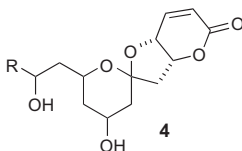


FIGURE 3 NOE conformation of the *syn*-stereochemical relationship to the lactone ring.

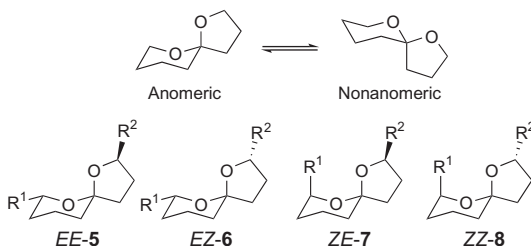
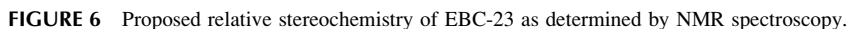
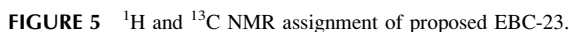


FIGURE 4 Stereochemical nomenclature of spiroacetals.

syn-isomer (**3**) with that of **1** because the Ley *et al.* paper⁵ did not report ^{13}C NMR data, although it was clear from above that it was a *syn* relationship at those positions.

Based on NOE (nuclear Overhauser effect) information at the time the stereocenter determination made was that shown in Figure 5. As the *syn* stereochemistry of the fused rings A and B had been established (see above), NOE correlations (NOE=through space interactions) with protons at C5 and C6 [4.5 ppm(t) and 5.05 ppm(m)] were first investigated. In the first instance, it was observed that a correlation between the two was present, which confirmed the *syn* configuration. Unfortunately, no useful correlation was observable when the proton at C5 (5.05 ppm) was irradiated; however, the C6 proton at 4.5 ppm correlated with the tetrahydropyran ring C13 proton at 4.4 ppm. This indicated that the stereochemistry at the ketal carbon (C8) was *EE* and was most likely a [6.5]-anomeric^{6,7} and not a [6.6]-spiroketal⁸ based on the chemical shift value of 106.5 ppm in the ^{13}C NMR [Note: these rings systems are most often called spiroacetals, but are more correctly spiroketals]. The *EE* stereochemical arrangement was the most favored due to the anomeric effect in the spiroketal, which we confirmed using DFT calculations of ground-state energies of the diastereomers.

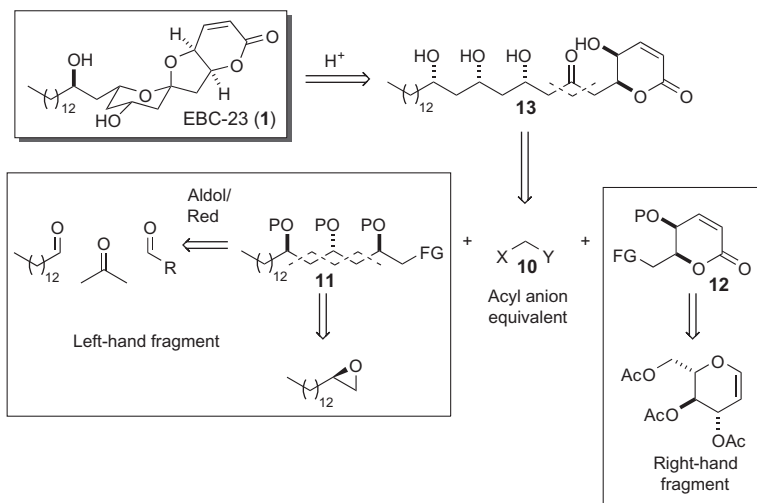
As a slight diversion, it would be useful for educational purposes to highlight spiroketal nomenclature further, but focusing on the *EE* configuration as it is pertinent to this case. In Figure 4, a [6.5]-spiroketal is shown in the anomeric and nonanomeric conformation. Taking the anomeric conformation, as indicated in structures **5–8**, when ring substituents attached to the carbon atoms at positions R¹ and R² are *cis*, then *Z* nomenclature is used. If *trans*, *E* nomenclature is applied.⁸



The *EE* stereochemistry also identified the C12 proton at 1.8 ppm as β , which in turn correlated to ring C13 proton at 4.1 ppm, also indicating β stereochemistry. Furthermore, the C13 proton at 4.4 ppm very weakly correlated with the long-chain methine proton at 3.8 ppm (C15), and because there were no OH peaks in the ^1H NMR spectrum showing hydrogen bonding, at the time I concluded that the stereochemistry at this position was α (Figure 5).

In summary, based on the above NMR evidence, I committed to structure **9** shown in Figure 6. It is at this point in the story that I draw the readers' attention to the fact that it has become increasingly common that natural products that have their chemical structures elucidated by NMR spectroscopy have those structures later revised, usually as a result of a natural product total synthesis campaigns!⁹ *Sleepless night 1.*

With the stereochemical assignment in hand, total synthesis could begin. Although we already had a pre-existing relationship with EcoBiotics for some years prior, this was the first major synthetic project. I remember the CEO, Dr. Victoria Gordon, asking me how long the synthesis would take and my guess was between 1–2 years, but I also said that natural product total synthesis was always fraught with danger and completion could take even longer. This worried both of us because from the company’s perspective, they needed it synthesized quickly to demonstrate proof of concept at minimal cost. From my perspective, my reputation was on the line knowing all too well that total synthesis never goes smoothly at the best of times (*Sleepless night 2*). A good case in point was our syntheses of vibsanin E and *epi*-vibsanin, which was a 10-year campaign, although the structures were more complex than that of our current target.¹⁰



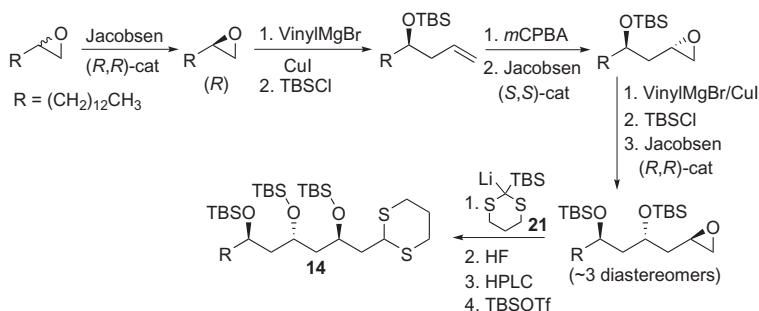
SCHEME 1 Retrosynthetic plan to attempt total synthesis of EBC-23.

3 RETROSYNTHETIC PLAN

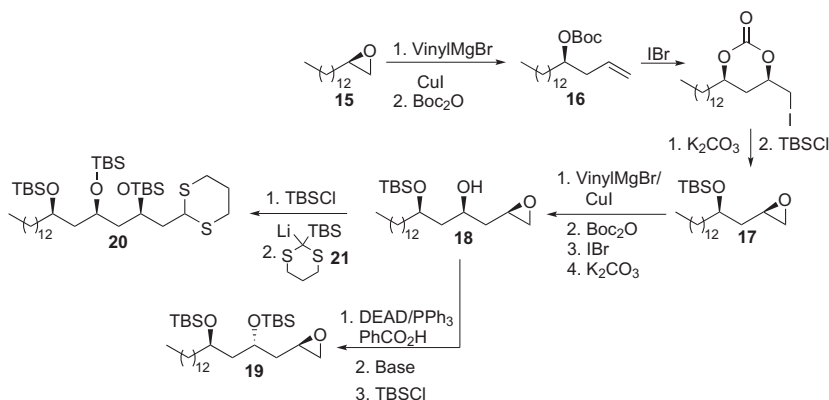
There was essentially one main approach (with a number of built in fallback strategies) that was convergent in nature and relied heavily on an acyl anion equivalent (**10**) to introduce both halves (LHF **11** and RHF **12**) and also acted as the spiroketal carbon center in the ketone oxidation state (i.e., **13**). Ketone **13** could then be treated with acid to cyclize the linear precursor to EBC-23 (**1**), driven thermodynamically by the anomeric effect (Scheme 1).

4 STARTING THE TOTAL SYNTHESIS

Initially, we set about constructing the left-hand fragment **11**, where the linking functional group (FG) seen in Scheme 1 was an epoxide and the acyl anion was a dithiane. This extensive amount of work was performed by Drs. Heiko Schill (University of Göttingen, Prof. Armin de Meijere), Rebecca Grange (University of Melbourne, Prof. Carl Schiesser), and Lin Dong (Chengdu Institute of Organic Chemistry, Prof. Liu-Zhu Gong). The first approach to LHF **11** was modeled on repetitive Jacobsen resolutions¹¹ with the idea that we could maintain ultimate stereochemical flexibility should our NMR assignment be incorrect. However, difficulties arose with the second and third Jacobsen resolutions (Scheme 2). The second worked to about 80% conversion, whereas the third resolution did not work at all, most likely due to the very lipophilic nature of the substrate. Nevertheless, the resulting three diastereomers were carried through and reacted with the anion of TBS-dithiane **21**, which underwent a Tietze–Smith linchpin reaction (discussed in greater detail below, see Scheme 8). The TBS groups were globally



SCHEME 2 An approach to the left-hand fragment.



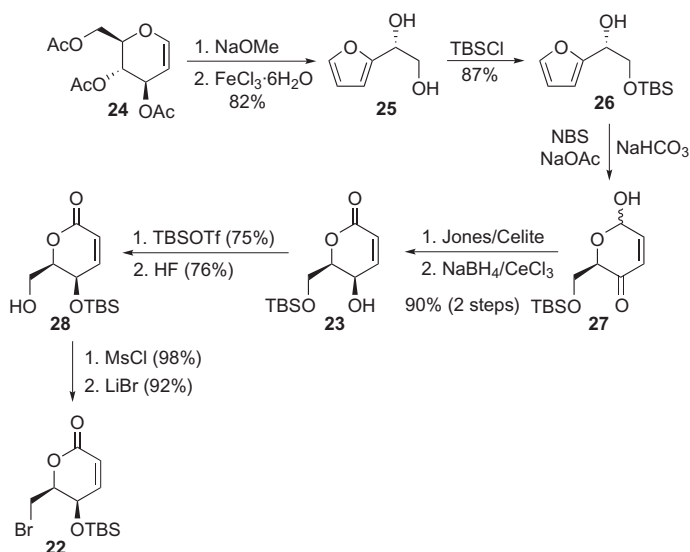
SCHEME 3 The second approach to the left-hand fragment.

deprotected to give the triol, which was purified by HPLC and the tris-TBS protection reintroduced with TBSOTf to give **14** (Scheme 2). Overall this sequence was long-winded, low-yielding and thus not going to be viable; hence another route was investigated.

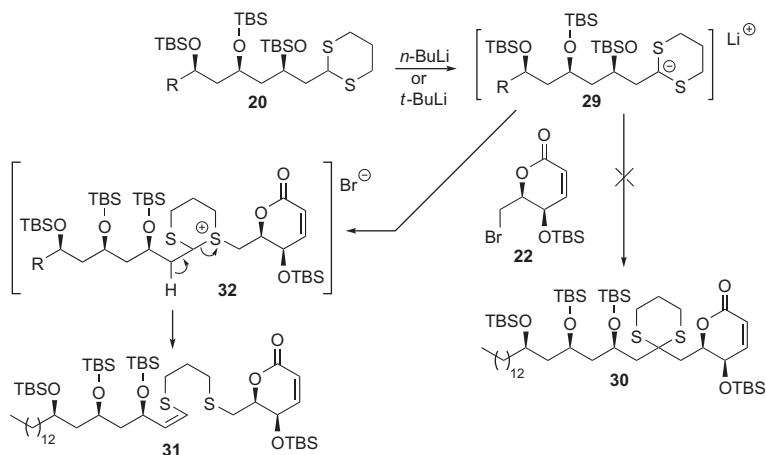
We turned to an iterative Bartlett iodocarbonate cyclization¹² strategy. Reaction of epoxide **15** with vinyl magnesium bromide, as seen above, followed by treatment with di-*tert*-butyl dicarbonate gave **16** (>95% over two steps). Treatment of **16** with iodine bromide quantitatively gave iodocarbonate, which on exposure to base followed by TBSCl produced epoxide **17** (56% over two steps). Repetition of this process afforded epoxy alcohol **18**, which under Mitsunobu conditions afforded the desired material **19** (Scheme 3). Although this was an improvement on the Jacobsen route (Scheme 2), it was still reasonably long-winded. That being said, we decided to react **18** with the anion of TBS-dithiane **21**. This gave **20** (Scheme 3) in a quantity sufficient to test dithiane alkylation with the right-hand fragment. The desired left-hand fragment **19** was kept in reserve due to the low quantity of material in hand.

Bromide **22** was chosen as the target right-hand fragment since classical dithiane umpolung chemistry revolved heavily around alkylation with alkyl bromides. A literature search revealed that hydroxylactone **23** had been reported by O'Doherty *et al.*¹³ This compound had been prepared in a succinct and clever way starting from commercial tri-*O*-acetyl-D-glucal **24**. We accidentally discovered that the first transformation to **25** could be improved¹⁴ using iron (III) chloride [Dr. Archim Porzelle (Technische Universität Darmstadt, Prof. Wolf-Dieter Fessner)]. Furan **25** was mono-protected using TBSCl in a straightforward manner to give **26**. The Achmatowicz reaction was deployed, which occurred quantitatively as reported by O'Doherty to give **27**. It was at this point that we encountered significant difficulty with the subsequent step, the Jones oxidation. Every time we went to repeat the Jones oxidation, we lost all the material. It was not until we made contact with Prof. O'Doherty that we were alerted to an omission in the experimental procedure that had inadvertently occurred. Although a minor omission, Celite[®] was critical as an additive to neutralize the Jones reagent, as the substrate (i.e., **27**) was very acid sensitive. The ensuing Luche reduction proceeded smoothly to give **23**. Now in new territory, protecting group “hokey pokey” was required to access **28**, which unfortunately could not be directly converted to bromide **22** in acceptable yields. Instead, a two-step process via mesylate formation and a Finkelstein reaction with lithium bromide afforded the target right-hand fragment **22** in 90% yield (Scheme 4).

With the two halves now available, dithiane **20**, possessing the undesired stereochemistry, was used as a test vehicle to attempt the key coupling of



SCHEME 4 An approach to the right-hand fragment.

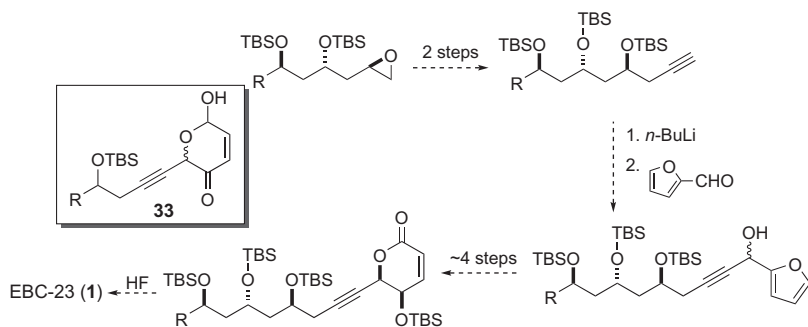


SCHEME 5 Failed attempt at uniting the right- and left-hand fragments.

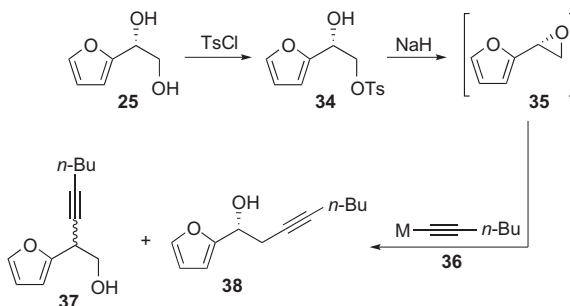
the left-hand fragment to the right-hand fragment (i.e., **22**). Utilizing a variety of strong bases and conditions to generate anion **29** and then subsequently quench with bromide **22** did not give on any occasion even a trace of the desired coupled product **30** (Scheme 5). Working up the crude reaction, we could see in the ^1H NMR a product that closely resembled compound **31**, which arises from S-alkylation and elimination of the dithiane (i.e., **32**) as opposed to C-alkylation (i.e., **30**). This was a disaster! *Sleepless night 3*. However, it had been reported once before by Corey and Seebach,¹⁵ when umpolung chemistry was first unveiled. Further consultation with the literature revealed that in some instances dithianes with large groups attached have failed to undergo reaction with alkyl halides, epoxides, and aldehydes,¹⁶ deprotonation being the major problem.¹⁷ Some fixes to this problem have involved making stannylated dithianes and then performing a transmetalation,¹⁸ but it was not possible to install tin functionality because of the nature of the Tietze–Smith linchpin reaction (more details below). We did, however, perform some deuterium quench experiments (CD_3OD), which showed $n\text{-BuLi}$ was not working, whereas $t\text{-BuLi}$ was providing at best a 50% yield of the desired anion **29**.

This heart-stopping result sent us spinning in a number of frantic directions trying to couple the two halves, but avoid dithiane S-alkylation. First, we switched to building the spiroketal from an acetylene (e.g., Forsyth methodology),¹⁹ which would allow us to also perform the Achmatowicz reaction and thus avoid the use of a bromide leaving group (Scheme 6). However, construction of a model system (**33**) quickly suggested stereocontrol of the alkyne addition to furfural was going to be an issue.

In an attempt to control the stereochemistry of addition, we investigated the use of chiral furan epoxide **35**, which was obtained from furan **25** via



SCHEME 6 Exploring back up routes to unite the right- and left-hand fragment.



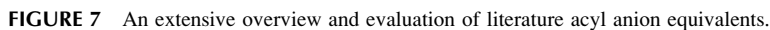
SCHEME 7 Developing chemistry involving the reactive furan epoxide **35**.

tosylate **34**. The epoxide could not be isolated but could easily be handled in solution. The only downside was that it showed mixed selectivity toward a range of nucleophiles, especially acetylides (e.g., **36**), giving regioisomers (**37** and **38**) in addition to showing poor stereoselectivity in the formation of **37** (Scheme 7).¹⁴ Therefore, this line of attack was abandoned.

5 UNDERSTANDING ACYL ANION EQUIVALENTS

Concluding that an acyl anion equivalent was required to couple both the LH and RH fragments, but nucleophilic sulfur atoms within the acyl anion equivalent needed to be avoided, we tested an extensive range of known acyl anion equivalents in epoxide ring-openings in an attempt to understand acyl anion reactivity (Figure 7).²⁰ You might have expected such a study to have already been reported in the literature; however, you would have been very wrong and, like us, very surprised.

All known acyl anion equivalents that contain a nucleophilic sulfur atom (unoxidized) open epoxides (e.g., **39–43**). Much to our surprise, all known

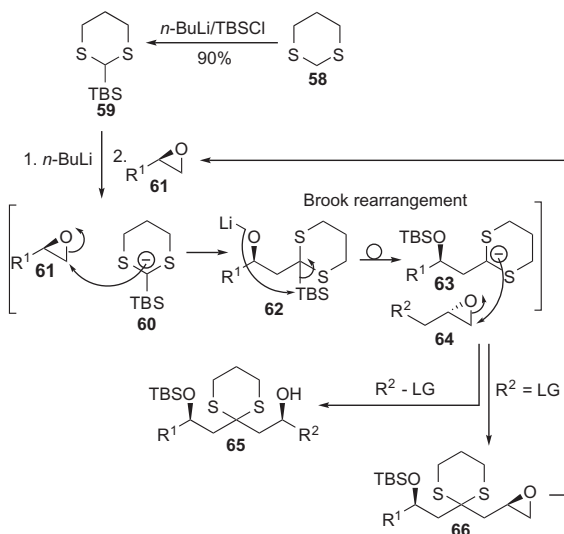


Sometime after the EBC-23 project had been completed, Dr. Wilhelm Eger (University of Jena, Prof. Ernst Anders), in collaboration with Prof. Tim Clark (University of Erlangen, Germany), ran an in-depth computational study into this phenomenon. That study, together with the experimental results,²⁰ demonstrated that dithianes, and their silyl derivatives, remain the most versatile, which may have been known prior to this study, but had not been proven. Furthermore, the study derived general design rules for the perfect acyl anion equivalent in the case of epoxide ring-opening. That is, “Second row substituents are superior to first row substituents, as resonance effects decrease anion reactivity, but polarization effects help stabilize the anions. As resonance effects decrease the reactivity, any substituent that enhances resonance decreases acyl anion reactivity and subsequent performance.”²⁰

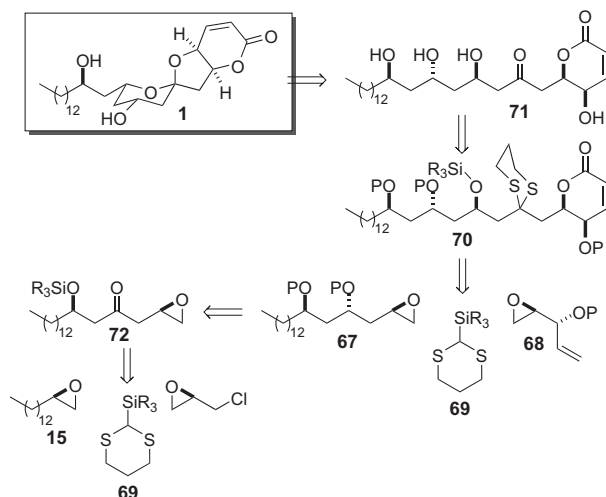
6 TIETZE–SMITH LINCHPIN REACTION

It was now clear that no reasonable substitute for the dithiane ring system as an acyl anion equivalent was available so the retrosynthetic deck was reshuffled building on what we had learned. This led us to reconsider the Tietze–Smith linchpin reaction,²¹ but in the form of Smith Anion Relay chemistry.²² A brief overview of these reactions is provided below (Scheme 8). Given that these methods are founded on the Brook rearrangement, a silyl group needs to be installed, as this FG migrates to produce a secondary anion. The silyl group, which can be virtually any member of this common protecting group class (another bonus of the methodology), is installed onto the dithiane ring. For example, **58** is treated with *n*-BuLi and the resulting anion quenched with TBSCl to give **59**. Exposure of **59** to *n*-BuLi gives anion **60**, which can react with an epoxide (e.g., **61**). This process gives in the first instance **62**, which then undergoes a Brook rearrangement, regenerating an anion at the dithiane carbon center (i.e., **63**). Anion **63** is then poised to undergo further *in situ* (one-pot) reactions. In the case of the Tietze–Smith linchpin process, further reaction with a second epoxide (e.g., **64**) is performed, leading to products of the type represented by **65**. If **64** contains a suitable leaving group, for example, a chloride (e.g., epichlorohydrin), then the resulting product is an epoxide (e.g., **66**), which can be used in a secondary cycle or relay (Scheme 8).

After becoming engrossed with this chemistry, we had an epiphany. Could the Tietze–Smith linchpin reaction be used twice? If this was to be executed the previously constructed right-hand fragment (i.e., bromide **22**) could not



SCHEME 8 Tietze–Smith linchpin approach to the left-hand fragment.



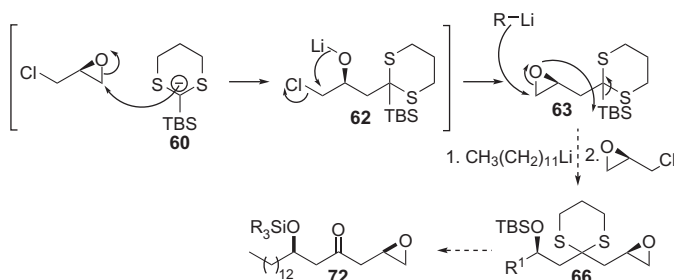
SCHEME 9 Revised retrosynthesis of EBC-23 based on the Tietze–Smith linchpin methodology.

be utilized, however, an obvious fix was to build the lactone downstream using ring-closing metathesis. The refined retrosynthesis was now as follows: silylated dithiane **69** would be deprotonated and then reacted with the chiral epoxide **15** and subsequently with epichlorohydrin. Removal of the dithiane to give ketone **72** and selective reduction should open access to the left-hand fragment **67**. Utilizing silylated dithiane **69** again, but in conjunction with the left-hand fragment **67** and the known higher functionalized epoxide **68** would hopefully lead to the advanced intermediate **70** after ring-closing metathesis (RCM). Finally, global deprotection (i.e., **71**), with Lady Luck on our side, might be expected to produce the desired target on treatment with acid (Scheme 9).

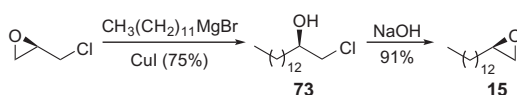
7 REFINING THE SYNTHETIC CAMPAIGN

With the refined retrosynthesis in place, some further cleaning of the edges was required before launching the campaign. First, a decision is needed to be made regarding the exact mode of construction being deployed for ketone **72**. Although only one route was shown in Scheme 9, there was another variation on the linchpin reaction that could give rise to **72**. Instead of using epoxide **15**, epichlorohydrin could function twice to give **66**, which leads to ketone **72** upon removal of the dithiane. However, although epoxide **63** could be easily obtained, various attempts to react it with the long-chain alkyl lithium failed to produce **66** efficiently (Scheme 10).

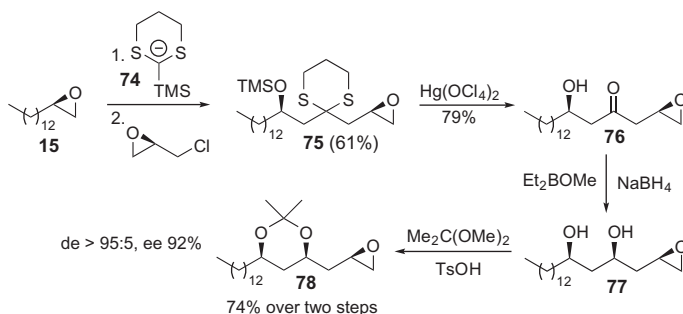
Second, now that it was a requirement to investigate the synthesis of **72** using chiral epoxide **15**, this epoxide was needed in large quantities.



SCHEME 10 Tietze–Smith linchpin failed approach to the left-hand fragment.



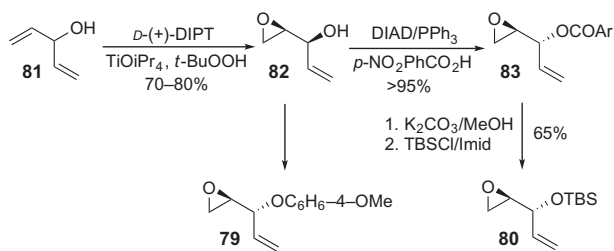
SCHEME 11 Generating epoxide **15** as a single enantiomer.



SCHEME 12 Successful Tietze–Smith linchpin approach to the left-hand fragment.

Previously, it had been prepared by Jacobsen epoxide resolution; however, a more efficient route was required. A collection of methodologies were tested, but these were surpassed by the method of Lepoittevin,²³ which gave **15** in high enantiomeric excess and in large quantities, via the chlorohydrin **73**, starting from epichlorohydrin as either enantiopode (Scheme 11).

Having smoothed the rough edges of the refined retrosynthesis, we could embark on the journey with some confidence. Initially, we discovered that substituting TBS-dithiane (**59**) for TMS-dithiane led to a fortuitous step reduction further along the sequence. Thus, reaction of **74** with (*R*)-epoxide **15**, and then with (*R*)-epichlorohydrin, gave the difunctionalized dithiane **75** in 61% yield (Scheme 12). However, when the dithiane function in **75** was oxidatively removed with mercury perchlorate, this did not give the desired ketone, but hydroxyketone **76** in high yield, that is, the TMS protecting group had also been removed, which did not occur with TBS. In the next step, however, we were unable to find conditions to facilitate an Evan's

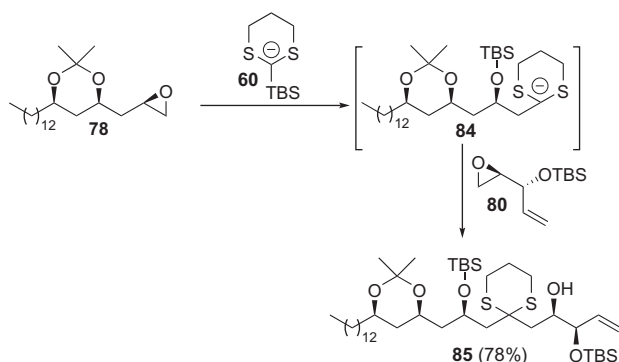
SCHEME 13 Synthesis of epoxides **79** and **80**.

anti-reduction²⁴ to access the desired stereochemistry (see **67** in Scheme 9 above). *Sleepless night 4*. With the pressure of delivery and own reputation hanging over our heads, we decided to investigate *syn*-selective reduction²⁵ hoping to obtain a left-hand fragment, albeit with the wrong stereochemistry, to test the remaining route. The *syn*-reduction worked perfectly, giving **77**, and after ketal protection,²⁶ the (stereochemically incorrect) left-hand fragment **78** (i.e., (*R,R,R*)-enantiomer) was obtained. We had decided to change the diol protection strategy from TBS to acetone to reduce steric demand.

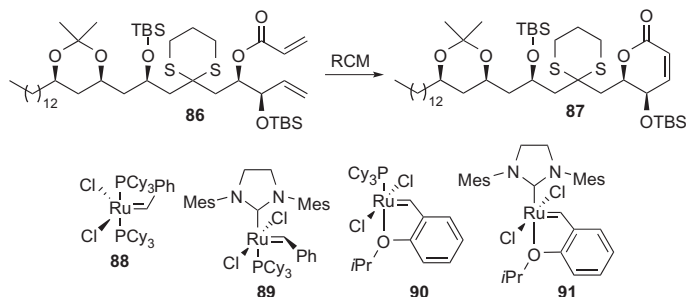
To achieve both the coupling and construction of the right-hand fragment, an enantiopure allyl epoxide of type **79** and **80** was required (Scheme 13). Synthesis of both epoxides could be realized starting from divinyl carbinol **81** via a direct enantiotopic group and diastereotopic face selective Sharpless epoxidation highlighted by Schreiber and others to give the known epoxide **82**.²⁷ Even with good literature support for the synthesis of **82**, it was not straightforward. We ultimately used a combination of procedures and modified the work-up. After these teething issues, we could access reasonable supplies although the reaction takes about 10 days! With **82** in hand, the Mitsunobu reaction could be employed to invert stereochemistry and simultaneously install the protecting group. In the case of the known epoxide **79**,²⁸ this could be undertaken in one step using *p*-methoxyphenol in the Mitsunobu reaction. Unfortunately, for epoxide **80** we needed a two-step process to introduce the TBS protecting group via ester **83** (Scheme 13).

Having ironed out the wrinkles in producing epoxides **68** and **79** (and **80**), the key linchpin coupling could be attempted. Our first attempt of reacting the dithiane anion **60** with **78** and **79** failed. *Sleepless night 5*. However, it was discovered that the change to a silyl protecting group (i.e., epoxide **80**) gave the long awaited transformation affording **85**, as shown in Scheme 14.

Confidence was now very high knowing that the next stage, the RCM, was just ahead and that this reaction was reported to work like a dream. Acylating the free alcohol with acryloyl chloride proceeded smoothly providing acrylate **86** in 82% yield. Unfortunately, the dream was soon shattered. *Sleepless night 5*. Contrary to literature precedent, RCM was not straightforward and substantial investigation was required to drive the formation of the requisite lactone **87**. The most popular catalyst utilized in



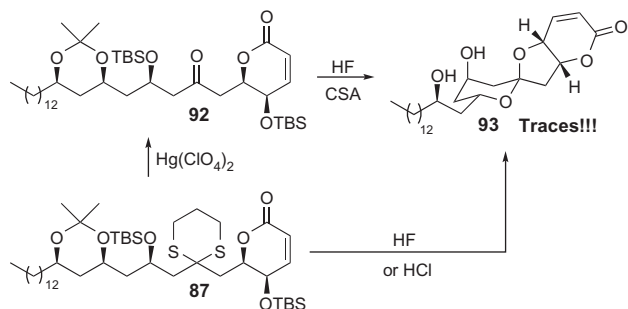
SCHEME 14 Uniting the left- and right-hand building block via a second Tietze–Smith linchpin.



SCHEME 15 Ring-closing metathesis.

the literature for the formation of lactones of this type, with hydroxyl substitution in the γ -position,²⁹ was the Grubbs first-generation catalyst **88**, but all attempts with this catalyst failed. The second-generation catalyst from the Grubbs group (**89**) and even the first-generation Hoveyda–Grubbs (**90**) catalyst again failed to deliver. It was only when the second-generation Hoveyda–Grubbs (**91**) catalyst was used under microwave irradiation that lactone **87** was obtained (65% yield) (Scheme 15).

We attributed the difficulties with this otherwise trivial RCM reaction to the close proximity of the dithiane ring to the metal center after catalyst coordination. This could allow a sulfur atom to coordinate to ruthenium, preventing catalyst turnover. A fix to this problem was not obvious as a dithiane was required as the acyl anion equivalent as determined above; nevertheless, dithiomethylmethane was briefly investigated as a dithiane substitute, but this resulted in lower yields at various points in the synthesis leading up to the acrylate. Since this work was originally reported, however, more RCM catalysts have become commercially available from various chemical suppliers and those might be able to overcome the difficulties we experienced.



SCHEME 16 Developing a deprotection sequence.

Accessing the full linear compliment (i.e., **87**) brought the project to a “do or die” point. Unmasking the ketone and alcohol functions, by global or partial deprotection, was critical in determining whether this stereochemical array would fold into the spiroketal final target. At this nexus, we were mindful that we did not have the correctly predicted stereochemistry, so it was likely that spiroketal folding would not occur.

For this part, we took guidance from a very well-researched review by Pihko.³⁰ Methods for direct conversion of **87** to **93**, that is, treatment with HF ·pyridine, aq. HF , or HCl , were first investigated. These provided only traces of the cyclized material **93** (Scheme 16). We resorted to a stepwise approach by first unmasking the ketone functionality (i.e., **92**) by deprotecting the dithiane **87**. Ketone **92** was then bombarded with a variety of acids (e.g., aq. HF , CSA) under a wide variety of conditions only to also afford trace amounts of the target **93** (Scheme 16).

8 COMPLETING THE TOTAL SYNTHESIS

What began as *Sleepless night 6* soon became one of the most pleasurable slumbers I had had in a few years. When Dr. Heiko Schill informed me that he had only obtained trace amounts of **93** I asked to see the ^1H NMR spectra, which had been obtained from HPLC fractions of the crude reaction mixture provided by Prof. Peter Parsons’ laboratory. Heiko did not realize it, but he was showing me spectra of the natural product!!! This was not his fault, because he was not involved in the elucidation part of the project and was not as familiar as myself with the natural product spectra. Nevertheless, how could this be? Surely, we did not make two errors in the stereochemical assignment (i.e., **9**). Yes, we did! As detailed in Figure 8, structure **93** and the mirror image **94** will have the same NMR spectra, and when compared to natural EBC-23(**1**) were an identical match except for the OH resonances. Because our synthetic sample was being measured at a concentration of <0.5 mg/mL, this was conducive to setting up extensive intramolecular

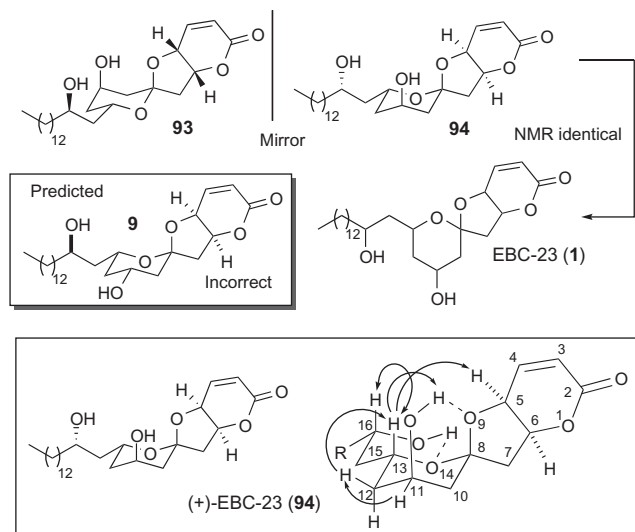
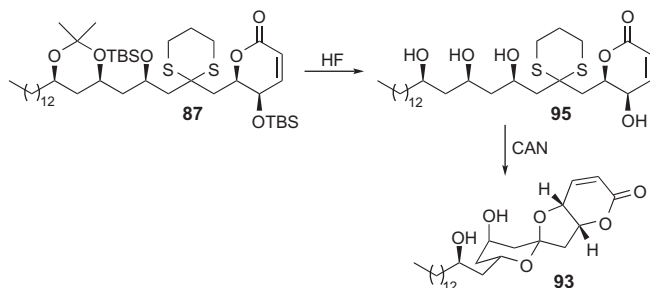


FIGURE 8 Understanding mistakes made in the spectroscopic stereochemical determination of EBC-23.

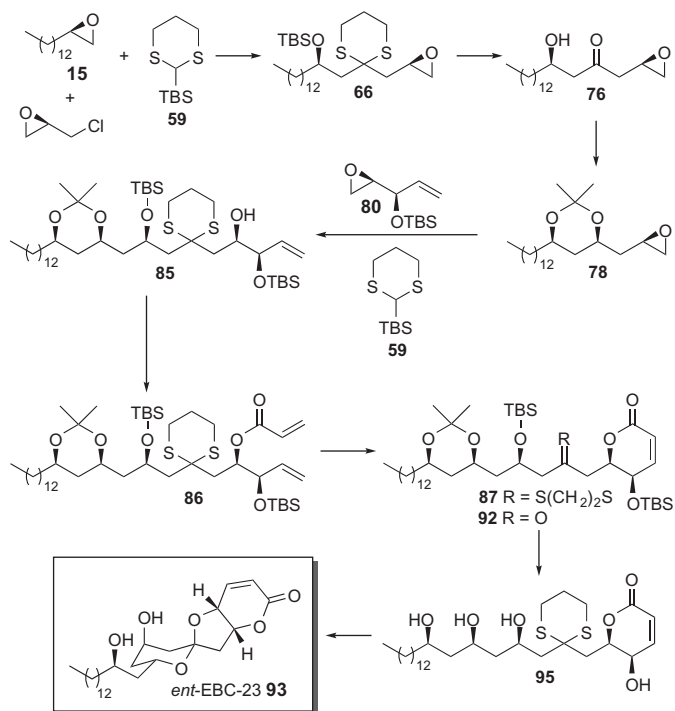
hydrogen bonding. Rerunning the NOE spectra on this sample provided definitive correlations not possible with the natural material. Why? In the case of the natural material, we had been provided with reasonable amounts and in relative terms we overloaded (e.g., 5 mg/mL) the NMR sample tube (i.e., measuring at higher concentration), quenching hydrogen bonding due to intermolecular exchange (Figure 8).

Although serendipity was at play in terms of the Evans *anti*-reduction not working (**67**, Scheme 9), we would have worked it out sooner or later. For example, we later determined that the conditions of the Evans reduction protocol, which include the solvents acetonitrile and acetic acid, were too polar to solubilize the “fatty” ketone **76** (Scheme 12). Simply reordering the reagent addition solved this when ketone **76** was added last.

We were not yet out the woods, however, as the yield of the final cyclization was at best 5%. Work by Ho *et al.*,³¹ demonstrated that cerium ammonium nitrate (CAN) can be used to deprotect dithianes. Because of the difficulty above when investigating direct cyclization, we decided to deprotect the alcohol functions first, before treating with CAN. Thus, treating **87** with hydrogen fluoride pyridine complex gave polyol **95**, which on exposure to CAN produced the target in a much improved yield of 54% over two steps (Scheme 17). Although surprised by the performance of CAN to both remove the dithiane ring system and efficiently promote the cyclization, we wondered why. Reports by both Smith³² and Evans³³ suggested that the spiroketal formation was most likely mediated by cerium via metal-templated preorganization.^{32,33}



SCHEME 17 Completing the total synthesis of EBC-23.



SCHEME 18 Overall successful synthetic route to EBC-23.

Comparison of the optical rotation of **93** to that of the natural material showed that the nonnatural isomer had been synthesized. The whole process was repeated with the enantiomers of the starting materials, which afforded material (i.e., **94**) matching the natural product in all aspects. *Sleepless nights were finally over.* The overall successful synthesis is shown in Scheme 18.

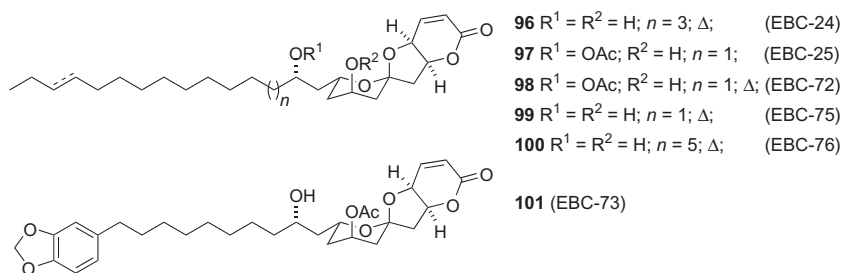
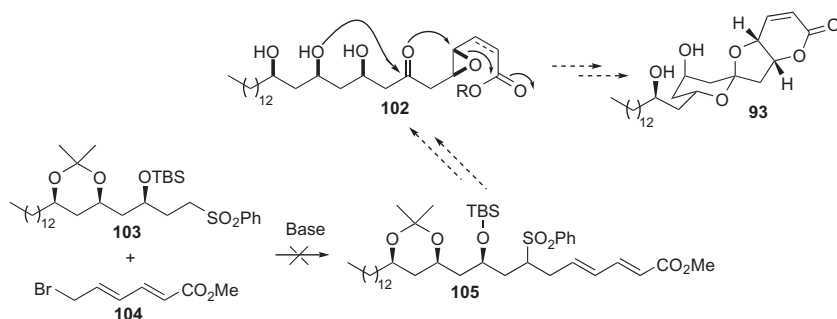


FIGURE 9 Other EBC-23 family members.

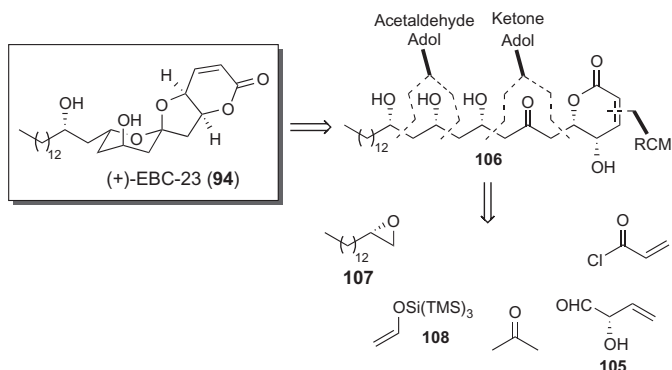


SCHEME 19 Exploring a biomimetic approach to EBC-23.

The absolute and relative stereochemical determination of (+)-EBC-23 (**94**) allowed us to determine the relative stereochemistries of the related EBC-23 family members of which there are quite a few (i.e., **96–101**) (Figure 9).

9 BIOMIMETIC ATTEMPTS

Considering our group had substantial expertise with the biomimetic synthesis of natural products,³⁴ a second-generation synthesis was briefly investigated based on a proposed biosynthetic pathway (e.g., **102**), which constituted an extension of that known from the related polyketide lactones already isolated from the Lauraceae family.³⁵ Since **103** was readily available from addition of phenyl methyl sulfone to **78**, we investigated coupling to allyl bromide **104**, as the literature³⁶ suggested that the allyl function seen in **104** could be converted into lactones of type seen in the EBC-23 system. Unfortunately, all attempts to access **105** via reaction of **103** and **104** failed (Scheme 19).



SCHEME 20 Yamamoto's synthesis of EBC-23.

10 YAMAMOTO SYNTHESIS

To complete the story, 2 years later the Yamamoto group published a synthesis of EBC-23 (**94**) using their “supersilyl” aldol chemistry.³⁷ The key to the retrosynthesis was the application of supersilyl enol ether **108** and epoxide **107** to forge most of the left-hand portion of the target, while acetone in the form of a second supersilyl unit brought the left- and right-hand linear units together followed by RCM. This approach lowered the overall number of steps from 15 to 10, although the Yamamoto group combined acylation, RCM, and HF·pyridine deprotection into a one-pot sequence. Our procedure is also amenable to such a one-pot sequence and so the difference in steps is about 3. The real test of any total synthetic route will be whether it performs on scale in the hands of the process chemists. This remains to be seen (Scheme 20).

11 CONCLUSION

In conclusion, working with industry on tough projects has many challenges, but can be very rewarding. Although I generated a number of gray hairs, and lost a lot of sleep, without doubt I have to say it was worth it.

Key points

1. Assisted a home-grown Australian company (EcoBiotics Limited).
2. Learned a lot of chemistry (advanced polyketide synthesis).
3. Filled a void in the literature (acyl anion equivalent study).
4. Provided an excellent training ground for post-docs to further their careers.
5. Working with a molecule that has potential human benefit.

ACKNOWLEDGMENTS

Drs. Victoria Gordon and Paul Reddell (EcoBiotics Limited) for entrusting the Williams' group with this very enjoyable and rewarding project, in addition, to a very fruitful longstanding collaboration. Emeritus Prof. William Kitching (University of Queensland) for discussions and mentorship. Prof. Peter Parsons (Queensland Institute of Medical Research) for mentorship and a longstanding collaboration in cancer biology. Drs. Dong, Schill, Grange, Porzelle, and Eger for their tour de force efforts in the laboratory and on the computer. The University of Queensland and EcoBiotics Limited for financial support.

REFERENCES

1. (a) Dong, L.; Gordon, V. A.; Grange, R. L.; Johns, J.; Parsons, P. G.; Porzelle, A.; Reddell, P.; Schill, H.; Williams, C. M. *J. Am. Chem. Soc.* **2008**, *130*, 15262–15263; (b) Dong, L.; Schill, H.; Grange, R. L.; Porzelle, A.; Johns, J. P.; Parsons, P. G.; Gordon, V. A.; Reddell, P. W.; Williams, C. M. *Chem. Eur. J.* **2009**, *15*, 11307–11318.
2. Reddell, P. W.; Gordon, V. A. WO 2007070984A1 20070628 PCT Int. Appl., 2007.
3. ACD/H and C NMR Predictor. ACD/Structure Elucidator, version 10.0, Advanced Chemistry Development, Inc., Toronto ON, Canada, www.acdlabs.com, 2007.
4. Saotome, C.; Ono, M.; Akita, H. *Chem. Pharm. Bull.* **2001**, *49*, 849–853, and references therein.
5. Ley, S. V.; Armstrong, A.; Díez-Martín, D.; Ford, M. J.; Grice, P.; Knight, J. G.; Kolb, H. C.; Madin, A.; Marby, C. A.; Mukherjee, S.; Shaw, A. N.; Slawin, A. M. Z.; Vile, S.; White, A. D.; Williams, D. J.; Woods, M. *J. Chem. Soc., Perkin Trans. 1* **1991**, 667–692.
6. Pihko, P. M.; Aho, J. E. *Org. Lett.* **2004**, *6*, 3849–3852.
7. La Cruz, T. E.; Rychnovsky, S. D. *J. Org. Chem.* **2007**, *72*, 2602–2611.
8. Jacobs, M. F.; Glenn, M. P.; McGrath, M. J.; Zhang, H.; Brereton, I.; Kitching, W. *ARKIVOC* **2001**, (vii), 114–137.
9. (a) For reviews, see: Nicolaou, K. C.; Snyder, S. A. *Angew. Chem. Int. Ed.* **2005**, *44*, 1012–1044; (b) Maier, M. E. *Nat. Prod. Rep.* **2009**, *26*, 1105–1124; (c) Suyama, T. L.; Gerwick, W. H.; McPhail, K. L. *Bioorg. Med. Chem.* **2011**, *19*, 6675–6701.
10. Williams, C. M. Harmata, M., Ed.; *Strategies and Tactics in Organic Synthesis*; Vol. 8; Elsevier: Amsterdam, 2012 pp 395–412.
11. Schaus, S. E.; Brandes, B. D.; Larrow, J. F.; Tokunaga, M.; Hansen, K. B.; Gould, A. E.; Furrow, M. E.; Jacobsen, E. N. *J. Am. Chem. Soc.* **2002**, *124*, 1307–1315.
12. Bartlett, P. A.; Meadows, J. D.; Brown, E. G.; Morimoto, A.; Jernstedt, K. K. *J. Org. Chem.* **1982**, *47*, 4013–4018.
13. (a) Harris, J. M.; O'Doherty, G. A. *Org. Lett.* **2000**, *2*, 2983–2986; (b) Harris, J. M.; Li, M.; Scott, J. G.; O'Doherty, G. A. Harmata, M., Ed.; In: *Strategies and Tactics in Organic Synthesis*; Vol. 5; Elsevier: Amsterdam, 2004 pp 221–253.
14. Porzelle, A.; Gordon, V. A.; Williams, C. M. *Synlett* **2007**, 1619–1621.
15. (a) Corey, E. J.; Seebach, D. *Angew. Chem. Int. Ed. Engl.* **1965**, *4*, 1075–1077; (b) Seebach, D.; Jones, N. R.; Corey, E. J. *J. Org. Chem.* **1968**, *33*, 300–305.
16. (a) Fürstner, A.; Fenster, M. D. B.; Fasching, B.; Godbout, C.; Radkowski, K. *Angew. Chem. Int. Ed.* **2006**, *45*, 5510–5515; (b) Kinoshita, M.; Taniguchi, M.; Morioka, M.; Takami, H.; Mizusawa, Y. *Bull. Chem. Soc. Jpn.* **1988**, *61*, 2147–2156; (c) Oppong, I.; Pauls, H. W.; Liang, D.; Fraser-Reid, B. *J. Chem. Soc. Chem. Commun.* **1986**, 1241–1244; (d) Hanessian, S.; Pougny, J. R.; Boessenkool, I. K. *Tetrahedron* **1984**, *40*, 1289–1301.

17. (a) Ide, M.; Yasuda, M.; Nakata, M. *Synlett* **1998**, 936–938; (b) Ide, M.; Nakata, M. *Bull. Chem. Soc. Jpn.* **1999**, 72, 2491–2499; (c) Lipshutz, B. H.; Garcia, E. *Tetrahedron Lett.* **1990**, 31, 7261–7264.
18. Seebach, D.; Willert, I.; Beck, A. K.; Groebel, B. T. *Helv. Chim. Acta* **1978**, 61, 2510–2523.
19. See for example Aiguade, J.; Hao, J.; Forsyth, C. J. *Org. Lett.* **2001**, 3, 979–982.
20. Eger, W. A.; Grange, R. L.; Schill, H.; Goumont, R.; Clark, T.; Williams, C. M. *Eur. J. Org. Chem.* **2011**, 2548–2553.
21. (a) Smith, A. B., III; Adams, C. M. *Acc. Chem. Res.* **2004**, 37, 365–377; (b) Imai, Y.; Kamon, K.; Kawaguchi, K.; Tajima, N.; Sato, T.; Kuroda, R.; Matsubara, Y. *Lett. Org. Chem.* **2009**, 6, 588–592; (c) Tietze, L. F.; Geissler, H.; Gewert, J. A.; Jakobi, U. *Synlett* **1994**, 511–512; (d) Smith, A. B.; Pitram, S. M.; Boldi, A. M.; Gaunt, M. J.; Sfougataakis, C.; Moser, W. H. *J. Am. Chem. Soc.* **2003**, 125, 14435–14445.
22. Smith, A. B., III; Tong, R. *Org. Lett.* **2010**, 12, 1260–1263.
23. Choukchou-Braham, N.; Asakawa, Y.; Lepoittevin, J.-P. *Tetrahedron Lett.* **1994**, 35, 3949–3952.
24. Evans, D. A.; Chapman, K. T.; Carreira, E. M. *J. Am. Chem. Soc.* **1988**, 110, 3560–3578.
25. Chen, K.-M.; Hardtmann, G. E.; Prasad, K.; Repič, O.; Shapiro, M. J. *Tetrahedron Lett.* **1987**, 28, 155–158.
26. Lipshutz, B. H.; Kozlowski, J. A. *J. Org. Chem.* **1984**, 49, 1147–1149.
27. (a) Häfele, B.; Schröter, D.; Jäger, V. *Angew. Chem. Int. Ed. Engl.* **1986**, 25, 87–89; (b) Hatakeyama, S.; Sakurai, K.; Takano, S. *J. Chem. Soc. Chem. Commun.* **1985**, 1759–1761; (c) Schreiber, S. L.; Schreiber, T. S.; Smith, D. B. *J. Am. Chem. Soc.* **1987**, 109, 1525–1529; (d) Zhi-cai, S.; Chun-min, Z.; Guoqiang, L. *Heterocycles* **1995**, 41, 277–287; (e) Nakatsuka, M.; Ragan, J. A.; Sammakia, T.; Smith, D. B.; Uehling, D. E.; Schreiber, S. L. *J. Am. Chem. Soc.* **1990**, 112, 5583–5601.
28. Evans, P. A.; Cui, J.; Gharpure, S. J.; Polosukhin, A.; Zhang, H.-R. *J. Am. Chem. Soc.* **2003**, 125, 14702–14703.
29. (a) Nicolaou, K. C.; Rodríguez, R. M.; Mitchell, H. J.; van Delft, F. L. *Angew. Chem.* **1998**, 110, 1975–1977; (b) Nicolaou, K. C.; Rodríguez, R. M.; Mitchell, H. J.; Suzuki, H.; Fylaktakidou, K. C.; Baudoin, O.; van Delft, F. L. *Chem. Eur. J.* **2000**, 6, 3095–3115.
30. Aho, J. E.; Pihko, P. M.; Rissa, T. K. *Chem. Rev.* **2005**, 105, 4406–4440.
31. Ho, T.-L.; Ho, H. C.; Wong, C. M. *J. Chem. Soc. Chem. Commun.* **1972**, 791.
32. Smith, A. B.; Doughty, V. A.; Lin, Q.; Zhuang, L.; McBriar, M. D.; Boldi, A. M.; Moser, W. H.; Murase, N.; Nakayama, K.; Sobukawa, M. *Angew. Chem. Int. Ed.* **2001**, 40, 191–195.
33. (a) Evans, D. A.; Trotter, B. W.; Coleman, P. J.; Côté, B.; Dias, L. C.; Rajapakse, H. A.; Tyler, A. N. *Tetrahedron* **1999**, 55, 8671–8726; (b) Evans, D. A.; Coleman, P. J.; Dias, L. C. *Angew. Chem. Int. Ed.* **1997**, 36, 2738–2741.
34. Mak, J. Y. W.; Williams, C. M. *Nat. Prod. Rep.* **2012**, 29, 440–448.
35. (a) Cavalheiro, A. J.; Yoshida, M. *Phytochemistry* **2000**, 53, 811–819; (b) Echeverri, F.; Arango, V.; Quiñones, W.; Torres, F.; Escobar, G.; Rosero, Y.; Archbold, R. *Phytochemistry* **2001**, 56, 881–885.
36. Ono, M.; Zhao, X. Y.; Shida, Y.; Akita, H. *Tetrahedron* **2007**, 63, 10140–10148.
37. Albert, B. J.; Yamaoka, Y.; Yamamoto, H. *Angew. Chem. Int. Ed.* **2011**, 50, 2610–2612.

Total Synthesis of the Crinipellins

Taek Kang and Hee-Yoon Lee¹

Department of Chemistry, KAIST (Korea Advanced Institute of Science and Technology),
Yuseong, Daejeon, South Korea

¹Corresponding author: leehy@kaist.ac.kr

Chapter Outline

1. Introduction and Background	271	4.1. Asymmetric Synthesis of the Substituted Cyclopentane Key Intermediate	283
1.1. Isolation and Structure	271		
1.2. Synthetic Analysis	272		
2. The First Approach	273	4.2. Formal Synthesis of (–)-Crinipellin B	286
3. The Second Approach: Formal Total Synthesis of Crinipellin B	279	4.3. Total Synthesis of (–)-Crinipellin A	288
4. Asymmetric Total Synthesis of Crinipellins	283	References	290

1 INTRODUCTION AND BACKGROUND

1.1 Isolation and Structure

In 1979, Steglich and coworkers reported the isolation of a crystalline antibiotic from submerged cultures of the basidiomycete *Crinipellis stipitaria* (Agricales) strain No. 7612, named “crinipellin” with undetermined structure,¹ later identified as *O*-acetylcrinipellin A.² Subsequently, further investigation on several strains of this fungus led to the isolation and structure determination of five crinipellins, named crinipellin A, *O*-acetylcrinipellin A, tetrahydrocrinipellin A, crinipellin B, and dihydrocrinipellin B² (Figure 1). The chemical structure of the crinipellins was elucidated using 1D and 2D NMR spectra, selective decoupling experiments, NOE difference measurements, and comparison of the NMR spectra of crinipellin A with hirsutane

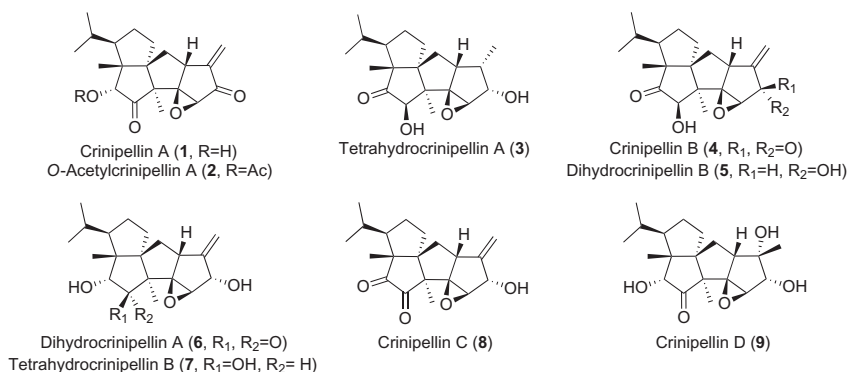


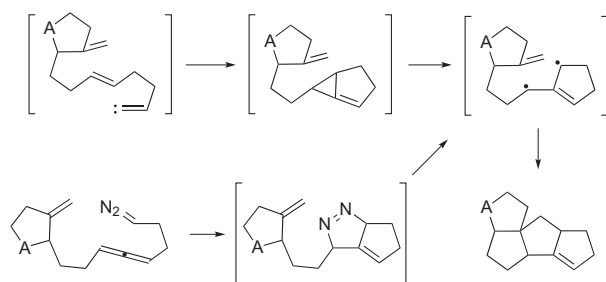
FIGURE 1 Members of the crinipellin family.

derivatives, complicatic acid and hypnophilin. Further confirmation was obtained by the single crystal X-ray diffraction analysis of crinipellin B. The absolute configuration of crinipellins was assigned by comparing the CD spectra with those of ent-3 β -hydroxy-5 α -androstan-17-one and the linear triquinane sesquiterpene hypnophilin. These assignments have yet to be verified, as the CD method of determining absolute stereochemistry is based on the empirical rules and often provides the opposite result with a slight difference in the substitution pattern of the same basic structure. Recently, Shen reported the isolation of four new crinipellins from the fungal strain *Crinipellis* sp. 113,³ named dihydrocrinipellin A, tetrahydrocrinipellin B, crinipellin C, and crinipellin D (Figure 1). While previously reported α -methylidene cyclopentanone-containing natural products (**1**, **2**, and **4**) exhibited strong antibiotic activity, antitumor and antibacterial assays of these new compounds showed no effect on the growth of tested bacteria or yeast but moderate activities against HeLa cells, notwithstanding the lack of an α -methylene ketone structural unit that was believed to be responsible for biological activities.

Crinipellins are presently the only natural products having a tetraquinane framework with the combination of linear and angular triquinane moieties. Each of these diterpenoids contains at least eight contiguous stereogenic centers, three of which are quaternary stereogenic carbon atoms. Also, crinipellins are embellished with a network of oxygen functionalities in various forms, such as epoxide, hydroxide, and carbonyl groups. Because of their unprecedented structural features and promising biological activities, crinipellin A, crinipellin B, and O-acetylcrinipellin A are attractive and challenging target molecules for total syntheses.

1.2 Synthetic Analysis

We recently reported tandem reaction strategies for obtaining triquinanes from linear substrates through trimethylenemethane (TMM) diyl [2+3]

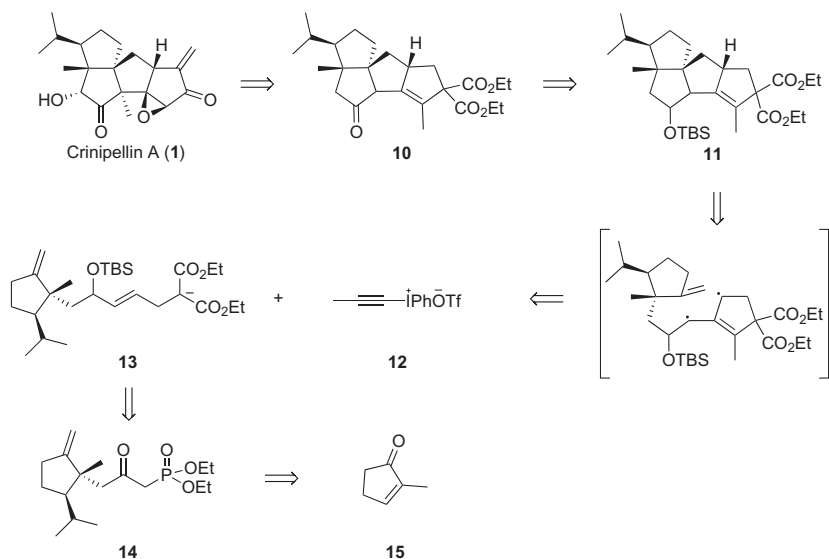


SCHEME 1 Tandem cycloaddition reactions toward tetraquinanes.

cycloaddition reaction.^{4a,f} The tandem cycloaddition reactions were successfully applied to the total synthesis of various triquinane natural products.⁴ In our effort to extend the scope of the tandem cycloaddition reaction via TMM diyl to the more complex and challenging structures, the total synthesis of the crinipellins was considered. Substrates possessing cyclopentane rings, through the tandem cycloaddition reaction strategies via TMM diyl, would produce tetracyclic products in one step (Scheme 1). The successful tandem cycloaddition reactions would mark the first cascade synthesis of tetraquinane structures, a process related to one that has been widely explored in the synthesis of polycyclohexane structures such as steroids.⁵ The challenge of the strategy was believed to be the tolerance of the tandem cycloaddition reaction toward the highly congested environment.

2 THE FIRST APPROACH

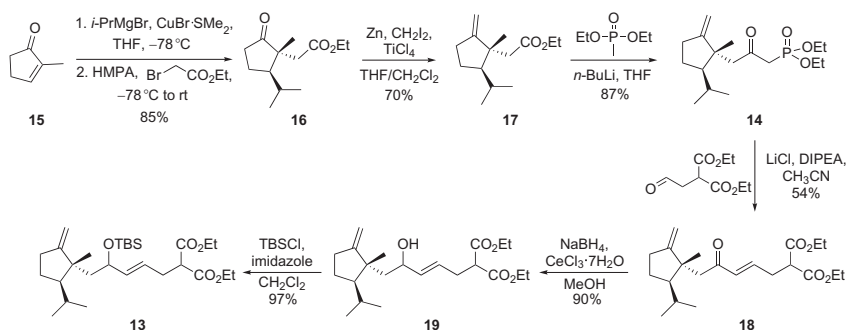
Our first approach to a tetraquinane was the tandem cycloaddition reaction strategy of alkylidene carbenes generated from alkynyliodonium salts.^{4c} Our initial synthetic analysis showed that the tetraquinane structure **11** could be assembled from the alkynyliodonium salt **12** and the nucleophile **13** through an alkylidene carbene-mediated TMM cycloaddition reaction. Though the tandem cycloaddition strategy looked fascinating for the synthesis of tetraquinane natural products, we could not convince ourselves to explore the strategy due to the relatively low efficiency of the tandem reaction strategy using carbene chemistry, which we encountered during the synthesis of angularly fused triquinanes. Nevertheless, Dr. Yeonjoon Kim, who developed the carbene-mediated tandem reaction strategy to the triquinane compounds via trimethylenemethane intermediates, tested the feasibility of tetraquinane synthesis right before defending his Ph.D. thesis. Yeonjoon observed the formation of tetraquinanes as minor products. This observation persuaded us to explore the total synthesis of crinipellins. The substrate for TMM cycloaddition reaction could be prepared from 2-methyl-2-cyclopenten-1-one **15** (Scheme 2).



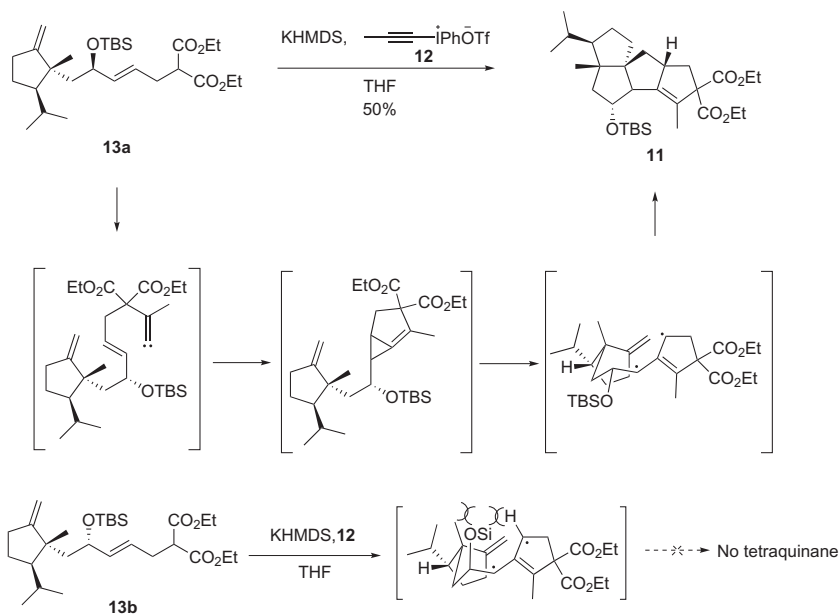
SCHEME 2 Synthetic analysis of crinipellins.

Copper-catalyzed 1,4-addition of isopropyl magnesium bromide to 2-methyl-2-cyclopenten-1-one **15** followed by alkylation of the resulting enolate with ethyl bromoacetate afforded the substituted cyclopentanone **16** stereoselectively. The ketone moiety of cyclopentanone was then converted to olefin **17** using $\text{Zn}-\text{CH}_2\text{I}_2-\text{TiCl}_4$ reagent⁶ as conventional Wittig-type reactions were complicated by the presence of the ester group. The phosphonate group was added to the ester **17** by treatment with the diethylmethyl phosphonate anion. The Horner–Emmons reaction of phosphonate **14** with diethyl 2-(2-oxoethyl)malonate produced enone **18**. The reduction of unsaturated ketone **18** with sodium borohydride and cerium chloride gave secondary allylic alcohol **19** as a mixture of epimers. The alcohol moiety was protected with a TBS group to afford the precursor **13** for cycloaddition reaction (Scheme 3).

Diastereomers of **13** were separated before the cycloaddition reaction since only one isomer was expected to adopt the sterically less demanding conformation in the transition state while the other diastereomer would suffer from severe steric congestion. Both diastereomers of precursor **13** were treated with KHMDS and the propynyliodonium salt, **12**. The tandem cycloaddition reaction of the substrate **13a**, to our pleasant surprise, gave tetraquinane product **11** in 50% yield, while **13b** did not yield any cycloaddition product. These results allowed us to determine the relative stereochemistry of **13a** and **13b** as depicted. The sequential formation of alkylidene carbene and the TMM diradical intermediates transformed the cyclopentane substrate with a linear chain into the tetracyclic compound (Scheme 4). The core structure



SCHEME 3 Synthesis of the cycloaddition reaction precursor from cyclopentenone.



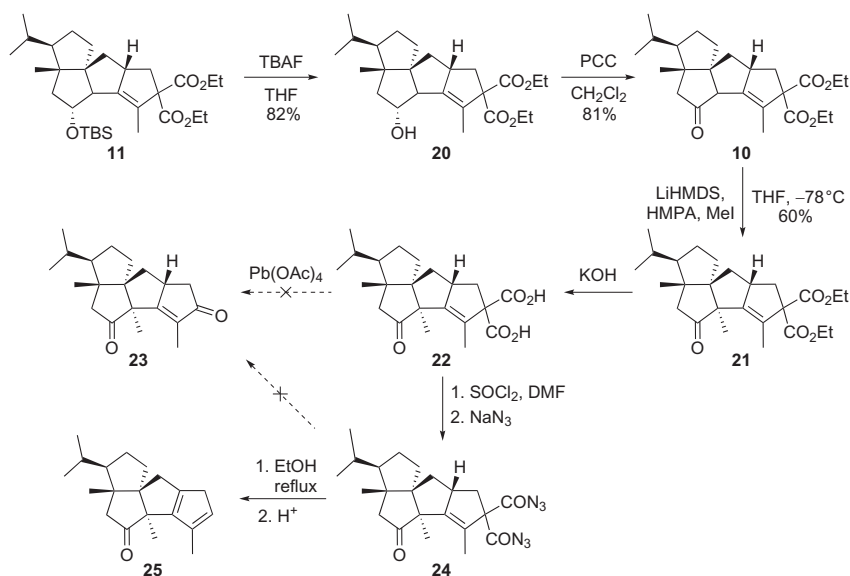
SCHEME 4 Tandem cycloaddition reaction toward a tetraquinane.

of the crinipellins was obtained in a seven-step sequence from 2-methylcyclopentenone. For the completion of the synthesis of crinipellins, what remained was the introduction of one quaternary methyl group, removal of the vinylic methyl group, and the conversion of the malonate unit into the ketone.

First, **11** was converted into the ketone **10** through deprotection of the TBS group with TBAF followed by PCC oxidation. At this stage, regioselective methylation of the enolate of **10** was highly desirable, though the selectivity of the enolate formation from **10** might well be toward the less substituted

side. Fortunately, base treatment (KHMDs, LiHMDS, LDA, *t*-BuOK, or NaH) of the ketone **10** followed by methylation produced only the desired product **21**. We believe that the tertiary hydrogen was more acidic due to the extra stabilization by the olefin in the molecule. The structure of tetraquinane **21** was deduced through extensive NMR experiments (^1H , ^{13}C NMR, COSY, and NOE). With the successful introduction of the quaternary methyl group, the next step was the removal of the unnecessary carbons in the structure. Transformation of the malonate unit into the corresponding ketone was investigated via Hunsdiecker-type reactions⁷ since other routes^{4g} would be too long and thus were not pursued. Oxidative cleavage of diacid **22** with $\text{Pb}(\text{OAc})_4$ did not produce the anticipated ketone **23** and double Curtius rearrangement of the bis(acylazide) **24** using NaN_3 produced the unexpected diene **25** instead of ketone **23** (Scheme 5).

Though conversion of the malonate unit of **21** into the corresponding ketone was not successful and it might take a long sequence of reactions to remove the extra methyl group, the successful introduction of the quaternary methyl group was quite encouraging. Thus, we decided to explore an alternate synthetic scheme that would eliminate unnecessary extra carbon atoms in the tetraquinane product by switching the position of the nucleophile and the iodonium salt. In this new synthetic route, the alkylidene carbene would not have to have the extra methyl group that was previously essential to prevent the rearrangement of the alkylidene carbene to the corresponding alkyne. We started the preparation of the required cycloaddition precursor from

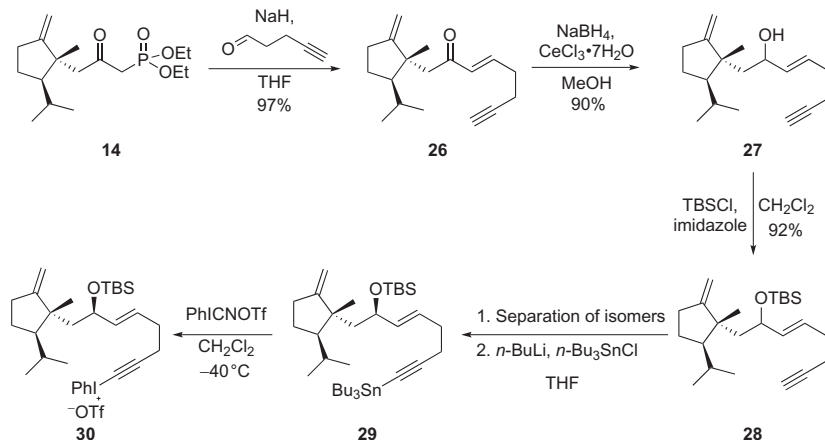


SCHEME 5 Functional group manipulation of the crinipellin tetracycle.

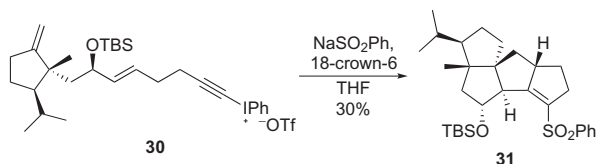
phosphonate **14**. The Horner–Emmons reaction of phosphonate **14** with pentynal produced enone **26**. The reduction of enone **26** with sodium borohydride and cerium chloride gave secondary alcohol **27** as a mixture of epimers. Protection of the alcohol as TBS ether and separation of the diastereomers afforded **28**. The alkynylstannane compound **29** was prepared from alkyne compound **28** with *n*-BuLi and tributyltin chloride. Due to the instability of **29**, it was used directly after workup without further purification. The alkynyliodonium salt **30** was prepared according to the procedure of Stang⁸ and used immediately in the next step (Scheme 6).

Alkylidene carbene was generated from nucleophilic attack of benzenesulfinate anion to iodonium salt **30** to produce the tetraquinane compound **31** in 30% yield. Benzenesulfinate (PhSO_2^-) was selected as the nucleophile as it showed relatively good efficiency for the cycloaddition reaction and could be easily removed in comparison to nucleophiles including CN^- , N_3^- , and PhS^- (Scheme 7). Though the tandem cycloaddition reaction was not as efficient as in the previous strategy, the cycloaddition product **31**, without any unnecessary carbons in the structure, was the bigger advantage.

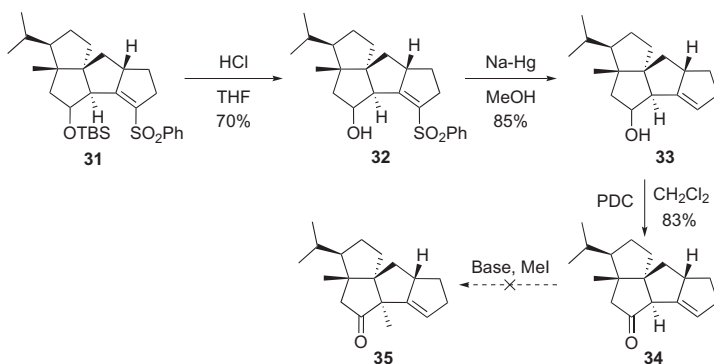
Tetraquinane **31** was converted into the ketone **34** through deprotection of TBS group with HCl followed by removal of the sulfone group with sodium amalgam and subsequent PDC oxidation of the alcohol. This modified



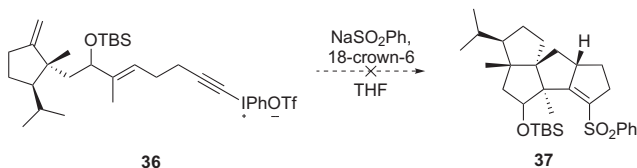
SCHEME 6 Preparation of alkynyliodonium salt containing precursor.



SCHEME 7 Tandem cycloaddition reaction triggered by nucleophilic addition reaction.



SCHEME 8 Removal of the added nucleophile and attempted methylation.



SCHEME 9 Attempted cycloaddition reaction with trisubstituted olefin.

synthetic strategy was explored by Dr. Su Young Ryou, then a second year graduate student with high enthusiasm for completing the total synthesis, since the introduction of the quaternary methyl group was expected to proceed without any trouble through the same protocol as for the ketone **10**. However, all the attempts at methylation through enolate formation from **34** did not yield any methylated product. (Scheme 8) While it took less than a month to achieve tetraquinane synthesis, the methylation became a nightmare for Su Young.

After almost a year of fruitless effort to find conditions for methylation of the ketone **34**, we concluded that the ketone of **34** was resistant to enolate formation. It is still amazing that a subtle conformational difference can make a drastic difference in the reactivity of a functional group.

Though it was ideal to introduce the methyl group prior to the formation of tetraquinane skeleton, the tandem cycloaddition reaction of the methyl-containing substrate **36** did not produce any cycloaddition product. While the preliminary interpretation of this failure was that the TMM diyl cycloaddition reaction would be sensitive to the steric environment, it turned out that the initial cyclopropanation reaction was sensitive to the substitution patterns of the olefin in the substrate, as the alternative cycloaddition reaction route via TMM yielded the tetraquinane product (Scheme 9).

At this point, Su Young was so frustrated that she decided to discontinue her year long struggle with the deceptively simple methylation. The total

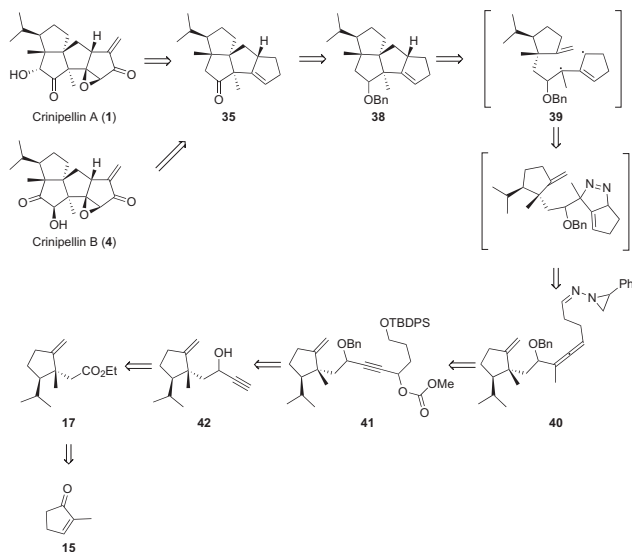
synthesis of crinipellins had to wait until a new tandem cycloaddition route that was highly efficient was developed.

3 THE SECOND APPROACH: FORMAL TOTAL SYNTHESIS OF CRINIPELLIN B

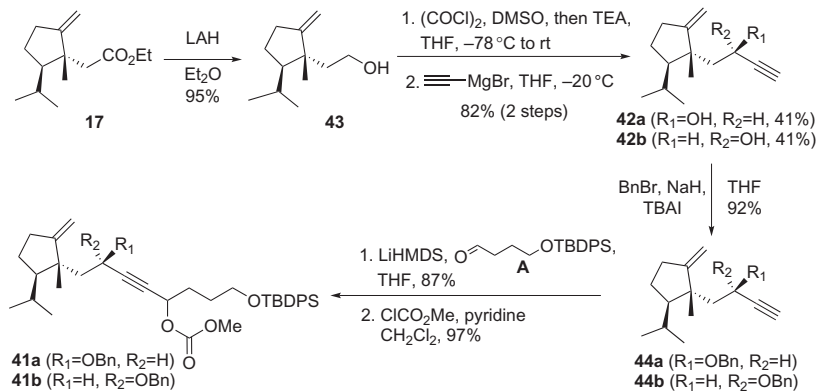
When Dr. Wonyeob Kim joined the tandem cycloaddition reaction via TMM project as a graduate student, we were on the verge of wrapping up the project as all the target compounds were too complex or sterically congested to produce the desired cycloaddition products. One day Wonyeob decided to test an alternative way of generating TMM via cyclopropanation on an allene moiety with a diazo functionality assuming that the diazo functionality would generate the alkyl carbene. We did not expect any better result from the new route as the process was believed to involve the carbene intermediate. However, when he ran the new tandem cycloaddition reaction for the first time, he could not believe the outcome. The yield of the reaction, even without any optimization effort, was almost quantitative, something that had not been observed before and was not expected from a synthetic route involving a carbene intermediate. Suddenly, we realized that we had developed a very efficient tandem cycloaddition route to triquinanes from linear substrates via a cycloaddition reaction of TMM diyl generated from the 1,3-dipolar cycloaddition reaction of allenyl diazo compounds.^{4f} Unlike the alkylidene carbene route to the triquinanes that suffered from relatively low efficiency and narrow substrate scope, the new tandem cycloaddition route showed versatility, efficiency, and wide applicability to natural product synthesis. Thus, we anticipated that the new tandem strategy would allow the precursor **40**, containing the trisubstituted allene for the introduction of the quaternary methyl group, to undergo tandem cycloaddition reactions. Cycloaddition reaction precursor **40** could be prepared from 2-methylcyclopentenone in a similar way to the synthesis of **13** (Scheme 10).

Preparation of the cycloaddition precursor **40** began with ester **17**. The ester functionality of **17** was reduced with LAH and the alcohol **43** was oxidized to the corresponding aldehyde using the Swern protocol. Due to the volatility of the aldehyde, oxidation was carried out in THF and the crude reaction mixture was treated with ethynyl Grignard reagent after rapid filtration through a pad of silica gel to remove insoluble materials to produce the alkynol **42**. Two diastereomers of **42** (**42a** and **42b**), were separated and were used in the next synthetic steps since we did not know the relative stereochemistry of the alcohols in **42a** and **42b**. The alcohol of **42** was protected as the benzyl ether and the anion of the terminal alkyne in **44** was added to the aldehyde **A** (Scheme 11). The resulting alkynol was activated as carbonate **41** to introduce the allene moiety through S_N2'-type reaction of an organocopper reagent.

The propargylic carbonate **41** was treated with a methyl organocopper reagent to produce the methyl-substituted allene compound **45** in good yield.



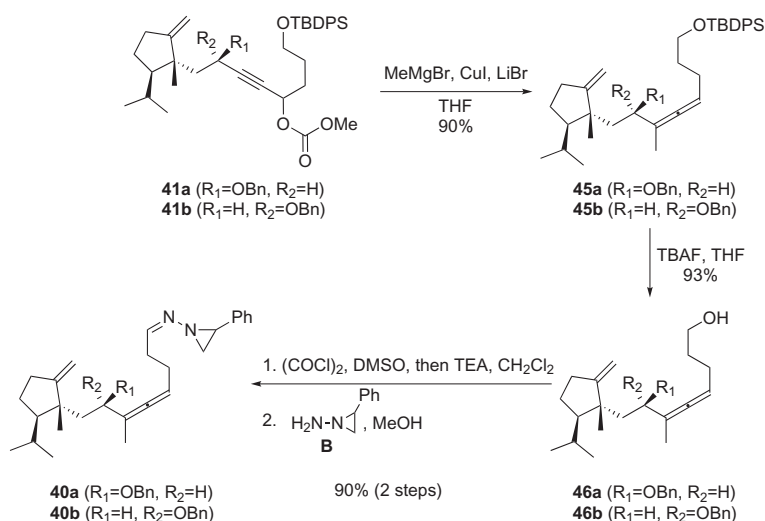
SCHEME 10 A new tandem strategy toward crinipellins.



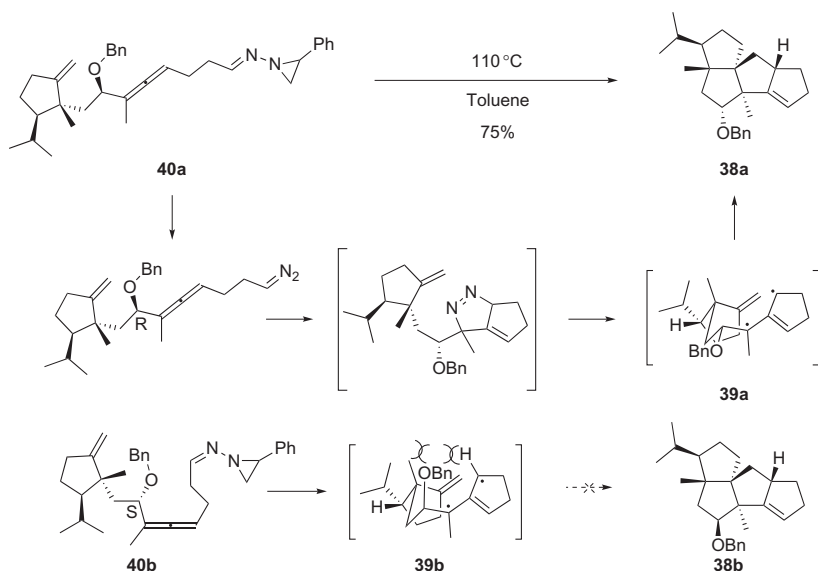
SCHEME 11 Preparation of the alkynol, the precursor for the allene compound.

Deprotection of the silyl ether followed by a Swern oxidation of the alcohol **46** provided the aldehyde. Subsequent condensation with aminoaziridine **B** in MeOH afforded allenyl aziridinylimine **40**, the cycloaddition precursor (Scheme 12).

When allenyl aziridinylimines **40** were heated to 110°C in toluene, as anticipated, only one allenyl aziridinylimine **40a** gave the tetraquinane product **38a** successfully through TMM diyl [2+3] cycloaddition reaction. Intramolecular [2+3] cycloaddition reaction of diazo compound with the allene moiety produced methylenepyrzole structure and the pyrazole ring lost a



SCHEME 12 Synthesis of the precursor for the cycloaddition reaction.



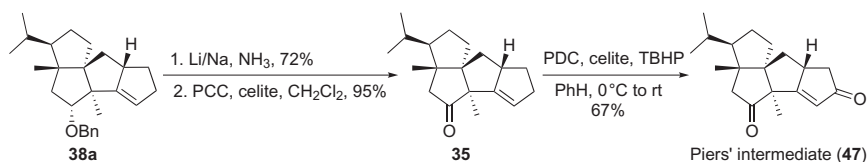
SCHEME 13 The tandem cycloaddition reaction to form the tetraquinane.

nitrogen molecule immediately to generate the TMM diyl. Subsequent [2+3] cycloaddition reaction of the sterically less demanding intermediate **39a** gave the tetraquinane structure and thus confirmed the relative stereochemistry of **40a** and **40b** (Scheme 13). This successful tandem cycloaddition reaction also proved that the previously failed tandem cycloaddition reaction through

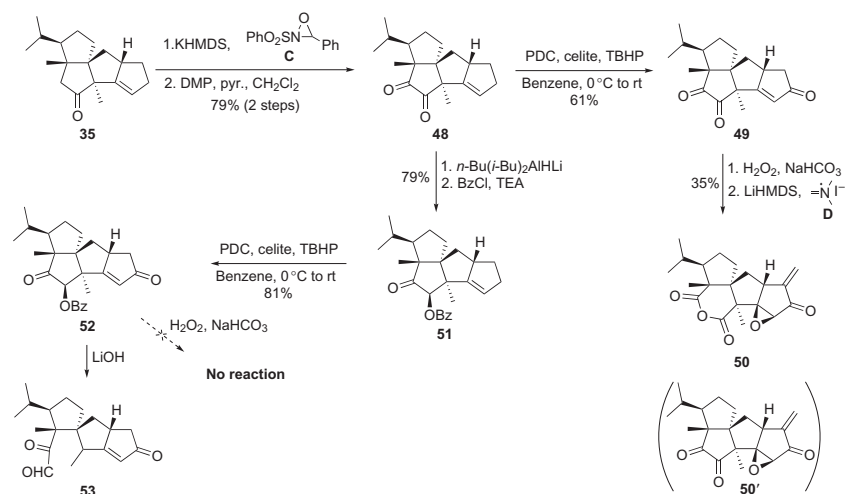
alkylidene carbene intermediate was due to the sensitivity of the cyclopropanation reaction of the alkylidene carbene with the trisubstituted olefin. Otherwise, the overall efficiency and the yield should have been similar in both strategies.

With the tetraquinane **38a** in hand, completion of the total synthesis of a crinipellin required only functional group manipulation. Deprotection of the benzyl ether of the tetraquinane **38a** under Birch conditions and PCC oxidation of the resulting alcohol yielded ketone **35**. Allylic oxidation of **35** with PDC and TBHP in benzene furnished dione **47**, which was an intermediate in Piers' total synthesis of crinipellin B.⁹ Thus, the structure of dione **47** was confirmed by the comparison of the NMR spectral data of **47** with the data reported by Piers. With this confirmation, we completed the formal synthesis of crinipellin B (Scheme 14).

Our brief exploration of an alternative synthetic route to crinipellins from **35** via dione **48**, which was deemed to be a good intermediate for the completion of the synthesis without the protecting group chemistry, turned out to be an ill-fated expedition (Scheme 15). α -Hydroxylation with Davis' reagent (C) followed by Dess–Martin periodinane (DMP) oxidation¹⁰ produced the dione



SCHEME 14 A formal total synthesis of crinipellin B.



SCHEME 15 Ill-fated endeavor of functional group manipulation.

48 and the dione was converted into trione **49** through allylic oxidation with PDC. The nucleophilic epoxidation of **49** followed by methylenation of the ketone using Eschenmoser's salt (**D**)¹¹ was initially thought to produce **50'**, another Piers' intermediate that was two steps away from crinipellin B. Instead, the obtained product was **50**, the over-oxidized product whose structure was only deduced through mass spectrometry. To avoid the oxidation of the dione, **48** was reduced with DIBAL-*n*-BuLi to form **51** chemo- and stereoselectively after the benzylation of the alcohol. Allylic oxidation of **51** produced the enone **52** with good efficiency. However, the usual epoxidation reaction did not proceed at all. The sudden loss of the reactivity toward nucleophilic peroxide reaction was presumably due to the blocking of the reaction site by the benzoate of **52**. To relieve the steric hindrance by the benzoate, the ester was hydrolyzed with base only to produce the ring cleavage product **53** through the retro-aldol-type reaction. Replacement of the protecting group with the *t*-butyldimethylsilyl group did not change the reactivity of **52** at all.

4 ASYMMETRIC TOTAL SYNTHESIS OF CRINIPELLINS

In our formal synthesis of (±)-crinipellin B, we verified that the relative stereochemistry of protected hydroxyl group in the cycloaddition precursor **40** was crucial. Therefore, the stereoselective synthesis of **40** would be desirable. We realized that the asymmetric synthesis of **40** could be a good solution to control the relative stereochemistry as well.

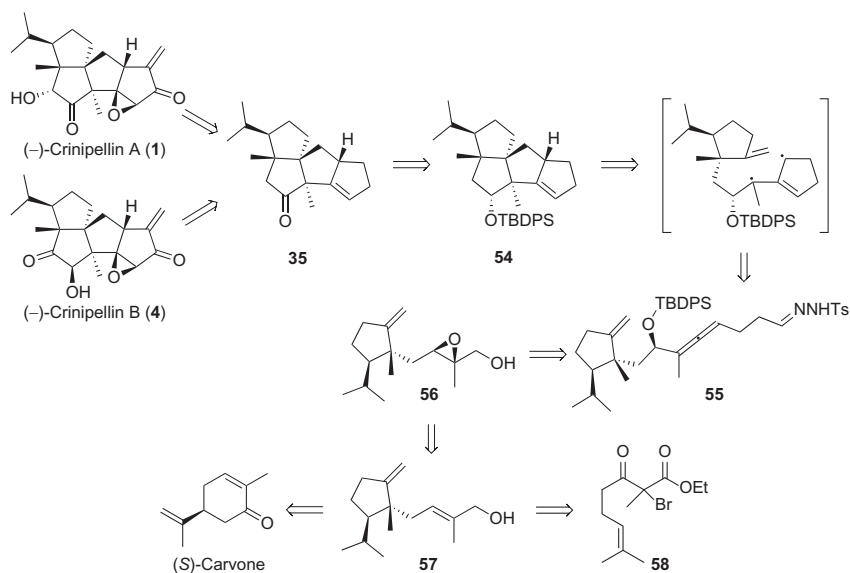
For asymmetric synthesis, we had to prepare the enantiomerically pure allene **55** with the proper relative stereochemistry. The allene moiety could be synthesized from epoxy propargylic derivative **56** through S_N2'-type reaction with a Grignard reagent. The epoxy propargylic substrate would be synthesized from allylic alcohol **57** via Sharpless epoxidation¹² for introducing the appropriate stereochemistry of the protected allenyl alcohol. For the stereoselective synthesis of **56**, the allylic alcohol **57** would be prepared enantioselectively (Scheme 16).

To obtain a chiral intermediate, we tried several methods, including synthesis through an asymmetric radical cyclization reaction and synthesis from a chiral starting material, as described below.

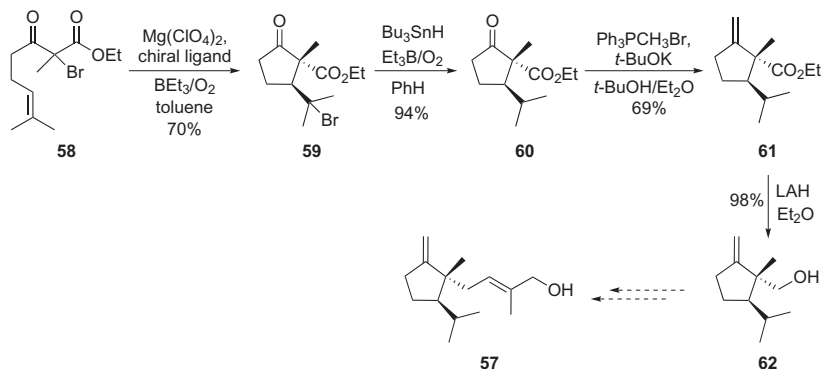
4.1 Asymmetric Synthesis of the Substituted Cyclopentane Key Intermediate

4.1.1 Synthesis Through Asymmetric Radical Cyclization Reaction

We first tested enantioselective introduction of the isopropyl group and methyl group using the highly enantioselective atom-transfer radical cyclization reaction developed by Yang¹³ to obtain the optically pure intermediate for the total synthesis.



SCHEME 16 Analysis of asymmetric total synthesis of crinipellins.



SCHEME 17 Asymmetric radical cyclization to the cyclopentane ring.

Following Yang's report, the atom-transfer radical cyclization reaction of **58** provided chiral cyclopentane ring **59**. The bromide of **59** was removed by radical dehalogenation reaction to produce **60**. Wittig olefination followed by reduction of the ester group gave chiral alcohol **62** that could be easily converted into the allylic alcohol **57** (Scheme 17).

Though the stereochemical control of the isopropyl and methyl groups on the cyclopentane ring using the atom-transfer radical cyclization reaction, as well as further functional group modifications, were successful, this strategy revealed critical problems for our synthesis. First of all, the radical cyclization reaction produced small amounts of undesired diastereomeric side product

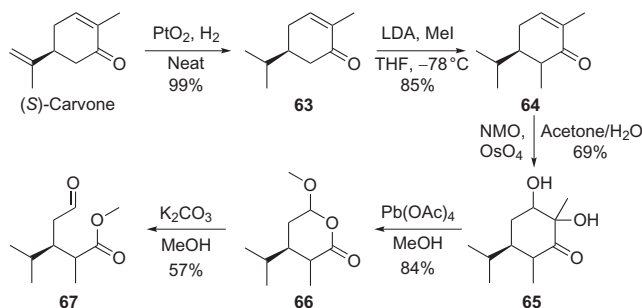
that was not easily separable. In addition, the product yield was not consistent in the Wittig olefination step, probably due to the existence of the ester group. More critically, the reaction was not suitable for large-scale reaction because high dilution was required for the intramolecular radical reaction.

4.1.2 Synthesis from (*S*)-Carvone

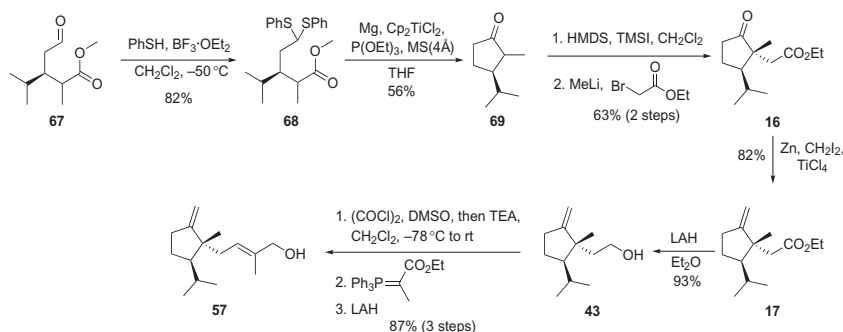
Another approach to the synthesis of an optically pure intermediate for the asymmetric total synthesis of crinipellins was utilizing the stereocenter of (*S*)-carvone. To convert the cyclohexane ring of commercially available (*S*)-carvone to the cyclopentane ring, (*S*)-carvone was hydrogenated selectively with PtO_2 catalyst to give cyclohexenone **63**. After the methylation of the enolate of the ketone **63** to form a mixture of diastereomers **64**, the cyclohexenone ring was degraded via osmium tetroxide oxidation followed by cleavage of dihydroxyketone with lead acetate into the lactone **66**. Hydrolysis of the lactone **66** with potassium carbonate afforded the aldehyde **67** (Scheme 18).

Since the direct coupling of aldehyde-ester **67** through the McMurry coupling reaction¹⁴ was not successful, a modified McMurry coupling of the thioacetal¹⁵ of **67** was used to form cyclopentane ring. Treatment of thioacetal **68** with magnesium, bis(cyclopentadienyl) titanium(IV) dichloride and triethylphosphite afforded cyclopentanone **69**.¹⁶ Alkylation of the thermodynamic enolate of **69** with ethyl bromoacetate produced **16** stereoselectively. The ketone moiety of **16** was converted to olefin **17** using $\text{Zn-CH}_2\text{I}_2\text{-TiCl}_4$ reagent to avoid the byproduct formation from the Wittig olefination reaction. Finally, the ester of **17** was extended into the allylic alcohol **57** through a four-step sequence (reduction–oxidation–Wittig reaction–reduction) (Scheme 19).

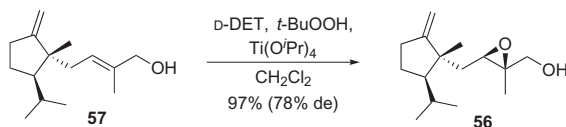
Sharpless epoxidation of allylic alcohol **57** produced the desired epoxide **56** along with 20% of the undesired diastereomer. Allylic alcohols with the substitution pattern of **57** are well known to produce low enantioselectivity



SCHEME 18 One carbon deletion sequence of carvone.



SCHEME 19 Asymmetric synthesis of cyclopentane intermediate.



SCHEME 20 Asymmetric epoxidation of the allylic alcohol.

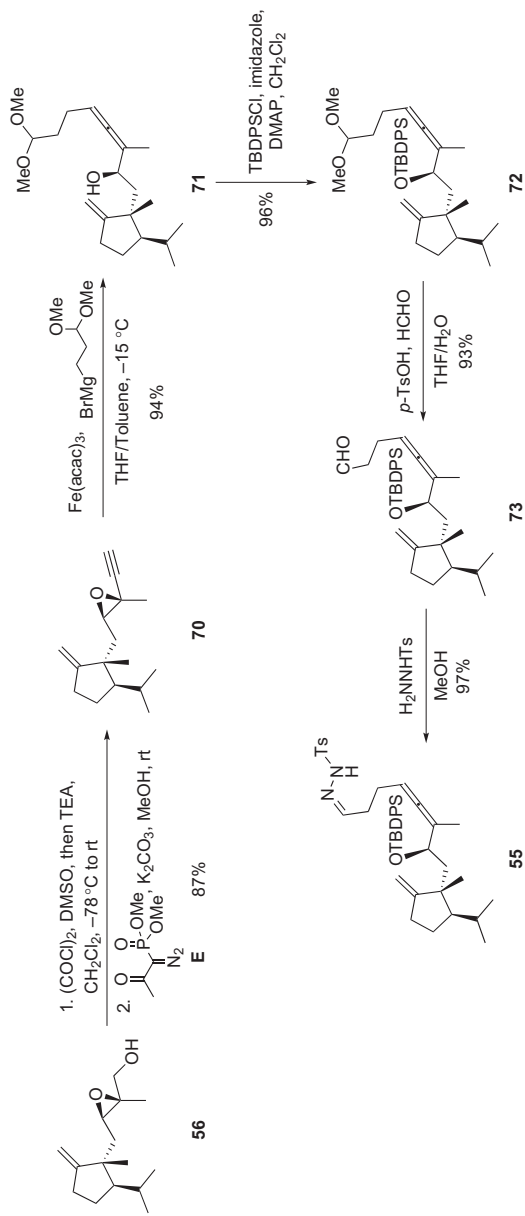
in the Sharpless epoxidation reaction. Now, we were ready for the asymmetric total synthesis of crinipellins ([Scheme 20](#)).

4.2 Formal Synthesis of (–)-Crinipellin B

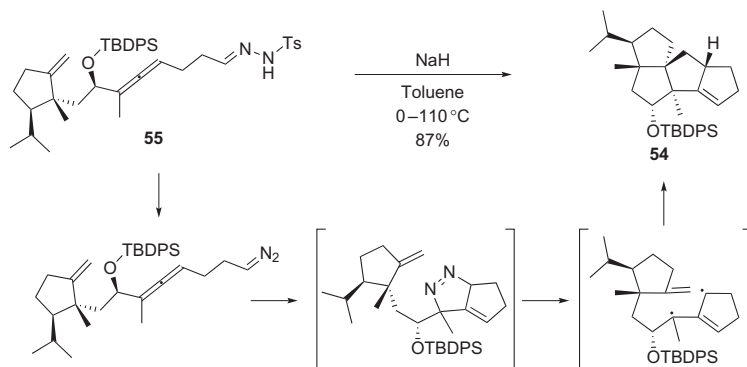
From the chiral epoxide **56**, the TMM cycloaddition precursor **55** for construction of the tetraquinane structure was prepared in a straightforward manner. Oxidation of epoxy alcohol **56** by the Swern protocol followed by treatment with Bestmann–Ohira reagent (**E**)¹⁷ produced alkyne **70**. Iron-catalyzed S_N2' -type reaction¹⁸ of **70** afforded an allene moiety as a diastereomeric mixture in a 1:1 ratio and this mixture was used in the next step without the separation of isomers. Allenyl alcohol **71** was protected as a TBDPS ether to give *O*-silylated allene **72**. Deprotection of the acetal of **72** was delicate as the allenyl moiety was not stable under acidic condition. Fortunately, treatment of **72** with *p*-toluenesulfonic acid monohydrate in presence of formaldehyde afforded aldehyde **73**, and subsequent treatment with *p*-toluene sulfonylhydrazide furnished the precursor **55** for the tandem cycloaddition reaction ([Scheme 21](#)).

Treatment of substrate **55** with sodium hydride in toluene followed by heating gave tetraquinane structure **54** successfully via TMM diyl [2+3] cycloaddition reaction in 87% yield ([Scheme 22](#)).

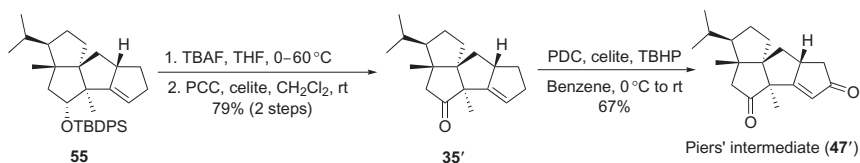
The synthesis of chiral Piers' intermediate **47'** was accomplished in the same manner as before ([Scheme 23](#)).



SCHEME 21 Preparation of the cyclization precursor.



SCHEME 22 Tandem cycloaddition for the asymmetric synthesis of the tetraquinane.



SCHEME 23 Another formal synthesis of crinipellin B.

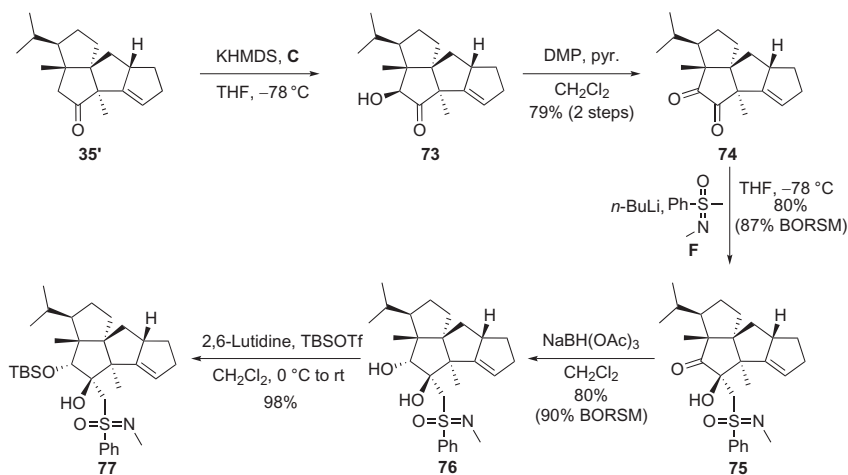
At this point, since the asymmetric total synthesis of crinipellin B could be completed following Piers' route, we decided to focus on the total synthesis of crinipellin A.

4.3 Total Synthesis of (–)-Crinipellin A

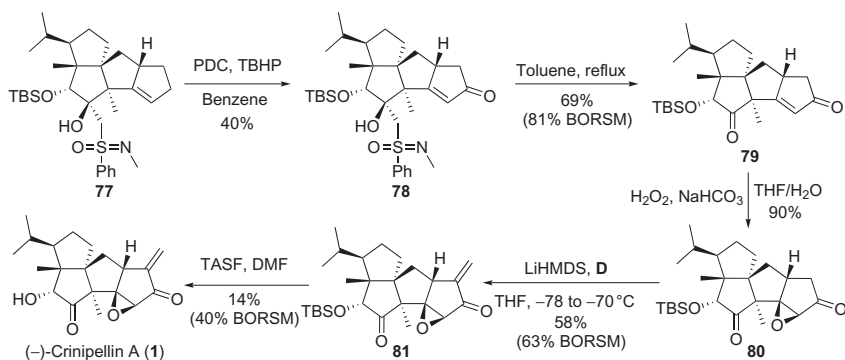
To achieve the synthesis of (–)-crinipellin A, introduction of the proper stereochemistry of the α -hydroxyketone would be the challenge of the synthesis. Because direct α -hydroxylation reaction of **35'** using Davis' oxaziridine (**C**)¹⁹ gave **73** having opposite stereochemistry of crinipellin A, inversion of the stereochemistry was necessary. Since direct inversion of the stereochemistry through Mitsunobu reaction did not proceed at all, selective reduction of the dione **74** was pursued. If selective, the stereochemistry of the resultant alcohol would be the desired one for crinipellin A. Based on prior experience, the dione **74** could be chemo- and stereoselectively modified depending on the nucleophile. After DMP oxidation of **73**, treatment of diketone **74** with various hydride sources reduced the undesired ketone selectively. This result inspired us to use the selectivity in a different context. If we added a nucleophile to the undesired ketone that would produce the β -alcohol and this alcohol could direct the stereochemistry of the reduction of the remaining ketone. However, after the stereoselective reduction of the desired ketone, the other ketone had to be regenerated. For that purpose,

we chose (*S*)-(+)-*N,S*-dimethyl-*S*-phenylsulfoximine (**F**). This reagent also allowed us to resolve **74** further. As anticipated, addition of the anion of (*S*)-(+)-*N,S*-dimethyl-*S*-phenylsulfoximine (**F**)²⁰ produced **75** stereoselectively. The stereochemistry of this tertiary alcohol was used for the stereoselective reduction of the other ketone of **75**. Thus, hydroxyl group-directed stereoselective reduction of the remaining ketone with sodium triacetoxyborohydride produced diol **76** with the correct stereochemistry found in crinipellin A. The secondary alcohol was protected with a TBS group selectively to give alcohol **77** (Scheme 24).

With the correct stereochemistry of the alcohol in **76**, the total synthesis of (–)-crinipellin A was completed in a straightforward fashion, a circumstance only possible because of our previous experience with functional group manipulations in crinipellins. Allylic oxidation of alcohol **77** using PDC and TBHP produced enone **78**. From the previous experience, we knew we had to regenerate the ketone. The sulfoximine group was removed easily by simply refluxing in toluene to give diketone **79**. Treatment of **79** with hydrogen peroxide under basic conditions produced the epoxide **80** without any of the trouble encountered in the previous synthetic effort. The ketone **80** was treated with LiHMDS and Eschenmoser's salt (**D**) to afford the α -methylene ketone **81**. That left only one step toward crinipellin A and thus, Taek Kang was very excited, though we knew the deprotection might not be easy, since the conjugated enone would be reactive toward any nucleophilic reagent. In fact, the final deprotection was not easy, and Taek, who was wrapping up the total synthesis, had to spend several months on this operation. The final deprotection of the TBS group was troublesome presumably due to the reactivity of the conjugated enone of **81**. Various deprotection conditions such as TBAF, TBAF/NH₄F, TBAF/AcOH, HF·Pyr., HF/urea, HF/TEA, NH₄F·HF,



SCHEME 24 Selective functionalization of the dione.



SCHEME 25 Completion of the total synthesis of crinipellin A.

SiF₄, and TASF were tested and the product decomposed under most reaction conditions. Only TASF gave desired (–)-crinipellin A, with low conversion due to instability of the epoxynone of **81** under the reaction conditions. With a small amount of the final product in hand, Taek was able to obtain spectral data and was convinced that he had crinipellin A. To obtain enough of synthetic crinipellin A the deprotection reaction was carefully monitored. Thus, the reaction was stirred for 15 min, and then filtered through a pad of silica gel rapidly to minimize the decomposition of the starting material and the product. Recovered starting material was recycled several times to produce appreciable amounts of (–)-crinipellin A (Scheme 25).

Finally, the structure of the synthetic (–)-crinipellin A was confirmed by comparing NMR spectral data of the synthetic material to that of natural (–)-crinipellin A. The spectroscopic data and optical rotation for synthetic (–)-crinipellin A were identical to the data reported for the natural (–)-crinipellin A.

In summary, we have accomplished the first asymmetric total synthesis of crinipellin A along with the formal total synthesis of crinipellin B. The very unique tetraquinane core structure of crinipellins was constructed efficiently through a tandem cycloaddition reaction via TMM diyl. The absolute stereochemistry of crinipellins was also confirmed through our asymmetric total synthesis.

REFERENCES

1. Kupka, J.; Anke, T.; Oberwinkler, F.; Schramm, G.; Steglich, W. *J. Antibiot.* **1979**, *32*, 130–135.
2. Anke, T.; Heim, J.; Knoch, F.; Mocek, U.; Steffan, B.; Steglich, W. *Angew. Chem. Int. Ed. Engl.* **1985**, *24*, 709–711.
3. Li, Y.-Y.; Shen, Y.-M. *Helv. Chim. Acta* **2010**, *93*, 2151–2157.

4. (a) Lee, H.-Y.; Kim, Y. *J. Am. Chem. Soc.* **2003**, *125*, 10156–10157; (b) Lee, H.-Y.; Kim, W.-Y.; Lee, S. *Tetrahedron Lett.* **2007**, *48*, 1407–1410; (c) Lee, H.-Y.; Yoon, Y.; Lim, Y.-H.; Lee, Y. *Tetrahedron Lett.* **2008**, *49*, 5693–5696; (d) Lee, H.-Y.; Jung, Y.; Yoon, Y.; Kim, B. G.; Kim, Y. *Org. Lett.* **2010**, *12*, 2672–2674; (e) Yoon, Y.; Kang, T.; Lee, H.-Y. *Chem. Asian J.* **2011**, *6*, 646–651; (f) Kang, T.; Kim, W.-Y.; Yoon, Y.; Kim, B. G.; Lee, H.-Y. *J. Am. Chem. Soc.* **2011**, *133*, 18050–18053; (g) Kim, W.-Y.; Kim, B. G.; Kang, T.; Lee, H.-Y. *Chem. Asian J.* **2011**, *6*, 1931–1935; (h) Lee, S.-S.; Kim, W.-Y.; Lee, H.-Y. *Chem. Asian J.* **2012**, *7*, 2450–2456; (i) Lee, H.-Y.; Song, S.-B.; Kang, T.; Kim, Y. J.; Guem, S. J. *Pure Appl. Chem.* **2013**, *85*, 741–753; (j) Kim, Y.-J.; Yoon, Y.; Lee, H.-Y. *Tetrahedron* **2013**, *69*, 7810–7816.
5. (a) Brunoldi, E.; Luparia, M.; Porta, A.; Zanon, G.; Vidari, G. *Curr. Org. Chem.* **2006**, *10*, 2259–2282; (b) Razzak, M.; De Brabander, J. K. *Nat. Chem. Biol.* **2011**, *7*, 865–875.
6. (a) Takai, K.; Hotta, Y.; Oshima, K.; Nozaki, H. *Tetrahedron Lett.* **1978**, *19*, 2417–2420; (b) Lombardo, L. *Tetrahedron Lett.* **1982**, *23*, 4293–4296; (c) Hibino, J.; Okaazoe, T.; Takai, K.; Nozaki, H. *Tetrahedron Lett.* **1985**, *26*, 5579–5580.
7. (a) Corey, E. J.; Casanova, J. J. *Am. Chem. Soc.* **1963**, *85*, 165–169; (b) Mahulikar, P. P.; Mane, R. B. *J. Chem. Res.* **2006**, 15–18.
8. (a) Omai, I. *Organotin Chemistry*; Elsevier: New York, 1989; (b) Williamson, B. L.; Stang, P. J. *Synlett* **1992**, 199–200.
9. (a) Piers, E.; Renaud, J. J. *Org. Chem.* **1993**, *58*, 11–13; (b) Piers, E.; Renaud, J.; Rettig, S. J. *Synthesis* **1998**, 590–602.
10. Dess, D. B.; Martin, J. C. *J. Org. Chem.* **1983**, *48*, 4155–4156.
11. Schreiber, J.; Maag, H.; Hashimoto, N.; Eschenmoser, A. *Angew. Chem. Int. Ed. Engl.* **1971**, *10*, 330–331.
12. Katsuki, T.; Sharpless, K. B. *J. Am. Chem. Soc.* **1980**, *102*, 5974–5976.
13. Yang, D.; Gu, S.; Yan, Y.-L.; Zhu, N.-Y.; Cheung, K.-K. *J. Am. Chem. Soc.* **2001**, *123*, 8612–8613.
14. Takeda, T.; Tsubouchi, A. *Org. Synth.* **2013**, *82*, 1–470.
15. Rahim, M. A.; Sasaki, H.; Saito, J.; Fujiwara, T.; Takeda, T. *Chem. Commun.* **2001**, 625–626.
16. Horikawa, Y.; Watanabe, M.; Fujiwara, T.; Takeda, T. *J. Am. Chem. Soc.* **1997**, *119*, 1127–1128.
17. (a) Ohira, S. *Synth. Commun.* **1989**, *19*, 561–564; (b) Müller, S.; Liepold, B.; Roth, G. J.; Bestmann, H. J. *Synlett* **1996**, 521–522.
18. Fürstner, A.; Méndez, M. *Angew. Chem. Int. Ed.* **2003**, *42*, 5355–5357.
19. Davis, F. A.; Vishwakarma, L. C.; Billmers, J. M.; Finn, J. J. *Org. Chem.* **1984**, *49*, 3241–3243.
20. Johnson, C. R.; Zeller, J. R. *Tetrahedron* **1984**, *40*, 1225–1233.

Note: Page numbers followed by “f” indicate figures, “t” indicate tables, and “s” indicate schemes.

A

Abamines, 15–18, 19s
 Abamine SG, 15–18
 Acetic acid, 99, 124–125, 265
 Acetyl chloride, 188–189
 Achmatowicz reaction, 255, 256
 AcOOH, 104
 Acrylation, 237
 Acryloyl chloride, 262–263
 Actinophyllic acid, 208
 Acylaminal formation, 191–192, 191s
 Acyl anion equivalents, 257–258, 258f
 Acylation, 218–220
 Acyliminium ions, 184, 190
 Adam’s catalyst, 173
 AgOTf, 40, 45
 Aldehyde *ent*-6 synthesis, 93–94, 94s
 Aldehyde preparation, 93–95
 Alder ene reaction, 84
 AlH₃, 15–18
 Alkaloids, 113–130, 114–115
 Alkene reduction, 40–41, 41s
 2-Alkoxy carbonyl allylboronates, 85–86
 2-Alkoxy carbonyl allylic zinc reagents, 83
 γ -Alkylation, 164s
 Alkylidene carbene, 273, 274–275, 276–277
 Alkylidene-2*H*-indolium ion, 116–118
 Alkynyldiol fragment, 43–44, 44s
 Alkynylodonium salt, 273, 277s
 Alkynyl-substituted aldehyde fragment, 44–45, 44s
 Allenyl aziridinylimines, 280–282
 Allylboration, 85
 Allylboration/lactonization reaction, 96–99, 98t, 99f
 Allylboronates, 85, 88–89
 Allylic alcohols, 285–286
 Allylic amination, 140–141, 143–144
 Allylic carbonates, 82–83
 Allylic oxidation, 170, 172–173, 282–283, 289–290
 Alverine, 19–20, 21s
 Amathaspiramide, 133–139
 Amathaspiramide A, 144–147
 Amathaspiramide alkaloids, 132–133, 133f

Amathaspiramide F, 131–154, 134–136, 148–152
 Amathaspiramides A–F, 137–139
Amathia wilsoni, 132–133
 Amide variants, 199–200, 199s
 Amido trioxadecalin synthesis, 185, 186s
 Aminoquinolines, 115–116
 Amino-substituted chroman spiroacetals, 37–38, 38s
 Annulation, 218–220
 Anomeric effect, 253
 Anticipated selective dimerization, C-2 symmetric substrate, 61, 62s
 Antifungal naftifine, 15, 18s
 Anti-inflammatory activity, 244–245
 Antimalarial, 115–116
 Antimalarial activity, flindersial and borrierial alkaloids, 115–116
 Arenediazonium salts, 2
 Argabin, 80–81, 80f
 Aromatic carbonates, 148
 γ -Arylated allylic amines, 11, 12s
 Arylation, allylamine derivatives, 13, 13s
 Arylation, N-substituted allylamine, 13–14, 14s
 Arylcyclopentene, 23–24, 24t
 Aryldiazonium salts, 2–3, 3f
 Asymmetric β -lactone formation, 193–194
 Asymmetric radical cyclization reaction, 283–285
 Atropisomerism, 229
 Axial chirality, 228–229

B

Bacillus subtilis, 241–244
 Barbier-type additions, 83
 Bartlett iodicarbonate cyclization, 254
 Barton–McCombie protocol, 40–41
 Bcl-xL protein, 53
 Benzenesulfinate, 277
 Berkeley Pit Lake, 34
 (–)-Berkelic acid, structure of, 34, 34f
 Bestmann–Ohira reagent, 286

- Betaine, 172
 BF₃·OEt₂, 96–97, 124, 188–189, 192–193, 257–258
 Biaryl bond formation, 241, 242*t*
 BiBr₃, 192–193
 Bicyclooctadienes diesters, 57, 58*s*
 Bicyclooctadienes synthesis, 60, 60*s*
 Bimetallic oxovanadium catalysts, 228, 242*t*
 6,6'-Binaphthopyranone, 226–228, 227*f*, 241–245
 BINOL, 229, 230*f*, 234
 Biologically active kavalactones, 11, 11*s*
 Biomimetic synthesis, 267
 Biosyntheses, flinderole B, 125–126, 126*s*
 Biosynthesis, 118–119
 Biosynthesis, borreverines, 116–118, 117*s*
 Biosynthesis, kingianins, 71
 Bis(cyclopentadienyl) titanium(IV) dichloride, 285
 Bis(triphenylphosphoranylidene)ammonium chloride (PNPCL), 46–47
 1,10-bis(diphenylphosphino)ferrocene (dppf), 13–14
 Bisindole alkaloids, 209–210
 Bisoxazoline ligand, 121
 Bistriarene C, 229
 9-Borabicyclo[3.3.1]nonane (9-BBN), 40–41
 Borrerine, 116–118, 121–122, 122*s*, 124, 125–126, 127–128
 Borreverines, 114–115, 116–118, 117*s*, 122, 124–125, 127–128, 129
 Bronsted acid catalysts, 86
 Brook rearrangement, 259
 Brown crotylation, 188
 Bu₄NF, 195–196
 BuOK, 275–276
 (*S*)-(–)-3-Butyn-2-ol, 43–44
- C**
 Cacchi's methodology, 14, 14*s*
 Caged core structure, 163–165
 Calphostin A, 232
 Calphostin D, 234
 Carbamate, 23, 23*s*
 Carbene-mediated tandem reaction, 273
 Carbocupration, 85
 β-Carboline, 121–122
 Carbopalladation, 10–11
 Carborhodation, 84
 Carbonyl allylboration reaction, 95–96
 Carvone, 93–94, 107–108, 109*f*
 (*R*)-Carvone, 88
 (*S*)-Carvone, 93–94, 285–286
 Catalytic cycle, allyl acetates, 7–8, 9*s*
 Catalytic cycle, Heck–Matsuda reaction, 3–4, 4*s*
 Catalytic decarbonylation, 216–218
 Catalyzed vs. uncatalyzed aldehyde allylboration reactions, 95–96, 97*t*
 CBS-oxazaborolidine, 160–161, 169
 CDCl₃, 106–107
 Central chirality, 228–229
 Cerium ammonium nitrate (CAN), 265
 Cerium chloride, 274
 Chemoselective allylic oxidation, 172–173
 Chinensioidide, 80–81
 Chinensioidide and α-methylene γ-lactones, 80–81
 Chinensioidide B, 80–81, 80*f*
 Chinese folk medicine, 80–81
 Chiral copper complex, 234, 235*s*
 Chiral iridium-based catalyst, 84–85
 Chiral lactones synthesis, 238, 238*s*
 Chiral pool, 88
 Chloromethyl pinacolboronate, 91
 5-Chloropent-1-yne, 91
 Chloroquine, 115–116
 Chroman spiroacetals, 37, 38*s*
 Chromatographic method, 59–60
 Chromium carbonyl arene complex, 232–234
 Cinacalcet, 18–20, 20*s*
Cinnamomum laubatii, 249–250
 Claisen rearrangement, 133–134
 Codonopsinine, 4
 Column chromatography, 94–95
 Competition bioassay method, 70
 Complicated acid, 271–272
 Copper-based allylation reagents, 85
 Cp₂Zr(H)Cl, 138–139, 196–197
 Crabtree's catalyst, 170–171
 Crinipellin, 271–291
 Crinipellin A, 288–290
 Crinipellin B, 271–272, 282, 282*s*, 286–288
 Crinipellin C, 271–272
 Crinipellin D, 271–272
 Crinipellin tetracycle, 276*s*
Crinipellis stipitaria, 271–272
 Cross-coupling reactions, 228, 230–231
 Crystal structure, side product, 101, 101*f*
 C-2 symmetric and meso substrates dimerization, 61, 63*s*
 Cu(OTf)₂, 119–120
 Curtius degradation, 23, 24*s*
 Curtius rearrangement, 133–134, 138
 Cyanation, 195–196

Cyanohydrins, 47–48
Cyanosilylation, 46–47
Cyclic aldehydes, 88–90, 89s
Cyclic olefins, 21, 22s, 23s
Cycloaddition, 54, 55f, 278, 278s, 279
[4+2]-Cycloaddition, 36
[2+3]-Cycloadditions, 119–120, 272–273, 280–282
Cyclohexenone, 159–160, 166
Cycloisomerization, 36
Cyclooctadiene derivatives, 59
Cyclooctadienes, 53
Cyclopentene scaffolds, 21–30
Cyclopentenone, 275s

D

Davis' reagent, 282–283, 288–289
DDQ, 11
De Brabander's synthesis, (–)-berkelic acid, 36, 36s
Dehydrogenation, 218–220
Desmethylflinderole, 121–122
Dess–Martin periodinane (DMP) oxidation, 172–173, 282–283, 288–289
Dethe synthesis, flinderole B, 119–120, 119s
DFT calculations, 251
Diacetylene, 57, 58s
Diastereomers, 274–275
Diastereoselective epoxidation, 87, 104, 105s
Diastereoselective reduction, 171t
Diastereoselectivity, 41, 42s, 150, 151s
1,5-Diaza-*cis*-decalin ligand, 234
Diazaspiro[4.4]nonane, 132–133
DIBAL-H, 91, 188
DIBAL-*n*-BuLi, 282–283
Dichamanetin, 245
2,3-Dichloro-5,6-dicyano-1,4-benzoquinone, 239–240
Diels–Alder reactions, 52, 116–119, 124, 156, 157, 157f, 168–169
Diethyl 2-(2-oxoethyl)malonate, 274
 α,α' -Dihalo ketone, 156
Dihydrocrinipellin A, 271–272
Dihydrocrinipellin B, 271–272
Diketone, 175s
Dimerization, 1,3-cyclohexadiene, 55
Dimethyl-(D)-malate, 46
Dimethylisoborreverine, 114–115, 121–122, 126–127, 129
(*S*)-(+)-*N,S*-Dimethyl-*S*-phenylsulfoximine, 288–289

1,3-Dimethyl-3,4,5,6-tetrahydro-2(1*H*)-pyrimidinone (DMPU), 47–48
Diphenylphosphoryl azide (DPPA), 217–218
Direct hydrogenation, alkene, 41, 42s
Disubstituted allylboronate synthesis, 91
2,6-di-*t*-butyl-4-methylpyridine, 4–6
(di-*t*-butylphosphino)ferrocene, 83–84
2,6-di-*tert*-butylpyridine, 192–193
Dithianes, 253–254, 258
DMP. *See* Dess–Martin periodinane (DMP)
DNA polymerase inhibitors, 80–81
Double homologation, kingianin A, 65, 66s
DPPA. *See* Diphenylphosphoryl azide (DPPA)
D-proline, 134
Dysidea frondosa, 167

E

EBC-23, 249–250, 250f
ecFABF(C163Q), 158f
EcoBiotics, 252
E-crotyl boronates, 95–96
Effects of acid, borrerine dimerization, 122–125
Electrochemical reaction, 46
Electrophilic epoxidizing agent, 87–88
Electrophilic halomethylboronic esters, 85–86, 85s
Enantioselective Heck–Matsuda reaction, 3, 3s
Enantioselective pyrrolidine formation, 121, 121s
Enantioselective transformations, 113–114
Endocyclic enecarbamates, 4, 5s
endo-Diels–Alder reaction, 125
 γ -Enolate, 163–164
Ent-3 β -hydroxy-5 α -androstan-17-one, 271–272
Epichlorohydrin, 259, 261–262
epi-vibsanin, 252
Epoxidation, 102–104
Epoxidation vs. oxymercuration, 102–104
Epoxide, 256–257, 257s
Eravacycline, 226f
Eschenmoser's salt, 282–283, 289–290
Escherichia coli, 241–244
Et₂BOME, 185–186
Ethyl amides, 55, 56f
Ethyl bromoacetate, 274, 285
Ethyl chloroformate, 144
Et₃N·HF, 188
Evans reduction, 265
exo-hydride attack, 161

F

FabF enzyme, 158–159
Favorskii rearrangement, 88
Felkin–Anh model, 188–189
Felkin model, 188–189
Fingolimod, 26–27, 28^f
Finkelstein reaction, 15–18, 255
Flack parameter, 107–108
Flavasperone, 234
Flinderole optical activity, 127–128
Flinderoles, 113–115, 118–120, 121–124, 125–128, 129
Flindersia species, 114–115
Formal [4+2]-cycloaddition, 39
Friedel–Crafts allenylation, 120–121
(+)-Fronodosin A, 167–179
Fronodosin B, 176–177
FtsZ, 226–228
FtsZ inhibitor, 226–228
Fukuyama synthesis, amathaspiramides A–F, 137_s
Furan, 157^f
Furan–TBCP cycloaddition reaction, 167
Fürstner’s synthesis, (–)-berkelic acid, 36–37, 37_s

G

GDP, 244
Gelsemine, 225–226, 226^f
Geminal dimethyl moiety, 176–177
Ghaffar–Parkins catalyst, 188–189
Ghosez’s reaction, 238–239
Gilenya, 26–27
Gliocladin C retrosynthesis, 210–211
Gong’s catalyst, 234, 236_s
Gossypol, 231–232
Gram-positive bacteria, 158–159
Grieco elimination, 87–88, 99–101, 100_s
Grignard reagent, 279
Grubbs catalyst, 23
Grubbs II catalyst, 102
GTP, 244
GTPase, 226–228
GTPase assay, 241–244

H

Halogenation, 230–231, 230_s
HBr, 192–193
HCl, 264
HClO₄, 37–38
HCT116, 200

Heck–Matsuda reaction, 1–2, 2_s, 10–11, 10_s
Heck mechanisms, unactivated olefins, 11–12, 12_s
Helical chirality, 228–229
Hemoglobin, 115–116
1-Heptyne, 44–45
Heteroannulation method, 83–84
Hexacyclinol, 225–226, 226^f
HF-pyridine, 264, 268, 289–290
HF/TEA, 289–290
HF/urea, 289–290
High-pressure liquid chromatography (HPLC), 53
Horner–Emmons reaction, 274, 276–277
Hoveyda–Grubbs catalyst, 262–263
Hunsdiecker-type reactions, 275–276
Hybrid analogs, 198
1,2-Hydride shift, 175
Hydroboration, 40–41
Hydrophobicity, 201
3-Hydroxyethylindole, 120–121
 α -Hydroxylation reaction, 282–283, 288–289
Hydroxymethylene ketone, 165–166
Hydrozirconation, 190–192
Hypnophilin, 271–272

I

IBX, 135–136
IBX-promoted dehydrogenation, 164–165
Indium, 83
3-Indoleacetic acid, 120–121
Indoles, 211–212
Interleukin-8, 167
Intramolecular alkylation, 162–163
Intermolecular RCDA reaction, 66–67, 67_s
Intramolecular alkylation reaction, 162–163
Intramolecular Friedel–Crafts allenylation reaction, 120–121
Intramolecular rhodium-catalyzed Alder ene reaction, 84
Iodine bromide, 254
Iodine–lithium exchange, 36–37
Iodoetherification, 60–61, 61_s, 65, 65_s
Iodonium salts, 11–12
(+)-Ipc₂BCl, 185–186
Irciniastatin A, 186–187
Iridium-catalyzed transfer hydrogenation reaction, 84–85
Iron (III) chloride, 255
Isoborreverines, 114–118, 117_s, 121–124, 125–126, 129
Isolation of, (–)-berkelic acid, 47–48, 47_s

Isomerized olefin, 25, 27s
Isoprenylated indole, 118–119
2-Isoprenylated tryptamine, 116–118
2-Isoprenylskatole, 119–120
Isopropyl magnesium bromide, 274

J

Jacobsen epoxide resolution, 260–261
Jacobsen resolutions, 253–254
Japp–Klingemann reaction, enol, 10, 10s
Johnson–Lemieux conditions, 185–186
Jones oxidation, 255
Jones reagent, 255

K

Keck allylation, 237, 238–239
KHMDS, 274–276
Kinetic reduction, 160–161
Kingianin A, structure of, 52
Kingianin D synthesis, 68, 68s
Kingianin F, 54–55, 56f, 56s
Kingianin F synthesis, 68, 68s
Kingianin H synthesis, 68, 69s
Kingianin J synthesis, 69, 70s
Kingianin synthesis, intermolecular RCDA approach, 71, 72s
Korupensamine synthesis, 232–234, 233s
Krische allylation, 188–189

L

Lactone, 9, 10s
LAH, 279
L-aspartic acid, 237
LDA, 9, 136, 275–276
Lewis acid, 124, 172–176
Lewis/Bronsted acid catalysis, 95–96, 97t
LiAlH₄, 104–106
LiBH₄, 192–193
LiEt₃BH, 104–106
LiHMDS, 275–276, 289–290
Lindlar catalyst, 57, 238
Lithium aluminum hydride (LAH), 43–44
Lithium bis(trimethylsilyl)amide, 46
Lithium diisopropylamide (LDA), 47–48
L-proline, 134–135
Luche reduction, 160–161, 255

M

Majoral's acylimine formation, 190–191, 191s
Malachite green, 245
Malaria, 115–116

Manchand reaction, 69
Markovnikov addition, 102–103
Mastigophorene A, 231–232
Matrix metalloproteinase-3, 34
Matsuda's acid-mediated N-acyl aminal epimerization reaction, 190, 191s
McMurry coupling reaction, 285
*m*CPBA, 104
Mefloquin, 115–116
(MeO)₃CH, 195–196
MeOTf, 190, 192–193
Metal-catalyzed cycloisomerization reaction, 37
Metal-catalyzed [2,3]-Stevens rearrangement, 131–154, 140–141, 141s
Methylative dimerization, 125–127
Methyl chloroformate, 91
2-Methyl-2-cyclopenten-1-one, 273, 274
 α -Methylene γ -lactone, 80–81
Methyl triflate, 126–127
Methyl 2,4,6-trihydroxybenzoate, 48–49
Mg(ClO₄)₂, 37–38, 191–192, 194
MgBr₂–Et₂O, 134–135
Michael addition, 163
Michael–Dieckmann condensation, 235–236
Michael–Dieckmann cyclization, 239–240
Michellamine biaryl linkages, 232–234, 233s
Michellamines A–C, 229
MnO₂, 104–106
Morita–Baylis–Hillman adducts, 84–85
Muscle relaxant, 19–20
Mycalamides, 184–185

N

NaBH₄, 185–186
N-acylaminal formation, 194
NaH, 275–276
NaN₃, 275–276
Naphthopyranone monomer, 239–240
Naphthopyran-2-ones, 235–236, 236s
n-BuLi, 276–277
NCI60 tests, 71, 73t, 74t, 75t, 76t
Nef reaction, 134
NH₄F·HF, 289–290
Nigerone, 234
Nitrile hydrozirconation, 190–192
N-methylquinolinium hexafluorophosphate (NMQPF₆), 184
NMR spectroscopy, 252
NOE. *See* Nuclear Overhauser effect (NOE)
Non-*N*-acylaminal-containing analogs, 199–200

(*S,S*)-Noyori transfer hydrogenation catalyst, 169
N-protected allyl amine derivatives, 11–21
 Nuclear Overhauser effect (NOE), 24, 251
 Nucleophilic epoxidation, 282–283

O

O-acetylcrinipellin, 271–272
 Olefination, 178–179
 Organocopper reagent, 279–280
ortho-bromophenyl carbonate, 148
ortho-tolyl carbonate, 148
 Osmium tetroxide oxidation, 285
 Osumundalactone, 250–251, 250*f*
 Ovarian cancer cell line, 34
 Oxabicyclo[3.2.1]octadiene, 158*f*
 8-Oxabicyclo-[3.2.1]-octane ring system, 156
 Oxaphosphetane, 172
 Oxa-Pictet–Spengler reaction, 35–36
 Oxidative addition, 7–8
 Oxidative carbocation formation, 184, 184*s*
 Oxidative cleavage of silyl ether, 106, 107*s*
 Oxidative couplings, 241
 Oxidative dimerization, 232, 232*s*
 Oxidative homocoupling, 228
 Oxocarbenium, 184
 Oxyallyl cation, 156
 Oxygen-substituted chroman spiroacetals, 38–39, 39*s*
 Oxymercuration, 102–104, 103*s*
 Ozonolysis, 146–147
 Ozonolytic cleavage, 188–189

P

Palladium catalysis, 82–83
 Palladium-catalyzed allylic amination, 140–141
 Palladium-catalyzed reactions, 167–168
 Palladium-catalyzed [2,3]-Stevens rearrangement., 141, 141*s*, 142*s*
 Palladium(II) complex, 37–38
 Paterson aldol, 192–193
 PC190723, 226–228
 PCC, 282
 Pd₂(dba)₃, 4–6
 Pd(MeCN)₄(BF₄)₂, 37–38
 Pd(OAc)₂, 4–6
 PDC, 138, 277–278, 282–283, 289–290
 Pederin, 192–194

Pederin analogs, 197*s*, 198
 Pederin/psymberin hybrid structures, 198, 198*f*
 Pedestatin, 198, 198*s*
 Penta-substituted arene, 188, 188*s*
 4-Pentyn-1-ol, 88
 Perylenequinones, 234
 Petersen olefination, 64
 Ph₃As nucleophile, 175*s*
 Phenyl methyl sulfone, 267
 Phleichrome, 232, 234
 Phosphine mediated ring-opening, 172*s*, 173
 Photochemical racemization, 229
 Photoredox catalyst, 66, 67*s*
 Photoredox radical coupling, 211–212
 Pimentosin, 228, 237–241
 Pivaloyl chloride, 190–191
 Planar chirality, 228–229
 Platensimycin, 158*f*
 Platensimycin retrosynthetic analysis, 159*s*
 PNPCI, 46–47
 Polarimetry, 127–128
 Polysubstituted cyclopentanes, 91–93, 93*s*
 Prehomologated diol, 64, 64*s*
 Propellane ring system, 114–115
 Protecting groups, 90–91
 PtO₂, 285
 Psymberin, 186–190, 187*f*, 195–196, 195*s*
 Pyridine-*d*₅, 106–107
 Pyridinium dichromate, 106
 Pyrrolidine, 118–120, 121*s*, 124, 125
 Pyrroloindolines, 211–212

R

Racemic *endo* Diels–Alder products, 56–57
 Radical cation, 184
 Radical cation Diels–Alder (RCDA) approach, 55–59
 Radical cation reaction, 57, 58*s*
 Radical cyclization, 82, 283
 RCM. *See* Ring-closing metathesis (RCM)
 Redox manipulations, 104–106, 106*s*
 Reduction, epoxide, 104–106
 Regioselective hydroalumination, 85–86
 Relative stereochemistry, *syn*- and *anti*-123a, 24, 25*s*
 Reserpine, 225–226, 226*f*
 retro-Mannich reaction, 146–147
 retro-Michael reaction, 136–137
 Retrosynthesis and retrosynthesis, 52
 Retrosynthetic analyses, kavalactones, 9, 9*s*
 Retrosynthetic analysis, 159–160

Retrosynthetic analysis, (–)-berkelic acid, 42–43, 43s
Retrosynthetic analysis, chinensioid B, 86–88
Retrosynthetic analysis, VPC01091, 28, 28s
Retrosynthetic plan, 253
Retrosynthetic synthesis, α -methylene γ -lactones, 81, 81f
Rhodium-catalyzed cycloisomerization protocol, 84
Rhodium π -allyl species, 84
Ring-closing metathesis (RCM), 87, 102, 102s, 259–260, 262–263
Ring opening/elimination, 172–173
Robinson annulation, 163, 165–167
Rochelle salts, 43–44

S

Sakaguchi synthesis, amathaspiramide F, 136–137
Sakai's approach, 121–122, 122s
Sandmeyer, and Meerwein reactions, 2–3
Scandium (III) triflate, 96–97
Schramm's C-azanucleoside, 4
Schwartz's reagent, 138–139
Secondary metabolites, 33–34
Selective iodolactonization, acids, 65, 65s
Sesquiterpene lactones, 80–81, 80f
Seven-membered ring generation, 99–102
Sharpless epoxidation, 262, 283, 285–286
SiF₄, 289–290
Silver-catalyzed synthesis, chroman spiroacetal, 40, 40s
Silver-mediated hydrolysis, 157
Silver triflate, 40
Smith Anion Relay chemistry, 259
SnCl₂, 135–136
Snider's synthesis, (–)-berkelic acid, 35–36, 35s
S_N2'-type reaction, 279
Sodium amalgam, 277–278
Sodium borohydride, 274, 276–277
Sonogashira coupling, 136
Spectroscopic stereochemical determination, 264–265, 265f
Sphingosine 1-phosphate (S1P), 26–27, 28f
Spiciferrin, 36
Spiroacetalization, 36–37
Spiroacetals, 251, 251f
Spiroketal, 251
Staphylococcus aureus, 226–228

Staunton–Weinreb annulation, 235–236, 239–240
Stereochemistry, 148–150, 150s
Stereoconvergent resolution, 161
Stereoselective arylation, allylic esters, 6–11
Stereoselective Heck–Matsuda reaction, 4–6, 5t
Steroidal inhibitors, 80–81
[2,3]-Stevens rearrangement, 131–154, 139, 140–144
Stierle's original and Fürstner's revised structure, (–)-berkelic acid, 35, 35f
Substrate-directed Heck–Matsuda reaction, 4–30, 16t, 26s
Supersilyl aldol chemistry, 268
Suzuki coupling, 57, 58s
Suzuki–Miyaura cross-coupling, 170
Suzuki reaction, 232–234
Swern oxidation, 279–280
Swern protocol, 279, 286
syn-pentane interaction, 97–99

T

Talarodexine A, 237–241
Talarodexine B, 237–241
Talarodexine lactone synthesis, 238–239, 239s
Tandem cycloaddition reactions, 272–273, 273s, 275s, 280–282, 281s, 286, 288s
TBAF. *See* Tetrabutylammonium fluoride (TBAF)
TBAF/AcOH, 289–290
TBAF/NH₄F, 289–290
TBHP, 282, 289–290
TBSCl, 259
TBSOTf, 253–254
t-BuLi, 255–256
t-butyl acetate, 193–194
Tertiary alcohol installation, 102–108
Tethered phosphonate-stabilized anions, 82
Tethered substrates preparation, 61, 62s
Tetrabutylammonium fluoride (TBAF), 47–48, 289–290
Tetrabromocyclopropene (TBCP), 157
Tetracyclic core synthesis, 39, 40s, 45, 45s
Tetracycline, 226f
Tetrahalocyclopropenes, 179
Tetrahydrocrinipellin A, 271–272
Tetrahydrocrinipellin B, 271–272
Tetraquinane, 275s, 280–282, 281s
TFA, 125
Theopederin, 184–185

Theopederin D, 184–187
 Thermo gravimetric analysis, 2–3
 β -Thujaplicin, 157–158
 Tietze–Smith linchpin failed approach, 260, 261s
 Tietze–Smith linchpin reaction, 253–254, 255–256, 259–260
 TMM, 278, 279, 280–282, 286, 290
 TMM diyl cycloaddition reaction, 278
 TMSCN, 192–193, 195–196
 TMS-dithiane, 261–262
 TMSOTf, 188–189, 195–196
 Toste group's synthesis, flinderole B, 120–121, 120s
 Total synthesis, 131–132
 Totarol, 245
 Trauner synthesis, amathaspiramide F, 134, 135s
 Trialkylphosphine ring opening, 172–176
 Tributyltin chloride, 276–277
 Tributyltin hydride, 40–41
 Triflates, Aryl, 11–12
 Triflic acid, 125
 Trifluoroacetic acid, 150–152
 Triketopiperazine (TKP), 210–211
 Trimethylenemethane (TMM), 272–273
 Trimethylsilyl chloride, 106
 Trimethylsilyldiazomethane, 150–152
 Tri-*O*-acetyl-D-glucal, 255
 2,6,7-Trioxabicyclo[2.2.2]octane (OBO) ester, 238–239
 Trityl ether, 6
 Tropical rainforests, 249–250
 Tsuji–Trost reactions, 6–7
 Tsuji–Wacker oxidation, 166–167
 Tubulin, 226–228
 Tumor necrosis factor- α , 80–81
 Type I and type II allylation reagents, 95, 96f

U

Ullman coupling, 231–232
 α,β -Unsaturated lactones, 237–239

V

Vanadium catalysts, 234, 236s
 Vancomycin, 128
 Vibsanin E, 252
 Vilsmeier–Hack formylation, 44–45
 Vioxanthin, 228
 Viriditoxin, 226–228, 235–236, 237–241
 Visible light photocatalysis, 208–209
 Vitamin D receptor inhibitors, 80–81
 VO(acac)₂, 241
 V(O)F₃, 234
 VPC01091 synthesis, 26–27, 28f, 29–30, 30s

W

Weinreb amide, 6
 Wittig condensation, 170
 Wittig–Horner–Emmons–Wadsworth olefination, 82
 Wittig olefination reaction, 284, 285
 Wittig-type reactions, 274
 Wöhler, 225–226
 Woodward-inspired annulation strategy, 220–222
 Woodward–Wilds, 163

X

Xiao, 121
 X-ray diffraction analysis, 271–272

Y

Yamamoto's synthesis, 268, 268s
 Yuechukene, 127–128

Z

Zantrin Z3, 244
 Z-crotyl boronates, 95–96
 Zimmerman–Traxler chair-like transition state, 95–99
 Zinc–copper reagent, 85
 Zinc-mediated Barbier-type allylations, 83
 Zn(OTf)₂, 195–196
 ZnBr₂, 240
 Zn-CH₂I₂-TiCl₄, 274, 285
 ZnCl₂, 136, 138